AD

TECHNICAL REPORT
72-10-FL

INVESTIGATION OF THE ENERGETICS OF WATER BINDING IN DEHYDRATED FOODS AT VERY LOW MOISTURE LEVELS IN RELATION TO QUALITY PARAMETERS

by

D.R. Heldman, F.W. Bakker-Arkema,
P.O. Ngoddy, G.A. Reidy,
M.P. Palnitkar and D.R. Thompson

Michigan State University,
Agricultural Engineering Department,
Department of Food Science
and Human Nutrition,
East Lansing, Michigan 48823

Contract No: DAAG 17-67-C-0165

Approved for public release;
distribution unlimited.

June 1972

UNITED STATES ARMY
NATICK LABORATORIES
Natick, Massachusetts 01760

Food Laboratory
FL-139

Approved for public release; distribution unlimited.

Citation of trade names in this report does not constitute an official indorsement or approval of the use of such items.

Destroy this report when no longer needed. Do not return it to the originator.

AD_____

TECHNICAL REPORT
72-10-FL

INVESTIGATION OF THE ENERGETICS OF WATER BINDING IN DEHYDRATED FOODS AT VERY LOW MOISTURE LEVELS IN RELATION TO QUALITY PARAMETERS

by

D. R. Heldman
F. W. Bakker-Arkema
P. O. Ngoddy
G. A. Reidy
M. P. Palnitkar
D. R. Thompson

Agricultural Engineering Department
Department of Food Science and Human Nutrition
Michigan State University
East Lansing, Michigan 48823

Contract No. DAAG 17-67-C-0165

Project reference:
1J062110A034

Series: FL-139

June 1972

Food Laboratory
U. S. ARMY NATICK LABORATORIES
Natick, Massachusetts 01760

FOREWORD

The amount and physico-chemical state of water of low and intermediate moisture foods is one of the prime considerations in textural and flavor qualities.

The work covered in this report had two general objectives: First, to provide practical information on the effects of a multitude of variables on the eating qualities of precooked freeze-dried beef, including the effects of final plate temperature in the freeze-drier, and the role of in-package water activity on mechanical and sensory properties. Second, to present basic information on the energy relations encountered in the sorption of water by low and intermediate moisture foods -- information which is of value to the food engineer in the designing of equipment and in cost analysis of the freeze-drying process.

The report presents a large volume of data on both of the above objectives. Information of practical importance deals with quantitative relationships between the sorption of water along the isotherm and textural properties of beef as affected by the plate temperature, initially and after storage, under different conditions. Information of engineering or theoretical significance covers the calculations of the thermodynamic properties of the meat-water system, analysis of the physical parameters necessary in the construction of a sensitive calorimeter for the measurement of the energy of sorption, and prediction of thermodynamic quantities using a single isotherm. In addition to the above, information which can be of value to the food technologist and the food engineer includes literature discussion and data on (a) percent water present in various intermediate moisture foods, (b) changes in food qualities (flavor plus texture) along the isotherm, (c) calorimetric measurements in foods, (d) sensory texture profiling, (e) theories of water sorption, and (f) construction of mechanical models for evaluation of effects of storage on textural properties.

On the part of the Contractor, the main investigator was Dr. D. R. Heldman and his co-investigator Dr. F. W. Bakker-Arkema; research associates were Drs. P. O. Ngoddy, G. A. Reidy, M. P. Palnitkar, and D. R. Thompson.

On the part of the Government, the Project Officer was Dr. John G. Kapsalis and the Alternate Project Officer was Mr. John E. Walker, Jr.

TABLE OF CONTENTS

TABLE OF CONTENTS (Continued)

TABLE OF CONTENTS (Continued)

List of Tables

List of Figures

ABSTRACT

The thermodynamic and texture properties of low and intermediate moisture foods are discussed on the basis of the moisture sorption isotherm. Information is presented on the effects of final plate temperature in the freeze-drier and of in-package relative humidity on the textural properties under different storage conditions.

1. Introduction

1.1. Importance of Water Activity in Foods

Water, comprising 60-95 percent of the total weight of food, is by far the dominant and the most important component of common foods, which may also contain fat, protein, carbohydrate, mineral and other groups of substances. Therefore, water is an important factor to consider in perishability of foods. The water molecule and its association with biological substances is still a subject of controversy in spite of considerable literature available on the subject. Kuprianoff (1958) proposed that moisture associated with biological material could exist as free moisture, chemically bound moisture and adsorbed moisture. Various workers defined bound water on the basis of the technique used for its measurement. No definition of so-called "bound water" is accepted universally. The concept of bound water associated with biological materials cannot be ignored since some characteristic and sometimes irreversible changes take place when water is removed from a biological material by freezing, by evaporation or even by binding chemically. Fennema (1970) gave some guidelines to describe the water associated with biological materials.

> "There is no such thing as free water, all water associated with food is bound. The relative boundness of water associated with a given biological material changes as a continuum. That is at low moisture levels water is less mobile in comparison to the water at higher moisture levels."

The ratio of vapor pressure of a food material over the saturation vapor pressure of pure water would probably be the simplest and least meaningful definition of water activity. Numerically water activity is the equilibrium relative humidity divided by one hundred.

From the thermodynamic point of view, the water activity (a_w) has a different meaning. Water activity of a given material means its relative chemical potential with respect to the chemical potential of pure water to which a value of 1 is arbitrarily assigned. The following thermodynamic relation effectively describes the link between the chemical potential of water in a biological material (μ_w) and the chemical potential of pure water (μ_w). This link is truly what is called water activity. The term R_gT is the product of the universal gas constant (R_g) and the absolute temperature (T).

$$\mu_w = \mu_w^o + R_g T \, \mathrm{Ln} \, a_w \qquad (1\text{-}1)$$

In general the smaller the chemical potential of water in food, the smaller the driving force for chemical reactions involving water.

1.1.1. Relationship to dehydration processes: It is well known that the latent heat of vaporization increases to a value well above the values known for pure water as food is dried to low moisture levels. Latent heat of vaporization values especially at low moisture levels become very important when designing the equipment to be utilized in the dehydration process. Moisture equilibrium isotherms for a given product provide the information

needed to compute various energy levels with which water associates with the product.

1.1.2. Influence on product texture: Due to the obvious relationship between texture of dry and intermediate moisture foods and moisture content, there will be a corresponding relationship to water activity. There have been no consistent research results which illustrate the water activities at which the texture of dry or intermediate moisture foods is most desirable.

1.1.3. Relationship to sensory evaluation: The heat of adsorption or the amount of heat released as a product adsorbs moisture, may be as important to product quality as the latent heat of vaporization is to the design of a dehydration process. The most obvious relationship between product quality and thermodynamic parameters is that described by heat of immersion. This particular parameter best describes the heat released and sensed by the person consuming a dry or intermediate moisture food product. Although the magnitude of this value or parameter is relatively small, it must be considered in the overall sensory evaluation of dry food product. Difficulties in direct calorimatric experimental measurement of small thermodynamic quantities such as heat of immersion place increased emphasis on indirect evaluation from moisture equilibrium data.

1.1.4. Influence on storage stability: The understanding of water activity in relation with the food materials has been partly responsible for the development of intermediate moisture foods. Brockmann (1969) reported that the intermediate moisture foods are a class of heterogenous groups of foods which owe their stability to reduced water activity but contain too much water to be regarded as dry. In general, an intermediate moisture food can be consumed, without rehydration, and is shelf stable without refrigeration or thermal processing. It is well known that the water activity has a dramatic influence on the growth of bacterias, yeasts and molds. Water activity and equilibrium moisture values are extremely useful in selecting the environmental conditions necessary to establish or maintain the desired product properties.

1.2. The Role of Thermodynamics in Moisture Equilibria.

The thermodynamics of moisture sorption in food products influences virtually every phase of manufacturing, handling and consumption. The design of the system for moisture removal will be determined by the products binding energy for water. The properties of the dry product are directly dependent on the particular moisture level which exists. In addition, the hygroscopic characteristics and thermodynamics of moisture adsorption will determine the manner in which rehydration proceeds in the product.

The thermodynamics related to moisture sorption provide a macroscopic description of the sorption process. Based on available theory, thermodynamic parameters can be computed from the accurate moisture equilibrium isotherm data. As mentioned earlier latent heats of vaporization are useful in designing dehydration processes and the heats of adsorption are important to the sensory properties of foods. The recent trend towards the development of dry and intermediate foods has created renewed interest in the evaluation of thermodynamic parameters related to the moisture phenomena. There seems to be considerable evidence that the storage stability of dry and intermediate moisture foods may be related in some manner to thermodynamic parameters although it is difficult to develop an obvious relationship between them.

1.3. Calorimetric Investigations.

Many processes with small heats of reaction are being studied with microcalorimeters. The magnitude and the variations with time of some reaction heats have been shown to be of considerable importance in processes of the food industry. Microcalorimetric measurements are expected to be valuable both for the analysis and control of food processes. Because of the accuracy required of microcalorimetric measurement a detailed analysis of the instrument is necessary.

In principle the design and operation of microcalorimeter is simple. The basic parts of the calorimeter include the product under study, one or more thermometric measuring devices, perhaps an electric heater, devices for mixing and a vessel for confining the reaction. In microcalorimeter the environment ambient to the reaction vessel is of utmost importance. Even small temperature gradients between the environment and the reaction vessel can cause heat transfer rates of the same order of magnitude as the thermal effects of the reaction.

1.4. The Role of Freeze-dried Foods.

Freeze-drying is a unique form of food dehydration which may have considerable application in some foods which cannot be dried by other available processes. The process seems to be well adapted to drying of beef and other meat products, but quality of the product needs to be improved. Both flavor and texture quality need to be considered.

One approach to improvement of freeze-dried food quality is to investigate basic mechanisms which occur during the process or during rehydration of the freeze-dried product. After these mechanisms are described and understood, the processes can be modified in a manner which will reduce their influence on flavor and texture of the product.

1.5. Objectives of the Research.

The research results to be presented and discussed in this report were completed in three rather distinct phases. There were separate objectives for each phase of the investigation, but the overall objectivesinvolved the use of results from each phase. The objectives include the following:

1. To determine the influence of processing temperature of precooked freeze-dried beef on the adsorption and desorption moisture equilibrium characteristics of the product.
2. To utilize moisture equilibrium data to evaluate the thermodynamic parameters which describe the product.
3. To use moisture equilibrium characteristics and thermodynamic parameters of freeze-dried beef as a basis for improving moisture.
4. To analyze microcalorimetric measurements of foods.
5. To evaluate the texture of precooked freeze-dried beef at various water activities by using sensory panels and objective methods.
6. To investigate the influence of storage time and temperature on the texture of precooked freeze-dried beef.
7. To investigate relationships between thermodynamic parameters of precooked freeze-dried beef and rheological parameters of the product.

2. Literature Review

2.1. General Remarks

Water, in many respects, is a unique compound. Chemical reactions and physical interactions in which it participates influence every gross characteristic of a biological material. The moisture content of a biological product controls its mechanical (texture, hardness, chewiness, etc), enzymic, chemical, physical and even microbiological characteristics. Recently Labuza et al, (1970) stated that at moisture contents below those of fresh foods, water still has solvent properties including the ability to dissolve the solids and to allow the diffusion of reactants.

Since the objective of this report is related to the estimation and importance of thermodynamic energy parameters for low and intermediate moisture foods with regards to the moisture sorption phenomena, it is not intended to review the vast amount of literature available on the subject of moisture sorption phenomena.

For convenience, the literature on the subject of moisture sorption phenomena can be divided into two classes, the approach of physical chemists and engineers and the approach of food scientists. The physical chemists are primarily interested in investigating the underlying principles of moisture sorption phenomena. Their approach is to obtain a theoretical moisture equilibrium isotherm to account for sorptive behavior of biological materials, making use of sound physicochemical laws governing the moisture sorption. Not entirely different from the above mentioned theoretical approach, food scientists rely largely on experimental work and investigate the changes in a given food system with respect to moisture content which is so closely related to equilibrium relative humidity. In general, both the approaches focus on the same goals, namely, better food and the role of water in food quality.

2.2. Moisture Sorption Phenomena

Moisture equilibrium isotherms are the most convenient way to represent the sorption characteristics of a given biological substance. In addition, it proves to be a good starting point for further theoretical analysis of moisture sorption phenomena. Bio-scientists are primarily interested in only one adsorbate (water vapor) and numerous adsorbents (biological materials) which are characterized by great complexity and heterogeneity in physical structure, each being an assemblage of strongly hydrated high molecular weight compounds mostly belonging to classes called proteins, carbohydrates, and lipids. Since the complete quantitative representation of components in a given biological material is difficult, the combined or average behavior of large numbers of individual components is dealt with in relation to water activity and the adsorbent-adsorbate complex. However, it is obvious that the weight of adsorbate adsorbed on a given adsorbent depends on the characteristics of both adsorbent and adsorbate.

Adsorption is commonly divided into two classes, namely, physisorption and chemisorption. Physical adsorption could be relatively rapid as compared to chemisorption. Physical adsorption is caused by intramolecular forces between molecules of water vapor and the surface of adsorbent (polar sites of adsorbent). In general the polar-molecules--the molecules possessing

the following polar groups: $-NH_2$, -NH, -OH, $-COOH_2$, etc.--are considered to be sorptive sites on the adsorbent because the positive and the negative charges in the above molecules are not symmetrically distributed. The formation of a physically adsorbed layer may be similar to condensation of a vapor to form liquid.

Considerable efforts have been devoted to the development of quantitative theories to account for usually sigmoid shaped moisture equilibrium isotherms of biological materials. Labuza (1968) reviewed some of the theories and s tated that there are three basic theories to explain the moisture sorption phenomena, (1) the kinetic concept of Langmuir, (2) Polayanis' adsorption potential theory, and (3) Zsigmody's capillary condensation theory. Recently Ngoddy (1969) critically reviewed several moisture sorption theories in terms of their applicability, assumptions and limitations. According to his hypothesis, if the physical structure of a given biological material is represented mathematically in terms of pore size distribution function and an idealized geometry, its moisture equilibrium isotherm shape canbe predicted. Ngoddy (1969) applied his theory to several biological materials and was able to show good agreement between experimental and theoretical moisture equilibrium isotherms. Adamson (1967) noted that the theoretically derived relationships for moisture equilibrium isotherms from different models have been found to yield equations which are graphically and even algebraically identical.

The applicability of theoretical equations explaining the moisture sorption phenomena based on some mathematical model system to real food systems is somewhat limited due to their great complexity. Even if a given theoretical equation does predict a moisture equilibrium isotherm, in most cases it fails to explain the relation between food stability and moisture levels. Finally the general drawback of the theoretical prediction equation is that it depends on the experimental determination of a parameter used in its derivation.

Strasser (1969) reported that the moisture sorption isotherm can be expressed by the following formula:

$$M = f(P/P_o)_T$$

Moisture content (M) of food at constant temperature (T) is a function of water activity (a_w). Strasser (1969) further remarked that a more sensitive indication of the sorption properties of food might be obtained if isobars were measured at low temperatures. Sorption isobars can be determined by varying the temperature of a food and keeping the partial vapor pressure of water about the food constant as expressed by the folllowing formula:

$$M = f(T)_P$$

Another method of expressing moisture content is by using isosters as expressed by the following equation:

$$P = f(T)_M$$

Procedures for obtaining water vapor sorption isotherms have been described in detail by Taylor (1961), Karel and Nickerson (1964) and Hofer

and Mohler. (1962). Ngoddy (1969) described a more sensitive and accurate method of obtaining the moisture equilibrium. This system uses an electro-balance which records the sorptive changes automatically and continuously.

Biological substances usually exhibit a prominent hysteresis effect. This indicates that the equilibrium moisture content for a given relative humidity is higher during desorption than adsorption (Chung and Pfost, 1967). Several theories have been advanced to account for the phenomena of hysteresis, based mostly on the pore structure of the adsorbent, which is assumed to play a dominant role in hysteresis.

2.3. Water Activity and Food Stability

One of the basic theories of adsorption of gases or vapors was proposed by Brunauer, Emmett and Teller (1939). The BET equation leads to the determination of the amount of gas or vapor adsorbed in the first monomolecular layer (M_1). This monomolecular layer moisture value was first related to optimum moisture content of dehydrated food by Salwin (1959). Whether a BET monomolecular layer value does represent an optimum moisture level is debatable according to Rockland (1969). However, the existence of an optimum moisture level for dehydrated food is well established (Cuendet et al, 1954; Huelsen and Bemis, 1955; Martin,1958; Mitchell and Enright, 1957; Roby and Simon, 1959; and Salwin, 1963). Rockland (1957), Rockland, et al.(1961) reported an optimum moisture content of walnut kernels above and below which they deteriorated at a more rapid rate. Deterioration reactions occurring below the optimum moisture value were characterized as auto-oxidative, resulting in the development of typical rancid flavors and odors. Scott (1957) and Webb et al.(1960) demonstrated that microbiological proliferation occurred at high equilibrium relative humidity values.

With the development of intermediate moisture foods in recent years, food stability acquired a much boarder meaning than just optimum moisture value commonly expressed for dehydrated foods. There is no reliable theoretical method to predict the stability region for a given food system.

2.3.1. Rockland's local isotherm concept: Rockland (1969) specified three types of local isotherms (Figure 2-1). Type L I is associated with water bound by polar to ionic groups such as carboxyl and amino groups. Type L II may consist of water hydrogen bonded to hydroxyl and amide groups, and Type L III is characterized by unbound or free water. Optimum stability region, according to Rockland (1969), appears to be associated with L II - L III region as shown in Figure 2-1. Some typical physical, chemical and biological changes associated with local isotherm regions L I, L II and L III are shown in Table 2-1.

Table 2-1 -- Some product characteristics within localized moisture sorption isotherms (Rockland, 1969).

Local Isotherm I	Local Isotherm II	Local Isotherm III
Dry	Dry	Moist
Hard	Firm	Soft
Crisp	Flexible	Flaccid

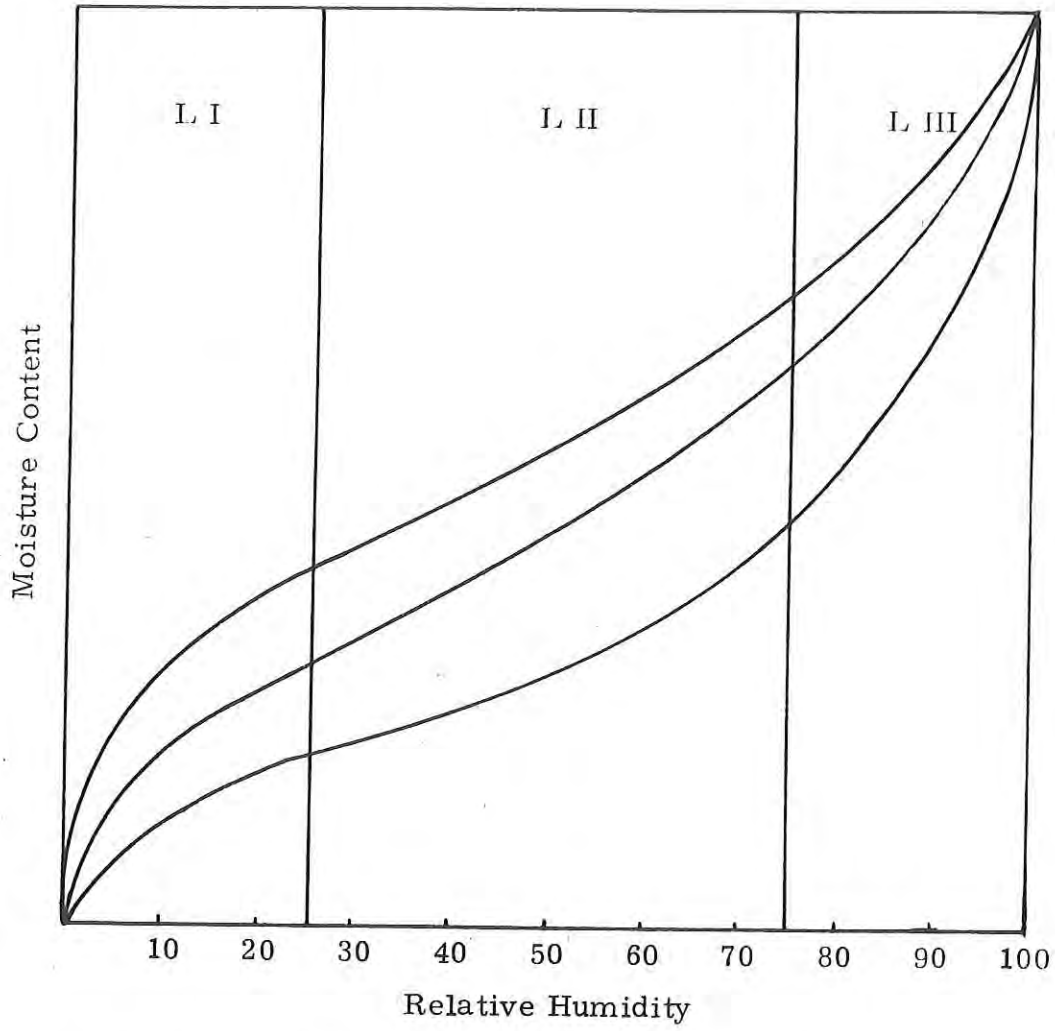

Figure 2-1. --Hypothetical separation of local isotherms (Rockland, 1969).

(Continuation of Table 2-1)

Glazed	Normal Dry Surface	Syneresis
Shrunken	Normal Size	Swollen
Static Charge	Non-adherent	Sticky
Darkened	Normal Color	Browning
Rancid Odor	Normal Odor	Off Odor
Rancid Falvor	Normal Flavor	Off Flavor
Autoxidation	Minimal Chemical Changes	Enzymatic Reaction
Microbicidal	Microbiostatic	Microbial Growth

Rockland used Henderson's (1952) semi-empirical equation of the moisture sorption isotherm to establish his local isotherm concept. If this concept should hold for intermediate moisture foods, then the chances for improved shelf stability are increased by structuring the food to obtain L II type sorption isotherm. An understanding of water activity thus could be tied with food stability, leading to innovation in formulation and processing of food products. It is evident that the available control factors are temperature, vapor pressure and composition of a food.

TABLE 2-2. -- Some intermediate moisture foods (Bone, 1970).

Item	% Water	Item	% Water
Mayonnaise	16	Canned Biscuits	39
Canned Bacon	16	Swiss Cheese	39
Margarine	16	Chocolate Syrup	39
Butter	16	Waffles	40
Citron Candy	18	Luncheon Meat	40 - 55
Pound Cake	19	Pork Link Sausage	42
Marshmallow	15-35	Cooked Ham	42
Doughnuts	19	Tortillas	42
Honey	20	Canned Sardines	47-57
Raw Bacon	20	Cooked Hamburger	47
Fruit Cake	23	Fresh Coconut	47
Dried Fruits	24	Dried or Chipped Beef	48
Foundation Cake	25	Apple Pie	48
Table Syrup	25	Sweetened Cranberry Sauce	48
Biscuits	27	Corn Bread	49
Sweetened Condensed Milk	27	Egg Yolk	49
Jams, Marmalades	28	Cream Cheese	51
Gingerbread	30	Canned Tuna Fish	52
Angel Food Cake	32	Apple Butter	53
Jellies	35	Corned Beef, Uncooked	54
Canned Orange Juice Concentrate	35	Raw Hamburger	55
White Bread	35	Pancakes	56
Cheddar Cheese	39	Baked Macaroni and Cheese	58

Food stability is not an absolute term. In fact, food stability could be visualized as a function of several interdependent factors such as color, texture, flavor, and nutritive value, in addition to moisture content. It seems logical, however, to correlate the food stability with water activity, although it may be difficult to develop a logical relationship between them. Bone (1970) stated that the control of water activity is the basic control factor in the preservation of non-refrigerated intermediate moisture foods that have extended shelf life. Table 2-2 illustrates some examples of intermediate moisture foods (Bone, 1970). Prevention of microbiological growth is, of course, a dramatic feature of water activity control. Table 2-3 indicates the approximate lower limits of water activity at which growth can occur for various kinds of organisms.

Table 2-3. -- Approximate lower limits of a_w for microorganism growth (Bone, 1970)

Microorganism	Lower Limits of a_w
Bacteria	0.91
Yeast	0.88
Molds	0.80
Halophillic Bacteria	0.75
Xerophillic Fungi	0.65
Osmophillic Yeasts	0.60

2.4. Microcalorimetry

Thermal effects accompany many chemical and biological phenomena. The magnitude of these effects may be of considerable theoretical and practical importance. The stability and structure of molecules, the conditions of chemical equilibria and the heat exchange in industrial processes can all be calculated from a knowledge of these thermal effects.

Many processes have been studied by calorimetric methods. Heats of combustion and other processes that evolve large quantities of thermal energy have been extensively investigated. The advent of microcalorimetric measurements has extended the range of calorimetric studies. Various examples of these microthermal processes have been reviewed by Swietoslawski (1946).

Provisions must be made in a microcalorimeter for either eliminating or measuring the heat transfer between the reaction vessel and its environment. It is possible to measure the heat loss by continuously recording the temperature difference between the reaction vessel and a jacket surrounding the vessel. This technique requires that either the temperatures of the reaction vessel and the jacket be uniform or that the temperature difference between the two surfaces be taken at a number of locations. The heat loss can be eliminated by maintaining the jacket at the same temperature as the reaction vessel. This system also requires the surface temperatures to be uniform. Both of these techniques require extremely accurate thermal measuring or control apparatus in addition to that required to determine the heat evolved.

The heat loss can be measured by using twin vessels inside a thermally uniform jacket. If both are treated identically but the reaction takes place in only one of the vessels, the effect of time variations in the temperature

of the jacket can be eliminated. The difference in thermal gradients between each vessel and the jacket is identical to the thermal gradient between a reaction vessel and an absolutely constant environment. It is very difficult to maintain a constant thermal environment for long periods of time, but the thermal gradients in a twin vessel microcalorimeter can be easily measured with thermocouples. Calvet and Pratt (1963) have shown that the temperature of the reaction and reference vessels need not be uniform if a number of thermocouples are judiciously placed around the surface of each vessel. The principle requirement is that the temperature of the jacket remains uniform. Well stirred baths of water or other liquids have frequently been utilized to maintain the temperature uniformity condition. A simpler design and a more stable ambient condition are achieved by substituting a solid metallic sink for the well stirred bath.

At least two microcalorimeters are commercially available. Sunner and Wadso (1966) reported on a commercially produced Swedish microcalorimeter that is capable of measuring the heat of immersion. A French built microcalorimeter is being imported and marketed by Imass Corporation. This instrument has sufficient sensitivity to measure the heat of immersion but the instrument is not designed for this type of application.

Even with several microcalorimeters commercially available, most experimentors will probably build their own instruments. Wilhoit (1967) indicated that the specifications of each experimentor differs sufficiently to require modification of existing instruments or construction of new ones. A review of microcalorimeters by Thompson (1970) indicated that most experimentors are developing their own equipment.

Many design parameters or characteristics of microcalorimeters are well established. However, some characteristics and experimental techniques are still selected arbitrarily. Several authors have discussed the optimum use of temperature sensors. Other authors have discussed electric circuits both for heater supplies and for recording the electric potential from thermoelectric sensors. A few authors have discussed calibration techniques and also methods of finding the reaction heat from temperature data. On the other hand, the size and shape of the sinks for twin vessel microcalorimeters appears to be arbitrary.

It is very difficult to evaluate the effectiveness of the metallic sinks experimentally. Microcalorimeters require temperature measurement equipment with the highest sensitivities available for measuring the temperature difference between the reaction and comparison vessel. However, this temperature difference is much larger than the temperature variation in a good sink. Some indication of the effectiveness of the metallic sink can be obtained by increasing the reaction heat to a level that causes measurable thermal variation within the sink. Unfortunately, it is not easy to relate the latter measurements to the effectiveness of the sink for reactions with small heat outputs. Both radiative and convective heat transfer characteristics are functions of the thermal gradient. Therefore, the ability of a sink to maintain a uniform temperature with reactions of low heating value is not the same as its effectiveness with reactions of higher heating value. Furthermore, because of the exacting requirements of similarity between the reaction and comparison vessels and their cavities, the cost of testing several physical models is extremely high.

2.5. Food Texture

The exact definition of texture in relation to food-stuffs has been a subject of considerable controversy in the literature. Definitions have varied so much that Matz (1962) and Elder and Smith (1969) appear justified in concluding that texture or rheological properties of foods will have different meanings to individuals, depending on the particular industry of interest e.g. cereal, dairy or confectionary processing.

A dictionary definition of texture is "an identifying quality; the disposition or manner of union of the particles of a body or substance". An alternative definition for texture of food is offered by the Institute of Food Technologists (Kramer, 1959):

> "The mingled experience deriving from the sensations of the skin in the mouth after ingestion of a food or beverage. It relates to density, viscosity, surface tension and other physical properties of the material being sampled".

However, when referring specifically to meat, Ball et al. (1957) state that "texture of cooked meat is the feel of smoothness or fineness of the muscle tissue in the mouth".

The various suggestions for definition of texture found in the literature are thoroughly reviewed by Matz (1962) and Szczesniak (1963), who concluded that the two important elements of texture are:

(1) physical structure of the material (geometry);
(2) the way the material handles and feels in the mouth (surface and mechanical properties).

Szczesniak (1963) suggested a total of eight mechanical characteristics which would completely describe a food; cohesiveness, hardness, adhesiveness, viscosity, elasticity, (primary parameters) and brittleness, chewiness, gumminess (secondary parameters). The definitions offered are rather vague and confusing, with some overlaping. Two useful parameters however,which have satisfactorily described freeze-dried beef texture (Reidy and Heldman, 1970); are

Hardness: the force necessary to attain a given deformation on the first bite; and

Chewiness: the energy required to masticate a solid food product to a state ready for swallowing.

Matz (1962) notes that hardness is not considered a fundamental property of solids but a composite property dependent on the elastic moduli and elastic limit.

The Szczesniak (1963) texture profile was critically examined by Sherman (1969) who questioned both the classification of primary and secondary parameters made by Szczesniak and also the significance of the definitions of elasticity, chewiness and gumminess. Sherman suggested a modified texture profile by classifying analytical characteristics; elasticity, viscosity, adhesion to palate as secondary characteristics; and masticatory and non-masticatory mechanical properties as tertiary characteristics. The usefulness of such

debate is questionable, since it ignores the problem of relating texture of a particular food to meaningful, easily measured rheological characteristics. Both of the profiles offered by Sherman and Szczesniak easily distinguish between different foods (e.g. candy, meat and cheese) but are not sensitive to texture differences in the same product (e.g. meat cooked for various time-temperature combinations, or meat of different moisture contents). It is generally accepted that a sensory panel can detect texture differences in the same product, and the ability of a panel to rank meat on a tenderness scale is a typical example.

However, despite the fact that no simple satisfactory definition of texture exists it may be accepted that consumers have a good concept of texture on a comparative basis when considering specific food items.

2.5.1. Texture evaluation by sensory panel: Szczesniak, et al (1963) developed a standard rating scale for texture parameters and correlation between objective and the sensory methods of texture evaluation.

A texture profile is the sensory analysis of the texture complex of a food in terms of its mechanical, geometrical, fat and moisture characteristics, to degree of each present and the order in which they appear from first bite through complete mastication. Szczesniak, et al (1963) selected foods to represent individual points on the scale of hardness, brittleness, chewiness, gumminess and adhesiveness. The samples were evaluated by subjective (sensory panel) and objective methods (texturometer, viscometer, etc) and good correlation between subjective and objective evaluations was illustrated. The resultant scales are the basis of quantitative organoleptic texture evaluation or can be called a complete texture profile. The texture profile encompasses the entire range of parameter intensities encountered in food products.

Mention should be made of the fact that texture of a food is that general class of characteristics other than aroma, color and flavor, which makes up the appearance, mouthfeel and handling properties of foods. The texture profile method uses the A.D. Little flavor profile method as a model. (Brandt, et al; 1963).

2.5.2. Objective evaluation of texture: The objective methods developed by food technologists to evaluate texture are numerous. Although Metzner (1956) has stated that particle size distribution and rheological tests can be used to describe food texture in a scientific and qualitative way, practically every mechanical device available is empirical. Several reviews appear in the literature which classify and describe texture measuring instrumentation, most notably Pearson (1963) and Schultz (1957) - meat tenderness measurement; Elder and Smith (1969) - non-Newtonian and semi-solid foods; Kramer and Twigg (1959) - fruits and vegetables; Szczesniak (1963) - general review; and Bourne (1966), who classified the physical methods of texture evaluation into seven groups.

The seven classifications of Bourne (1966) are:

1. Force measuring
2. Distance measuring
3. Time measuring
4. Energy measuring
5. Ratio measuring
6. Multiple measuring instruments; and
7. Multiple variable instruments.

In fact, most methods fall into the force measuring category. There is considerable overlap between the instrumentation and, if anything, Bourne's review only helps to emphasize the empirical approach which exists.

The rheological property which is measured to indicate texture of liquid foods is viscosity - either "true" viscosity for Newtonian fluids or an "apparent" viscosity for non-Newtonian fluids. An apparent viscosity is frequently referred to as "consistency" by food technologists. There are many viscosity measuring instruments available including capillary viscometers, the Bostwick consistometer, the Scott viscometer, the Brabender visco-amylograph, Corn Industries viscometer, Bloom gelometer, the Brookfield, Fann V-G and Rotovisco viscometers. Nearly all of these methods are discussed by Elder and Smith (1969).

The fact that texture is a useful guide to maturity or ripeness of fruits and vegetables has led many people to develop methods for mechanically evaluating the quality of fruits. Over forty years ago, Magness and Taylor (1925) developed a probe pressure tester, which is still widely used today. The force necessary for the plunger to penetrate a given depth into a fruit or vegetable is used as an index of maturity. Martin (1937) developed a tenderometer which proved extremely successful in predicting raw pea quality. Pea samples are compressed and sheared when an upper hinged set of grids engages with a similar stationary bottom set. An instrument which also applies a combination of compression and shear forces is the Kramer shear press (Kramer et al., 1951 and Kramer, 1961), an apparatus which allows the use of a number of different test cells, depending on the product being tested. The force recorded to penetrate the product is used as an index of quality. Penetrometers, such as the Bloom gelometer, indicate the consistency of gels or soft foods e.g. jellies, cheese, bread. A standard weight is allowed to fall onto the product and the resistance to sinking following impact is taken as a guide to consistency (Szczesniak, 1963).

Shearing devices are most frequently utilized in the meat industry (Pearson, 1963; Lowe, 1949; Szczesniak, 1961-64; Deatherage and Garnatz, 1952; Bockian et al., 1958). The most popular instrument is undoubtedly the Warner-Bratzler shear (Bratzler, 1932). A cylindrical meat sample is placed in a triangular hole in the center of a 1/32" thick steel blade. The blade is pulled through parallel plates by a gear system powered by a constant speed motor, and the necessary force is measured. Pearson (1963) reported that the correlation between sensory evaluation and Warner-Bratzler shear forces was about 0.75 on average, and suggests that the disappointing results may be due to the fact that the shear force fails to account for the time-load effect. Presumably this might reflect more accurately the work required in chewing. The Warner-Bratzler shear was compared with the Kramer shear press by Burrill et al. (1962) who did not find any significant difference between both instruments when used on cooked beef. Of interest perhaps was their finding that the Warner-Bratzler shear nearly always gave a higher correlation with sensory evaluation than did the Kramer press. Harrington and Pearson (1962) found a high correlation between shear values and chew counts on meat, as suggested by Lowe (1949). Miyada and Tappel (1956) described a grinding machine which they suggested could predict meat tenderness. However, Bockian et al. (1958) could only find a correlation of the order - 0.6 with taste panel results when working with cooked beef.

Proctor et al. (1955) developed a denture tenderometer at Massachusetts Institute of Technology in an effort to simulate mastication of food in the mouth. The instrument was fitted with a lower (stationary) set of dental plates, while a similar upper set was fitted to allow both vertical and lateral movement. A force-penetration relationship was recorded as the food sample was compressed and allowed to recover. This system was then modified by Friedman et al. (1963) at General Foods Company who developed the texturometer, while the General Foods Texture Profile was simultaneously developed (Brandt et al., 1963). The basic change from the M.I.T. denture tenderometer was the replacement of the dentures by a plunger and plate. The force-distance diagram which resulted allowed the measurement of a number of texture parameters as follows (see Figure 2-2):

$$\text{Hardness} = L_1$$

$$\text{Adhesiveness} = A_3$$

$$\text{Cohesiveness} = A_2/A_1$$

$$\text{Elasticity} = 68.5\text{-}B$$

$$\text{Chewiness} = L_1 \times (A_2/A_1) \times (68.5\text{-}B)$$

$$\text{Gumminess} = L_1 \times (A_2/A_1)$$

The constant 68.5 was the same measurement B made on a completely inelastic material such as clay.

An exhaustive study to examine the suitability of the General Foods texturometer to describe meat texture was carried out for the U.S.Army Natick Laboratories by General Foods (1965). The Kramer shear press and Warner-Bratzler shear were also used. Foods tested included fresh meat, dehydrated pork, turkey and other meats, and pre-cooked freeze-dried beef with emphasis placed on the latter product. The texturometer was found to be highly suitable for measuring meat texture and gave good correlations with taste panel evaluations. However, it was not possible to select any one of the three instruments as being superior, and all three instruments were able to differentiate between the important sample (muscle, animal) and processing (cooking time) variables incorporated into the design. Although General Foods recommended that their Texturometer and Kramer shear press be used for future research on meat texture, they offered little substantiating evidence to justify neglecting the Warner-Bratzler shear.

The tenderometer approach was once again modified by Bourne (1968) for adaption onto the Instron testing machine, which basically is a constant strain rate (vertical motion) apparatus. Borne points out that with the Instron, the horizontal measurements are exact measurements of penetration - in contrast to the General Foods Texturometer, which has a rotating motion. The following texture parameters can be evaluated on the Instron (Figure 2-3):

$$\text{Hardness} = L_1$$

$$\text{Elasticity} = B_2$$

$$\text{Cohesiveness} = A_2/A_1$$

$$\text{Chewiness} = L_1 \times B_2 \times (A_2/A_1)$$

$$\text{Gumminess} = L_1 \times (A_2 \times A_1)$$

Figure 2-3 illustrates a typical response on the Instron Testing Machine for pre-cooked freeze-dried beef found by Reidy and Heldman (1970), using

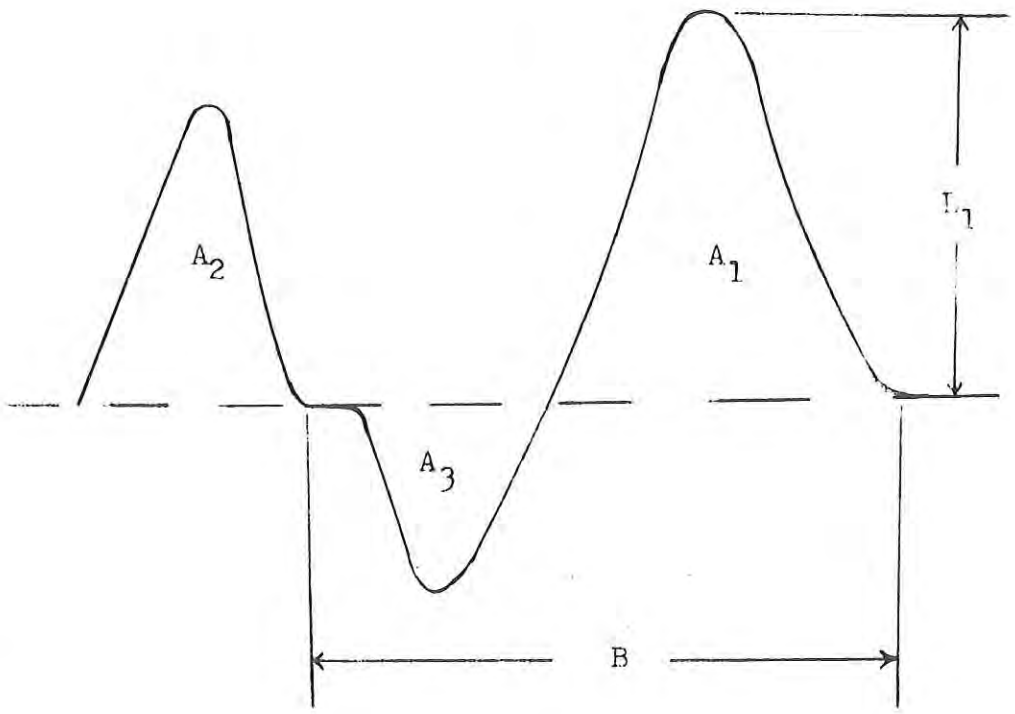

Figure 2-2. Typical Texturometer curve (Friedman et al., 1963).

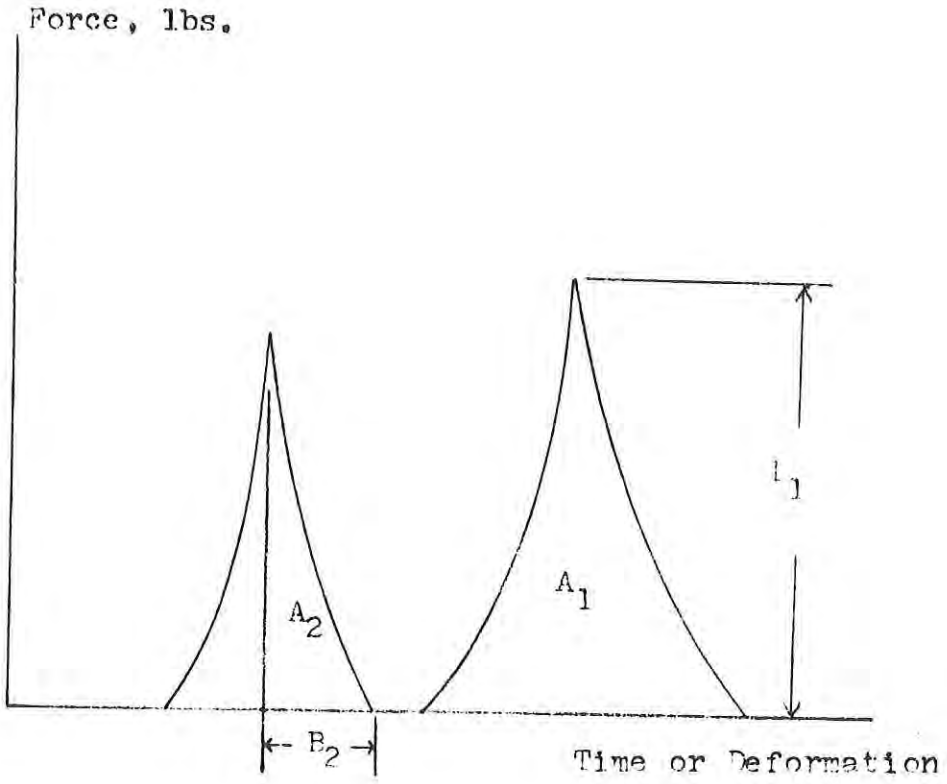

Figure 2-3. Typical force-deformation response for pre-cooked freeze-dried beef from Instron Testing Machine (Reidy and Heldman, 1970).

Bourne's (1968) approach. Reidy and Heldman (1970) investigated the influence of freeze-dried beef, and found that product texture, as indicated by hardness and chewiness values defined above, was least desirable at water activities of 0.4 to 0.6 and with product freeze-dried at a plate temperature of 105°F.

Previous investigations into texture of pre-cooked freeze-dried beef were carried out by Kapsalis (1967) and U.S. Army Natick Laboratories (1965). The objective of the latter research was to examine the suitability of the Texturometer, Kramer Press and Warner-Bratzler Tenderometer for meat texture measurement, as previously stated, and did not examine the influence of water activity on product texture as did Kapsalis (1967). Kapsalis (1967) used an instrument called a Masticometer, developed in Sweden, which in fact was a further modification of the Texturometer and gave a response similar to those obtained by the Instron (Figure 2-2) and Texturometer (Figure 2-1). Dehydrated foods tested included pre-cooked beef and chicken, as well as sandwiches of cheese, chicken and beef. Kapsalis (1967) found that hardness values increased to a maximum at an equilibrium relative humidity of 66% and decreased at relative humidities greater than that. However, since samples had been stored for up to five and a half months, it is possible that texture changes were emphasized due to storage effects.

2.5.3. Engineering properties of food: On the engineering side, agricultural products have received considerable attention in recent years with regard to their mechanical strength and this may be due to the increasing demand for mechanical harvesters. Certainly the majority of papers publishing data on physical properties of foods make no mention of texture but frequent references to "harvesting machinery", "processing equipment" and "damage by bruising" can be found. The terminology used e.g. "apparent Youngs Modulus" also suggests that the intended application of this data is mostly in machine development. However, Mohsenin et al. (1963) do suggest that loading and unloading curves of fruits and vegetables under compression can reveal certain mechanical properties which "should be of importance in evaluating textural characteristics". They further demonstrated from the relationship between modulus of elasticity and stage of maturation of apples that a greater rate of change and more consistent data can be obtained if measurements can be defined in engineering terms.

Researchers apparently soon realized that the mechanical behavior of biological systems is complicated, and concluded that simple mechanical tests which are easily interpreted would be most meaningful (Finney, 1963). Consequently the literature is composed mainly of simple tension and compression tests to give some idea of mechanical strength, and creep and relaxation tests to indicate behavior with time. Morrow and Mohsenin (1966) reviewed the experimental methods applied to agricultural products to determine parameters. They noted that the fundamental assumption of homogeneity, isotropy and continuity are violated in such tests but recommended that violations could be disregarded by adopting a "black-box" approach i.e. merely examining inputs and outputs. Therefore "apparent" rather than actual parameters could be used.

Although McClelland and Spielrein (1957) treated plants as simple supported beams and concluded that the biological materials tested obeyed the established laws of mechanical behavior, the results of Huff (1967) seem to verify the complexity of biological materials. Huff (1967) investigated the behavior of

potato tubers when tested in tension and computed mean values of four mechanical properties. Estimations of tensile strength, strain at failure, failure modulus and unit strain engergy at failure varied with the location in the tuber from which the specimens were taken, and with length of storage. Properties further varied with strain rate, demonstrating viscoelastic behavior. Potato firmness was also measured by Bourne and Mondy (1967) using the Instron Universal Testing Machine. Standard cylindrical samples and whole potatoes were deformed using a metal punch, and the results compared with sensory panel ratings. A correlation coefficient of 0.8 was found. Earlier interest in mechanical properties of potatoes had been shown by Hansen (1952) who measured the resistance of potatoes to pressure, abrasion and impact loading. The necessary pressure to force a piston a certain depth into the tuber was indicative of resistance to pressure; the torque or energy required for removing the skin indicated abrasion resistance; and a measurement of the depth of bruised tissue resulting from impact by a falling steel ball showed how well the potato could withstand brusing damage.

The simple pressure method of Magness and Taylor (1925) for determining fruit maturity already described may possibly be replaced by a sophisticated sonic technique developed by Abbott, et al (1968). By vibrating cylindrical sections of fruits and vegetables at their natural frequencies internal friction coefficients and Young's Modulus could be determined. Of more interest is their finding that as a fruit gradually ripens, the "stiffness coefficient" (measured by applying sonic energy to the whole fruit) decreased. Mohsenin and Gohlich (1962) determined yield points for apples by applying strains at various rates of loading. They suggested also that the force-deformation relationship was approximately linear. The effect of different chemical solutions on the apparent Young's Modulus of apples, pears and potatoes was demonstrated by Somers (1965). Somers (1965) also did stress relaxation tests and showed how the time for 20% relaxation differed with the chemical treatment. Creep and relaxation tests were performed on McIntosh apples by Morrow and Mohsenin (1966), who simulated the stress-strain response to that of a simple three element model - an elastic spring and Maxwell element arrangement in parallel. Morrow and Mohsenin (1966) point out that the elastic relaxation modulus will not equal the inverse of the elastic creep compliance obtained by instaneous load application because instantaneous loading and deformation do not truly take place.

Other foods which have been investigated for rheological behavior include marshmallow, carmel and chocolate, cottonseed, butter and grans. Bourne (1967) applied single compression loading to marshmallows. The response obtained could be simulated by a model of several springs of varying heights with different values of Hooke's constant arranged in parallel between two flat plates. The effect of chemical composition of caramels and chocolate on mechanical behavior was demonstrated by Morrow (1969). Samples were subjected to bending and uniaxial compression. The response of butter to static and dynamic testing was investigated by Diener and Heldman (1968). For stresses below the yield point, a model consisting of parallel viscous and Maxwell elements in series with parallel viscous and plastic elements simulated the stress-strain relationship. Clark, et al (1968) performed cyclic stress and cyclic strain tests on cottonseed and fitted an equation to the experimental data. They also derived entities called "Loss Coefficient" and "Quality Factor" which had been discussed by Lazan (1965) as useful properties of non-linear materials. Zoerb (1958) investigated the energy requirements for shearing grains of different moisture content.

The field of biomechanics ie. mechanics applied to biology, has also witnessed much activity in recent years. A fairly complete bibliography on the field, with

references classified according to subject matter, has been presented by Fung (1968). The emphasis to date has centered around simple elongation tests to collect data on yield stresses and stress-strain relationships at different strain rates, as a basis for the design of artificial limbs or sinews to be used for surgical transplants. Results indicate that in general, tissues exhibit non-linear viscoelastic behavior.

3. Theoretical Considerations

In an effort to provide a basis for computations, results and discussion to be presented in this report, theoretical developments utilized will be presented as separate portions. The developments have been initiated in a separate but not unrelated manner. The proposed theory of moisture sorption leads to a new approach to mathematical description of equilibrium isotherms. The approach to prediction of thermodynamic parameters from moisture equilibrium data is unique in many ways. The rheological models for describing dry and intermediate moisture foods is necessary to allow interpretation of product texture in terms of basic product properties.

3.1. Theory of Moisture Sorption in Foods

Several attempts (Smith, 1947; Henderson, 1952; Young and Nelson, 1967; Chung and Pfost, 1967; Strohman and Yoerger, 1967) have been made to develop a predictive model for the sorption of vapors by biological and polymeric materials. However, in terms of well established evaluative criteria for sorption theories (Adamson, 1967), we can safely say that there does not exist in the current literature any generally satisfactory model of water sorption by biological materials. The primary reason for this almost universal inadequacy is that each one of the existing sorption models has emanated from either one of three fundamental concepts none of which is self sufficient as an exclusive theory of sorption. The basic concepts are (a) Polanyi's Adsorption Potential Theory, (b) The Kinetic Concept as exemplified by the B-E-T theory of multimolecular adsorption and its numerous modificatins; and (c) Zsigmondy's "Capillary Condensation" theory.

Although these theories have not succeeded in their individual capacities in producing a generally satisfactory predictive model of moisture sorption by biological materials, thei apparent complementary character indicates, as has been suggested by Kühn (1964), that the funadmental concepts may be successfully integrated into a coordinated and self-contained model of sorption.

As a broad statement of the problem, a generalized model based on the assumption that each of the above theories correctly describes some specific aspect of the problem is proposed. Specifically, in this section, an attempt has been made to construct an isotherm equation for biological materials based primarily on the B-E-T and capillary condensation theories and somewhat indirectly on the potential theory.

This integrated theory will be justified if the porous nature of a given biological material can be considered fundamental to its sorptive behavior. In the light of the best available knowledge in the area of sorption, it is reasonable to consider the adsorption process by biological products as resulting from mono and multi-layer phenomena up to the incidence of hysteresis, the subsequent isotherm progress into the region of hysteresis is attributed to both multi-molecular adsorption as well as capillary condensation on the porous solid.

3.2. Mathematical Description of Equilibrium Isotherms

3.2.1. A physical model of water adsorption by bio-materials: The physical picture advanced here is illustrated in Figure 3-1 which shows an organic tissue in a vaporous atmosphere of water a a specified pressure and temperature. The tissue is visualized as a random network of small pores, the diameter of one of the pores has been magnified for illustrative purposes. The pores are interstices between ill-fitting cellular building blocks which make up the tissue. We assume for our present purposes that these intercellular passage ways can be treated as cylinders

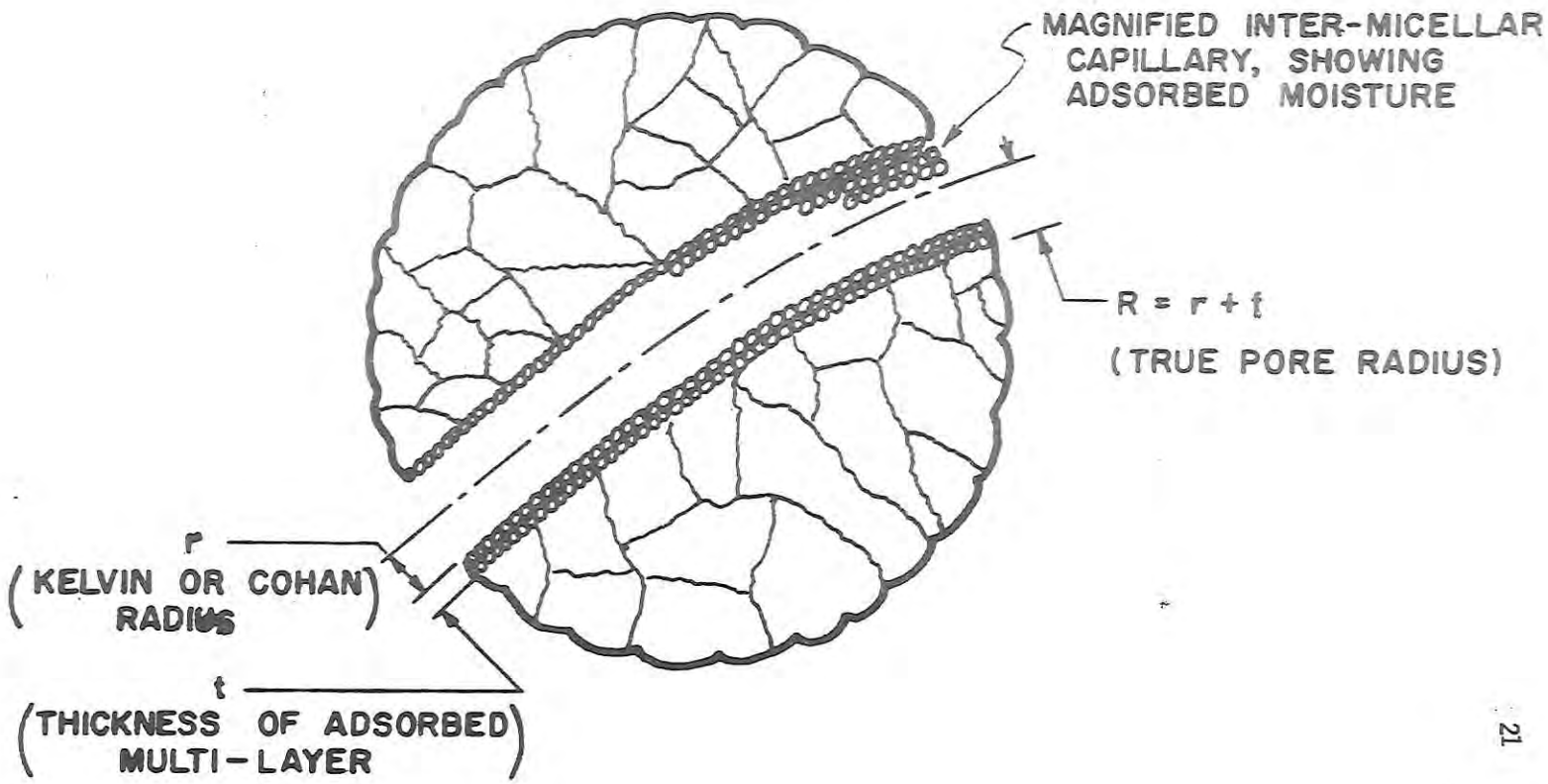

Figure 3.1. Pictorial representation of an organic tissue as a random network of small, irregular pores. The diameter of one pore is magnified for illustrative purposes.

or interconnected spheroidal "ink bottles" (see Figure 3-2) with rough walls in intersecting with other pores.

The sorption of water vapor by the tissue can now be thought of as a process by which the pores are isothermally filled or emptied of water vapor under the influence of surface forces active on the pore walls. While this does not preclude its basic organic or biological nature, the position is taken here that unique modes of behavior such as respiration, and "water active" sites which characterize biological materials in their natural state, exert a tremendous influence on the nature and distribution of surface forces. In consequence, it is logical to assume that the "live processes" find commensurate expression in the energy and entropy configurations associated with the sorptive process.

As a macroporous body, the pore filling process proceeds due to the operation of two mechanisms: (a) molecular adsorption, and (b) capillary condensation. At any stage in the process, its adsorptive capacity is measured by the adsorptively utilizable volume of the constituent pores. The practical objective of the physical model is now to characterize these pores sufficiently in terms of size, and size distribution to make the computation of the aforementioned volume possible.

3.2.2. Pore characterization: In its strictest sense, the term "capillary condensation" is applied to the particular adsorption mechanism described by Lord Kelvin. In this mechanism, the equilibrium vapor pressure of a liquid in a cylindrical capillary is reduced below its saturation value by negative hydrostatic pressure arising from tensile components of curved surfaces of tension of the liquid. The reduction in pressure is related to the radius of curvature of the meniscus by the well known Kelvin equation:

$$r_k = \frac{2\,\sigma\,\overline{V}}{R_g T \ln\,(P_o/P)} \qquad (3\text{-}1)$$

In this form, complete wetting is assumed to occur so that the wetting angle of the sorbate is zero.

Although equation (3-1) is basically descriptive of such microscopic phenomena as capillary rise and depression, Zsigmondy (1911) and later Foster (1932) applied it to the relationships between adsorption and pre size in microporous adsorbents. Their principal assumption was that the adsorbate exists as a condensed liquid in the capillaries of the sorbent and has properties characteristic of the bulk liquid phase. Investigators generally consider that the Kelvin equation can be used with reliability for the calculation of pore size along the desorption path of the isotherm (Flood, 1967, p. 55).

Wheeler (1945) proposed an improved theory which took into account the effects of multi-layer adsorption. Two new assumptions were made. First it was assumed that at any point in the desorption branch of the isotherm, all pores larger than a certain radius R, are covered with adsorbed multi-layer of thickness t, whereas all pores smaller than R are filled by capillary condensation. Secondly, since all unfilled pore walls have an adsorbed layer of thickness t, the radius of the meniscus in a filled pore, where it joins a larger pore, is assumed not to be R, but a smaller radius (R-τ). This means in effect that under conditions of capillary

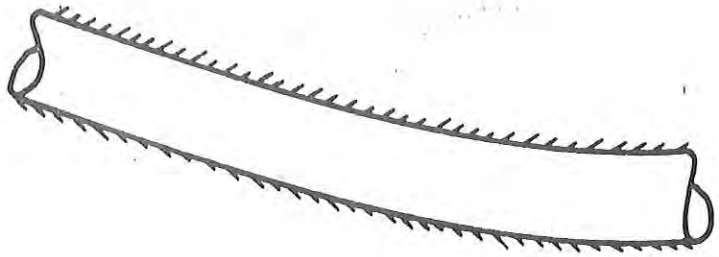

(a)

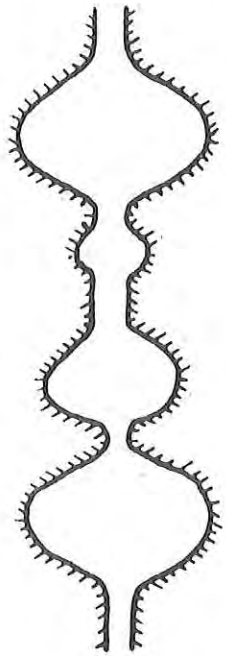

(b)

Figure 3-2. Shapes of capillaries.

(a) Cylindrical capillary

(b) Interconnected spheroidal "Ink Bottles".

adsorption, it is not the pore of the true physical radius, R, which is important, but rather, a pore whose radius has been effectively diminished by the thickness of an adsorbed multi-layer. Wheeler thus argued that the Kelvin equation applied not to the actual pore radius but to the effective radius of the "inside annular tube" (see Figure 3-3a) left after multi-layer adsorption has taken place. The maximum true pore radius, R, which will be filled by both molecular adsorption and capillary condensation at a relative vapor pressure P/P_o is thus given by:

$$R = t + r_k \qquad (3\text{-}2)$$

Because of its Kelvin component, the Wheeler equation (3-2) is applicable only to the desorption branch of the isotherm. However, Cohan (1938) and Coelingh (1939), working independently, concluded that along the adsorption curve, the capillary condensed liquid assumes a cylindrical instead of a hemispherical meniscus (see Figure (3-3b), and showed that for this case, the Kelvin equation is modified to the form:

$$r_c = \frac{\sigma \bar{V}}{R_g T \ln(P_o/P)} \qquad (3\text{-}3)$$

The Wheeler equation can now be generalized to the form:

$$R = r + t \qquad (3\text{-}4)$$

where $r = r_c$ for adsorption; and $r = r_k$ for desorption. With r defined as a function of the variable P/P_o, the thickness t , now needs to be similarly defined in order to complete the characterization of R.

Halsey (1948) employed the concept of cooperative adsorption to refine the B-E-T theory. This concept implies that adsorbate molecules influence each other by horizontal interaction during the adsorption process. He derived the following semi-empirical relation for the adsorbed multi-layer thickness:

$$t(A^\circ) = \tau \left(\frac{Q_{st}}{R_g T \ln(P_o/P)}\right)^{\Omega} \qquad (3\text{-}5)$$

where Q_{st} = isosteric heat of sorption, Ω empirical exponent.

In Figure (3-4), a plot of the Halsey equation (3-5) in the modified form:

$$n = \frac{X}{X_m} = \left(\frac{1.75}{\ln(P/P_o)}\right)^{\frac{1}{2}} \qquad (3\text{-}5a)$$

is superposed on a set of empirical data for several biological materials. If the scatter of the individual points of Figure 3-4 is accepted as within the limits of uncertainty to be expected because of the specific nature biological systems, then t is defined by the Halsey equation in the specialized form:

$$t(A^\circ) = 3.2 \left(\frac{1.75}{\ln(P_o/P)}\right)^{\frac{1}{2}} \qquad (3\text{-}6)$$

where for the water molecule, τ is taken to be roughly equal to the molecular

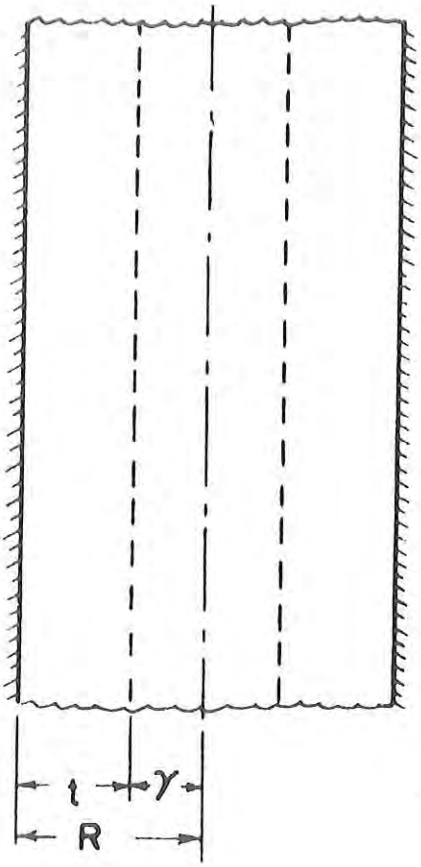

Figure 3-3(a) Cylindrical capillary of radius R, showing the "inside annular tube" r which may be given either by the Cohan or Kelvin equation.

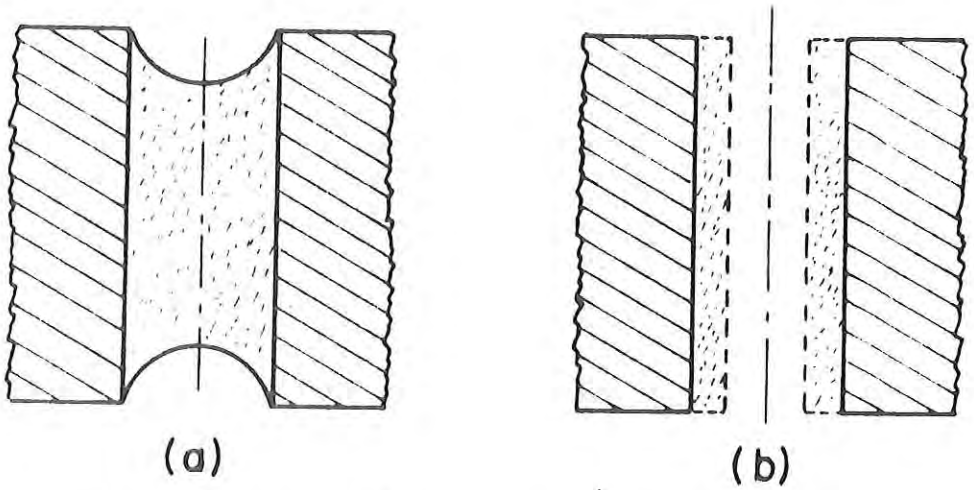

Figure 3-3(b) Capillary menisci: (a) Hemispherical (Kelvin) meniscus. (b) Cylindrical (Cohan) meniscus.

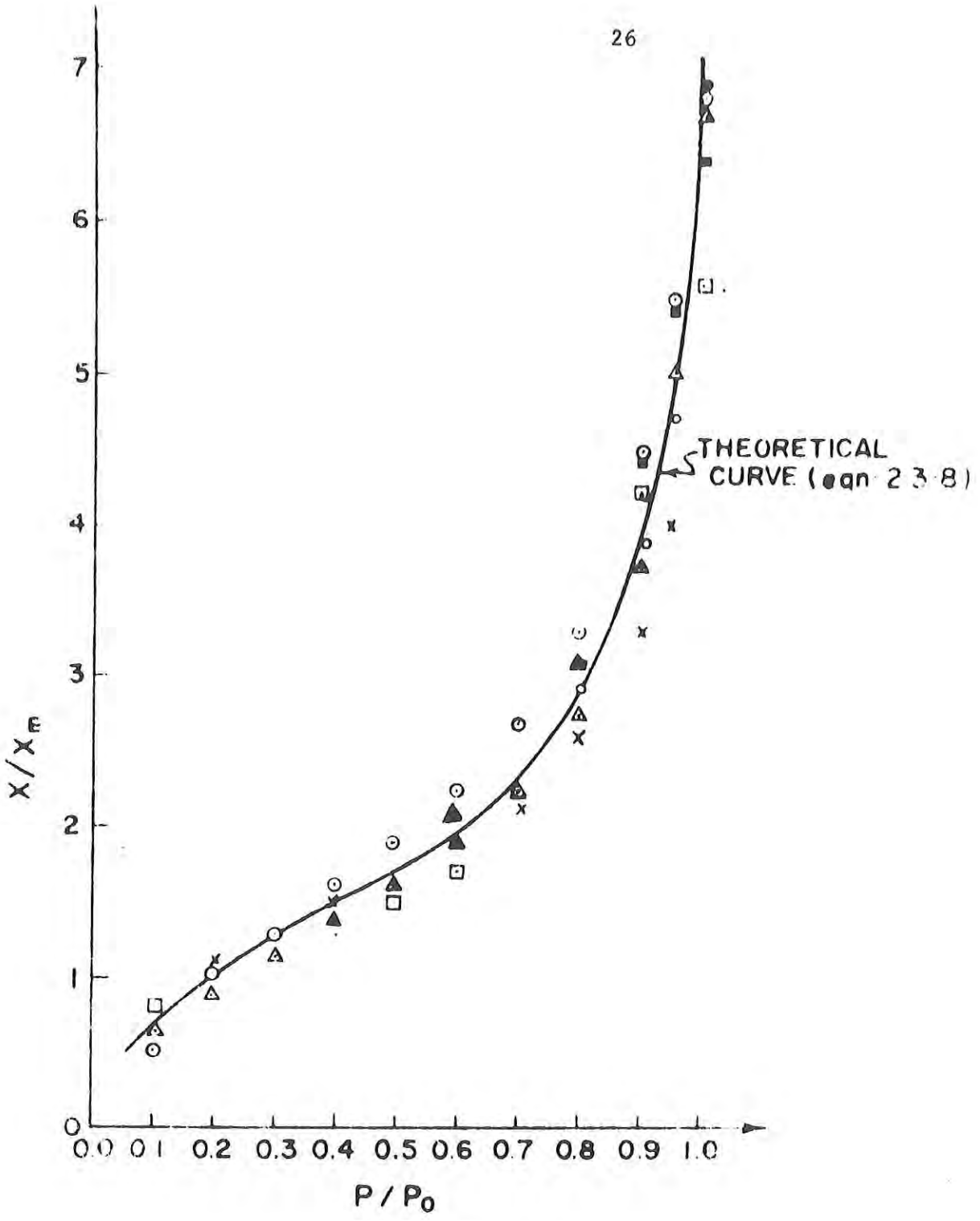

Figure 3-4. Plot of X/X_m against P/P_o.

⊙ wood 20°C isotherm. △, cotton 10°C isotherm. o, cotton 20°C isotherm. ▲, cotton 30°C isotherm. x, corn 4°C isotherm.

⊡, Ground freeze-dried beef 10°C isotherm. ■, ground freeze-dried beef 22.2°C isotherm.

diameter, d, for lack of a better approximation.

Equation(3-6) in a slightly different form was used by Shull (1948); Dollimore and Heal (1964); and Visanathan and Sastri (1967) for the calculation of the adsorbed multi-layer. It is adopted here in preference to the B-E-T 3-parameters equation from which $n = X/X_m$ is derivable, for a number of reasons. It is consistent with the concept of mobile adsorbed film. It has a form convenient for usage in a larger context.

3.2.3. The isotherm equation: With R fully defined as a function of P/P_o, the equation for the adsorption isotherm is developed as follows:

The generalized Wheeler equation (3-4) specifies the P/P_o value at which condensation will occur in a capillary of radius, R. Such condensation will occur on the adsorbed layers of water molecules already covering the concave surfaces of a porous system. If such condensation leads to a significant reduction in the radius of curvature of a concave surface or open ended capillary, condensation will continue (by spontaneous phenomena) on this surface as long as the radius of curvature continues to reduce. In this discussion, a pore is defined as any void region in a porous material which is partially or completely filled by the combined consequence of molecular and capillary adsorbed moisture. Also the pore radius will be considered to mean the radius of curvature of a surface on which the above described filling-process started to occur; this radius is defined by the generalized Wheeler equation 3-4.

If a porous system of organic tissue, has a given distribution of pore radii, one can say that at a specified vapor pressure, pores of radius equal to or less than the value determined by the Wheeler equation(3-4)will be completely filled. That is, if the volume of a pore in a porous system is expressed by the function:

$$v_R = \varphi_1 (R) \tag{3-7}$$

and if the number of pores of radii between R and R + dR is given by:

$$dN(R) = \varphi_2(R)\, dR \tag{3-8}$$

then the volumes of all pores with radii in the domain (R,R + dR) is:

$$dv_R = v_R\, dN(R) = \varphi_1 (R) \times \varphi_2 (R)\, dR \tag{3-9}$$

Thus, the sum of the volumes of all pores whose radii are equal to or less than R is given by the integral:

$$V_a = \int_{R_m}^{R} [\varphi_1 (R) \times \varphi_2 (R)]\, dR \tag{3-10}$$

where R_m, the lower limit of integration is used in recognition of the so-called "molecular sieves" effect which assumes that adsorbed molecules in the first approximation, cannot penetrate into pores smaller than their own diameter.

Equation(3-10) is an integral isotherm equation defining the adsorptive volume of the porous adsorbent. In order to solve this integral equation explicitly, it is necessary to obtain explicit analytic functions for (a) the pore geometry, $\varphi_1(R)$ and (b) the pore-size distribution, $\varphi_2(R)$. de Boer (1958) has shown that a wide variety of geometric models are possible. However, only two broad classes of these geometric shapes are consistent with the assumptions of the present development - these geometric forms are:

(i) The Cylindrical type pore model for which:

$$\varphi_1(R) = \pi L(R) R^2 \qquad (3\text{-}11)$$

where L(R) = variable length of pore.

(ii) The Interconnected Spheroidal "Ink Bottle", pore model for which:

$$\varphi_1(R) \quad \frac{4}{3} \pi R^3 \qquad (3\text{-}12)$$

Wheeler (1945) suggested and Shull (1948) demonstrated that pore size distributions of porous sorbents may be represented by simple analytical relationships of:

(i) The Maxwellian type for which:

$$\varphi_2(R) = A \frac{R}{R_o} \exp\left[- R/R_o\right] \qquad (3\text{-}13)$$

(ii) The Gaussian type for which:

$$\varphi_2(R) = A \exp\left[- \beta^2 \left(\frac{R}{R_o} - 1\right)^2\right] \qquad (3\text{-}14)$$

Gregg and Sing (1967) have further suggested the possible utilization of:

(iii) The Log-Normal distribution for which:

$$\varphi_2(R) = A \exp\left[- \beta^2 \left(\ln R/R_o - 1\right)^2\right] \qquad (3\text{-}15)$$

No closed form solution to equation (3-10) is possible when any one of the above analytical functions is used to define $\varphi_2(R)$, the worst of them is mathematically intractable, the best leads to unwieldy end results. In the attempt to overcome this difficulty, Foster (1948) and Kühn (1964) have recommended:

$$\varphi_2(R) = K_1 R^{\gamma} \qquad (3\text{-}16)$$

where the symbol γ is an exponent dependent on the product. Equation (3-13) is essentially of an exponential character, and for the most simple cases, it reduces to a simple power function in which γ can assume constant numerical

values, being positive or negative, integral or fractional.

A detailed computation of the pore-size distribution of several biological materials was done by Ngoddy (1969) using a modified Cranston and Inkley (1957) scheme. The results show that if the spheroidal "ink bottle" geometric model is assumed, $\varphi_2(R)$, as defined in equation (3-8) is well described by the power law equation (3-13).

Combining the "ink bottle" pore geometry with the power function distribution of pore radii in equation (3-10) yields:

$$V_a = \frac{4}{3} \pi K_1 \int_{R_m}^{R} R^{3=\gamma} \, dR \tag{3-17}$$

Equation (3-14) integrates to:

$$V_a = \frac{\xi}{\eta} (R^{\eta'} - R_m^{\eta'}) \tag{3-18}$$

where

$$\xi = \frac{4}{3} \pi K_1 \tag{3-19}$$

and

$$\eta' = 4 + \gamma \tag{3-20}$$

Equation (3-18) is simplified geometric expression of the adsorptively utilizable volume of a porous adsorbent. The exponent η can have positive or negative, integral or fractional values.

Substitution of the generalized Wheeler equation (3-4) into equation (3-18) and using the Cohan equation (3-3) together with the specialized Halsey equation (3-6) yields:

$$V_a = \frac{\xi}{\eta'} \left\{ \left[3.2 \left(\frac{1.75}{\ln P_o/P} \right)^{\frac{1}{2}} + \frac{\sigma \bar{V}}{R_g T \ln(P_o/P_m)} \right]^{\eta'} - \left[3.2 \left(\frac{1.75}{\ln P_o/P} \right)^{\frac{1}{2}} + \frac{\sigma \bar{V}}{R_g T \ln (P_o/P_m)} \right]^{\eta'} \right\} \tag{3-21}$$

where P_m is the vapor pressure corresponding to the adsorbed monolayer or point "B" of the isotherm.

Equation (3-21) is an isotherm equation relating the specific adsorbed volume of the adsorbent, V_a, with relative vapor pressure. It shows strange deviations from experience in that it gives zero adsorption, $V_a = 0$, at $P = P_m$, and negative values of V_a at pressure, $P < P_m$. This means that isotherms

calculated with equation (3-21) must start not at $P/P_o = 0$, but at a low relative vapor pressure $P_m/P_o > 0$. This irregularity stems from the fact that the choice of the lower limit of integration, R_m, in equation (3-10) while conforming with the specifications of the "molecular sieves" effect, overlooks the contribution to V_a due to the partial filling of the first mono-layer in the vapor pressure range $0 \leq P \leq P_m$. Yet, the choice of R_m is substantiated in the now accepted agrument (Wheeler, 1945) that the Kelvin or Cohan radius is inapplicable in the low pressure range $0 \leq P < P_m$. In order to correct for this irregularity, a shift of the reference axes of the isotherm plot was performed, thereby reducing equation (3-21) to the form:

$$V_a = \frac{\xi}{\eta'}(Z^{\eta'} - \lambda^{\eta'}) \qquad (3\text{-}22)$$

where

$$Z = 3.2 \left(\frac{1.75}{\ln \chi_1}\right)^{\frac{1}{2}} + \frac{\sigma \bar{V}}{R_g T \ln \chi_1} \qquad (3\text{-}23)$$

$$\lambda = 3.2 \left(\frac{1.75}{\ln \chi_2}\right)^{\frac{1}{2}} + \frac{\sigma \bar{V}}{R_g T \ln \chi_2} \qquad (3\text{-}24)$$

$$\chi_1 = (P_o + P_m)/(P + P_m) \qquad (3\text{-}25)$$

$$\chi_2 = (P_o + P_m)\, P_m \qquad (3\text{-}26)$$

Equation (3-22) is a volumetric isotherm equation defining the specific adsorbed volume due to molecular and capillary phenomena within the intermicellular capillaries of the tissue. It is reducible to its gravimetric equivalent by a process which converts the specific adsorbed volume to specific adsorbed mass. This can be accomplished by introducing the appropriate density term into equation (3-22) to obtain the terminal relation:

$$M_a = \rho \frac{\xi}{\eta'} (Z^{\eta'} - \lambda^{\eta'}) \qquad (3\text{-}27)$$

where, in view of the demonstrated variable compressibility of the adsorbed water "film" (Katz, 1933); Stamm and Seborg, 1935; and Stamm, 1938), ξ is an undefined function which is dependent on the magnitude of the intermolecular forces, the surface-impressed pressure and possibly the isotherm temperature. Polanyi's Adsorption Potential theory describes the adsorbed multi-layer as resembling the atmosphere of a planet with the highest compression at the surface of the solid and the density falling off outwards. Babbitt (1942) insists that any theory of adsorption must account for this adsorption compression. Stamm and Seborg (1935) demonstrated that actual adsorption compression values can be obtained, and that adsorption compression extends to the fiber saturation point. A density function for the adsorbed water film reflecting these points of view was derived by Ngoddy (1969). The function is of the semi-theoretical form:

$$\frac{\rho}{\rho_o} \mu^* \left(\frac{Q_{st}}{Q_{st^o}} \right) \qquad (3\text{-}28)$$

(3-28)

where the determinitive function, μ^*, is defined for a class of biological materials of interest p_o and Q^o_{st} are the saturation values of sorbate density and isosteric heat of sorption respectively.

3.3 Simulation of Heat Sinks in Microcalorimetry

This study attempted to numerically model a cross section of a cylindrical Individual cylindrical cavities for the reaction and comparison cells were included. The effectiveness of the sink was determined by computing the relative error in the temperature measurements. That is the temperature measurements from the simulated real system were compared with measurements from a reaction vessel enclosed in an absolutely constant environment. With this model it is possible to compare the effectiveness of various sink designs.

3.3.1. Selection of a numerical method: A numer of numerical methods have been suggested for the solution of the transient heat conduction equation. These methods are classified as either implicit or explicit methods. Several implicit methods were considered but rejected because of the large amount of computer time required for their solution and the difficulty of programming them in three dimensions. Although a two-dimensional model was to be developed it was considered advisable to select a numerical technique and a grid system that could be easily generalized to include the third dimension should this be found to be necessary.

Three explicit methods were considered for the model. The forward difference technique was considered because it is the most commonly used explicit method. The stability of the forward difference technique is dependent on the size of the time and space increments. This technique could not be employed in the model of the heat sink because the space increment must be varied to account for the unusual configurations. This would cause instability for any reasonable time step.

In 1957 Saul'ev suggested a new explicit technique. Allada and Quon (1966) compared an extension of the technique suggested by Saul'ev with some other numerical methods. Their method, the alternating-direction-explicit-procedure, or ADEP, was much faster than any of the implicit techniques. They concluded that the ADEP appears to combine the computational ease of explicit with the stability of implicit methods.

Barakat and Clark (1966) compared another extension of a Saul'ev method with various numerical techniques. The extension reported by these authors utilizes the same molecule equation as the Allada-Quo extension, but solves the equation twice at each node for each time step. First, the equation is solved for each node beginning at one corner of the object being thermally modeled and progressing to the opposite corner. Second, the equation is resolved proceeding through the array of nodes in the opposite direction. Barakat and Clark claimed that a more accurate model was obtained by averaging these two solutions for each time step. Their technique required twice the computer time of the technique proposed by Allada and Quon. Barakat and Clark also employed

the von Neumann method for stability analysis which is described by Richtmyer (1957) to show that either of the extensions of the Saul'ev method are unconditionally stable.

The Saul'ev technique was selected for the numerical model of the heat sink. The model was written so that either the Allada-Quon or the Barakat and Clark extensions could be applied.

3.3.2. The grid system: The irregular boundary of the heat sink made the selection of a coordinate system difficult. The selection was based on three criteria. The primary interest is in the temperatures around the cavities. Therefore, the system must accurately model the heat sink in these areas. The ease of programming the boundary conditions in a general way was also important. The purpose of the model is to test a number of different sink designs. Thus, the grid system should be such that the computer can determine the boundary conditions for each node of the system. Finally, it is difficult to guarantee that a computer program actually performs the operation intended. The probability of errors existing in the program can be greatly reduced in the final program is developed from an initial crude but simple model. If the original model is sufficiently simple the errors in it can be removed with reasonable certainty. If the ensuing modification are of modest magnitude, it is possible to maintain a low probability of errors occurring in the program.

For the first crude model a cartesian network was constructed on the cross section of a metallic sink, Figure (3-5). A cell, the smallest area enclosed by the lines in the network, was considered to lie entirely in the sink or entirely outside the sink depending on whether more of its area lay inside or outside of the boundary of the sink. The dashed line in Figure (3-5) illustrates the resulting simulated boundary. The temperature nodes used in the heat transfer calculations were considered to be located at the centroid of each cell. A convective boundary condition was assumed both to the cavity and to the outside of the sink. Since none of the nodes were located on the boundary, the temperature at the wall was not known. Therefore, it was necessary to write two simultaneous equations, one for the convective boundary condition and one for conduction from the wall of the sink to the nearest node. These two equations were then solved to give a multiplicative constant of heat transfer between the node and the ambient given by:

$$c_5 = \frac{hA}{hD + k} \quad [cm] \tag{3-29}$$

such that

$$q = kc_5 \ (T_\infty - T_{i,j}) \ [cal/sec] \tag{3-30}$$

where:

A is the boundary area, cm^2
D is the distance from the node to the surface, cm.
h is the conductive heat transfer coefficient, $cal/°C\text{-}cm^2$

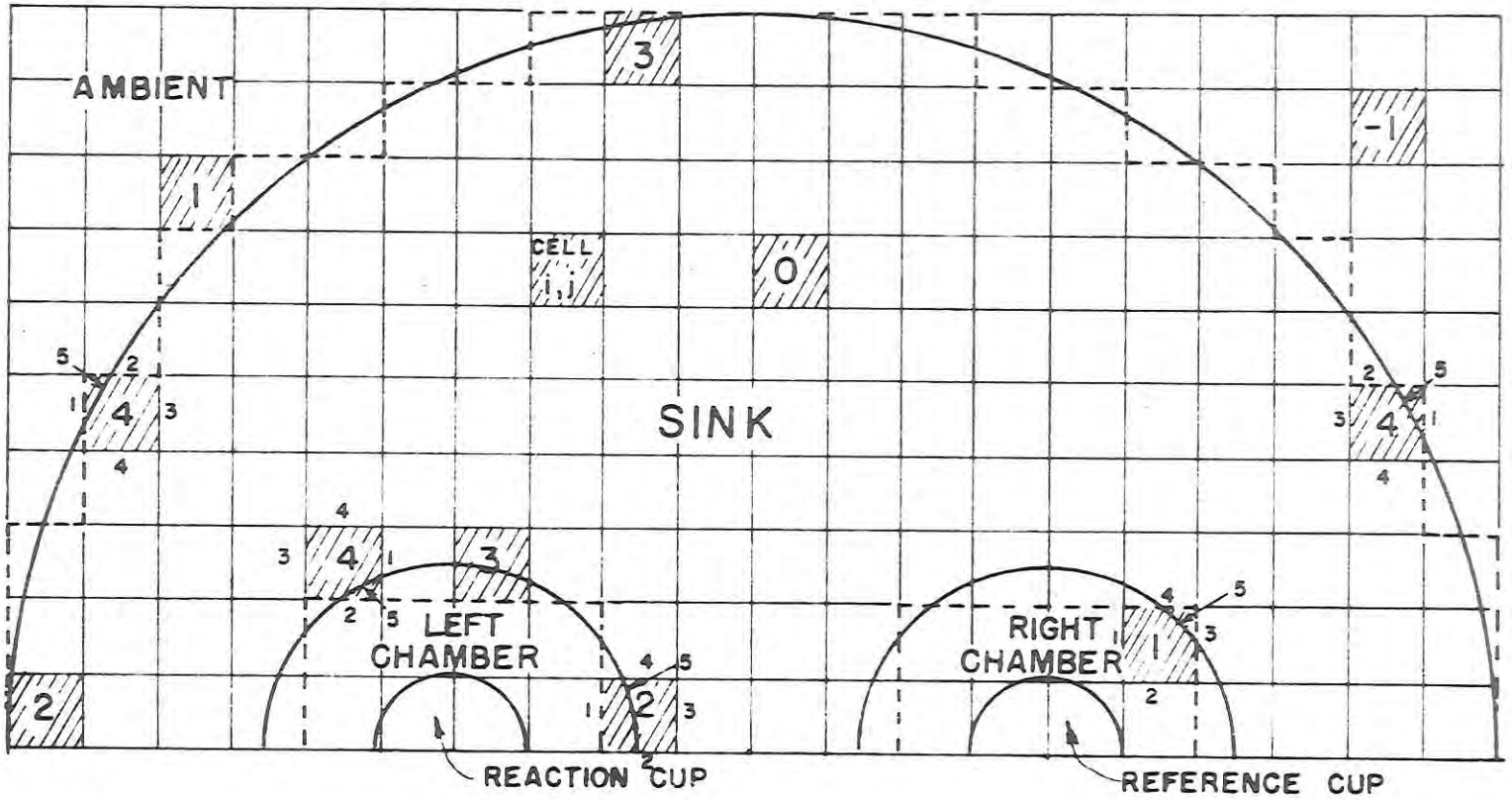

Figure 3-5. The grid system for the model of the sink.

k is the thermal conductivity of the sink, cal/°C-cm-sec
q is the rate of heat transfer, cal/sec
T_∞ is the ambient temperature, °C.

$T_{i,j}$ is the temperature of the node in the cell of interest. These equations were appropriately employed in the Saul'ev model.

The model of the sink was refined to improve the approximation at the boundary. In the refined model the size and shape of each cell lying on the boundary of the sink was modified. For programming purposes each cell was recognized as having one of six possible relationships with respect to the boundary of the sink. In Figure (3-5) the integers 1 through 4 have been assigned to cells representing each of the six types. Notice that any given type may be located in any quadrant of the external or internal boundaries of the sink. Thus once the thermal relationships for a cell are known in one quadrant they can be immediately inferred for another quadrant merely by judiciously changing the numbering of the sides of the cell.

For the mathematical model the boundary of the sink was replaced in each cell by a straight line. The straight line intersected the border of the cell at the same location as did the boundary of the sink. The numerical value of the cell's volume, the areas for heat transfer to other cells, and to the ambient, and the distance from the temperature node in this cell to the adjacent temperature nodes and to the boundary were all adjusted. The temperature node for each cell that was intersected by the boundary was assumed to lie at the centroid of the remainder of the cell. The derivation of the mathematical relationship for these adjustments and the resulting computer model are listed in the appendix of the thesis by Thompson (1970).

Adjustments must also be made to the distance and area for heat transfer of cells adjacent to the ones intersected by the boundaries. In final form the computer program would accept information on the thermal characteristics, the heat transfer values, the radii of the sink and chambers, the location of the chambers and the function describing the heat produced by the reaction. The model would then determine the necessary boundary conditions, computes the temperatures of the reaction and comparison cells and finds the temperature distribution in the sink for each time step. The model also computes the temperature of a reaction vessel in an absolutely constant thermal environment and prints out the relative error at given time intervals.

3.3.3. Tests of the model: The accuracy of the model was tested with several techniques. The computation of the boundary conditions by the model was checked with hand calculations on the various cell types. The application of the Saul'ev method and the stability of the techniques were checked by printing out the entire array of temperatures for each time step. It was thus possible to see if the technique was being correctly applied to every node.

The ability of the model to accurately predict transient thermal behavior in the sink was also observed. The size of the cavity and the reaction heat were both reduced to zero. The initial temperature of the sink was then set to a numerical value of one and the ambient temperature was established at zero.

The transient temperature was predicted by the model at various locations agreed with the curves published by Boelter et al. (1942).

Although Saul'ev technique has been shown by Barakat and Clark (1966) to by unconditionally stable large oscillations were observed. For large time steps and small cell sizes the coefficient in front of the temperature of the node of interest at the previous time becomes negative. Physically this is a violation of the second law of thermodynamics and can cause damped oscillations. In a rectangular object this condition will rarely occur. However, in the irregular shaped heat sink some boundaries cells are extremely small. Large time steps caused these cells to introduce large oscillations which spread through the entire model.

Two adjustments were made to decrease the probability of the occurrence of these oscillations. The size of the boundary cells was limited to a triangular cell with side lengths at least 1% of a regular cell's dimensions. Also the heat transfer from the ambient was always employed at the future time. Even with these adjustments it was still necessary to limit the size of the time step. The maximum time step that did not produce oscillations was found experimentally to be:

$$\Delta t_s = \frac{(\Delta x)^2}{10\ \alpha} \qquad (3\text{-}31)$$

where

Δt_s is the time step, sec.
Δx is the distance between nodes, cm.
α is the thermal diffusivity, cm^2/sec.

The maximum cell size that could be employed without introducing errors due to the boundary approximation was investigated. It was found that the distance between nodes should not be greater than 1/4 of a chamber diameter. Increasing the distance between the nodes from 20 to 40% of a chamber diameter caused the predicted relative error to increase 15%. Decreasing the distance between nodes below 25% of a chamber diameter did not change the predicted relative error.

The Allada-Quon technique was compared with the Barakat-Clark method. The results obtained from each were nearly the same; therefore, the Allada-Quon procedure was adopted to reduce the necessary computer time.

3.4. Thermodynamics of Moisture Sorption in Foods

Adamson (1967) stated that it is not necessary phenomenologically to state whether the process is adsorption, absorption or solution; the same thermodynamic relations could be applied for all the cases. In general, the thermodynamic processes to be considered are of two general types: integral and differential.

1. Integral Processes. For adsorbent (Z_1) and adsorbate (Z_2) the following general equation can be written:

$n_s\ Z_1$ (adsorbent at T°K) + $n_w\ Z_2$ (adsorbate liquid at pressure P and temperature T°K)

$\longrightarrow$ (system comprising of n_s Z_1 and n_w Z_2) (3-32)

This process represents the adsorption of n_w moles of water (Z_2) initially in liquid, upon n_s moles of Z_1 (adsorbent).

2. Differential processes. n_w Z_2 (liquid) $\rightleftharpoons$ n_w Z_1 (adsorbed on Z_1 n'_w/n_s constant) (3-33)

Equation (3-33) represents an adsorption of n_w moles of liquid adsorbate, on the infinitely large amount of Z_1 (adsorbent) which already hold n'_w moles of adsorbent. The mole ratio n'_w/n_s increases only infinitesimally.

3.4.1. Thermodynamics of adsorbate. The major portion of the thermodynamic treatment of the moisture sorption phenomena has been devoted to adsorbate (water vapor). In most cases partial free energy, enthalpy and entropy values are reported as cal/g water or cal/g mole of water.

Calculation of partial heats of sorption $\overline{\Delta H_w}$ is conveniently carried out by using the Clausius-Clapeyron equation (Kapsalis, 1967).

$$\text{Ln } P = \frac{\overline{\Delta H_T}}{MW_w \cdot R_g} \cdot \frac{1}{T} + K \qquad (3\text{-}34)$$

where P -- partial vapor pressure of water at temperature T,

T -- absolute temperature

R_g -- Universal gas constant

K -- constant of integration

MW_w -- molecular weight of water

In practice, the isosteric values ofequilibrium vapor pressure (P) on a log scale are plotted against 1/T on a linear scale. The slope of any isoster is given by $\frac{\overline{\Delta H_T}}{2.303 \; R_g \; (MW_w)}$. The $\overline{\Delta H_T}$ obtained from the slope of an isoster is the sum of the enthalpy of sorption $\overline{\Delta H_w}$ and the latent heat of vaporization or condensation (L). The $\overline{\Delta H_w}$ enthalpy of sorption is also the differential heat of wetting and is obtained by subtracting latent heat of vaporization (L) from the $\overline{\Delta H_T}$ value.

Davis and McLaren (1948) and Dole and McLaren (1947) gave the following relation to calculate the integral heat change:

$$\Delta H = \frac{R_g \; T_1 \; T_2}{T_2 - T_1} \int_o^{n_w} \text{Ln} \; \frac{X_1}{X_2} \; dn \qquad (3 - 35)$$

where X_2 is relative vapor pressure (P/Po) at the higher temperature (T_2) which produces the same number of moles of water sorption as at lower temperature (T_1) for which X_1 applies and n_w is the moles of water per 100 g of dry substance.

Partial molar free energy for water vapor (adsorbate) is calculated by using the following relation (Kapsalis, 1967):

$$\tilde{\Delta} G_w = \frac{\tilde{dG}}{dn} = R_g T \text{ Ln } X = R_g T \text{ Ln } \frac{P}{Po} \qquad (3\text{-}36)$$

The integral free energy change for water vapor accompanying the sorption process was calculated by using the following equation:

$$\Delta G_w = - R_g T \int_o^1 n_w \, d \text{ Ln } \frac{P}{Po} \qquad (3\text{-}37)$$

where n_w is the number of moles of water sorbed per 100 g of dry substances. The integration of the right hand side of the above equation is commonly carried out by parts as follows:

$$\int_o^1 n_w \, d \text{ Ln } \left(\frac{P}{Po}\right) = \int_o^1 n_w \, \frac{P}{Po} \, d \left(\frac{P}{Po}\right) \qquad (3\text{-}38)$$

In this process P/Po is considered as an independent variable. In practice, a plot of $n_w \frac{P}{Po}$ vs P/Po is made and the total area under the curve multiplied by RT gives the integral free energy ΔG_w.

Calculation of corresponding entropy changes for water vapor (adsorbate) is carried out by using the following relations:

$$\tilde{\Delta} S_w = \frac{(\Delta H_w - \tilde{\Delta} G_w)}{T} \qquad (3\text{-}39)$$

$$\Delta S_w \quad \frac{(\Delta H_w - \Delta G_w)}{T} \qquad (3\text{-}40)$$

3.4.2. Thermodynamics of adsorbent. Adamson (1967) pointed out that the bulk of thermodynamic treatment of sorption phenomena was focused primarily on the contribution of adsorbate and very little emphasis was placed on adsorbent. The Gibbs-Duhem equation (1875) permits the calculations of the energy contribution of adsorbent from the knowledge of its composition.

Gibbs-Duhem equation. -- Houghen et al. (1962) stated that

> the Gibbs-Duhem equations are rigorous thermodynamic relations that are valid for conditions at constant temperature and pressure. They are of particular value in minimizing the number of experimental data necessary to evaluate the properties of a system and for detection of inconsistent and erroneous measurements.

The general form of the Gibbs-Duhem equation can be written as for a constant temperature and pressure:

$$n_1 \, d\mu_1 + n_2 \, d\mu_2 = 0$$

where n_1 and n_2 are moles of substances 1 and 2, μ_1 and μ_2 are chemical potentials or partial properties. The standard states or reference states are substances described by μ°_1 and μ°_2.

Thus

$$\mu_1 = \mu^\circ_1 + R_g T \, \text{Ln} \, a_1 \qquad (3\text{-}42)$$

$$\mu_2 = \mu^\circ_2 + R_g T \text{Ln} \, a_2 \qquad (3\text{-}43)$$

where a_1 and a_2 are the activities of substances 1 and 2.

The derivation of the Gibbs-Duhem equation is given in several textbooks of chemical thermodynamics (Houghen et al., 1962, page 974). Stitt (1958) reported that the thermodynamic quantities pertaining to the sorption process can be obtained from the temperature dependence of sorption isotherms. At equilibrium the Gibbs chemical potential (partial Gibbs free energy) for water must have the same value throughout the system and furthermore this quantity must be the same in the solid material as in the vapor phase. Copeland and Young (1961) and Wu and Copeland (1961) studied the adsorption isotherms for $BaSO_4$-H_2O system. The thermodynamic analysis of the $BaSO_4$-H_2O system by the above authors revealed that the heats of sorption values computed utilizing the Gibbs-Duhem equation were in good agreement with the similar values obtained by calorimetry on the $BaSO_4$-H_2O system. Copeland and Young (1961) reported that the magnitude of surface forces during sorption of water on $BaSO_4$-H_2O system usually is very small and can be ignored. There seem to be similarities between water sorption in the $BaSO_4$-H_2O system and the sorption of water vapor on various foods. In accordance with the above observations, it was felt that the contribution due to surface forces during water vapor sorption of food products need not be included in this investigation.

With reference to liquid water as a standard state, the change in the partial Gibbs function per g of water for a transfer of an infinitesimal quantity from pure liquid (vapor pressure P) to equilibrate solid with vapor pressure P is given by:

$$\overline{\Delta G_w} = \frac{R_g \, T}{MW_w} \, \text{Ln} \, \frac{P}{Po} \qquad (3\text{-}44)$$

which is similar to equation (3-36).

The corresponding free energy change per g of solids (dry material as standard state) can be found by application of the Gibbs-Duhem equation:

$$N_w \, d\left(\overline{\Delta G_w}\right) + N_s \, d\left(\overline{\Delta G_s}\right) = 0 \qquad (3\text{-}45)$$

$$\overline{\Delta G_s} = -\int_o^P \frac{N_w}{N_s} \, d\left(\overline{\Delta G_w}\right) \qquad (3\text{-}46)$$

where N_w is the weight fraction of water.

N_s is the corresponding weight fraction of solids

also $N_w + N_s = 1$.

The overall change in Gibbs function for the entire process of dry sorbent combining with water to form 1 g of material at equilibrium pressure P is given by

$$\overline{\Delta G} = N_w \Delta G_w + N_s \overline{\Delta G_s} \qquad (3\text{-}47)$$

The $\overline{\Delta H_w}$ the change in partial heat function per g of water for the sorption on an infinitesimal quantity from pure liquid to equilibrated material of specific moisture content is obtained by using the equilibrium moisture sorption data at various temperatures. The Clausius-Clapeyron equation can be rewritten in the following form:

$$\left[\frac{d \, Ln \, \frac{P}{Po}}{dT}\right] M = - \frac{MW_w \, \overline{\Delta H_T}}{R_g \, T^2} \qquad (3\text{-}48)$$

which is also given as equation (3-34).

The enthalpy due to solids portions ($\overline{\Delta H_s}$) is once again obtained by using the Gibbs-Duhem equation:

$$N_w \, d \, (\overline{\Delta H_w}) + N_s \, d \, (\overline{\Delta H_s}) = 0 \qquad (3\text{-}49)$$

$$\overline{\Delta H_s} = - \frac{N_w}{N_s} d \, (\overline{\Delta H_w}) \qquad (3\text{-}50)$$

and the total enthalpy contribution of making 1 gm of product by mixing N_w of water and N_s of solids is given by:

$$N_w \overline{\Delta H_w} + N_s \overline{\Delta H_s} = \overline{\Delta H} \qquad (3\text{-}51)$$

The entropy function can be calculated by using

$$\overline{\Delta S} = \frac{\overline{\Delta G} - \overline{\Delta H}}{T} \qquad (3\text{-}52)$$

3.5. Indirect Prediction of Heats of Immersion in Foods

3.5.1. Effective molecular weight of solid in biological substances. Thermodynamic treatment of moisture sorption on biological products would besimplified and more meaningful if the effective molecular weight of solids (EMW_s) in the biological substances was known. Stitt(1958) first observed the need of knowing the effective molecular weight of solids and indicated that if this value was known, then it would be possible to express the thermodynamic parameters on a molar basis.

It is well known from the thermodynamics that the free energy changes, enthalpy changes and entropy changes are best discussed when a process is described as follows:

$$aA + bB \rightleftharpoons cC + dD \qquad (3\text{-}53)$$

where a moles of substance A and b moles of substance B react to form c moles of C and d moles of D.

Such a description for a biological process would be very difficult because of the complex nature of the biological product. If is assumed that the solids in a given biological material form one phase of the system while the other phase is water under equilibrium conditions. By extending this analogy, an effective mole fraction which would be representative of the solids portion of the biological substance can be defined. It should be noted, however, that an effective molecular weight of solids in a biological substance has no relation with the molecular weight as used in chemical terms.

The purpose of knowing the effective molecular weight of solids in biological substances is to develop a procedure with a sound thermodynamic basis to predict the thermodynamic parameters of low and intermediate moisture food utilizing moisture equilibrium data in a single temperature and to compare the results obtained by this procedure with the known method.

3.5.2. Possible methods of estimating the effective molecular weight. Freezing point depression, boiling point elevation and osmotic pressure measurements are some of the common methods used in the estimation of molecular weight of pure substances. If such data is available for biological products, it could be used for the estimation of the effective molecular weight of solids. This approach could be somewhat risky because much emphasis is placed on a single point whose experimental accuracy could be questionable.

The use of differential thermal analysis should be discounted since a food system changes significantly as the temperature is changed.

Hohner and Heldman (1970) used an interesting approach to determine the effective mole fraction in their studies with freezing rates of food systems by computer simulation. They developed the effective molar solute concentration by knowing the apparent specific heat and temperature relationship in the frozen product. This approach is probably more sound, since the computation involves the use of available data of apparent specific heats at various temperatures. They reported that the value of the effective molar concentration of solutes for cod fish was 0.0009 and for lean sirloin beef was 0.0007.

The validity of this approach will depend upon the extent to which the solution may be ideal at the composition corresponding to equilibrium relative humidities higher than 90 percent. Raoult's Law is defined as

$$P = X_w P_o \qquad (3\text{-}54)$$

and states that the vapor pressure of food (P) is proportional to mole fraction (X_w) and the saturation vapor pressure (P_o). Labuza (1968) stated that about 80-90 percent of the water in food exerts a vapor pressure equal to that of pure water ($a_w<1$). At higher equilibrium relative humidities, therefore, it may be assumed that Raoult's Law is valid.

3.5.3. Evaluation of thermodynamic parameters. There are several methods available to be used in the evaluation of thermodynamic parameters from moisture equilibrium data. In addition to direct use of the Clausius-Clapeyron equation, the Othmer procedure (1940) can be used if moisture equilibrium data is available at no less than two temperatures. The Brunauer, Emmett and Teller (BET) equation (1939) has been used widely to evaluate monomolecular moisture contents and allows the computation of latent heat values at that specific moisture content from equilibrium data at one temperature. In addition to the indicated limitations, these methods do not account for non-idealities existing in food products and do require careful use to obtain consistant results.

The Clausius-Clapeyron method is the most widely used method for the computation of total enthalpy ($\overline{\Delta H}_T$). The Clausius-Clapeyron equation was presented as equation (4-3). It may be recalled that the total enthalpy of sorption ($\overline{\Delta H}_T$), when applied to adsorption data represents the sum of the heat of adsorption and latent heat of condensation. If the procedure is applied to desorption data, the heat of sorption value would be the sum of latent heat of vaporization for pure water plus heat of desorption at any moisture content level. The Clausius-Clapeyron equation has been utilized by Kapsalis (1967) to determine the partial molal heat of sorption for various dry foods including freeze-dried beef. As would be expected, the heat of sorption increased dramatically as the moisture content was reduced to low levels.

An alternate approach to determination of latent heat values was proposed by Othmer (1940), who utilized the Clausius-Clapeyron equation to derive the following expression:

$$\text{Log}\ \frac{P_2}{P_1} = \frac{L}{L'}\ \frac{P'_2}{P'_1} \qquad (3\text{-}55)$$

where L and L' represent latent heat of vaporization for the product and the latent heat of vaporization for pure water respectively. Obviously equilibrium date is required for at least two temperatures. Preferably, the equilibrium data would be available at more than two different levels. Rodriguez-Arias (1956), Heldman, et al. (1965) and Strohman and Yoerger (1967) have applied the Othmer method to computation of latent heats of vaporization for various biological substances. In all of these applications the method has been applied to desorption data in an effort to evaluate the latent heats of vaporization necessary for design of dehydration equipment.

The method of Brunauer, Emmett and Teller (1939) utilized the following equation:

$$\frac{P}{M(P_O - P)} = \frac{1}{M_1\, c} + \frac{c - 1}{M_1\, c} \cdot \frac{P}{P_O} \qquad (3\text{-}56)$$

where M_1 and c are the constants evaluated from the BET analysis. In most applications to food products, the constant M_1 has been computed and is referred to as the moisture content of the product when a monomolecular layer of moisture is adsorbed on surfaces of the material. Salwin (1959) utilized

this monomolecular layer value to define a minimum moisture content for the stability of a food product in storage. The second constant (c) is defined by the following expression:

$$c = \text{Exp} \frac{(E_1 - L)}{R_g T} \qquad (3\text{-}57)$$

where E_1 represents the heat of sorption for the moisture in the monomolecular layer and L is the latent heat of vaporization or condensation for a free water surface. It is interesting to note that the energy constant of the BET equation as defined by equation (3-37) has not been utilized to compute the heats of sorption for food products.

3.5.4. Proposed method. The approach to be presented in this investigation is considerably different than the approach utilized by previous methods for computation of thermodynamic parameters in food products. The approach will utilize basic thermodynamic expressions and will assume initially that a dry food or intermediate moisture food product can be treated as a two-phase system. The two phases are the liquid phase and the solid phase of the product. Utilizing this assumption, any dry or intermediate moisture food product will exist due to the mixing of two phases. This so-called mixing process lends itself to description by two thermodynamic expressions. The first of these expressions is the free energy of mixing as follows:

$$\tilde{\Delta} G_m = X_w R_g T \text{ Ln } a_w + X_s R_g T \text{ Ln } a_s \qquad (3\text{-}58)$$

Equation (3-58) is expressed in terms of mole fraction of water (X_w), mole fraction of solids (X_s), activity of water (a_w) and activity of solids (a_s). The second expression is the entropy of mixing expressed as :

$$\tilde{\Delta} S_m = - X_w R_g \text{ Ln } X_w - X_w - X_s R_g \text{ Ln } X_s \qquad (3\text{-}59)$$

which defines the entropy value in terms of the mole fraction of the two phases in the system. Utilizing these two expressions and experimental equilibrium moisture data, the necessary thermo-dynamic parameters and other parameters describing the food system can be computed.

Equations (3-58) and (3-59) deserve somewhat more discussion at this point. First of all, it must be pointed out that equation (3-58) is a rigorous thermodynamic equation and is applicable to both ideal and non-ideal systems, while equation (3-59) is applicable to a class of non-ideal solutions which Hildebrand and Scott (1950) called "regular solutions." For ideal solutions the enthalpy of mixing is zero, while for regular solutions the enthalpy of mixing is relatively small. The concept of mixing as applied to an adsorption process may be somewhat more difficult to explain. Since mixing of two phases results in a free energy change and an increase in entropy, the assumption at this point is that the adsorption process (the mixing of liquid and solids) results in the same type of free energy change and entropy increase within a food system.

An example of equations (3-58) and (3-59) reveals that evaluation of free energy change or entropy increase can only be accomplished if the mole fraction values for water and solids are known. In general, mole fraction can be defined in the following manner:

$$X_1 = \frac{\frac{W_1}{MW_1}}{\frac{W_1}{MW_1} + \frac{W_2}{MW_2}} \qquad (3\text{-}60)$$

which defines the mole fraction value in terms of the weights and the molecular weights of each component. In a given food system, as defined in this investigation, all parts of equation (3-60) would be known except the molecular weight of the solid phase of the system. This molecular weight value must be considered an effective molecular weight (EMW) rather than one which would be defined in a chemical manner. As described earlier, Raoult's Law (equation 3-54) can be used in a region of high equilibrium relative humidity (>90 percent). Using equation (3-54), all the quantities in equations (3-58) and (3-59) can be defined except the activity of solids (a_s). The desired water activity and corresponding equilibrium moisture content values can be selected from the equilibrium moisture isotherms. The remaining quantity, the solids activity (a_s), is not readily available in order to compute the changes in free energy defined in equation (3-58).

Since the solutions or food systems considered in this investigation are not ideal, procedures which will account for this non-ideality must be considered. In thermodynamics, the procedure normally utilized to account for non-ideality is to introduce an activity coefficient defined for solids in the following manner:

$$a_s = X_s \cdot \gamma_s \qquad (3\text{-}61)$$

where the activity coefficient (γ_s) accounts for the non-ideality in the system. An activity coefficient of one would indicate that the water activity and mole fraction are equal. Unfortunately, equation (3-61) alone will not allow computation of solids activity in the food system. An additional equation must be introduced in order to accomplish this objective.

In a two-component system (solids and water), it is possible to ascertain the thermodynamic changes in one component from the thermodynamic changes of the second component by using the convenient form of the Gibbs-Duhem equation (3-41) as follows:

$$X_w \; d \; Ln \; \gamma_w + X_s \; d \; Ln \; \gamma_s = 0 \qquad (3\text{-}62)$$

Using equation (3-61) and (3-62) the activity coefficient of solids can be determined by graphical integration. Since the dry solids in a given food system is considered a standard state, the activity of solids at this point is considered equal to one. This explanation will become more evident as an actual example is illustrated. By knowing the activity coefficient of solids, activity of solids can be calculated using equation (3-61). The

free energy of mixing ($\Delta \tilde{G}_m$) can be computed using equation (3-58). The procedure outlined up to this point allows evaluation of free energy change and an increase in entropy for the mixing of two phases. Evaluation of these two thermodynamic parameters allows the evaluation of a third parameter, enthalpy of mixing ($\Delta \tilde{H}_m$), as follows:

$$\Delta \tilde{H}_m = \Delta \tilde{G}_m + T \Delta \tilde{S}_m \qquad (3\text{-}63)$$

Equation (3-63) represents the molar change in enthalpy of mixing of two phases in the system. There are several factors which must be emphasized when examining equation (3-63). The first concerns the acceptability of this expression to describe the enthalpy change which occurs during adsorption or desorption of moisture in a food system. The acceptability of this approach seems very likely but can only be proven by comparing results with known acceptable methods. The second factor is related to a distinct advantage of equation (3-63). Close examination of equations (3-58) to (3-63) indicates that equilibrium data are required at only one temperature for evaluation of latent heats of sorption results. Most procedures require at least three separate equilibrium moisture isotherms at three different temperatures. The success of utilizing this procedure could reduce the requirements for conducting of equilibrium moisture isotherm experiments to no more than one temperature.

3.6 Rheology of Foods

The rheological behavior of a system describes the manner in which the system will exhibit flow and/or deformation responses as a result of applied forces. Sometimes it is relatively simple to predict this response if the mechanical properties of the system are known. Due to the complex and heterogeneous nature of biological systems, however, it has been difficult to measure mechanical properties which will adequately describe the relationship between stress and strain. Consequently, a somewhat empirical approach has been used. Various combinations of ideal materials have been found to yield constitutive equations which, in effect, will express the influence of external disturbances on the behavior of a material due to its constitution. Frequently the limitations of perfect materials have presented the formulation of satisfactory constitutive equations and in such instances it has been necessary to propose relationships based purely on experimental results.

Therefore two approaches were used in seeking a model to adequately describe rheological behavior of pre-cooked freeze-dried beef at various water activities:

(a) combining simple elements of ideal materials, which led to Model 1; and
(b) proposing an empirical constitutive equation along guidelines suggested in the literature and on the basis of previous experience with the product, which led to Model 2.

To determine the values of the constants in both models, three different engineering tests were used, a relaxation test which recorded stress as a function of time; a creep test which measured strain changes with time; and a cyclic test in which strain was changed in a cyclic manner at a constant rate and the corresponding stress recorded. Any one of the three tests could be used to cross-check predicted results using the constants as evaluated by a different test. In addition, the response from the cyclic test allowed the two texture parameters, hardness and chewiness, to be evaluated.

The theory underlying the above three tests, and the method for calculating the constants in both Model 1 and Model 2 is described in the following sections.

The fundamental issue of interest is to determine the engineering parameters in Models 1 and 2, and use these parameters to predict hardness and chewiness values for pre-cooked freeze-dried beef. At that point, the common interests of the engineer and the food technologist in the physical characteristics of a food product will have been integrated.

3.6.1. Ideal materials. Deformation of a material may be elastic or inelastic (Mohsenin, 1968). Perfect elasticity is defined by Eirich (1958) as deformation which is independent of loading history, thus forming a conservative system in which all energy absorbed during deformation is reversible. However, most materials and particularly foods are not perfectly elastic and do not recover completely to their original shape prior to loading. Mohsenin (1968) suggests a property of biological materials he calls "degree of elasticity", defined as "the ratio of elastic deformation to the sum of elastic and plastic deformation when a material is loaded to a certain load and them unloaded to zero load".

In-elastic deformation can be divided into two categories, viscoelastic and viscoplastic. Viscoelastic behavior is characterized by a stress response dependent not only on the applied strain but also the rate at which strain is applied. The material may be composed of elastic and viscous elements which in combination display viscoelastic properties. A perfectly viscous material is defined by Prager (1956) as one which meets two requirements: (a) the deformation is dependent on the loading history and (b) the stress is proportional to the rate of deformation.

Similarly, a viscoplastic system consists of viscous and plastic materials. Again according to Prager (1956) the plastic material is similar to the viscous material in that deformation is dependent on the loading path, but different in that stress is independent of the rate of deformation. Malvern (1967) further states that the name perfectly-plastic is used for materials which do not show work-hardening properties beyond a yield point. Such materials may deform elastically upto a certain yield-stress point, beyond which the material will continue to deform without further additional stress.

The three classical ideal bodies representing elasticity, viscosity and plasticity are the Hookean body, Newtonian fluid and St. Venant body, respectively. These bodies serve as standards for analyzing stress-strain functions of real systems.

Hook's law states that stress is directly proportional to strain, i.e.,

$$\sigma = E\epsilon \qquad (3\text{-}64)$$

where E is Hook's constant or modulus of elasticity. In a Newtonian fluid, stress is directly proportional to strain rate, i.e.,

$$\sigma = \eta \dot{\epsilon} \qquad (3\text{-}65)$$

and the constant η is called viscosity. Integration of equation (3-65) shows that after a certain time period (t) strain will not return to zero when stress is removed, but will remain at the value corresponding to time (t).

A St. Venant body is likened to a block resting on a surface, with a friction factor between the block and surface preventing any movement from taking place. The block will not move until an applied stress ("yield stress") equals or slightly exceeds the static friction, but will then continue to move indefinitely under this stress until some external factor restricts or prevents further movement.

3.6.2. Rheological models; model 1. Using the three ideal bodies as building blocks, numerous combinations can be arranged differently to yield an almost infinite variety of models. Such models can, and have been used to satisfactorily represent macroscopic behavior of foods (Finney, et al., (1964); Diener and Heldman (1968); Mohsenin et al., (1963), Bourne (1967); Morrow (1965); Shama and Sherman (1966).

Some models are illustrated on Figure (3-6). The Hookean body is represented by a spring element and the Newtonian fluid by a viscous dashpot.

Depending not only on the number of elements used but also the manner of arrangement, mathematical equations may be formulated to describe the model. For example, consider the two simplest and most popular models: (a) a spring and dashpot in parallel, called a Kevin solid and (b) a series arrangement, referred to as a Maxwell fluid.

Let the subscripts 1, 2, m refer to the spring, dashpotand model:

(a)

$$\sigma_1 = E\epsilon_1$$

$$\sigma_2 = \eta \dot{\epsilon}_2$$

$$\sigma_m = \sigma_1 + \sigma_2$$

$$\epsilon_m = \epsilon_1 = \epsilon_2$$

$$\dot{\epsilon}_m = \dot{\epsilon}_1 = \dot{\epsilon}_2$$

$$\therefore \sigma_m = E\epsilon_m = \eta \dot{\epsilon}_m \qquad (3\text{-}66)$$

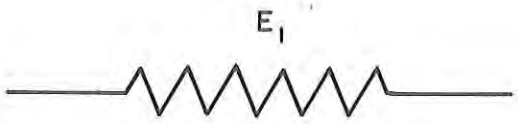

Elastic element $\sigma = E_1 \epsilon$

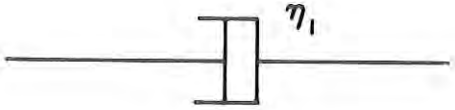

Viscous element $\sigma = \eta_1 \dot{\epsilon}$

Maxwell fluid $\dot{\epsilon} = \dot{\sigma} / E_1 + \sigma / \eta_1$

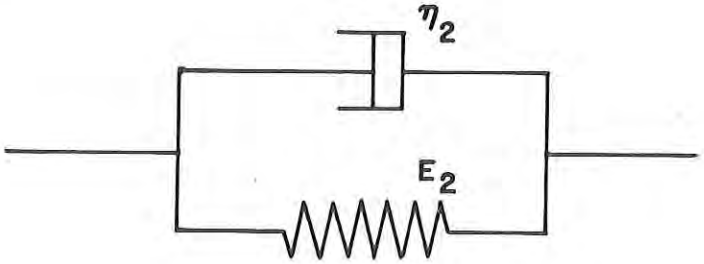

Kelvin solid $\sigma = E_2 \epsilon + \eta_2 \dot{\epsilon}$

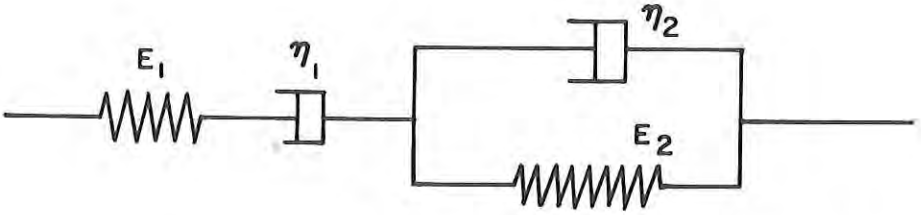

4-element solid $\ddot{\sigma} + \left(\frac{E_1}{\eta_2} + \frac{E_2}{\eta_2} + \frac{E_1}{\eta_1} \right) \dot{\sigma} + \frac{E_1 E_2}{\eta_1 \eta_2} \sigma = E_1 \ddot{\epsilon} + E_1 E_2 \dot{\epsilon}$

Fig 3.6 Simple viscoelastic models

(b) $\sigma_m = \sigma_1 = \sigma_2$

$\dot{\sigma}_m = \dot{\sigma}_1 = \dot{\sigma}_2$

$\varepsilon_m = \varepsilon_1 + \varepsilon_2$

$\therefore \dot{\varepsilon}_m = \dot{\varepsilon}_1 + \dot{\varepsilon}_2$

$= \frac{\dot{\sigma}_1}{E} + \frac{\sigma_2}{\eta}$

$= \frac{\dot{\sigma}_m}{E} + \frac{\sigma_m}{\eta}$ (3-66)

A similar approach yields equations for any other models chosen. The most frequently used models are the 3-parameter solid, 3-parameter fluid, 4-parameter solid, 4-parameter fluid. Behavior thus becomes a function of the particular arrangement and the relative values of the viscoelastic parameters.

Evidently the advantage of such models is that by inspection it is possible to judge how a material will behave but this is only feasible with a reasonable number of elements, i.e., 3 or 4, beyond which the variety of combinations becomes almost limitless. A further, and more serious limitation, is the assumption that <u>linear</u> viscoelastic behavior occurs, and most biological products probably do not act in this manner.

A model frequently recommended to simulate rheological behavior of foods is the 4-parameter fluid (see Figure 3-6). Preliminary relaxation tests confirmed that this model described the behavior of pre-cooked freeze-dried beef better than any other three or four element viscoelastic model, and it was decided to propose this arrangement, a Kelvin solid and Maxwell fluid in series, as Model 1. The model has the advantage of accounting for both solid and fluid response to applied stresses, a factor expected to become apparent especially at the higher water activity levels of the beef samples.

The mathematical equation for this arrangement is:

<u>Model 1</u>

$$\sigma + p_1 \dot{\sigma} + p_2 \ddot{\sigma} = q_1 \dot{\varepsilon} + q_2 \ddot{\varepsilon} \quad (3\text{-}67)$$

where

$$p_1 = \frac{(E_3/E_1 + \eta_3/\eta_1 + 1)}{(E_3/\eta_1)} \quad (3\text{-}68)$$

$$p_2 = \frac{\eta_3 \quad \eta_1}{E_1 \quad E_3} \quad (3\text{-}69)$$

$$q_1 = \eta_1 \quad (3\text{-}70)$$

$$q_2 = \frac{\eta_1 \quad \eta_3}{E_3} \quad (3\text{-}71)$$

All four constants E_1, E_3, η_1, η_3 may be calculated from any one of the three mechanical tests -- relaxation, creep, cyclic.

3.6.3. Formulation of constitutive equations: model 2. The fundamental problem facing researchers in rheology is the formulation of an equation of state

$$\sigma = f(\epsilon, \dot{\epsilon}, t, T, V, C_i) \tag{3.72}$$

that is, the relation between stress and strain, strain rate, time, temperature and physical composition variables (Frish and Simha, 1956). In equation (3-72) T represents absolute temperature, V volume and C_i particle concentration.

Bowen (1967) suggests, as a first step, a general set of equations which could describe physical properties of all materials. By imposing restrictions of elastic, plastic and viscous materials on the general equations, he formed more specific equations, e.g.,

$$\sigma = \sigma[T(t), g(t), F(t), \dot{F}(t)] \tag{3-73}$$

Clark (1968) interprets (3-73) to state that stress at time (t) is dependent on the temperature, temperature gradient, deformation gradient and the rate of change of the deformation gradient.

Further guidelines towards formulating constitutive equations can possibly be taken from dimensional analysis, which has been found very useful in establishing working formulas in fluid flow and heat and mass transfer. The basic concept of the method is that any mathematical equation which correctly expresses a physical phenomenon must be dimensionally homogeneous, i.e., the equation is valid, independent of the system of units used to measure the quantities involved. Charm (1963) attempted to use the dimensional analysis approach in food texture studies and proposed an expression relating the energy (P) required to masticate a food, to Young's modulus (E), a shear modulus (G), shear (S_s) and tensile stress (S_t), and the dimensions of the food sample (L). There is no evidence that any attempt was made to verify the equation suggested,

$$\frac{P}{LNE} = f\left(\frac{G}{E}, \frac{S_t}{E}, \frac{S_s}{E}, \mu\right) \tag{3-74}$$

N represents chews per minute and μ is Poisson's ratio, a dimensionless parameter.

Fung (1968) presented non-linear equations used in biomechanics. He proposed one equation of the form

$$\sigma = C\left[\epsilon\left\{1 - \epsilon + \frac{4}{3}\epsilon^2\right\}\right] e^{a\epsilon} \tag{3-75}$$

where C and a were constants. Haut and Little (1969) demonstrated that equation (3-75) could be used to describe rheological response of canine ligaments extremely well. Clark (1968) suggested an equation for cottonseed of the form

$$\sigma = C_1\epsilon + C_2\dot{\epsilon} + C_3\epsilon\dot{\epsilon} + C_4\int\epsilon dt \tag{3-76}$$

which satisfactorily predicted stress on the product under cyclic loading.

Adopting a general approach therefore, a second model was postulated on the assumption that food behaves in a non-linear viscoelastic manner and response to stress is a function of deformation or strain, strain rate, time, temperature, processing variables and compositional characteristics of the food, i.e., moisture, fat, sugar and protein contents, maturity; past history and physiological traits. This very general functional relationship could be simplified under the circumstances of this study which used samples of pre-cooked freeze-dried beef from only one muscle of one animal, was cooked at one temperature, freeze-dried at one plate temperature and tested mechanically at only one environmental temperature. Further, since moisture was the component whose content was varied over the equilibrium relative humidity range from 15 percent to 92 percent, it was assumed that rheological properties would be primarily a function of water activity. Thus a relationship of the form

$$\sigma = f(\epsilon, \dot{\epsilon}, t, a_w) \tag{3-77}$$

was assumed. Finally, at any one water activity a model exhibiting non-linear behavior was postulated, and proposed as an alternative model:

Model 2 $$\sigma = A\epsilon + B\epsilon e^{-t/\lambda'} + C \int_{t_n}^{t} d\epsilon \begin{cases} n = 0,2,4 \ldots; & \dot{\epsilon} \geq 0 \\ n = 1,3,5\ldots; & \dot{\epsilon} < 0 \end{cases} \tag{3-78}$$

The parameters A, B and λ' may be evaluated from the relaxation test, leaving the constant C to be determined from either the creep or cyclic test. Alternately, either the creep or cyclic test may be utilized to evaluate all four parameters.

The subscript n will denote whether strain is being increased, kept constant, or decreased. Normally, n = 0 such as for relaxation or creep, but for loading in a manner such as the cyclic test, n = 0, 2 ---- will denote the loading stages and n = 1, 3 will denote the unloading stages. This fourth term therefore in (3-78) will have a positive contribution to stress as strain increases, but negative as strain decreases.

3.6.4. Relaxation test. Under relaxation testing conditions, a strain ϵ_o is applied suddenly and kept constant, i.e.:

$$\epsilon = \epsilon_o H(t) \tag{3-79}$$

where H(t) is a step function defined as

$$H(t) = \begin{cases} 0 & -\infty < t < 0 \\ 1 & 0 < t < \infty \end{cases}$$

$$\therefore \dot{\epsilon} \; \ddot{\epsilon} = 0 \tag{3-80}$$

Constant strain $\epsilon_o H(t)$ for time greater than zero is illustrated on Fig. 3-8.

Model 1

$$\sigma + p_1 \dot{\sigma} + p_2 \ddot{\sigma} = q_1 \dot{\epsilon} + q_2 \ddot{\epsilon}$$
$$= 0 \tag{3-81}$$

The solution for this reduced homogeneous equation is given by Flugge (1967) as

$$\sigma = \epsilon_o \left[C_1 e^{-\lambda'_1 t} + C_2 e^{-\lambda'_2 t} \right] \tag{3-82}$$

where

$$\lambda'_1 = \frac{1}{2p_2} \left[p_1 - \sqrt{p_1^2 - 4 p_2} \right] \tag{3-83}$$

$$\lambda'_2 = \frac{1}{2p_2} \left[p_1 + \sqrt{p_1^2 - 4p_2} \right] \tag{3-84}$$

$$C_1 = \frac{(q_1 - \lambda'_1 q_2)}{\sqrt{p_1^2 - 4 p_2}} \tag{3-85}$$

$$C_2 = \frac{(-q_1 + \lambda'_2 q_2)}{\sqrt{p_1^2 - 4p_2}} \tag{3-86}$$

Model 2

$$\sigma = A\epsilon + B \epsilon e^{-t/\lambda'} + C \int_{t_n}^{t} d\epsilon$$

$$= \epsilon_o (A + B e^{-t/\lambda'}) \tag{3-87}$$

A typical relaxation stress-time relationship for biological materials is shown on Fig. 3-7.

From experimental curves, the values of C_1, C_2, λ'_1 and λ_2 in equation (3-82) may be estimated and by means of equations (3-83a) - (3.84d) and (3.68) - (3.71) the values of E_1, E_3, η_1, η_3 in Model 1 calculated. Thus equation (3-67) describing Model 1, can be used to predict creep and cyclic behavior for pre-cooked freeze-dried beef and consequently the texture parameters of hardness and chewiness.

Only three of the constants - A, B and λ - in Model 2 can be found from relaxation experiments since the term containing $d\epsilon$ equals zero under constant strain conditions. Therefore the fourth constant C must be evaluated from one of the other tests used - creep or cyclic.

A computer program using a non-linear estimation method for finding the best estimate of the constants in both models was available, and is briefly described at the end of this chapter.

3.6.5. Creep test. Deformation is recorded as a function of time due to a suddenly applied stress, σ_o H(t) which is kept constant.

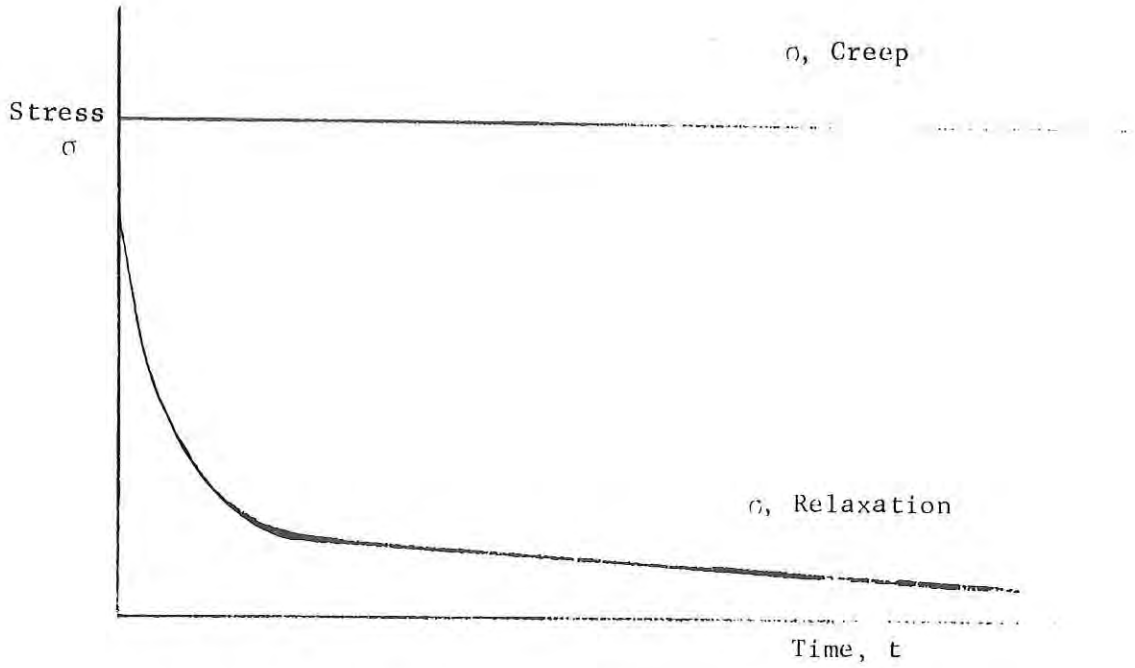

Figure 3-7. Typical σ - t relationship for creep and relaxation.

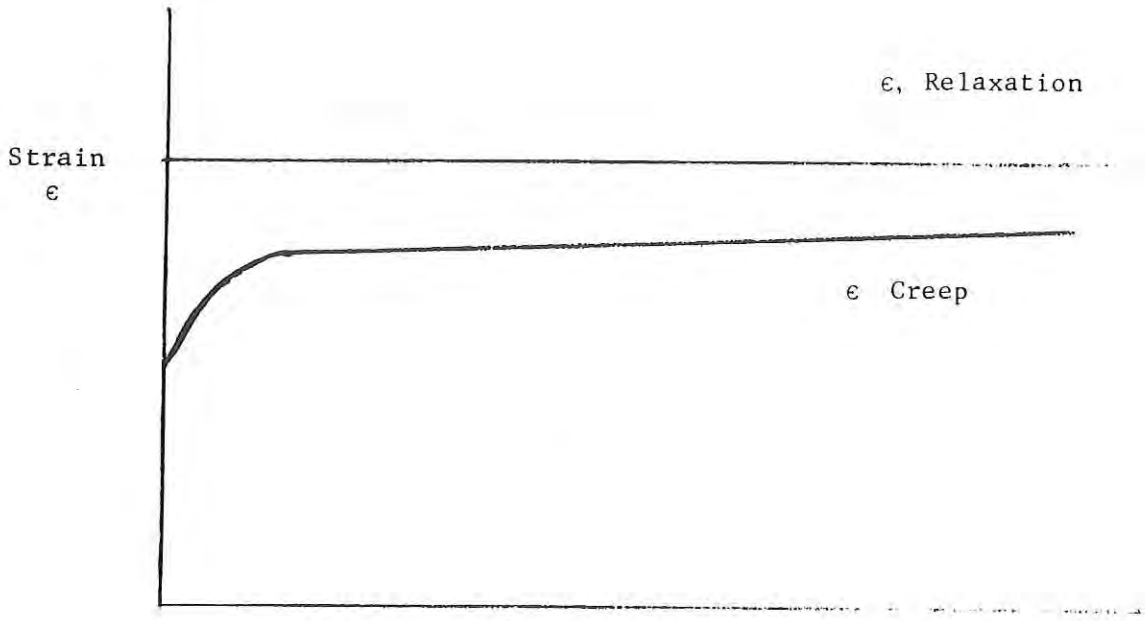

Figure 3-8. Typical ε - t relationship for creep and relaxation.

$$\sigma = \sigma_o H(t) \tag{3-88}$$

$$= \begin{cases} 0 & -\infty < t < 0 \\ \sigma_o & 0 < t < \infty \end{cases}$$

$$\therefore \quad \dot{\sigma} = \ddot{\sigma} = 0 \tag{3-89}$$

Stress and strain functions with time for the creep test may be seen on Figures 3-7 and 3-8.

Model 1

$$\sigma + p_1 \dot{\sigma} + p_2 \ddot{\sigma} = q_1 \dot{\epsilon} + q_2 \ddot{\epsilon} \tag{3-90}$$

$$\sigma = q_1 \dot{\epsilon} + q_2 \ddot{\epsilon}$$

The solution to (3-90) is also presented by Flugge (1967):

$$\epsilon = \sigma_o \left[C_3 + C_4 e^{-q_1 t/q_2} + \frac{t}{q_1} \right] \tag{3-91}$$

where

$$C_3 = \frac{p_1}{q_1} \quad \frac{q_2}{q_1^2} \tag{3-92}$$

$$C_4 = \frac{-1}{E_3} \tag{3-93}$$

Model 2

$$\sigma = A \epsilon + B \epsilon e^{-t/\lambda'} + C \int_{t_n}^{t} d \epsilon$$

Integration of the last term in Model 2 over time (t) to time (t = zero) yields,

$$C (\epsilon_t - \epsilon_o)$$

so that ϵ_t at any time (t) can be easily solved:

$$\epsilon_t = \frac{\sigma_o + C \epsilon_o}{A + B e^{-t/\lambda'} + C} \tag{3-94}$$

where ϵ_o is given by equation (3-95) below:

$$\epsilon_o = \frac{\sigma_o}{A + B} \tag{3-95}$$

In similar fashion to that outlined for the relaxation tests, the creep experimental data can be used to find C_3, C_4, q_1 and q_2 in equation (3-91) - which lead to the determination of E_1, E_3 η_1 and η_3 in Model 1 - and to find A, B, λ and C for Model 2 from equations (3-94 and (3-95).

3.6.6. Cyclic test. In cyclic tests, deformation takes place at constant rates (see Figure 3-9) i.e.

$$\dot{\epsilon} = + C_o \quad 0 < t < t_1;\ t_2 < t < t_3 \tag{3-96}$$

$$\dot{\epsilon} = - C_o \quad t_1 < t < t_2\ ;\ t_3 < t < t_4 \tag{3-97}$$

Model 1.

$$\sigma + p_1 \dot{\sigma} + p_2 \ddot{\sigma} = q_1 \dot{\epsilon} + q_2 \ddot{\epsilon}$$

$$= \begin{cases} q_1 C_o & 0 < t < t_1\ ;\ t_2 < t < t_3 \\ - q_1 C_o & t_1 < t < t_2\ ;\ t_3 < t < t_4 \end{cases} \tag{3-98}$$

a) $0 < t < t_1$

Writing the model in finite difference form, using constant time steps Δt,

$$\sigma(n) + p_1 \left[\frac{\sigma(n) - \sigma(n-1)}{\Delta t} \right] + p_2 \left[\frac{\sigma(n) - 2\,\sigma(n-1) + \sigma(n-2)}{\Delta t^2} \right] = q_1 C_o \tag{3-99}$$

$$\sigma(n) = \frac{q_1 C_o + \left\{ \dfrac{p_1 \sigma(n-1)}{\Delta t} + \dfrac{2 p_2 \sigma(n-1)}{\Delta t^2} - \dfrac{p_2 \sigma(n-2)}{\Delta t^2} \right\}}{\left\{ 1 + \dfrac{p_1}{\Delta t} \quad \dfrac{p_2}{\Delta t^2} \right\}} \tag{3-100}$$

Initial conditions, $\sigma(o) = \sigma(-1) = 0$.

b) $t_1 < t < t_2$

Solution is similar to equation (3-100) except for $- C_o$:

$$\sigma(n) = \frac{\left\{ -q_1 C_o + \left\{ \dfrac{p_1 \sigma(n-1)}{\Delta t} + \dfrac{2 p_2 \sigma(n-1)}{\Delta t^2} - \dfrac{p_2 \sigma(n-2)}{\Delta t^2} \right\} \right.}{\left\{ 1 + \dfrac{p_1}{\Delta t} + \dfrac{p_2}{\Delta t^2} \right\}} \tag{3-101}$$

Initial conditions:

$\sigma(o) = \sigma_{t_1}$, from (a) above

$\sigma^* (-1) = 2\sigma_{t_1} - \sigma_{t_1-t}$

c) $t_2 < t < t_3$

Equation (3-100) in (a) gives the solution for this part of the cylce.

Initial conditions:

$\sigma(o) = 0$

$\sigma^*(-1) = 2\sigma_{t_2} - \sigma_{t_2-t}$

d) $t_3 < t < t_4$

Solution is the same as (3-101) in (b) above.

Initial conditions:

$\sigma(o) = \sigma t_3$; from (c) above.

$\sigma^* (-1) = 2\sigma_{t_3} - \sigma_{t_3-t}$ (3-102)

The second initial condition i.e. $\overset{*}{\sigma}(-1)$ for parts (b), (c) and (d) is an approximation. Choice of the actual stress at any of the times $[t_1 - \Delta t)$, $(t_2 - \Delta t)$, $(t_3 - \Delta t)$]as the second initial condition would lead to an unstable solution. The predicted stresses after times t_1 and t_3 would continue to increase, even though strain is being decreased. Such behavior is physically impossible.

Therefore, if the values of E_1, E_3, τ_1 and τ_3 are previously shown from either the relaxation or creep experiments, it is possible to predict the stress-time relationship for cyclic loading conditions, which in fact also gives the texture profile on the Instron machine as used to objectively measure beef texture.

Model 2.

$$\sigma = A\epsilon + B\epsilon e^{-t/\lambda'} + C\int_{t_n}^{t} d\epsilon \qquad (3\text{-}103)$$

Referring to equations (3-96) and (3-97) and integrating the fourth term in Model 2, the solution for the cyclic test can be written as follows:

e) $0 < t < t_1$

$$\epsilon = C_o t \qquad (3\text{-}104)$$

$$\sigma = \epsilon(A + Be^{-t/\lambda'} + C) \qquad (3\text{-}105)$$

f) $t_1 < t < t_2$

$$\varepsilon = C_o t_1 - C_o (t - t_1) \tag{3-106}$$

$$\sigma = \varepsilon (A + Be^{-t/\lambda'} + C) - CC_o t_1 \tag{3-107}$$

g) $t_2 < t < t_3$

$$\varepsilon = \varepsilon_{t_2} + C_o (t - t_2) \tag{3-108}$$

$$\sigma = \varepsilon (A + Be^{-t/\lambda'} + C) - C \varepsilon_{t_2} \tag{3-109}$$

h) $t_3 < t < t_4$

$$\varepsilon = \varepsilon_{t_3} - C_o (t - t_3) \tag{3-110}$$

$$\sigma = \varepsilon (A + Be^{-t/\lambda'} + C) - C \varepsilon_{t_3} \tag{3-111}$$

Equations (3-104) through (3-111) will allow stress to be predicted as a function of strain and time provided A, B, λ and C have been found from relaxation or creep tests. The above equations will also permit the optimum values of A, B, λ and C to be found from cyclic experimental data, using the non-linear estimation method described below.

3.6.7. Non-linear estimation of parameters; GAUSHAUS program . The GAUSHAUS computer program (Meeter, 1964) for parameter estimation in non-linear models is one of several methods available (Hohner, 1970) and was used here mainly because of the supplementary statistics made available which gives the user valuable information as to the accuracy of the estimates. Basically, it is necessary to supply to the program first estimates of the required parameters, the theoretical model for calculating predicted results, and the experimental data. A comparison is made between the theoretical predictions from the model and the experimental data, and GAUSHAUS then continues to improve the parameter estimates until relative changes in the sums of squares between theoretical and experimental results have been minimized.

Output from the GAUSHAUS routine includes:
(a) optimum parameter estimates, with 95 per cent confidence limits.
(b) final predicted values of the model, also with 95 per cent confidence limits.
(c) sums of squares between theoretical and experimental values.
(d) correlation matrix of the parameters being estimated.

4. Experimental Considerations

A broad range of instrumentation and equipment types have been used in this investigation in an effort to accomplish the objectives of the research. The two primary areas of research included, (a) evaluation of equilibrium moisture characteristics and (b) evaluation of product texture. Several different types of instrumentation and procedures were utilized in these areas.

4.1. Equilibrium Moisture Content Determination

The equilibrium moisture contents of freeze-dried beef powder were determined from weight change measurements after the product had come to equilibrium with a known vapor pressure under vacuum. An equilibrium isotherm during moisture adsorption was generated after an initial removal of all produce moisture under vacuum to establish the zero percent moisture reference. After establishing the reference, the vapor pressure was increased and the second point on the isotherm was determined after the product was at equilibrium at that vapor pressure. This procedure was repeated at several successively higher vapor pressures to generate the entire adsorption isotherm.

After attaining equilibrium at the highest vapor pressure (95% RH), the vapor pressure was decreased to successively lower values, allowing time for the product to equilibrate at each point. This approach resulted in the generation of a desorption isotherm on the same product as was used for the adsorption isotherm.

The basic component of the system used for equilibrium moisture content determinations was an electrobalance. This balance was placed in a 5-in. diameter glass container with 1-in. diameter hangdown tubes as illustrated in Figures 4-1 and 4-2. A vacuum of less than 20 microns was maintained in this container. The balance and related instrumentation converted the sample weight change due to moisture adsorption or desorption into an electrical signal which is amplified in a 2-stage servo amplifier. This amplified signal was used to drive a strip-chart recorder which records the weight change of the product continuously.

The glass chamber containing the electrobalance was connected to a 13 mm inside diameter glass tube which was connected to a mechanical-diffusion type vacuum pump. A vapor trap was introduced immediately upstream from the vacuum pump at the location illustrated in Figure 4-2. This trap acted as a baffle to molecules of pumping fluid backstreaming from the diffusion pump and reduced the partial pressure of condensable vapors coming from the entire system.

The main vacuum line was connected to three vacuum gages which allow measurement of vacuum over the entire operating range. The gages included the following: (a) a mercury U-tube manometer used for measurement over the 5 to 760 torr range, (b) a McLeod gage designed for use in the 0.1 to 5 torr range and (c) a second McLeod gage designed for measurement in the 10^{-3} to 0.5 torr range. Each gage was connected through a separate stopcock so that measurements with any one of the three could be obtained at any time.

A third connection directly to the main vacuum line lead to the vapor source. The vapor source was in a 3-in. diameter glass tube, which had a detachable

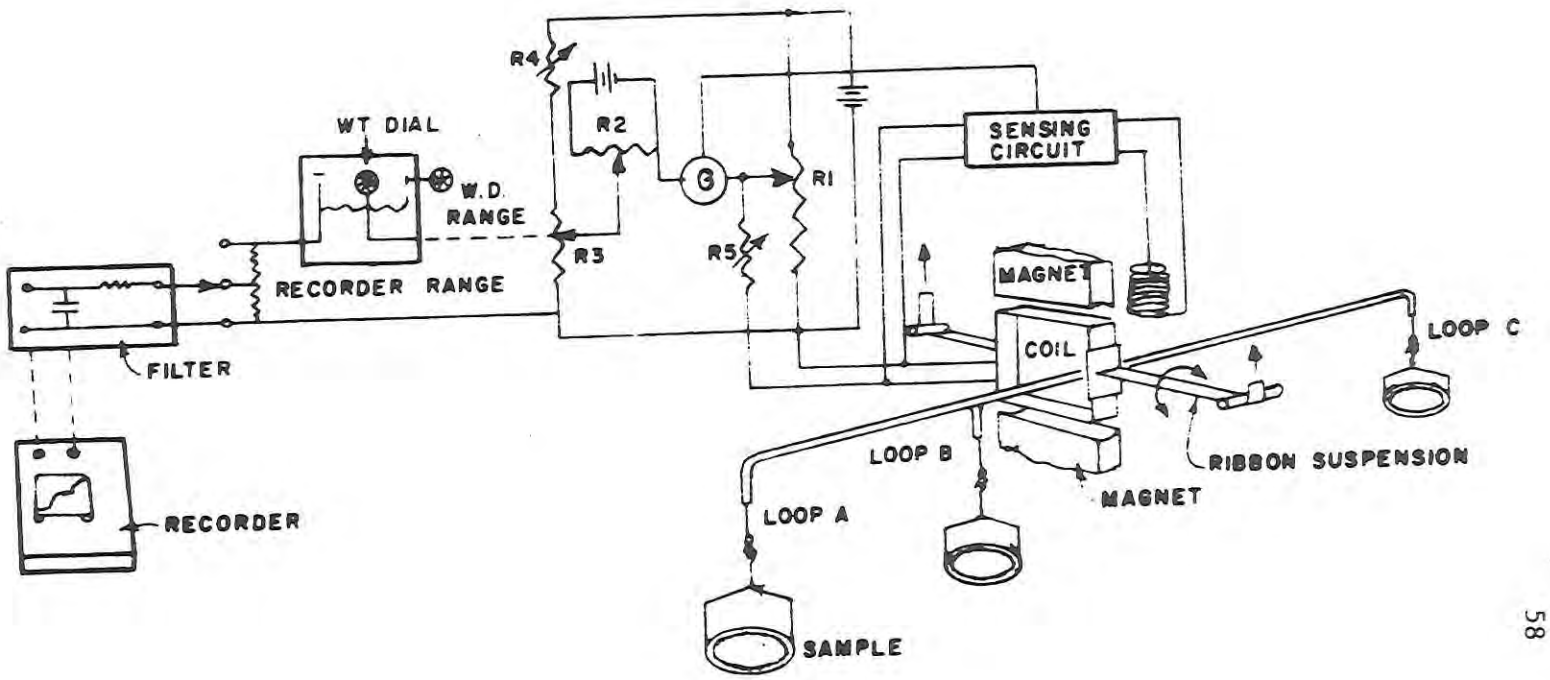

Figure 4-1. Principle of the Cahn-Electrobalance.

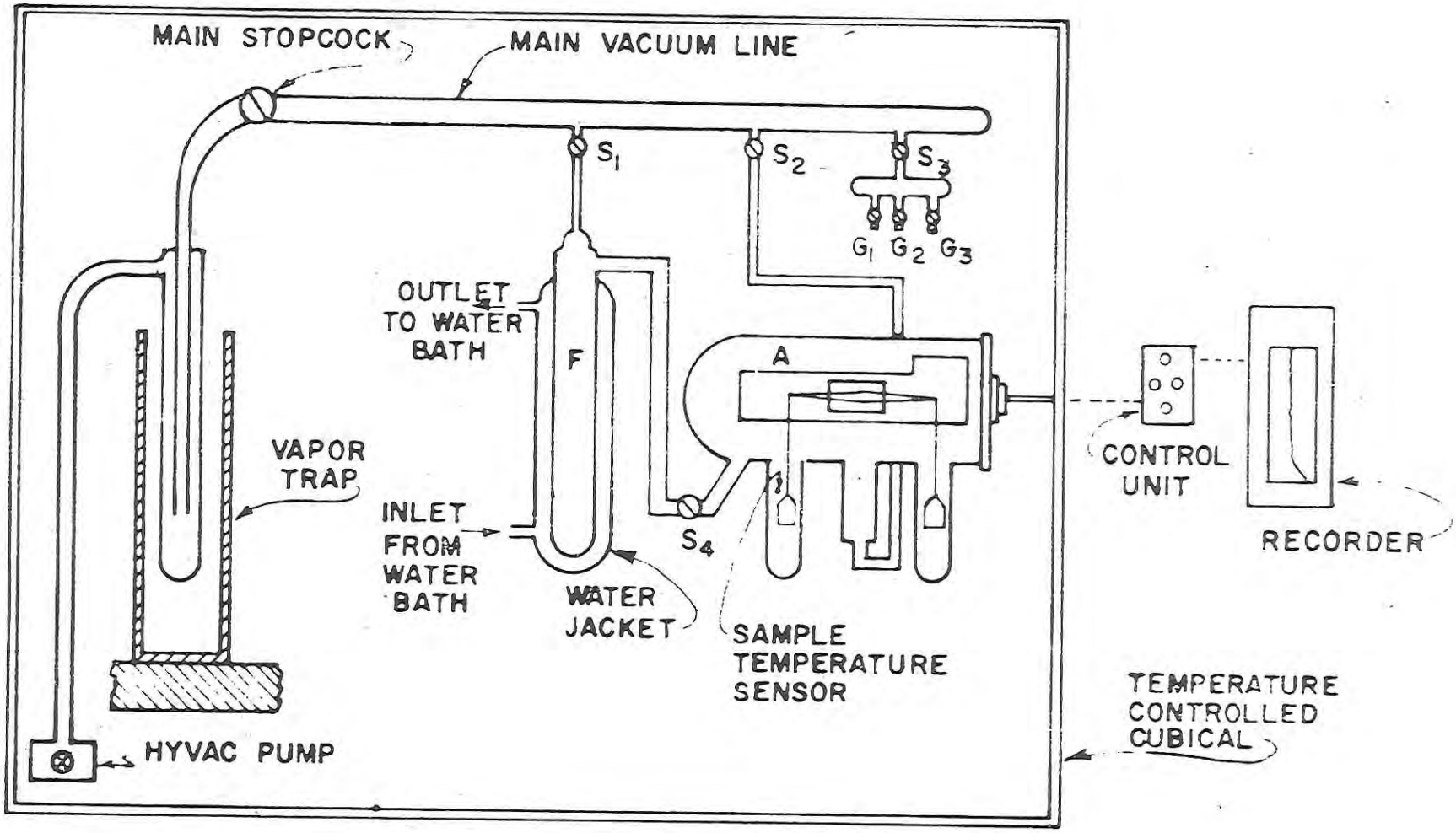

Figure 4.2. Schematic diagram of moisture sorption apparatus showing electrobalance assembly and related instrumentation.

lower portion for changing the vapor source solution. The upper portion of the vapor source tube was connected directly to the product hangdown tube of the electrobalance. The glass tube making this connection was 1/2-in. diameter and contained a stopcock for maintaining conditions around the product while changing solution at the vapor source. The vapor source was a water surface at various temperatures. Through the use of a series of water temperatures, the desired vapor pressure conditions were established in the system.

The entire system described with the exception of the servo-amplifier and the strip chart recorder was enclosed in a 5 by 4 by 9 ft. cubical which could be adjusted to any desired temperature in the range from 35 to 120°F. Water reservoirs were placed around the tubes containing the water vapor source and product to stabilize the temperature to the mean temperature of the cubical. Thermocouples placed in those locations indicated the desired temperatures were maintained to within $\pm$ 0.5°F.

4.2. Isothermal Differential Scanning Calorimeter

Figure 4-3 shows the schematics of instrumentation utilized for removal of water vapor and detection of the resultant heat loss. It consists of DTA console (DuPont-900 DTA), a calorimeter cell (DuPont-No. 900350), a vacuum pump and a time base recorder (Sargent-Model SR).

The isothermal program mode was used and the deviations from the isothermal conditions were recorded on the DTA console recorder. The 32°F temperature ice water in a thermas flask was used as a reference.

The external time base recorded indicated the difference between the cup and the sample temperature. The chart speed was 1 in./min. and the attenuation was varied with the recorder range selector.

The vacuum pump was set to pull a vacuum of less than 7 mm of Hg on the calorimetric cell within 15 seconds.

The samples were preconditioned to the required equilibrium relative humidity and temperature by an Aminco air conditioning apparatus (Figure 4-4). The moisture content of equilibrated sample was determined by oven method. Samples of about 3-20 mg were packed into cups as uniformly as possible for further DTA measurements.

4.3. Instron Testing Machine

The mechanical measurement of texture was carried out with the Instron Universal Testing Machine, floor model TT-BM, 2500 Kg capacity, with metric standard crosshead speed of 0.05 to 50.0 cm/min.

This machine has found many applications in the fields of texture evaluation and measurement of mechanical properties of agricultural products, (C. J. Morrow and N. W. Mohsenin (1966), G. F. Somers (1965), M. C. Bourne, J. C. Moyer and D. B. Hand (1966), M. C. Bourne (1966, 1965, 1967a, b, 1968)). The uses of the machine and a description are given by Bourne, et al, (1966). The use of the Instron to simulate the General Foods Texture Profile is described by Bourne (1968).

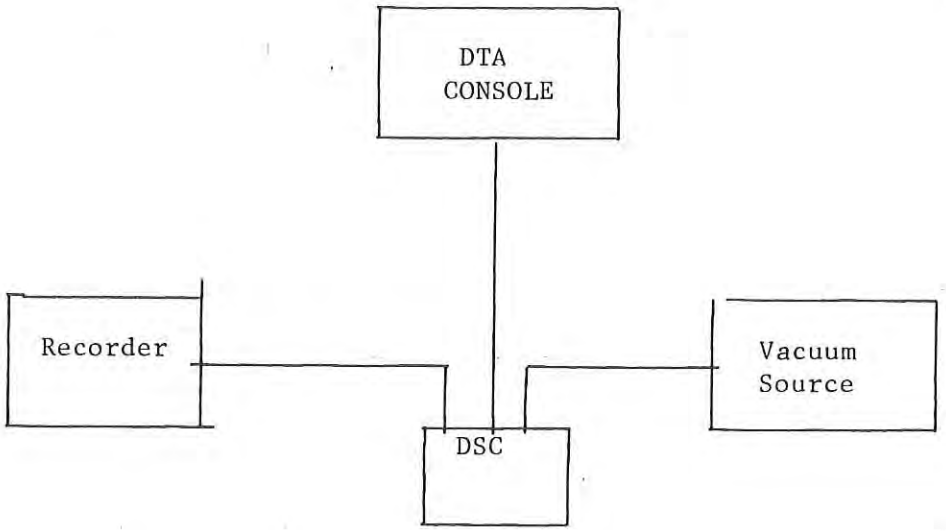

Figure 4-3. Isothermal differential scanning calorimetry (Schematic Diagram)

1. Air conditioning (Aminco) unit.
2. Equilibration chamber for pre-cooked freeze-dried beef cubes.
3. Laminar air flow element for measurement of air flow.

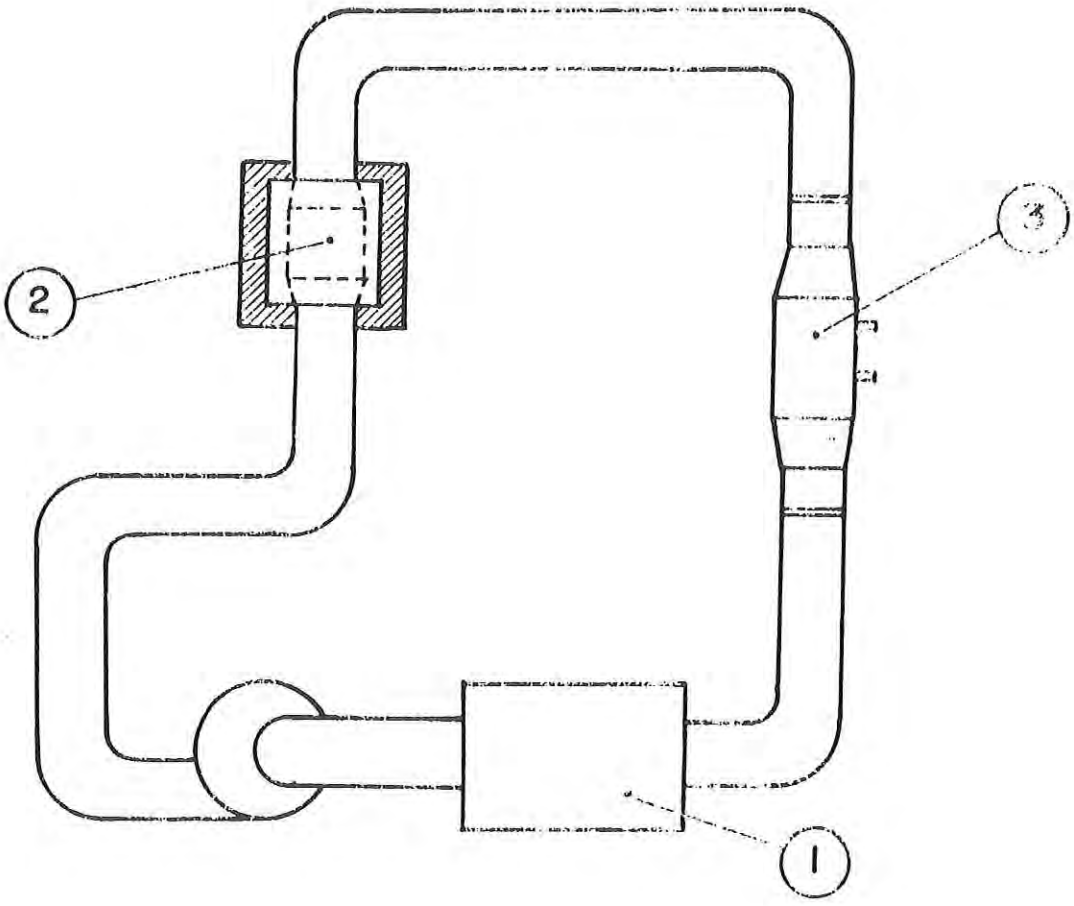

Figure 4-4. Apparatus used for equilibration of pre-cooked freeze-dried beef cubes.

A "loading cycling" test, which consists of complete compression-decompression cycles through a fixed stroke length, is only one of the many tests which are possible on the Instron. This type of test was suggested by Bourne (1968) as similar to the G. F. Texturometer curve, and was adapted as the objective method for texture measurement in this investigation.

The crosshead speed chosen was 2 cm/min. while a chart speed of 10 cm/min. was selected. Length of stroke was fixed at 4.5 mm. to correspond with a total compressive strain of 35%-40% of the samples. The diameter of the pressure probe, chosen after several preliminary trials, was 11/32 in. (Figure 4-5). A typical curve response is illustrated in Figure 4-6. Two primary parameters were of interest; hardness and chewiness. These can be calculated as follows (refer to Figure 4-6):

$$\text{hardness} = L_1 \ ;$$

$$\text{chewiness} = L_1 \times \frac{A_2}{A_1} \times B_2 .$$

The number of samples tested on the Instron instrument varied from 8 or 10 during early parts of the study to 15 or 20 for the remaining part. In all parts of the investigation the compression of the cube was perpendicular to fiber orientation.

4.4. Influence of Storage Conditions on Texture

A slightly different approach to product texture measurement was used in the second part of the study. To apply more of a shearing effect when penetrating the sample, a smaller probe of 3/16 inch diameter was selected.

Length of stroke was fixed at 2.5 mm. to correspond with a total compressive strain of about 20%. The crosshead speed chosen was 5 cm/min.

4.5. Relationship Between Engineering and Texture Parameters

An Instron Universal Testing Machine, table model TM, 200 kilograms capacity with standard crosshead speeds of 0.2 to 50 inches/minute was used to study cyclic behavior of pre-cooked freeze dried beef.

Three deformation rates were used, 0.5, 1.0 and 2.0 inch/minute; as in the other tests described below, five samples from different muscle locations were used. Data was collected on each sample from only two cycles since this response provided the necessary information for evaluating the texture parameters required.

4.6. Other Methods for Measurement of Product Properties.

4.6.1. Relaxation tests. The table model Instron Machine was used for relaxation testing as well as for cyclic testing previously described.

The cross head was set to deform the 0.4 inch cubes through 0.06 inch, or the equivalent of 0.15 strain. Ideally, a relaxation test involves instantaneous deformation. The crosshead speed used was 20 in./min., which applied the required deformation in 0.18 seconds. Any faster speed would have resulted in the crosshead slightly over-running the set stop-point and thus excessively deforming the samples.

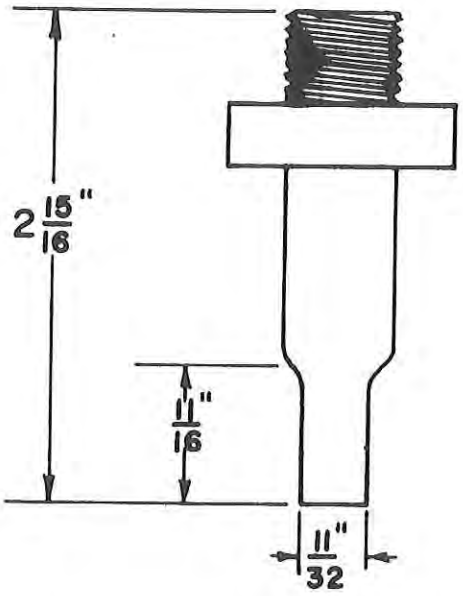

Figure 4-5. Probe used with Instron Testing Machine for compression - decompression tests.

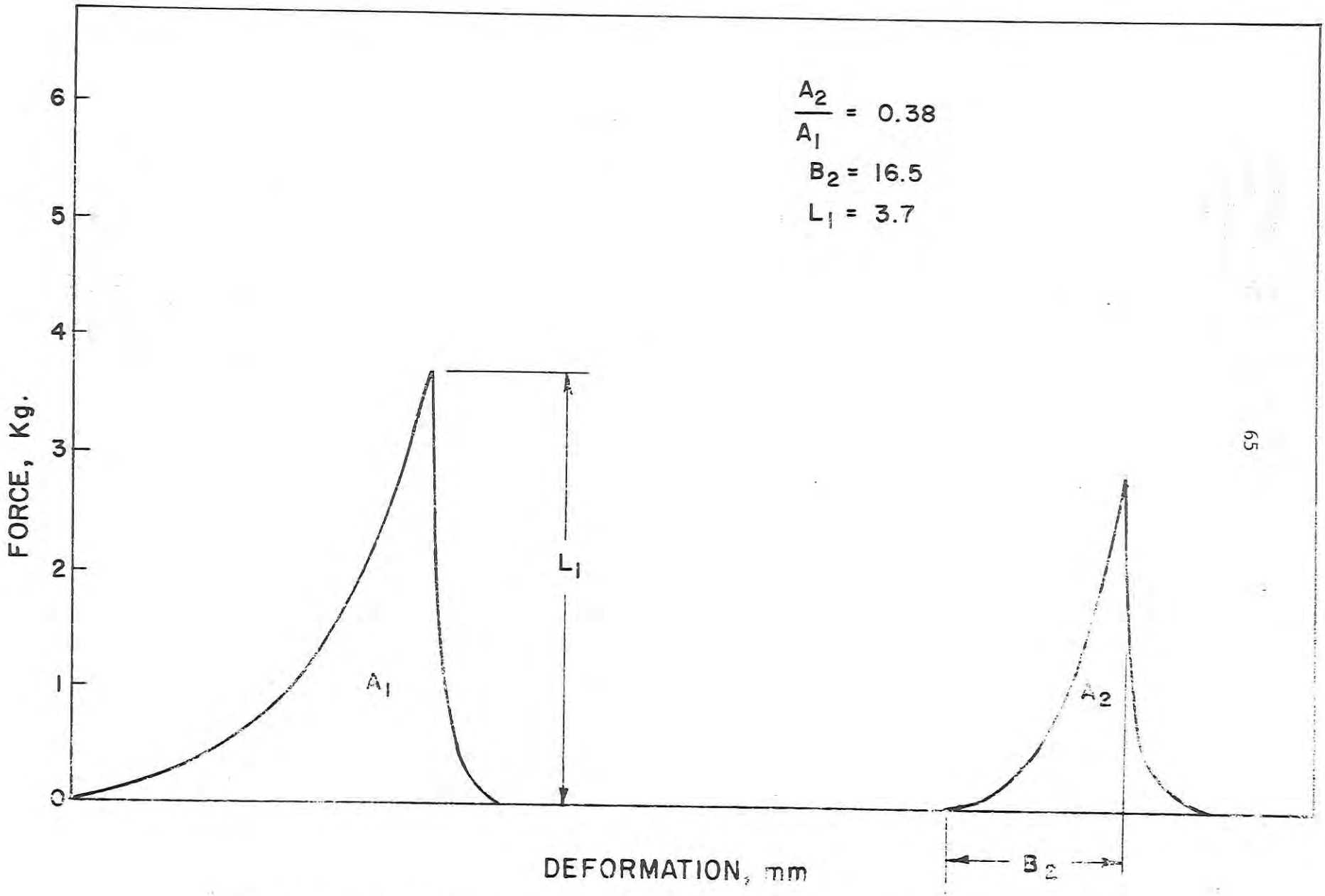

Figure 4.6 Typical force-deformation response for pre-cooked freeze-dried beef cube from Instron Testing Machine.

Since short time behavior was of prime interest, the change in stress (force divided by the cross-sectional area of the sample, 0.16 in.^{2}) over a time of 100 seconds was recorded. Mean behavior was evaluated by calculating the mean stress at every 1.2 second intervals up to 24 seconds, and at each 6 second interval thereafter.

4.6.2 Creep Tests. A creep test is the opposite to a relaxation test in that a sudden load is applied to the sample and held constant for a set period of time. The deformation or strain on the sample is recorded as a function of time.

The apparatus used for creep testing is illustrated schematically on Figure 4-7. First, the balance weight was positioned along the threaded arm (E) such that the part of the arm (C) to the left of the knife-edge (F) was exactly balanced. The pin (B) was raised upwards by the switch (A) so that it acted as a support for (C). The known weight (M) was then suspended from a point midway between the knife-edge (F) and the point of load application (H). The known weight used was 1 lb., and the effective force at (H) determined by calibration with a load cell, was 0.48 lb. The sample was inserted between (H) and a supporting stand (K) which could be raised or lowered by rotation of the threaded gear (D). A small glass plate (L) was placed on top of the sample to insure distribution of the applied load. The center point of the glass plate was placed to coincide with the center of the top surface area of the sample and the load application point.

The displacement rod of the linear variable displacement transducer (LVDT) was contacted by the adjustable screw (G) and set in a position which gave a reading of zero on the transducer-amplifier indicator (D ytronic 200D). At this stage the recording pen on the X-Y recorder (Moseley 7035A) was adjusted to the origin of the X-Y axes.

Creep testing was accomplished by releasing the switch (a) and allowing the supporting pin (B) to fall. Deformation of the sample was recorded through the LVDT by the X-Y recorder over a time period of 100 seconds.

4.7 Production Preparation.

4.7.1. Product description. The Longissimus dorsi muscle (low fat lean meat) was procured from Michigan State University food stores. This meat sample was utilized for the subsequent tests.

4.7.2. Cooking procedures. The product was cooked at an oven temperature of 325°F until the center of the roast attained the temperature of 160°F. A sensing element monitored the center temperature and automatically shut off the oven at the preset temperature of 160°F, simultaneously informing the operator that the cooking was complete.

4.7.3. Freeze-drying. The cooked meat was wrapped in a heavy duty aluminum foil, and frozen by storing at -20°F for 24-48 hours.

Freeze drying was carried out in freeze-dryer (virtis-Rep, Model 42) with a plate temperature setting of 105°F or 145°F as desired. Product temperature was measured by utilizing thermocouple junctions placed at the center of the product and a continuous recording potentiometer (Leeds-Northrup, Speedomax W Model). When the product temperature reached plate temperature, drying was

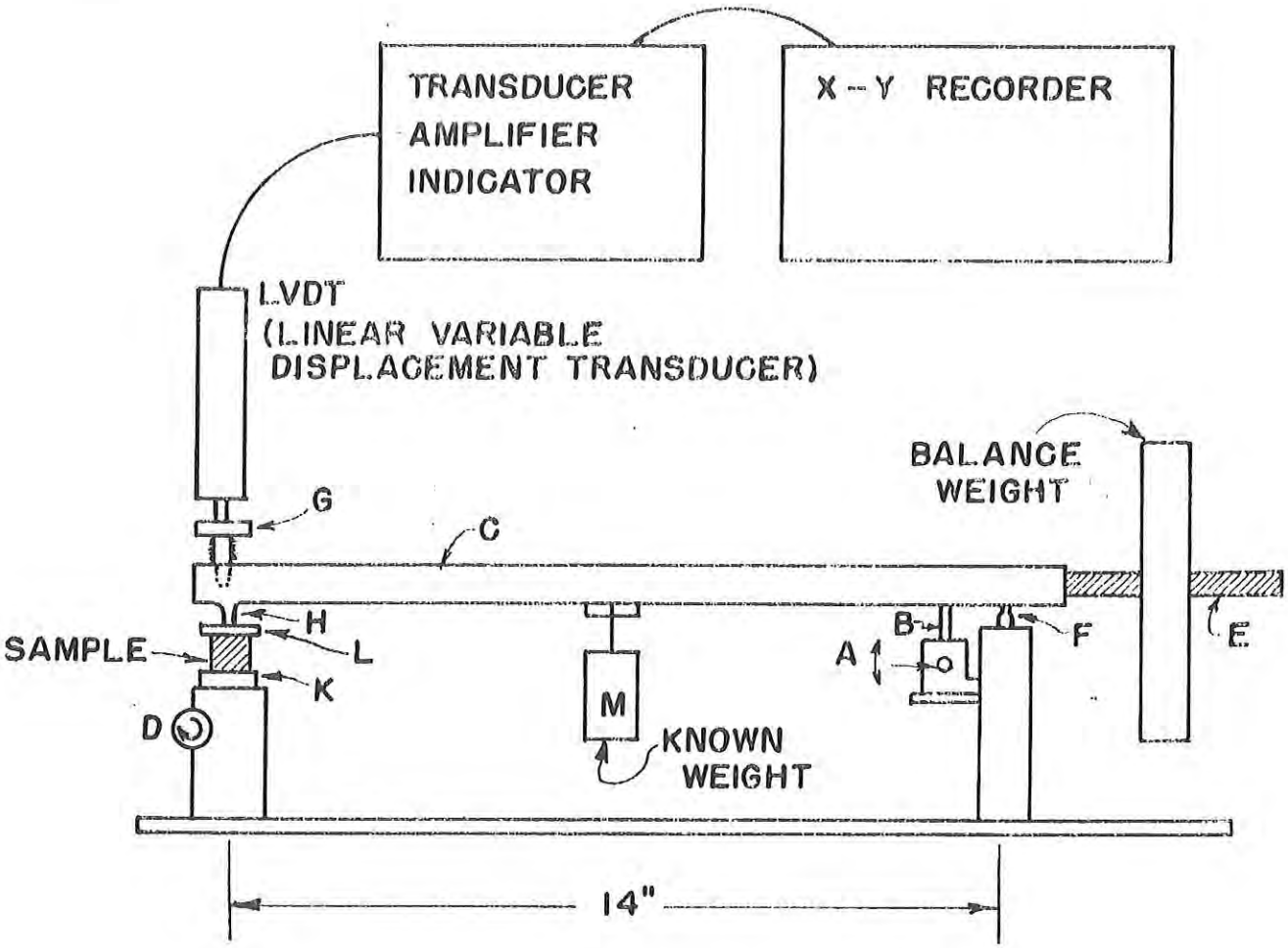

Figure 4-7. Schematic diagram of creep test apparatus.

assumed to be complete. The samples were subsequently stored in a desiccator at -20°F and utilized for testing purposes.

4.7.4. Precooked freeze dried beef powder preparation. The freeze dried product was ground in a Fritz-Patrick mill using a 0.063 in screen. The powder was placed in a sealed bottle which were stored in a desiccator at -20°F. Portions of the product to be used for equilibrium moisture determinations were equilibrated to the temperature of the experiment prior to the test.

4.7.5. Cubes for texture evaluation. After freezing (but prior to drying) the cooked roast was sealed in a heavy duty aluminum foil and labeled 1L, 2L, 2R, etc., to identify the location in the muscle from which the particular roast was cut. The number 1 through number 5 indicated the positions from the front to the rear of the muscle, respectively, while L and R denoted the left or right side.

A high speed band saw (Toledo, Model 5200-0-002) was used to cut the frozen beef into 1/2" cubes. Cubes were cut so that the fiber direction was as nearly perpendicular to a particular face as possible, to ensure that samples were similar in physical characteristics.

After several preliminary tests it was evident that a wide variation existed between results from samples similarly equilibrated, and it was felt that this could largely be attributed to non-homogeneities within the samples and to some irregularities in dimensions between samples. To overcome these problems, a small timber jig was assembled. By holding a cubed sample in the jig, which was clamped to the miter gage head on the table of a craftsman 18" band saw (Craftsman, Model 112, 23580), it was possible to cut off obvious non-homogeneities lying near the surface of the cubes and simultaneously reduce the cubes in size to a uniform dimension of 0.4 inch. The results reported refer to experiments using 0.4 inch cubes.

4.7.6. Moisture content of the product. The moisture contents of the freeze dried beef powder and beef cube (Parts I and II) was determined in a heated air oven procedure described by Triebold and Aurend (1963). An oven temperature of 80°C for 16 hr. was used to determine the product moisture content. The soxhlet extraction procedure was used to determine the fat content of the dehydrated product.

4.7.7. Beef component preparation. A portion of longissimus dorsi muscle was used for this purpose. Physically separable fat and connective tissue was removed from the sample. The sample was ground twine through 1 cm plate and once through 2 mm plate. The meat grinder head and plates were chilled to minimize the protein denaturation.

Raw beef was fractionated into actomyosin, water soluble component (sarcoplasmic fraction), connective tissue (collogen) and water insoluble component. All the fractionation procedures were carried at 3°C unless otherwise stated. The fractionation procedures are described in detail by Palnitkar and Heldman (1970).

4.7.8. Conditioning product for texture evaluation. The cubes from corresponding sections on both sides of the muscle were grouped together (i.e., 1R with 1L, 2R with 2L, etc), and from each of these five lots one sample was

randomly selected for mechanical testing. Thus for every test, five replications were run, as illustrated on Figure 4-8.

An Aminco Aire air-conditioning unit, capable of circulating air with controlled temperature and relative humidity (R.H.), was again used to equilibrate the beef samples. Samples were placed in the insulated chamber (2 on Figure 4-4) and equilibrated to moisture contents corresponding to 30, 50, 70, and 92% R.H. at a temperature of 80°F. Room temperature was 80°F, and room R.H. was 15%. The Aminco unit was incapable of circulating air at 15% R.H., so the samples at this low R.H. were allowed to equilibrate at room conditions.

Moisture content of the beef cubes equilibrated at 80°F, 15% R.H. was determined to by 3.1% (dry basis) using a hot air mechanical convection oven at 100°C for 18 hours. The dry weight corresponding to this moisture content was then used to calculate the moisture content at the higher relative humidities. The equilibrium condition was determined by weighing the sample cubes at 10-minute intervals until three successive readings indicated that a constant weight had been achieved. For the various tests carried out, the cubed beef samples were removed from the chamber of the Aminco Aire unit, one at a time. The resulting equilibrium moisture contents at 15, 30, 50, 70, and 92% R.H. were approximately 3, 6, 10, 16 and 30% (dry basis) respectively.

4.7.9. Establishment of conditions for storage evaluation. For storage studies only two temperatures were investigated -- 39°F and 100°F. At each of these temperatures, four equilibrium relative humidities were studied -- 0%, 25%, 50%, and 75%. As in the first study the Aminco Aire unit was utilized for conditioning the samples at the three highest equilibrium relative humidities.

After conditioning samples of precooked freeze dried beef were stored in sealed containers at 39°F and 100°F for a period of 6 months. After every one month 15 cube samples were tested for hardness and chewiness measurement by the objective methods described earlier.

4.8. Sensory Evaluation of Product

Two parameters, namely "hardness" and "chewiness" were selected for investigation. In addition the judges were asked to evaluate the heat evolved while chewing the sample. The "hardness" and "chewiness" provide the best overall description of the product texture. The "hardness" parameter provides an indication of product response during mastication. Both hardness and chewiness parameters were measured by sensory panel.

Judges were selected on the basis of previous experience and their willingness to serve as a member of the panel. The panel consisted of nine members, all students; six from the Food Science Department and three from the Agricultural Engineering Department.

The first phase of training involved basically the understanding of sensory definitions of "hardness" and "chewiness", acquaintance with standard rating scale and the correct method of evaluating sensory parameters. Table 4-1 and Table 4-2 were used to evaluate hardness and chewiness respectively. During the training period, the sensory panel was conducted twice weekly. Every panel was followed by discussion among the judges. Once every month, performance of the

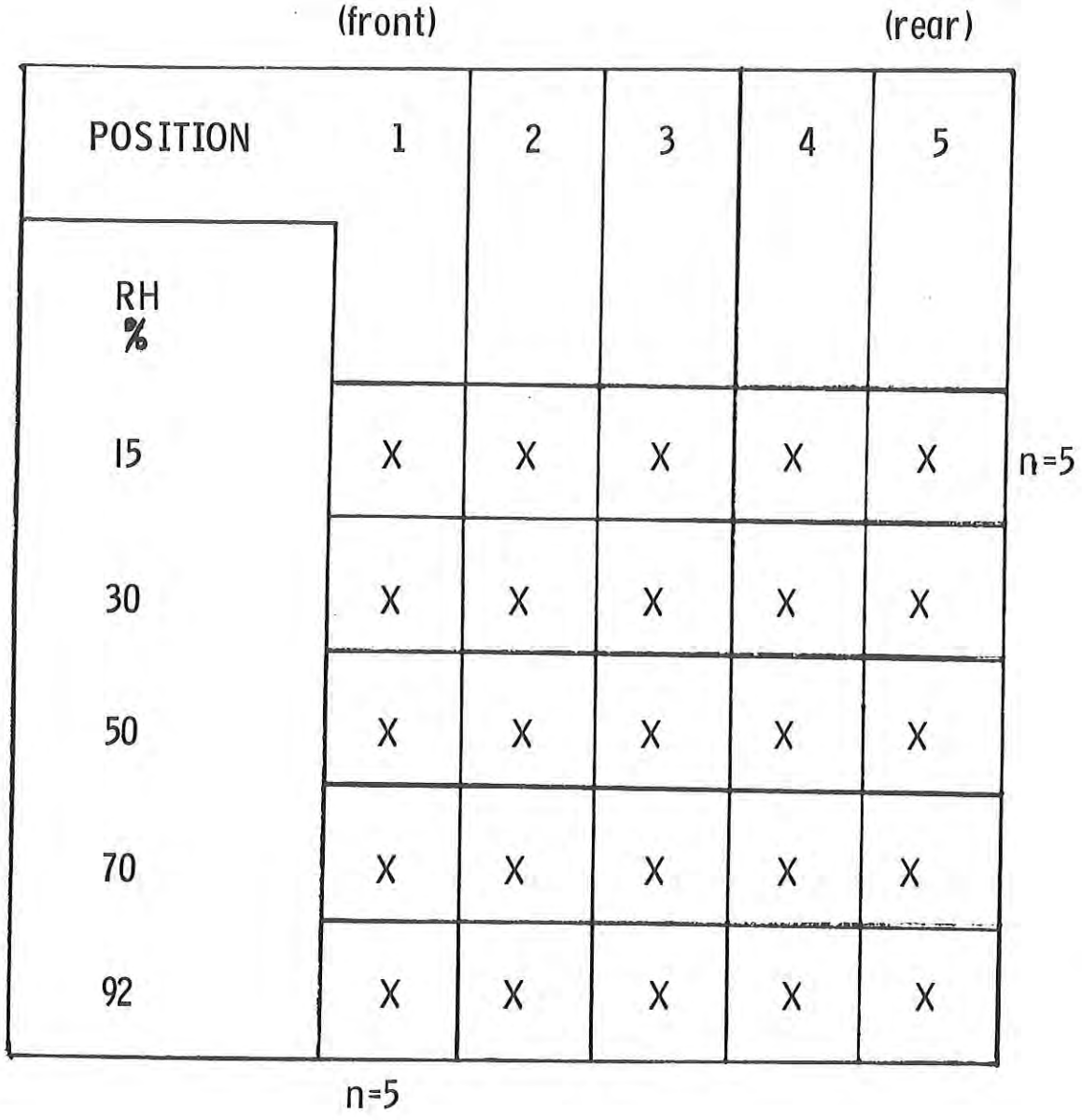

Figure 4-8. Experimental design for statistical analysis.

panel and individual judges was evaluated and discussed. The standard chewiness scale was modified slightly to incorporate additional standards and substitute some products which were more readily available.

In general, the judges indicated that the hardness scale was satisfactory. This was also confirmed by asking the judges to rank the products on the hardness scale according to degree of hardness. It was observed that the judges were able to rank the products according to the hardness scale.

The average number of chews and range for different reference points obtained during training period are given in Table 4-3. The results indicated that the average number of chews reported for a particular sample varied with the judges. For example, the average number of chews for the tootsie roll was 49-80.2. Even though considerable difference existed between the chewing ability between judges, each individual judge was relatively consistent.

After the completion of the training period the panels were conducted once per week. It should be mentioned that the modern sensory panel rooms located in the new Food Science Building were used. The air conditioned panel rooms can accommodate 20 people at one sitting. The samples were served from adjoining sample preparation rooms.

Three to four conditioned freeze dried beef cubes were served to the panel in duplicate. The samples were randomized on a paper plate. The instruction sheet (Table 4-4) and score sheet (Table 4-5) were provided to the judges with the sample. The reference products utilized during the training period were provided to the judges if any judge wished to confirm his memory.

Table 4-1.

HARDNESS SCORE SHEET

Name_____ Date_____

Technique for Evaluating Hardness (READ CAREFULLY)

1. For solids, place food between the molar teeth and bite down evenly, evaluating the force required to compress the food.
2. For semi-solids, measure hardness by compressing the food against palate with the tongue.
3. For olives, remove pimiento stuffing and compress slightly with the fingers.
4. For point 5 (olives) and point 6 (peanuts) bite crosswise.
5. Use the given standards for comparison purposes while evaluating unknown samples (if necessary).

Scale Value	Product	I	II	III
1	Cream Cheese			
2	Egg White			
3	Frankfurter			
4	Cheese			
5	Olives			
6	Peanuts			
7	Carrots			
8	Almonds			
9	Rock Candy			

Comments:

Table 4-2

CHEWINESS SCORE SHEET

Name_____ Date_____

Technique for Evaluating Chewiness (READ CAREFULLY)

1. Determine the force required to penetrate a gum drop in one-half of a second.
2. Place a standard in mouth and masticate at one chew per second at an applied force equal to that required to penetrate a gum drop in one-half of a second.
3. Count the number of chews required before the product is ready for swallowing. Repeat the procedure three times and determine the average number of chews.
4. Grade the unknown product according to average number of chews on the seven point Chewiness Scale.

Scale Value	Ave. No. of chews	Product	Ave. No. of chews (product)	I	II	III
1	(10.3)	Rye Bread				
2	(17.1)	Frankfurter				
3	(25.0)	Gum Drops				
4	(31.8)	Steak				
5	(33.6)	Black Crow Candy				
6	(37.3)	Nut Chews				
7	(56.7)	Tootsie Rolls				

Comments:

Table 4-3 Summary of results for chewiness parameter obtained during sensory panel training period.

Product	Mean Number of chews	Range in Number of chews
Rye Bread	11.2	8.9 - 15
Frankfurter	18	14 - 25.5
Gum Drops	22.8	18 - 31
Fudge	33.4	23 - 48.3
Black Crow Candy	37.3	30.3 - 48.9
Caramel	44.8	28 - 59.2
Tootsie Roll	66	49 - 80.2

Table 4-4

SENSORY PANEL

Score Sheet Guide

I. Hardness Evaluation for Freeze-dried Beef

A. Orient specimen so that product fibers are perpendicular to direction of bite.

B. Place specimen between molar teeth and bite down evenly to evaluate force required to compress.

C. Compare force required to standards in order to assign scale value.

D. Remember that hardness scale value is based on the very first response obtained from the specimen.

E. Assign a scale value to the nearest 0.25 point (7, 7.25, 7.5, 7.75, 8) and record.

II. Chewiness Evaluation for Freeze-dried Beef

A. Orient specimen in mouth the same as for hardness test.

B. Apply a force equal to that required to penetrate a gum drop in one-half second.

C. Chew the specimen at a rate of one chew per second with same force in each chew until the specimen is ready to swallow.

D. Be sure the specimen is as close to the condition at the time of swallowing as standards were at this point.

E. Record the number of chews.

III. Heat Evolved During Chewiness Evaluation

A. During the chewiness evaluation, try to sense an increase in temperature in the mouth (on tongue or palate).

B. Use the four-point scale on the score sheet to indicate your evaluation.

Table 4-5

TEXTURE SCORE SHEET

NAME _____ DATE _____

Hardness

Unknown

	I	II	III	IV	V
1. Cream Cheese					
2. Egg White					
3. Frankfurter					
4. Cheese					
5. Olives					
6. Peanuts					
7. Carrots					
8. Almonds					
9. Rock Candy					

Chewiness

(Record number of chews and scale number)

1.					
2.					
3.					
4.					
5.					
6.					
7.					

Heat evolved

1. None					
2.					
3.					
4. Evident					

5. Results and Discussion

5.1. Equilibrium Moisture Isotherms

Adsorption and desorption isotherms were obtained for precooked freeze-dried beef powder for the following isotherm temperatures: 40°F, 50°F, 72°F and 100°F. Figures 5-1 and 5-2 represent the adsorption and desorption moisture equilibrium isotherms for beef powder freeze-dried at 105°F plate temperature, while Figures 5-3 and 5-4 illustrate corresponding isotherms for beef powder freeze dried at 145°F plate temperature. Tables A-1 to A-4 show the adsorption and desorption data in a tabular form. The moisture content of precooked freeze-dried beef is expressed on non-fat dry matter basis (NFDM). The product freeze-fried with a plate temperature of 105°F has consistently higher sorptive capacity then 145°F product.

The equilibrium moisture isotherms for precooked freeze-dried beef show sigmoid shape as expected for most of the biological materials. The desorption curves show a general flattening tendency near saturation vapor pressure suggesting a type IV classification of Brunauer. The adsorption curves are strictly a sigmoid type II. Figures 5-5 and 5-6 show that as the temperature of the isotherm measurement was increased, the amount of water vapor absorbed by the material was decreased.

Figures 5-7 and 5-8 show the pronounced hysteresis behavior of the sample. These figures also indicate that the size of the hysteresis loop may be dependent upon the plate temperature utilized in freeze drying the product. In addition, Figures 5-7 and 5-8 reveal a considerable dependence of sorptive capacity on the freeze drying temperature.

The moisture equilibrium isotherms for raw beef components (actomyosin, connective tissue, water soluble component, sarcoplasmic fraction and water insoluble component) were measured at 50°F and 70°F. Typical moisture adsorption isotherms for three basic components of beef are presented in Figure 5-9. In general, moisture adsorption at low water activities appears to be limited for all three components. Water activities greater than 0.6 were required before actomyosin exhibited significant adsorption.

It should be mentioned that the actomyosin isotherm was determined at 72°F, at which actomyosin (being heat labile) may have partially denatured. The shape of the actomyosin isotherm was significantly different than the commonly known sigmoid shaped isotherms for foods (Figure 5-9), especially the steepness occurring at a $_w$ > 0.7. This indicates a possibility of water soluble component present in actomyosin preparation. Since KCl was used in the actomyosin preparation, traces of KCl left over in actomyosin may have caused this characteristic steepness at higher water activity values ($a_w > 0.7$)

The sarcoplasmic fraction adsorbed small amounts of moisture at low water activities (0.4) but the amount increased rapidly between 0.4 and 0.8. The moisture adsorption isotherm for connective tissue was the more typical sigmoid shape and moisture adsorption increased in a relatively uniform manner at all water activities. However, the amount of moisture adsorbed by the connective tissue at the higher water activities (>0.9) was less than that absorbed by either actomyosin or sarcoplasmic fraction.

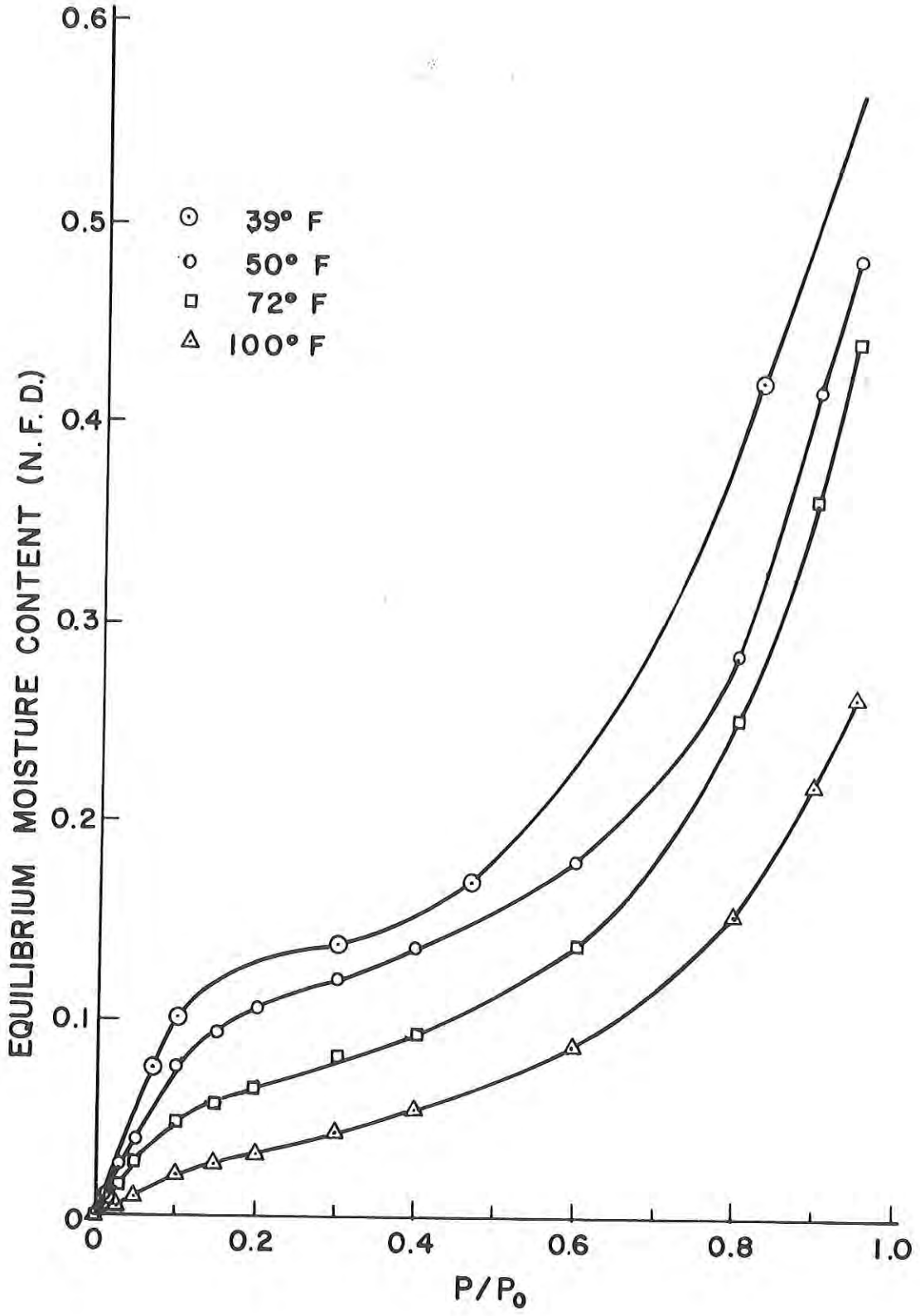

Figure 5.1. Adsorption isotherms for pre-cooked beef powder freeze-dried at 105°F plate temperature.

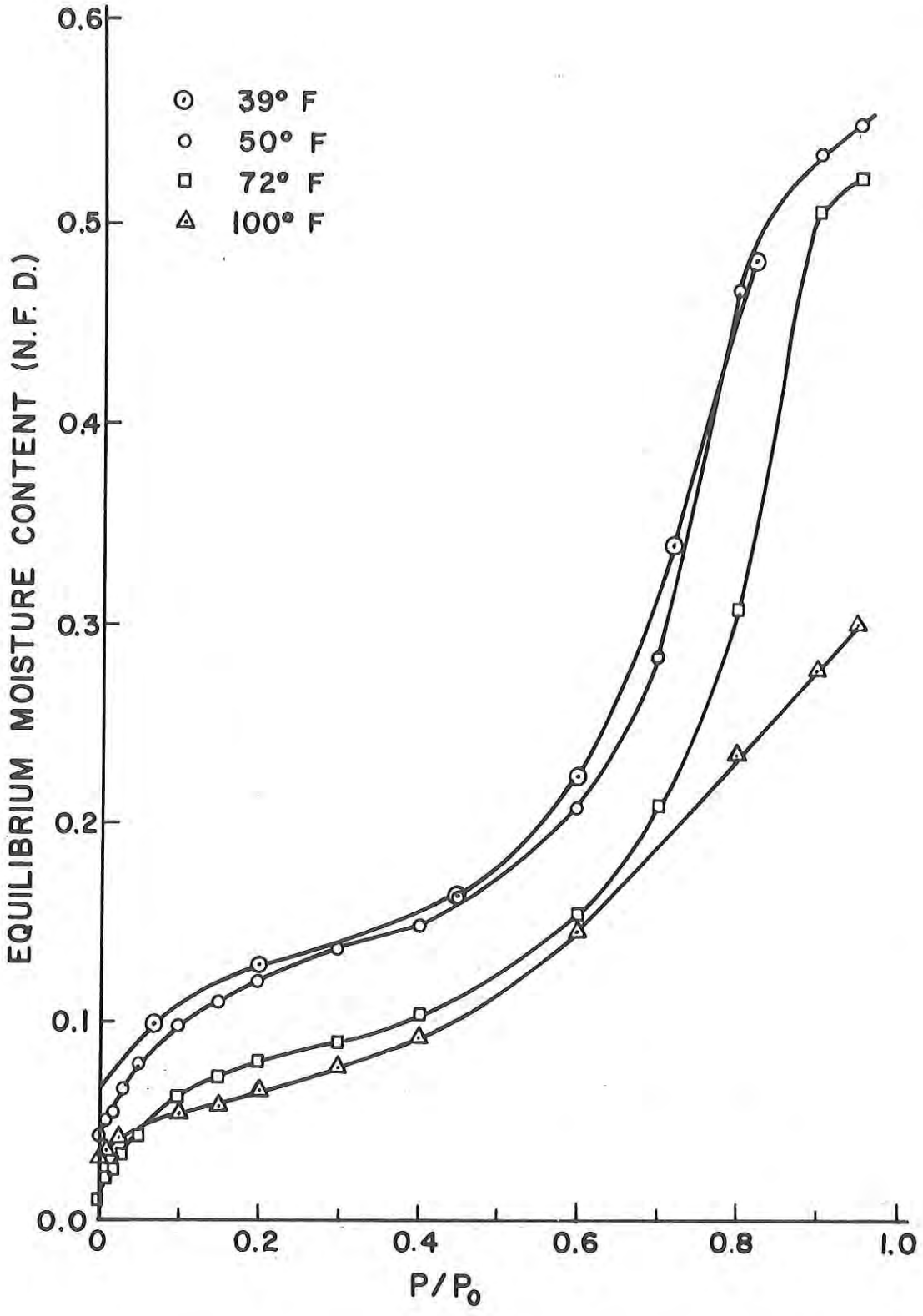

Figure 5-2. Desorption isotherms for pre-cooked beef powder freeze-dried at 105°F plate temperature.

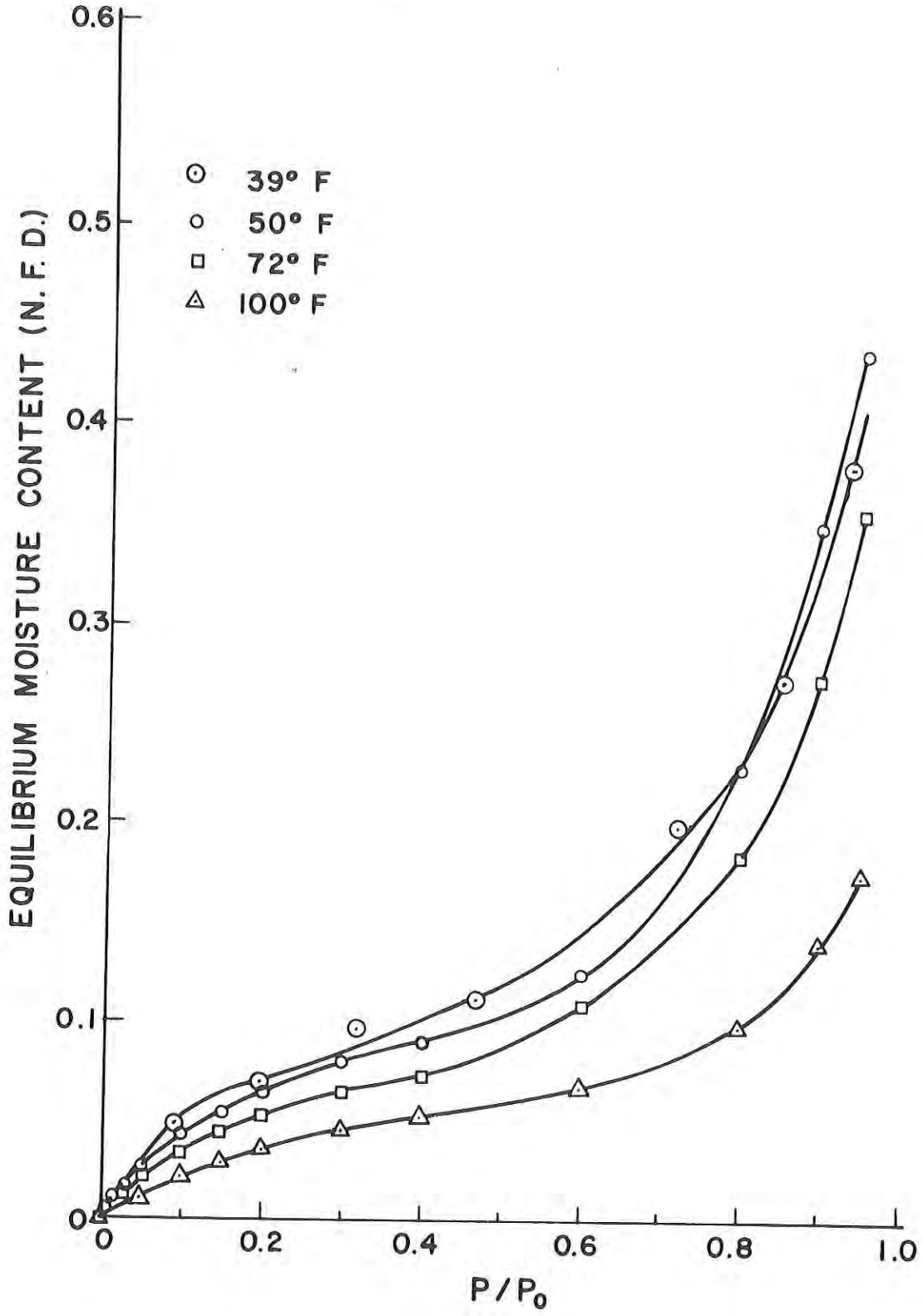

Figure 5-3. Adsorption isotherms for pre-cooked beef powder freeze-dried at 145°F plate temperature.

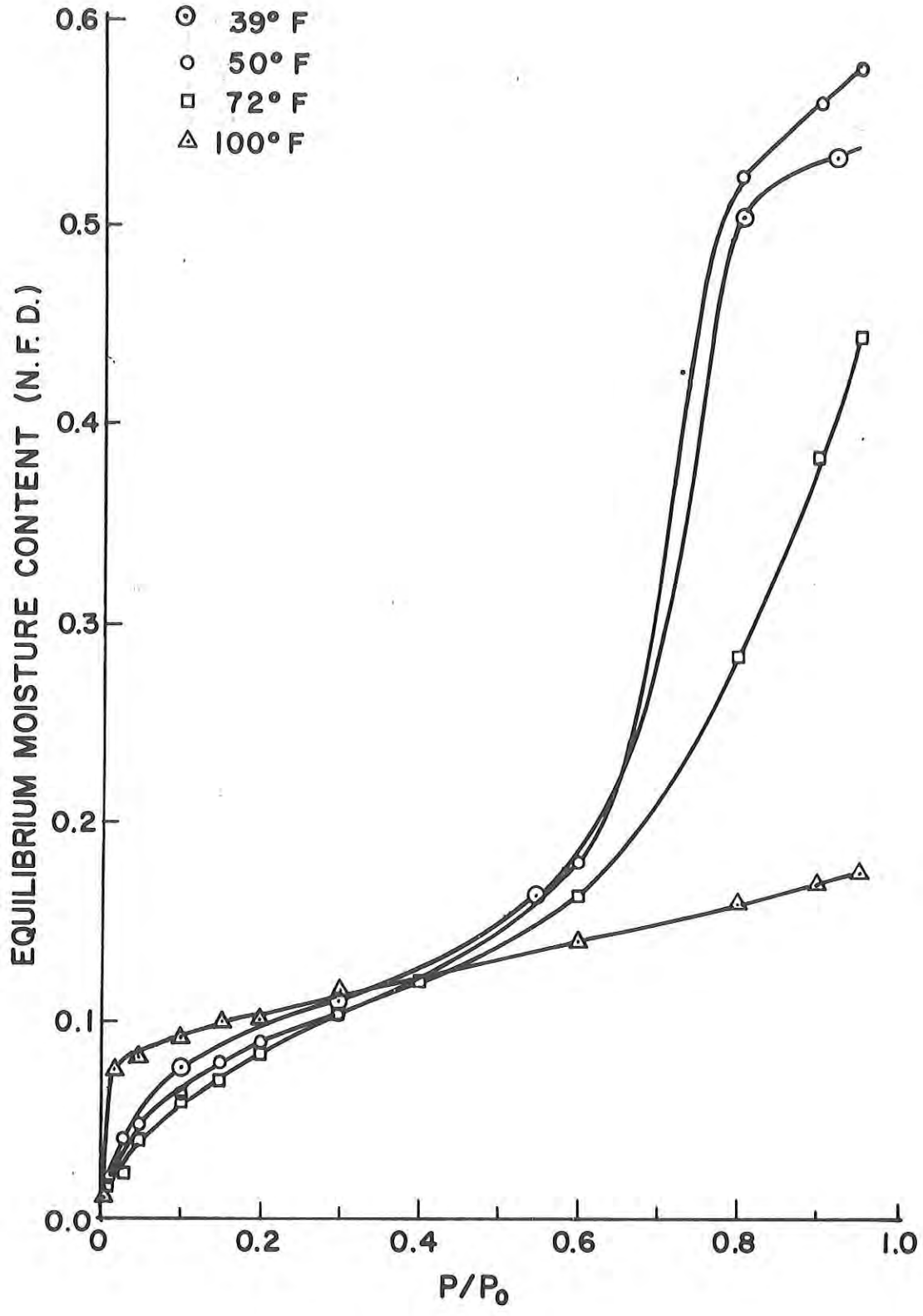

Figure 5-4. Desorption isotherms for pre-cooked beef powder freeze dried at 145°F plate temperature.

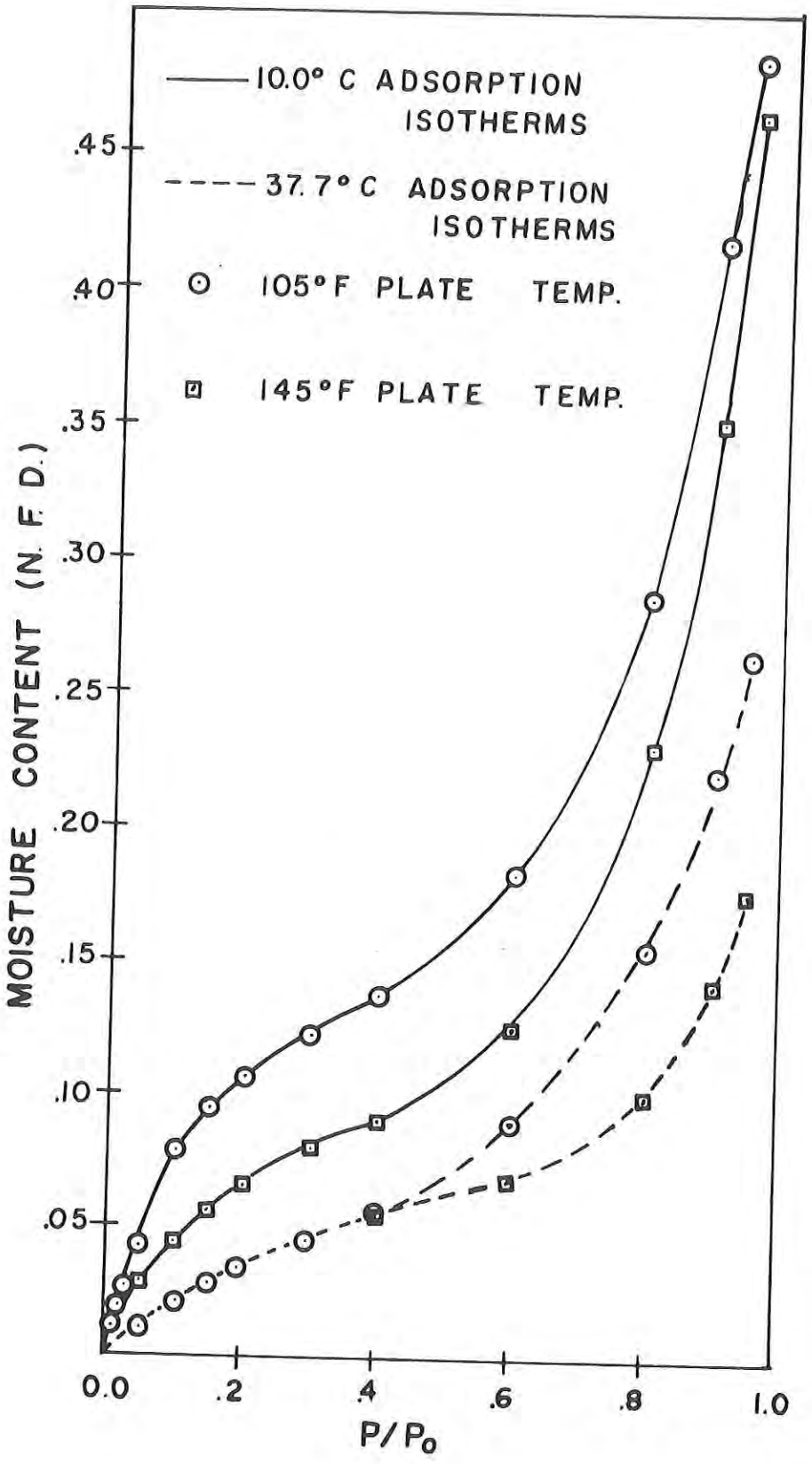

Figure 5-5. Comparative adsorption isotherm plots showing the effect of freeze drying (plate) temperature on the sorptive capacity of freeze dried beef powder.

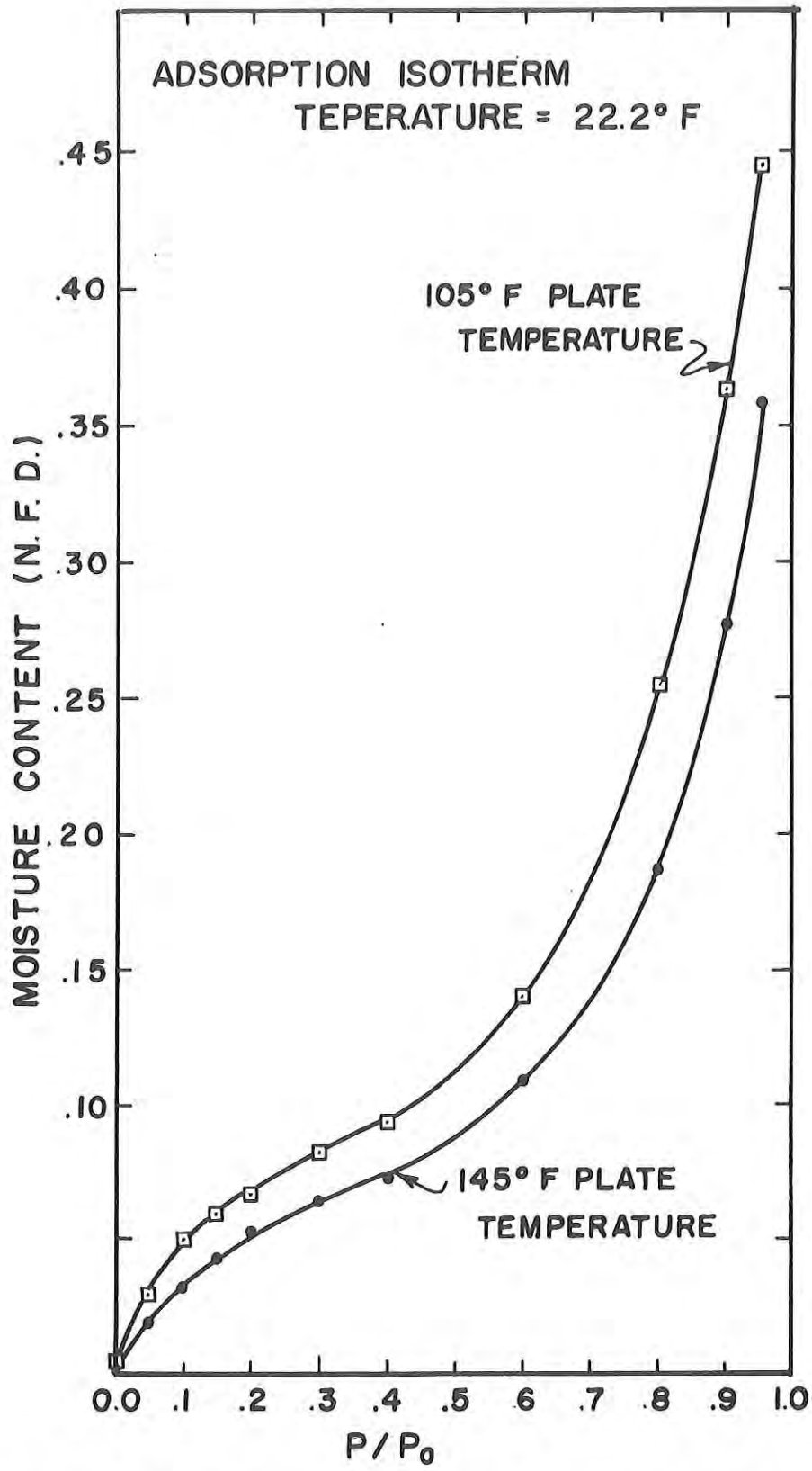

Figure 5-6. Comparative adsorption isotherm plots showing the effect of freeze drying (plate) temperature on the sorptive capacity of freeze dried beef powder.

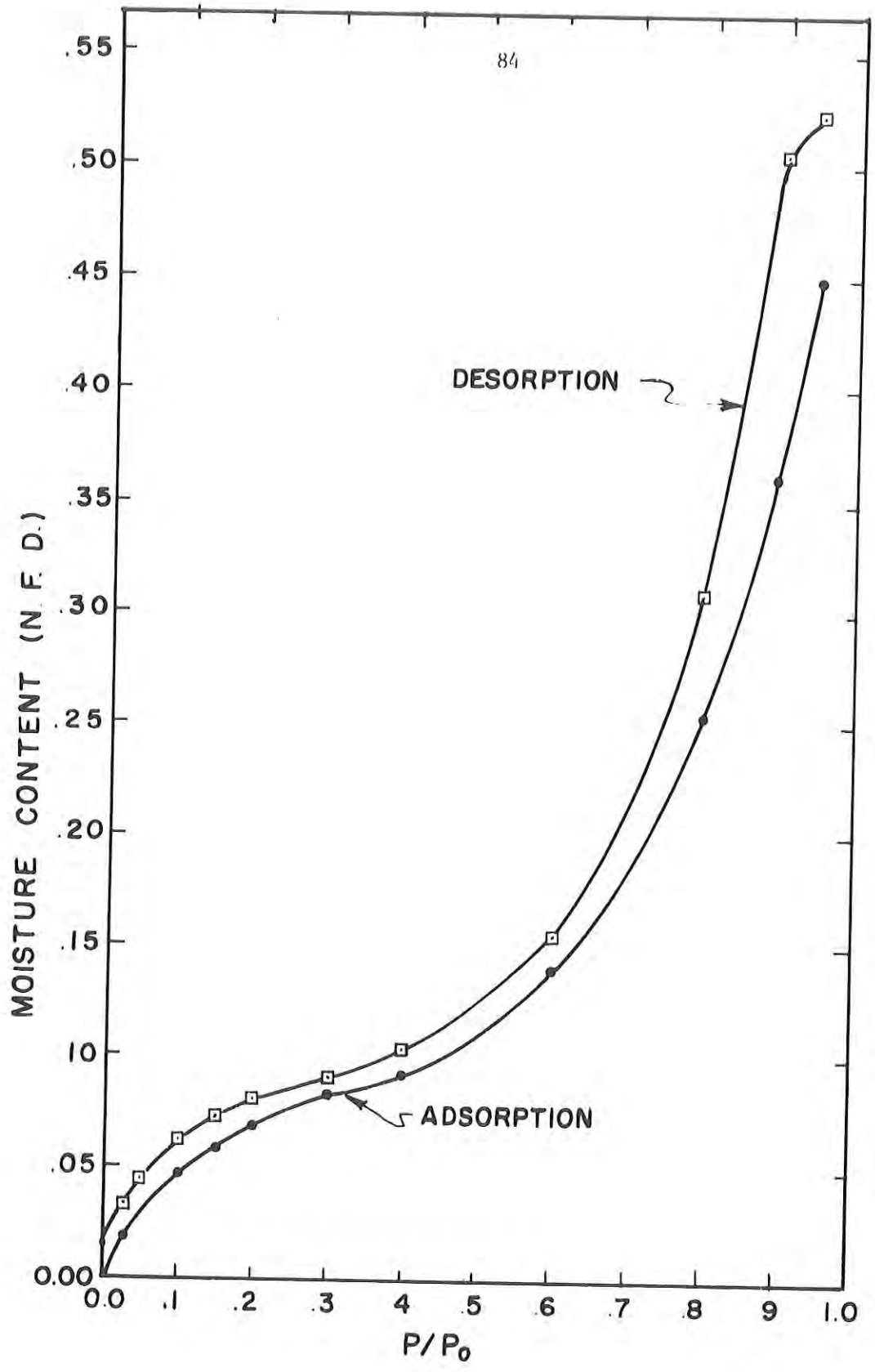

Figure 5-7. Sorption hysteresis in 72°F isotherm for pre-cooked beef powder freeze dried at 105°F plate temperature.

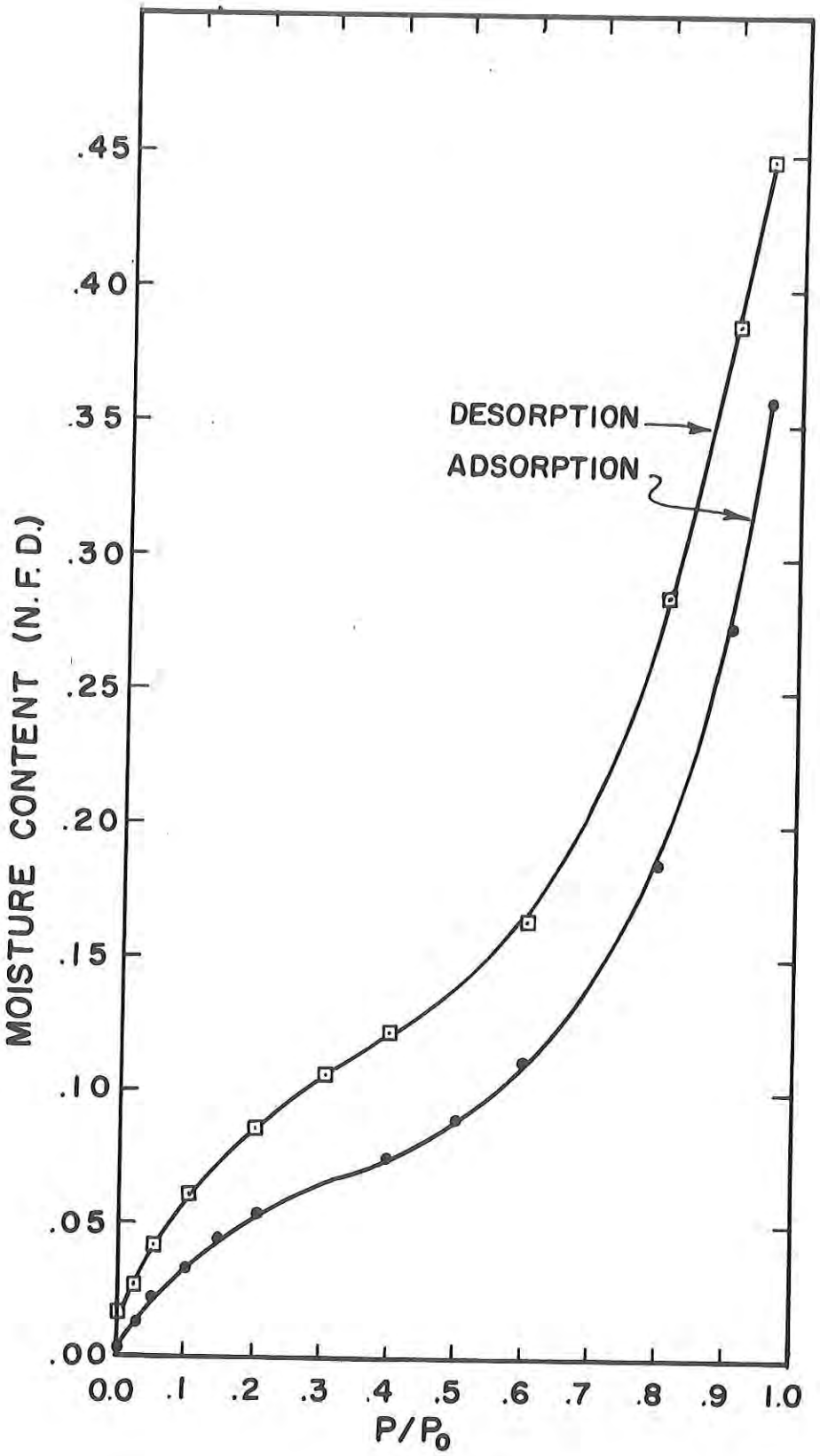

Figure 5-8. Sorption hysteresis in 72°F isotherm for beef powder freeze dried at 145°F plate temperature.

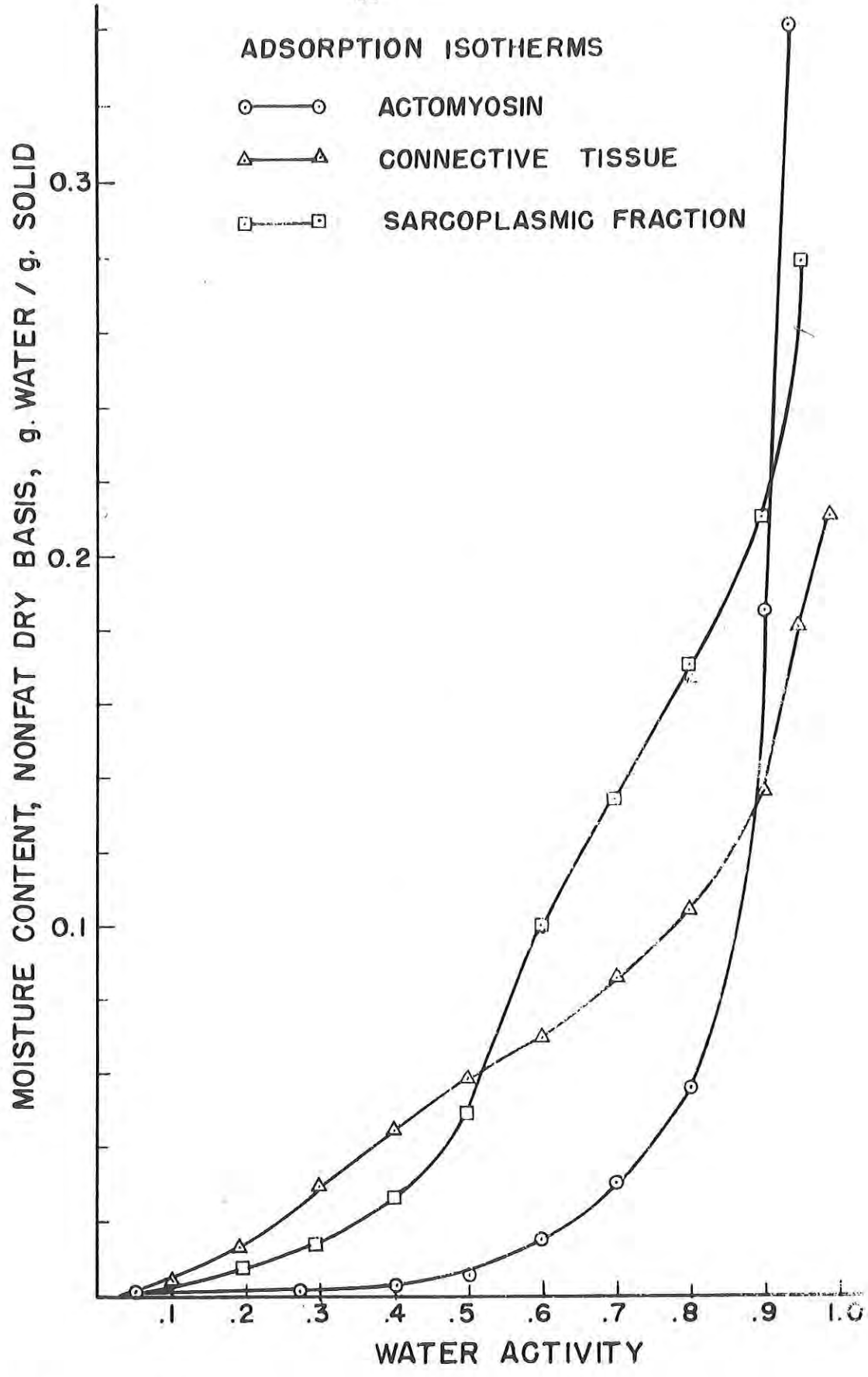

Figure 5-9 Moisture adsorption isotherms of major beef protein components at 70°F.

The influence of temperature on moisture adsorption isotherms is illustrated in Figure 5-10 for connective tissue at 52 and 70°F. The influence is as expected with the water activity decreasing from 0.77 to 0.65 at a moisture content of 0.1 g water per g solids as temperature was decreased from 70 to 52°F.

A comparison of the moisture adsorption isotherms for raw and precooked freeze-dried beef and the sarcoplasmic graction is presented in Figure 5-11. There are no significant differences in the amounts of moisture adsorbed by the raw and precooked freeze-dried products at any water activity selected, although the precooked product has a very typical sigmoid isotherm shape. Similarities between the isotherms for the sarcoplasmic fraction and the product (raw or precooked) exist only at water activities above 0.6. Reference to Figure 5-9 indicates that similarity between the connective tissue and raw-freeze-dried beef isotherms exists in the lower water activity range.

An examination of the moisture desorption isotherms for the sarcoplasmic fraction at 52 and 70°F (Figure 5-12) reveals a very abnormal shape. The influence of temperature is as expected, but the isotherm shapes indicate that large amounts of moisture are held by the component until the water activities are below 0.5. The results presented for the sarcoplasmic fraction are typical of the actomyosin and connective tissue fractions, also; revealing a very significant hysteresis effect.

The abnormal moisture desorption isotherm shape was not limited to the beef components as illustrated in Figure 5-13. Although the desorption isotherm for the precooked product exhibited a rather typical sigmoid shape, the desorption isotherm for the raw-freeze-dried product was very similar to isotherms obtained for product components. Again, relatively large amounts of moisture are held until the water activities are less than 0.5. These results tend to reveal the rather significant influence of heat on the moisture holding characteristics of beef components. There was no obvious difference in the moisture adsorption characteristics of raw and precooked beef, but significantly decreased capacity to hold moisture during desorption is observed for the precooked beef.

5.2. Verification of Isotherm Equation

5.2.1. Relationship to theory of moisture sorption. For the purposes of illustration, two sets of isotherms calculated with the volumetric equation 3-22 are presented in Figure 5-14. The specific adsorbed volume, V_a is plotted in its reduced form by dividing each calculated isotherm point by the corresponding calculated adsorbed volume at $P = 0.98\ P_o$. This reduction of all isotherm heights to 1 or 100% allows for a better comparison of characteristic forms of adsorption curves and facilitates the eventual matching of theoretical with experimental isotherms. The adsorbed volume at $P/P_o = 0.98$ is chosen as a relatively well defined point. In contrast, considerable doubt still exists among investigators (see for example Bangham and Sever, 1925) as to whether equilibrium is ever truly achieved at saturation. In consequence, the adsorbed volume at 100% relative humidity is not well defined. In these plots, the volumetric isotherm expression is chosen in preference to its gravimetric equivalent because it lends itself well for consideration on a

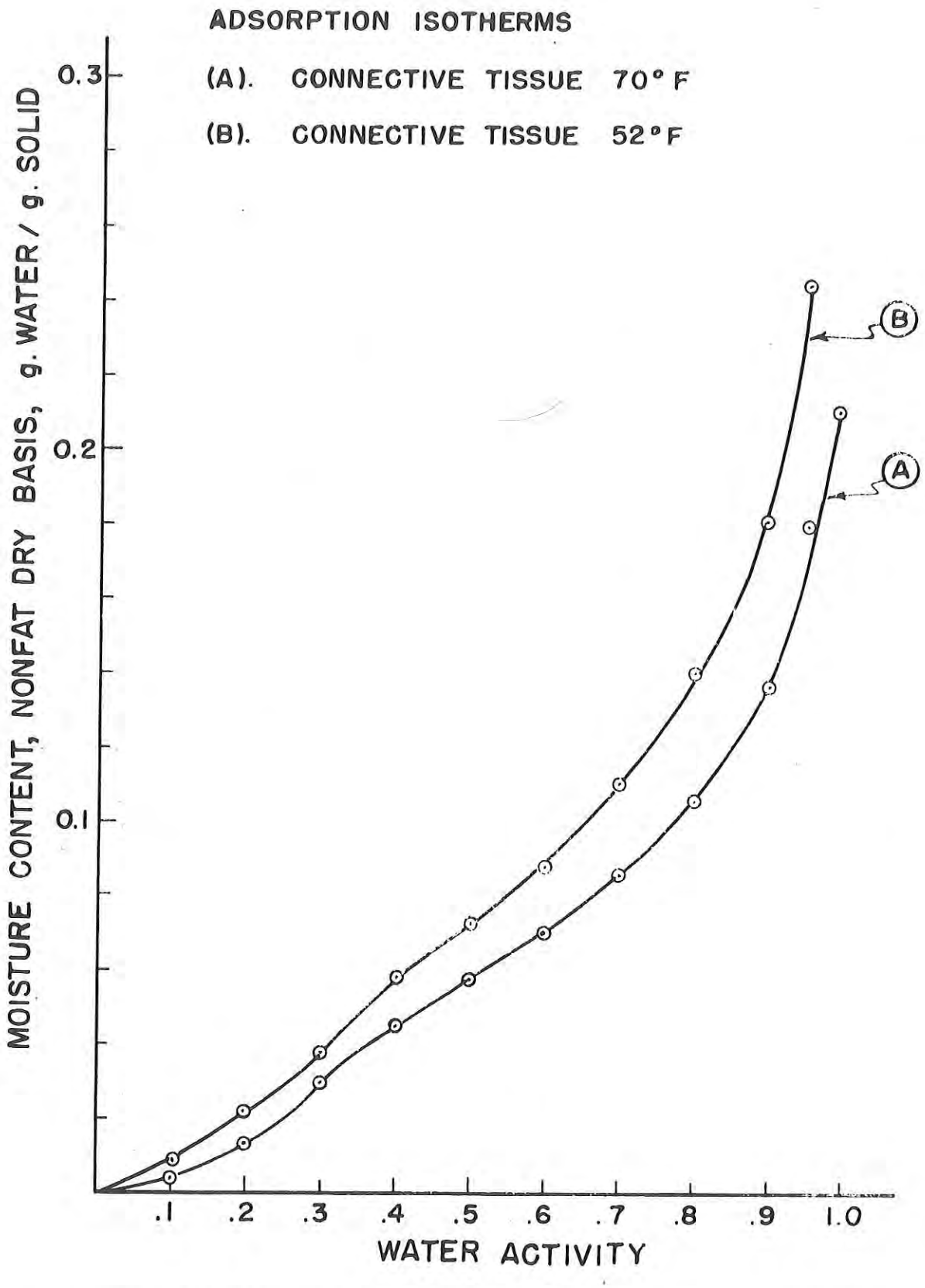

Figure 5-10 Influence of temperature on the moisture adsorption isotherms of connective tissue.

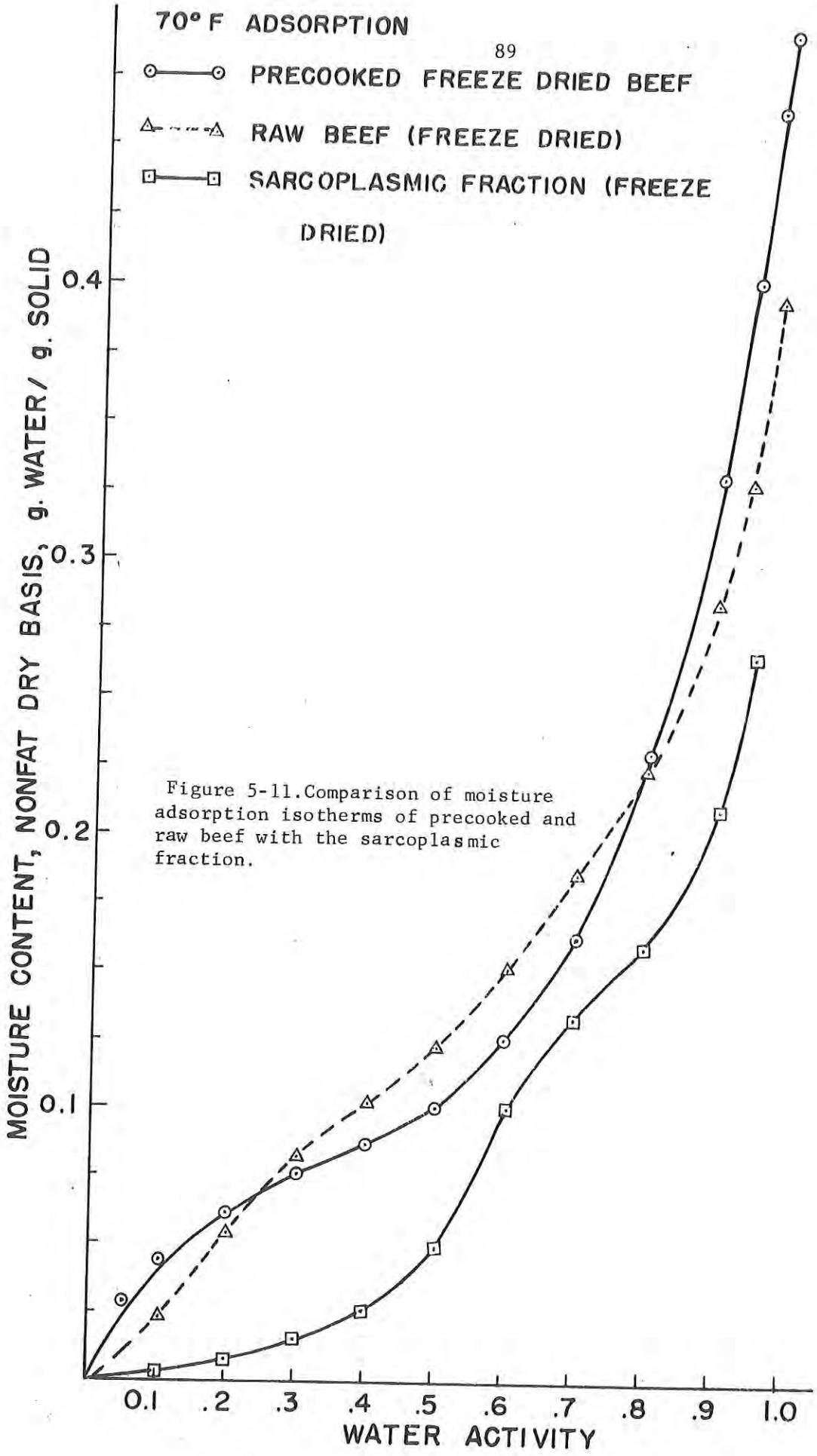

Figure 5-11. Comparison of moisture adsorption isotherms of precooked and raw beef with the sarcoplasmic fraction.

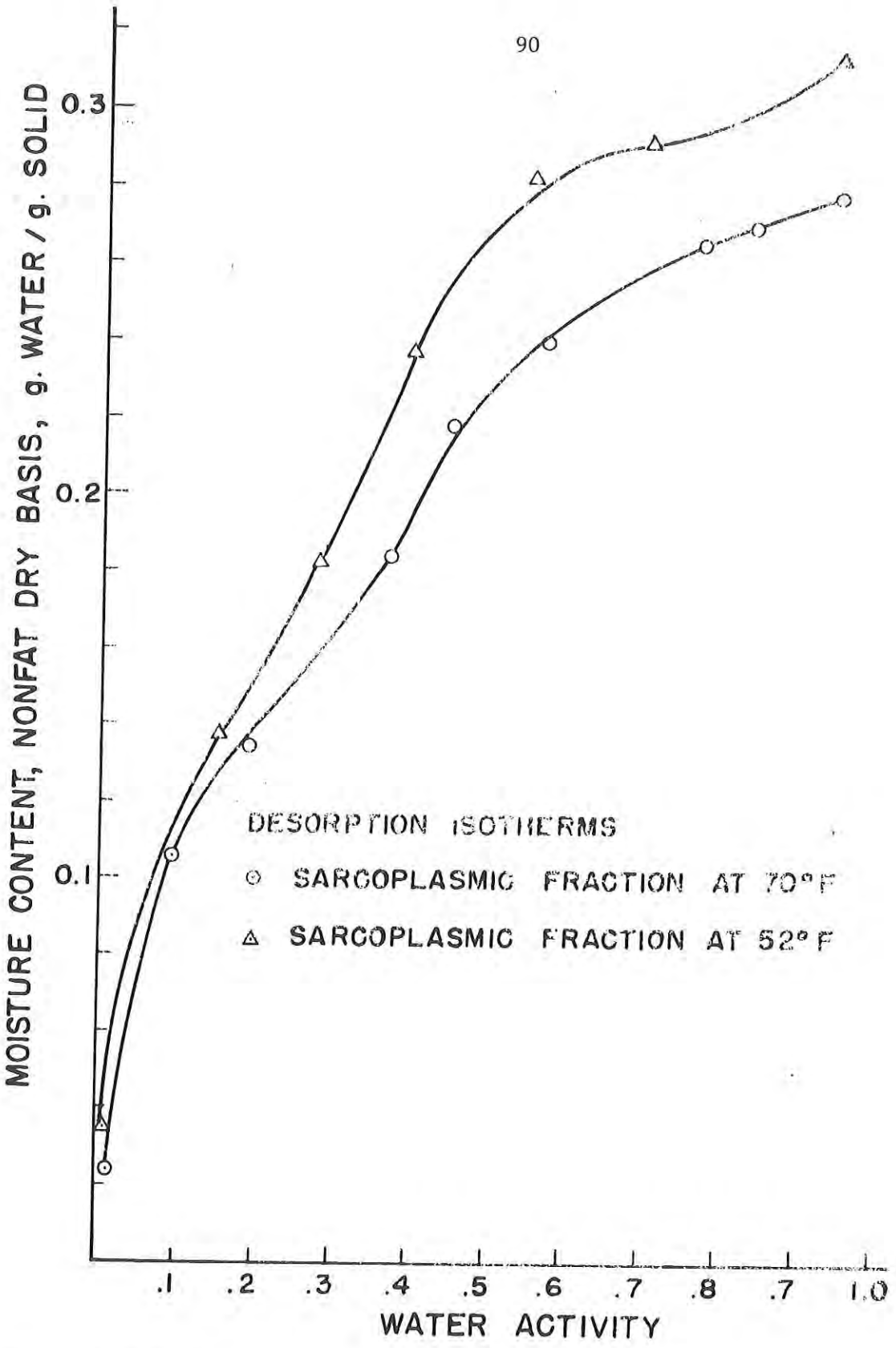

Figure 5-12 Influence of temperature on the moisture desorption isotherms of sarcoplasmic fraction.

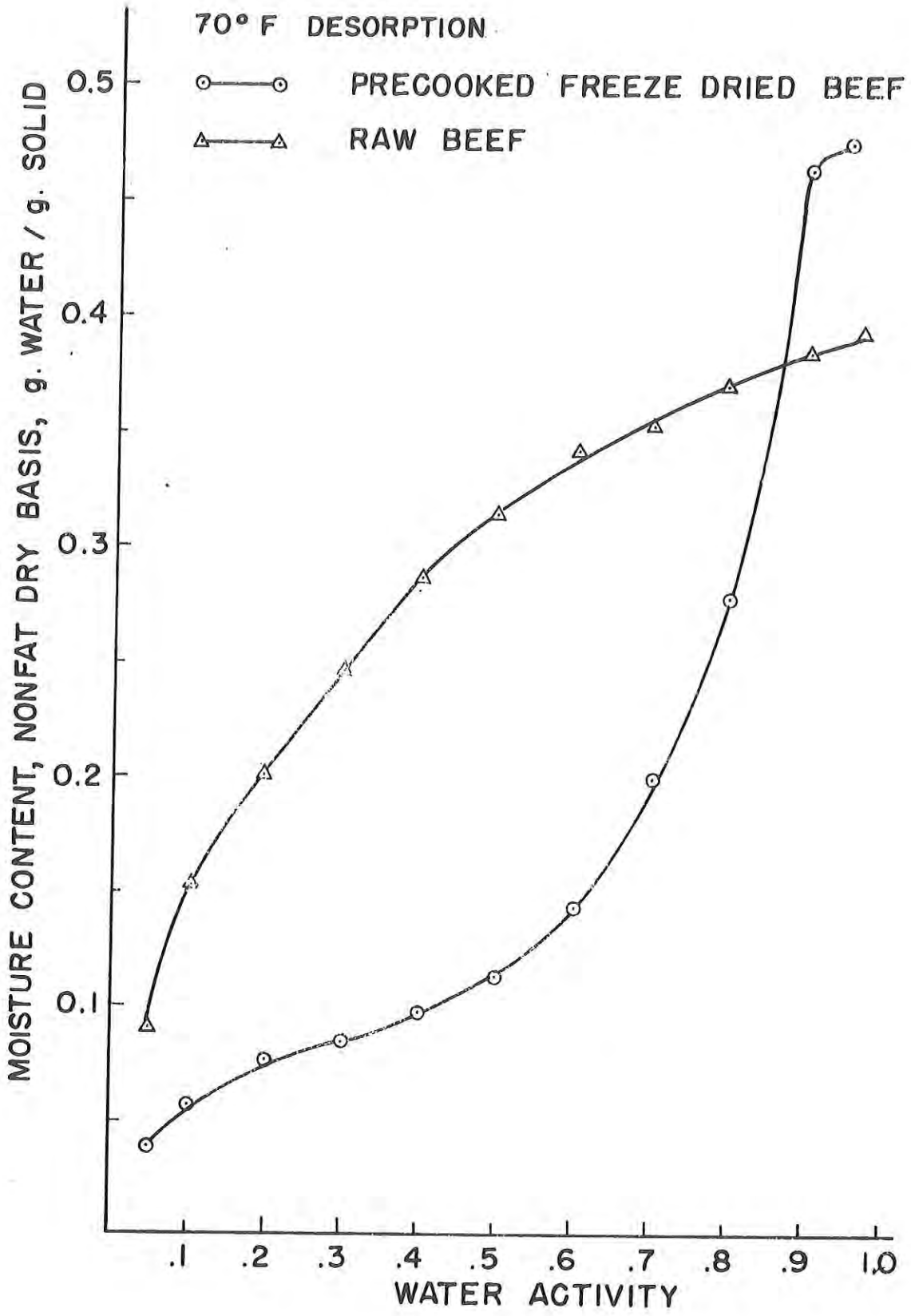

Figure 5-13 Comparison of moisture desorption isotherms of raw and precooked beef.

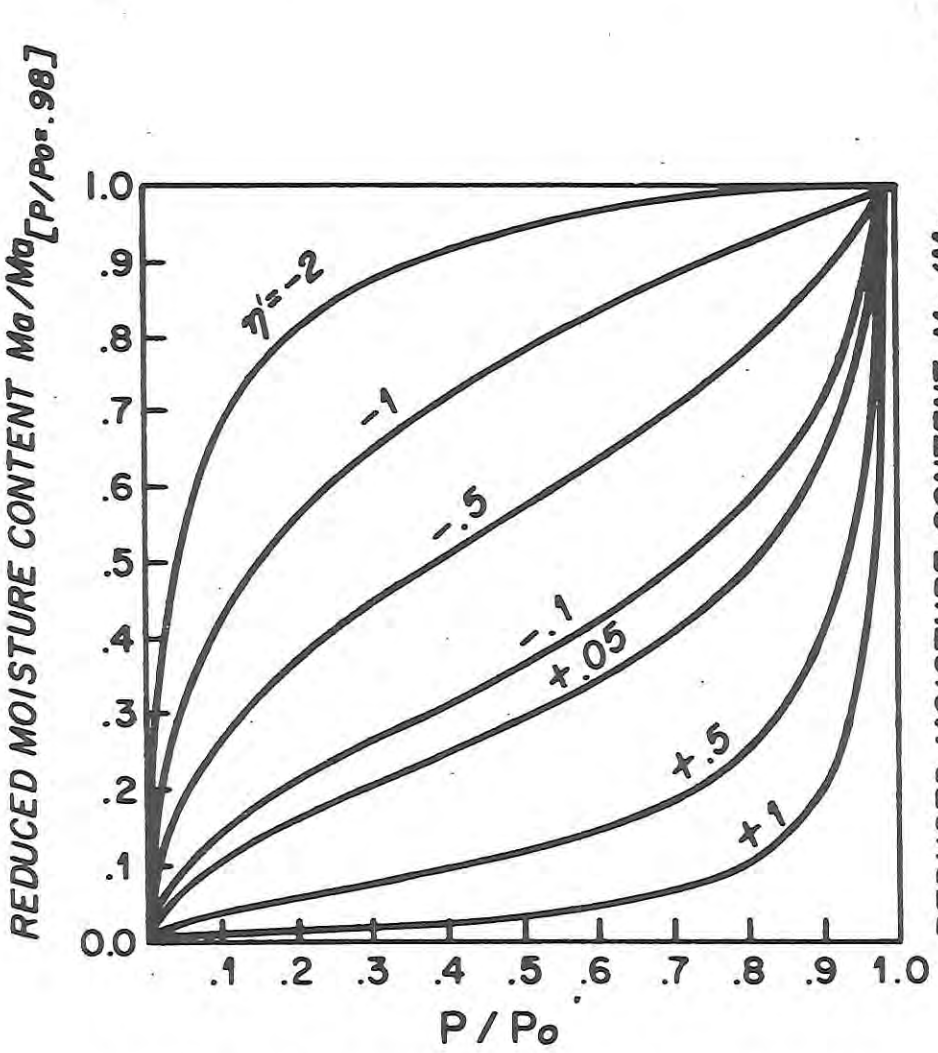

Figure 5-14.(a) Theoretical isotherms calculated with eqn. (3-22).

$P_m = (.008)P_o$, T = 10°C = 283°K

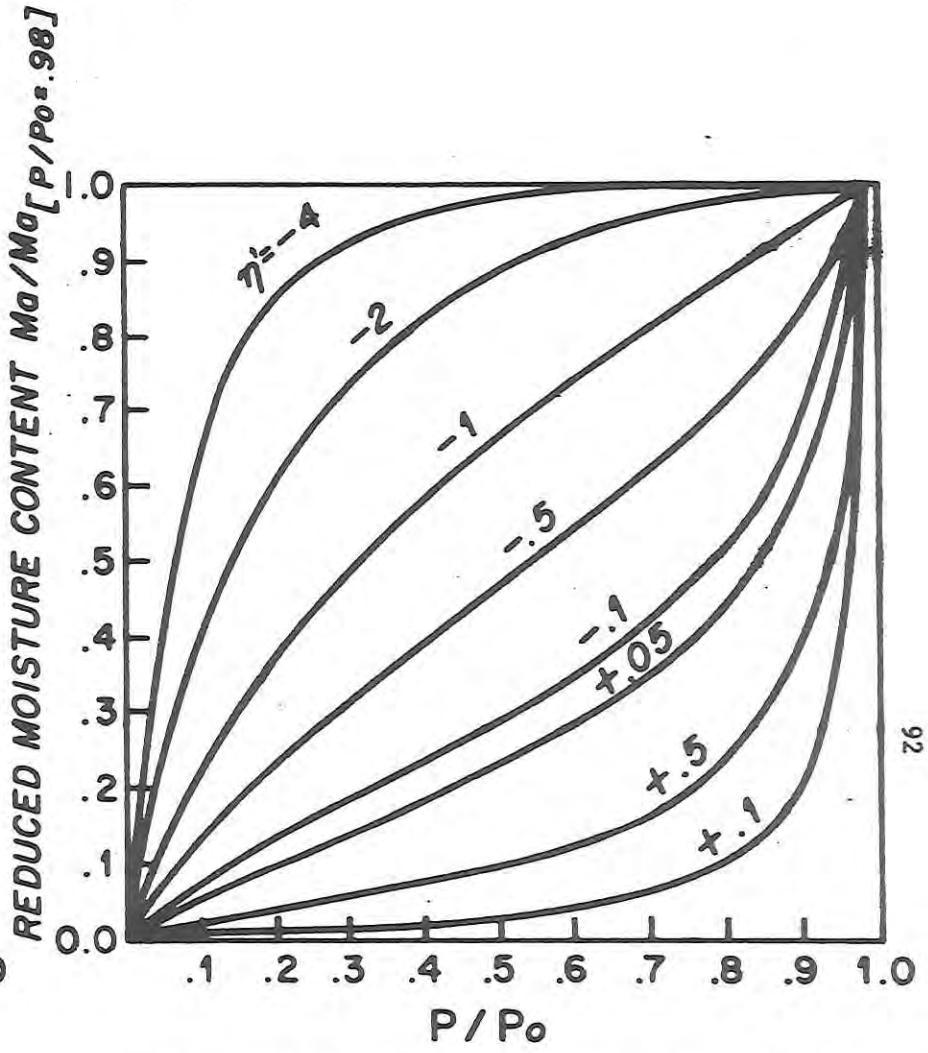

Figure 5-14.(b) Theoretical isotherms calculated with eqn. (3-22).

$P_m = (0.1)P_o$, T = 10°C = 283°K

general basis. The isotherm temperature used for the calculation of Figure 5-14 is 50°F. Two sets of theoretical curves are presented to illustrate the effect of the P_m value on the isotherm shape.

The curves are obviously very characteristic, showing (a) well defined initial "knees" at moderately positive values of η (the knees are clearly better defined at lower values of P_m, see Figures 5-14a and 5-14b), (b) certain linear parts, and (c) distinctive individual starting angles of the isotherms. All regular types of isotherms of the Brunauer classification are obtained merely by the variation of η. This finding not only appears to vindicate the leading premise of the generalized theory that the three basic concepts in adsorption are complementary, but also strengthens considerably, the significance of a purely power law distribution concept of pore-size.

5.2.2. The characteristic parameters of pore-structure -- η' and ξ. As the primary shape criterion for the sets of theoretical isotherms presented in Figure 5-14, η' may be viewed as the characteristic value representing the quantitative behavior of a porous sorbent at any relative vapor pressure. In the range $\eta' < 1$, the theoretical isotherms are clearly of the Langmuir-type. Sigmoid type II isotherms are defined in the range $-1 \leq \eta' \leq +1$; while η' values in the range, $\eta' > +1$, define type III isotherms. Since it is well recognized that the isotherms of most biological materials are sigmoid, it would seem logical that the main focus of the present investigation should be restricted to the intermediate range, $-\leq \eta' \leq +1$.

In equations (3.19) and (3.20), the parameters ξ and η' are defined respectively, as functions of the pore-size distribution parameters, K_1 and γ. From a detailed consideration of pore-size distributions in biological materials, Ngoddy (1969) has shown that the parameters, K_1 and γ, are both product and temperature dependent. Accordingly, the structural parameters, ξ and η', are uniquely defined not only for each sorbent system but also for each isotherm temperature. The temperature dependence of these parameters, demonstrate that considerable thermo-induced changes do take place in the sorbent pore structure during the adsorption process.

5.2.3. Prediction of adsorption isotherms. For our present purposes, the structural parameters, ξ and η', are empirically defined. To determine η' for a specific product and temperature, the empirical isotherm in its reduced volumetric form is superposed on a set of theoretical isotherms such as shown in Figure 5-14. The best matching η' and P_m values are thus selected. Based on these values of η' and P_m, the function

$$\left[\frac{Z^{\eta'} - \lambda}{\eta'}\right]$$

is defined for each relative vapor pressure. Combining the approximate density term, $\rho_1 \xi$ [based on Equation (3.28)], with the above function, the best fitting average ξ value, $\bar{\xi}$, is defined. It is now possible to define for each P/P_o value, the first approximation of the specific adsorbed mass defined by:

$$\rho_1 \cdot \bar{\xi}\left[\frac{Z^{\eta'} - \lambda^{\eta'}}{\eta'}\right]$$

The discrepancy between this approximate value and its empirical counterpart is minimized by the careful correction of the density term. This gives rise to a new set of density values, designated as ρ_2.

In Tables 5-1 to 5-4, the relevant parameters for raw freeze-dried beef slices (50°F and 104°F) and precooked freeze-dried beef powder (50°F and 100°F) are shown. The quantity,

$$\overline{\xi}\ \rho_2\ \left[\frac{z^{n'} - \gamma^{n'}}{n'}\right]$$

in each table represents the best prediction possible for the product and temperature under consideration. Predicted isotherms based on these tables are represented in Figures 5-15 and 5-16. The plots together with the standard error of estimates shown on each table are well within the limits of variability to be expected on account of the highly specific character of biological materials.

Because our present method of determining isosteric heat values by employing the Clausius-Clapeyron equation and the slopes of the so-called sorption isosteres, has well recognized inherent errors (Brunauer, 1945; Chapter 8, Ross and Oliver, 1964), the corrected density term, ρ_2, is justified. It is also clear that ρ_2, not only satisfies the essential implications of the adsorption potential theory, but also reflects the correct temperature dependence of the isosteric heat of sorption.

From Tables 5-1 to 5-4, n' and ξ, are both seen to increase with rising isotherm temperature. This trend indicates a progression from smaller to larger pores as the isotherm temperature rises. While a purely temperature-induced change in the sorbent pore structure may not seem very probable, Hammerle (1968) has shown that the so-called hydro-expansion in bio-materials is considerably temperature dependent. If the n' and $\overline{\xi}$ parameters for several biological materials are defined over a wide enough temperature range, the temperature dependence of these parameters can be formalized either on a general or specific basis, as a logical extension of the present work.

It is apparent from the Tables 5-1 to 5-4 that the parameter, P_m, as used in this study is quite different from the actual pressure corresponding to the mono-layer capacity. Part of this discrepancy can be traced back to the transformation of coordinate axes which became necessary in the original formulation. It appears that in the attempt to systematize the plots of the derived isotherm equation, the actual physical significance of P_m has been sacrificed.

5.3. Heat Sinks for Microcalorimeters

The computer program was utilized to test the effect of eleven design parameters of the metallic heat sinks for microcalorimeters. The parameters investigated include: the kind of metal in the sink, the heat transfer coefficient from the ambient to the sink, the external temperature control, the diameter of the sink, the distance between the center of the chamber and the center of the sink, the diameter of the chambers, the heat capacity of the twin reaction vessels, the amount of heat generated by the reaction, the length of the reaction, the overall heat transfer coefficient between the reaction vessel and the sink, and also the Calvet measurement configuration was compared

Table 5-1. Calculation of theoretical isotherm.

Product = raw freeze-dried beef slices
(Data taken from Saravacos, 1965)

Isotherm temperature = 50 °F.

P/P_o	M_a (Exptl.)	ρ_1	$\bar{\xi}$ = .1047	$[\frac{Z^{\eta'}-\lambda^{\eta'}}{\eta'}]$ $\eta' = 0.01$ $P_m = 0.10$	ρ_2	$\bar{\xi}\rho_2[\frac{Z^{\eta'}-\lambda^{\eta'}}{\eta'}]$	Error
.1	.030	1.360	"	.214	1.382	.030	.000
.2	.060	1.360	"	.390	1.382	.055	+.005
.3	.080	1.316	"	.556	1.382	.080	.000
.4	.100	1.316		.724	1.351	.101	-.001
.5	.120	1.316		.906	1.294	.121	-.001
.6	.142	1.164		1.110	1.241	.143	-.001
.7	.170	1.164		1.370	1.204	.172	-.002
.8	.200	1.164		1.710	1.132	.202	-.002
.9	.250	1.126		2.280	1.064	.253	-.003
.95	.310	1.062		2.860	1.050	.313	-.003
.98	.375	1.00	"	3.630	1.00	.38	-.005

Standard Error Estimate = ±0.0027

Table 5-2. Calculation of theoretical isotherm.

Product = raw freeze-dried beef slices (Saravacos, 1965)

Isotherm temperature = 104°F

P/P_o	M_a (Exptl.)	ρ_1	$\bar{\xi}$ = .136	$[\frac{z^{\eta'}-\lambda^{\eta'}}{\eta'}]$ η = .04 P_m = .10	ρ_2	M_a (Theoretical) $=\bar{\xi}\rho_2[\frac{z^{\eta'}-\lambda^{\eta'}}{\eta'}]$	Error
.1	.027	1.36	"	.126	1.600	.027	.000
.2	.050	1.36	"	.230	1.600	.049	+.001
.3	.065	1.316		.329	1.520	.066	-.001
.4	.080	1.316		.430	1.380	.080	.000
.5	.090	1.316		.539	1.270	.092	-.002
.6	.100	1.164		.666	1.145	.103	-.003
.7	.120	1.164		.821	1.145	.127	-.007
.8	.155	1.164		1.030	1.145	.160	-.005
.9	.215	1.126		1.400	1.145	.217	-.002
.95	.250	1.062		1.770	1.076	.258	-.008
.98	.300	1.000	"	2.280	1.000	.310	-.010

Standard Error Estimate = ±0.0048

Table 5-3. Calculation of theoretical isotherm.
Product = pre-cooked freeze-dried beef powder
Isotherm temperature = 50 °F.

P/P_o	M_a (Exptl.)	ρ_1	$\bar{\xi}$ = .454	$[\frac{Z^{\eta'}-\lambda^{\eta'}}{\eta'}]$ $\eta' = 0.1$ $P_m = 0.01$	ρ_2	$\bar{\xi}\rho_2[\frac{Z^{\eta'}-\lambda^{\eta'}}{\eta'}]$	Error
.1	.070	1.360	"	.0957	1.612	.070	.000
.2	.095	1.360	"	.1450	1.451	.095	.000
.3	.110	1.316	"	.1870	1.302	.110	.000
.4	.122	1.316	"	.2290	1.160	.132	-.010
.5	.135	1.316	"	.2750	1.160	.144	-.009
.6	.155	1.164	"	.3260	1.160	.171	-.016
.7	.191	1.164	"	.3900	1.160	.205	-.014
.8	.260	1.164	"	.4790	1.160	.252	-.008
.9	.380	1.126	"	.6350	1.160	.334	+.056
.95	.450	1.062	"	.7990	1.160	.420	+.030
.98	.483	1.00	"	1.0400	1.023	.483	.000

Standard Error Estimate = ±.0064

Table 5-4. Calculation of theoretical isotherm

Product = pre-cooked freeze-dried beef powder

Isotherm temperature = 100°F

P/P_o	M_a (Expt1.)	ρ_1	$\bar{\xi}$ =1.26	$[\frac{z^{n'}-\lambda^{n'}}{n'}]$ $n' = 0.2$ $P_m = 0.1$	ρ_2	$\bar{\xi}\rho_2[\frac{z^{n'}-\lambda^{n'}}{n'}]$	Error
.1	.0209	1.360	"	.0089	1.844	.020	+.009
.2	.0309	1.360	"	.0165	1.532	.031	.000
.3	.0391	1.316	"	.0240	1.292	.039	+.000
.4	.0500	1.316		.0319	1.248	.049	+.001
.5	.0591	1.316		.0407	1.248	.063	-.004
.6	.0791	1.164		.0512	1.248	.079	.000
.7	.1020	1.164		.0648	1.248	.100	+.002
.8	.1410	1.164		.0844	1.248	.132	+.009
.9	.2000	1.126		.1210	1.248	.190	+.01
.95	.2410	1.062		.1620	1.248	.254	-.013
.98	.2860	1.000	"	.2260	1.000	.284	+.002

Standard Error Estimate = ±.0064

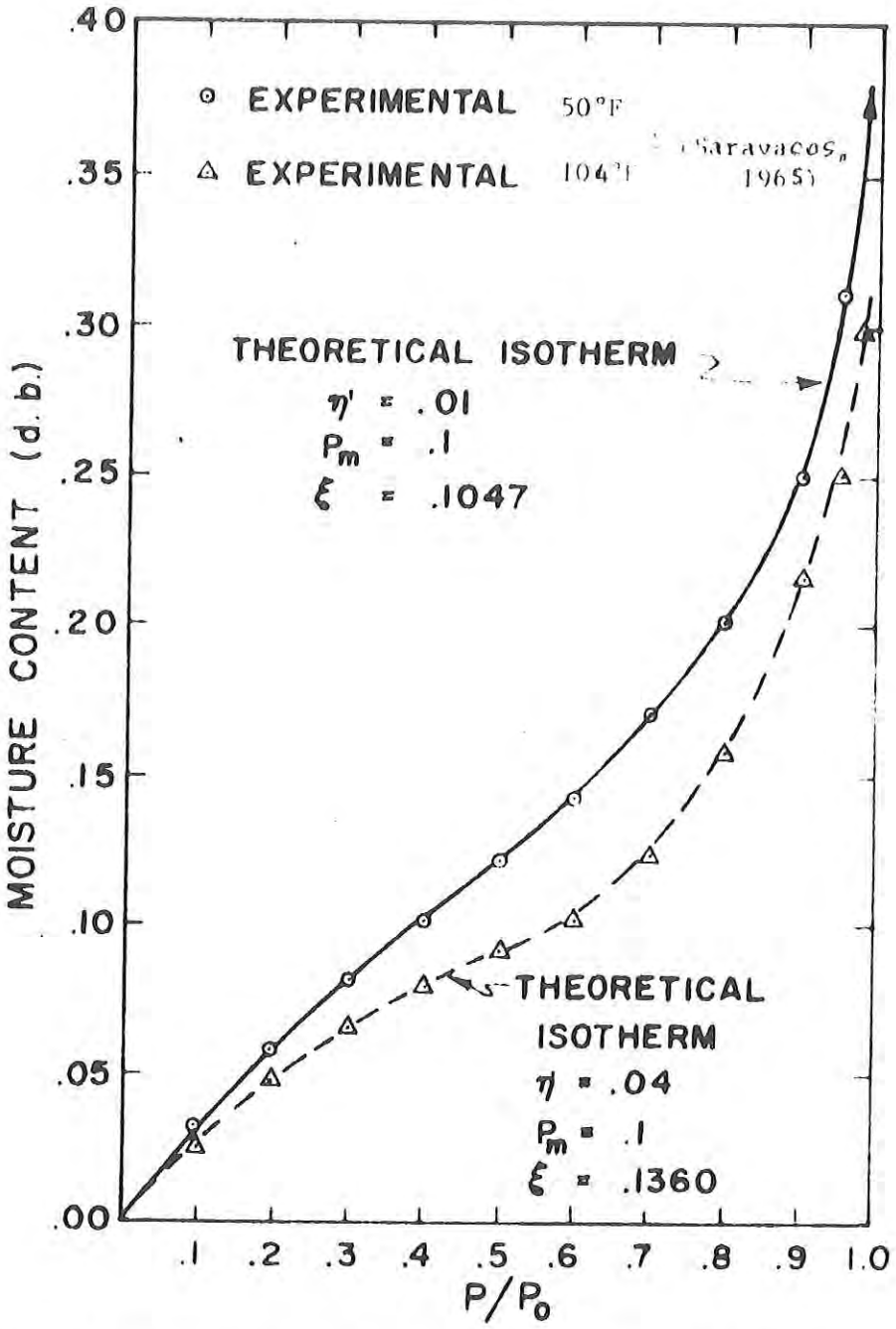

Figure 5-15. Comparison of experimental adsorption isotherm with calculated adsorption isotherms for raw freeze-dried beef in slices.

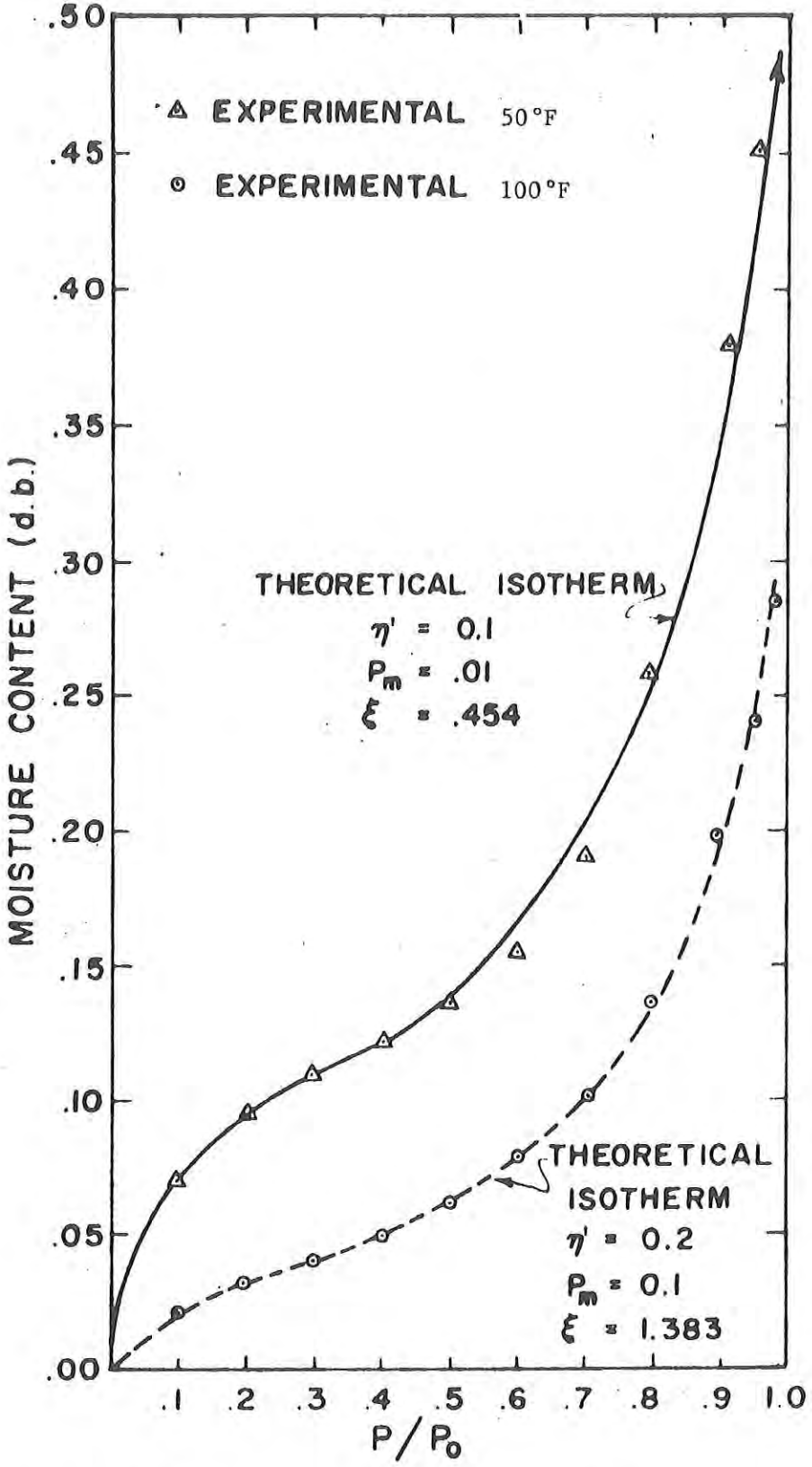

Figure 5-16. Comparison of experimental adsorption isotherms with calculated isotherms for pre-cooked freeze-dried beef powder.

with the configuration that has been proposed by Berger et al. (1968). In the Berger instrument both the reaction and reference vessles are located in a common oval cavity in the heat sink and only the temperature difference between the two vessels is measured. (A computer program is available to adjust the data of the Berger instrument for heat loss.)

The model was initially solved and then each of the parameters were individually varied the the model was resolved. Because of the large number of parameters very few of the inter-relationships were investigated. The study was restricted to the two-dimensional model of the sink. In effect, the model simulated a sink and twin reaction vessels of infinite length. In a real sink that totally encloses the twin vessels the relative error should be slightly less than was predicted by the model. The magnitude of this error was not investigated. The initial or standard conditions are listed at the bottom of Table 5-5, which summarizes the results of the investigation. The assumed functional form of the reaction heat is shown in Figure 5-17. The significance of the relative error depends on the measurement to be made with the instrument. For very precise measurements an error of 0.1% could be significant. However, for heat of immersion and for any measurements on biological materials the same error can usually be neglected. Therefore, for these measurements the standard aluminum sink is adequate.

Calvet and Pratt (1963) reported employing a silver sink with one of his microcalorimeters. The results in Table 5-5 show that a copper sink would provide approximately the same accuracy. The radiation heat transfer between the copper sink and the reaction vessels would be higher than with the silver, but if this was a serious disadvantage the copper could be plated with chromium or gold.

The heat transfer coefficients can have an important influence on the relative error. The effect of increasing the external heat transfer coefficient by a factor of 800 was only about one-tenth as large as the effect of increasing the internal heat transfer coefficients by a factor of four. However, if the external temperature was not uniform then the magnitude of the external heat transfer coefficient was very important.

Changes in the physical size caused only small variations in the relative error; increasing the diameter of the cavities by one centimeter, decreasing the distance between the cavities by two centimeters or decreasing the diameter of the sink by four centimeters changed the relative error by only 0.03 percent.

Variations in the physical size of the sink had only a small effect on the relative error in the two dimensional model. Changes in the third dimension, therefore, are not expected to be important either. This provides some justification for studying only the two dimensional problem also it indicated that the elaborate sinks reported by Calvet and Pratt (1963) are very little better than the simple cylindrical block employed by Berger et al. (1968).

Changes in the heat capacity of the reaction vessel, the amount of heat produced or the length of the reaction did not alter the relative error significantly.

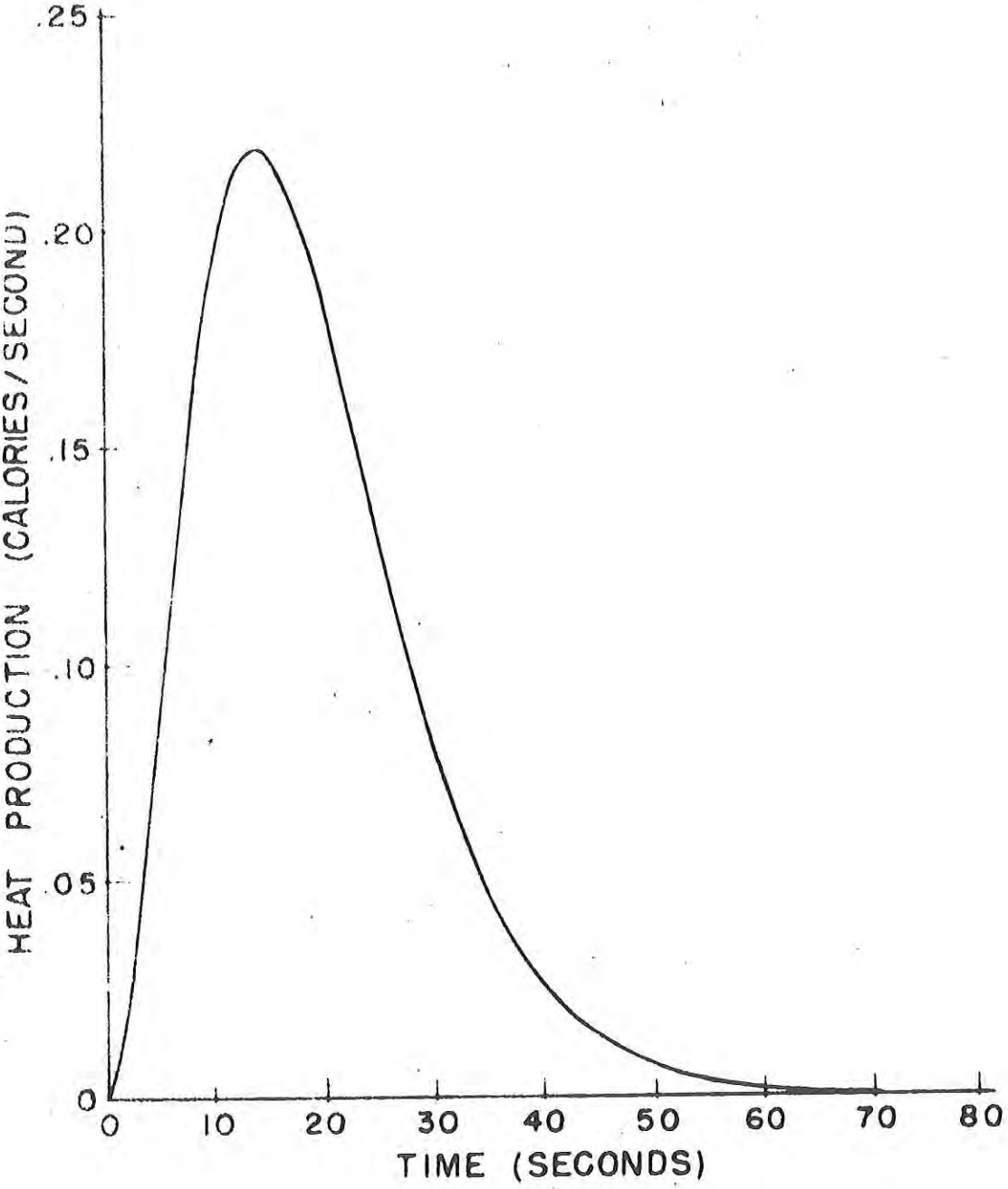

Figure 5-17. The Assumed Functional Form of the Reaction Heat.

TABLE 5-5. The maximum relative errors introduced by the non-ideal sink.

Parameter Varied	Predicted Maximum Per Cent Error
Standard conditions*	0.104
Silver heat sink	0.054
Copper heat sink	0.058
External heat transfer coefficient increased to 0.0136 cal./°C-cm^2-sec.	0.092
External heat transfer coefficient increased to 0.1 cal./°C-cm^2-sec.	0.067
Silver heat sink with external heat transfer coefficient of 0.0136 cal./°C-cm^2-sec.	0.050
Copper heat sink with external heat transfer coefficient of 0.0136 cal./°C-cm^2-sec.	0.054
Vary external temperature 0.1° C across the sink	0.126 or 0.082
Copper sink with external temperature varied 0.1° C and external heat transfer coefficient of 0.0136 cal./°C-cm^2-sec.	0.938
Copper sink with temperature variation and external heat transfer coefficient of 0.1 cal./°C-cm^2-sec.	3.56
Diameter of sink reduced to 16 cm.	0.131
Distance to cavity center reduced to 3 cm.	0.077
Diameter of cavity increased to 6 cm.	0.136
Size of reaction vessel reduced such that heat capacity is 6 cal./°C.	0.103
Heat of reaction reduced by a factor of 10	0.105
Reaction rate reduced by a factor of 10	0.099
Internal heat transfer coefficient increased to 0.001 cal./°C-cm^2-sec.	0.417
Berger Measurement technique	10

*The standard conditions were: an aluminum sink 20 cm in diameter with cavities 5 cm in diameter and located 4 cm off center. The heat transfer coefficients to the ambient and cups were 1.36×10^{-4} and 2.71×10^{-4} cal./°C-cm^2-sec., respectively. The heat capacity of each vessel was 15 cal./°C. Five cal. of heat was added during a period of 90 sec. The ambient was a uniform 0°. The Calvet measurement technique was simulated.

The large relative error shown in Table 5-5 for the Berger measurement technique does not reflect on the accuracy of this instrument. It does mean that data collected from similar instruments must be corrected for heat transfer. The thermocouple arrangement in the Berger instrument is easier to construct than the Calvet arrangement; however, it is necessary to apply corrections to the data collected from the Berger instrument but not to data from the Calvet.

It is unlikely that the sink simulated in this study would be the one needed for any particular microcalorimeter design. Therefore, the results are of limited value by themselves. However, they do provide evidence that any sink design should be checked for its effectiveness before the microcalorimeter is built. Faulty design can lead to large errors or to excessive construction costs. On the other hand, this model has shown that a well designed sink can reduce the associated errors to a negligible level without complicating the design.

5.4. Indirect Prediction of Heats of Immersion in Foods

Thermodynamic treatment of moisture sorption of biological products would be simplified and more meaningful if the effective molecular weight of solids (EMW_s) in the biological substances was known. Among the possible methods of estimating the effective molecular weight are the colligative properties such as freezing point depression, boiling point elevation and osmotic pressure measurements, are commonly used for pure substances. In this investigation the Raoult's law was used at higher relative humidities to compute the effective molecular weight of solids. The computation of the effective molecular weight and other thermodynamic qualities is illustrated as follows.

5.4.1. Computation procedure. The following example will illustrate the procedures used to compute total heats of sorption (ΔH_T) by the proposed method. The example will utilize equilibrium moisture adsorption data (Figure 5-3) for precooked freeze-dried beef at 72°F (plate temperature 145°F).

1. Computation of effective molecular weight (EMW_s)
   a. From the equilibrium moisture isotherms, the moisture content at the water activity of 0.95 is equal to 37.5 g water/100 g NFDM.
   b. Using Raoult's Law (equation 3.54)

$$X_w = \frac{P}{P_o} = 0.95$$

   c. Using equation (5-8) for mole fraction

$$.95 = \frac{\frac{37.5}{18}}{\frac{37.5}{18} + \frac{100}{EMW_s}}$$

Solving above, $EMW_s = 057.98$ for $X_w = 0.95$.

2. Computation of mole fraction of water (X_w) and mole fraction of solids (X_s) for a series of water activities.

By knowing the effective molecular weight of solids (950) and a given composition (a_w = 0.5, M = 8.5 g water/100 g NFDM) and using equation (5-8):

$$X_w = \frac{\frac{8.5}{18}}{\frac{8.5}{18} + \frac{100}{950}} = 0.818$$

and

$$X_s = \frac{\frac{100}{950}}{\frac{8.5}{18} + \frac{100}{950}} = 0.182$$

3. Computation of activity coefficient for water (γ_w).

The activity coefficient of water is expressed in terms of activity of water (a_w) and mole fraction of water (X_w) similar to equation (5-9) as follows:

$$\gamma_w = \frac{a_w}{X_w} = \frac{0.5}{.818} = 0.611$$

Values of γ_w at each moisture level are presented in Table 5-6.

4. Activity coefficient of solids (γ_s)

The calculation of activity coefficient of solids involves the integration of the Gibbs-Duhem equation (5-10). The integration of equation (5-10) was carried out by CDC 3600 digital computer. Figure 5-18 illustrates the method of integration. Results presented in Table 5-7 show the thermodynamic parameters obtained for the moisture equilibrium isotherm of precooked freeze-dried beef (plate temperature 145°F). In order to find the lower limit of integration of equation (5-9), the standard state of beef solids was considered as dry beef solids (low moisture content). Therefore the activity of precooked freeze-dried beef with moisture content of 2.7 g water/100 g NFDM corresponding to $\frac{P}{P_0}$ = 0.05 was considered to be equal to one. Equation (5-9) was utilized to calculate the activity coefficient of solids (γ_s). For the moisture content of 2.1 g water/100 g NFDM, X_s = 0.474 (Table 5-7); therefore the activity coefficient of solids at the standard state is:

$$\gamma_s = \frac{1}{0.474} = 2.109, \text{ where } \frac{X_w}{X_s} = 1.108$$

Above values fix the lower limit of integration and the constant of integration in equation (5-10) as follows:

Table 5-6. --Adsorption equilibrium moisture isotherm data for precooked freeze-dried beef (plate temperature 145°F) and some thermodynamic quantities.

$\frac{P}{P_0}$	M	X_w	X_s	$\frac{-X_w}{X_s}$	γ_w	$Ln\gamma_w$
0.050	2.100	0.526	0.474	-1.108	0.095	-2.353
0.100	3.200	0.628	0.372	-1.689	0.159	-1.838
0.150	4.300	0.694	0.306	-2.269	0.216	-1.532
0.200	5.200	0.733	0.267	-2.744	0.273	-1.299
0.300	6.400	0.772	0.228	-3.378	0.389	-0.945
0.400	7.100	0.789	0.211	-3.747	0.507	-0.680
0.500	8.500	0.818	0.182	-4.486	0.611	-0.492
0.600	10.900	0.852	0.148	-5.753	0.704	-0.351
0.700	14.200	0.882	0.118	-7.494	0.793	-0.231
0.800	18.400	0.907	0.093	-9.711	0.882	-0.125
0.900	27.400	0.935	0.065	-14.461	0.962	-0.038
0.950	35.700	0.950	0.050	-18.842	1.000	0.000

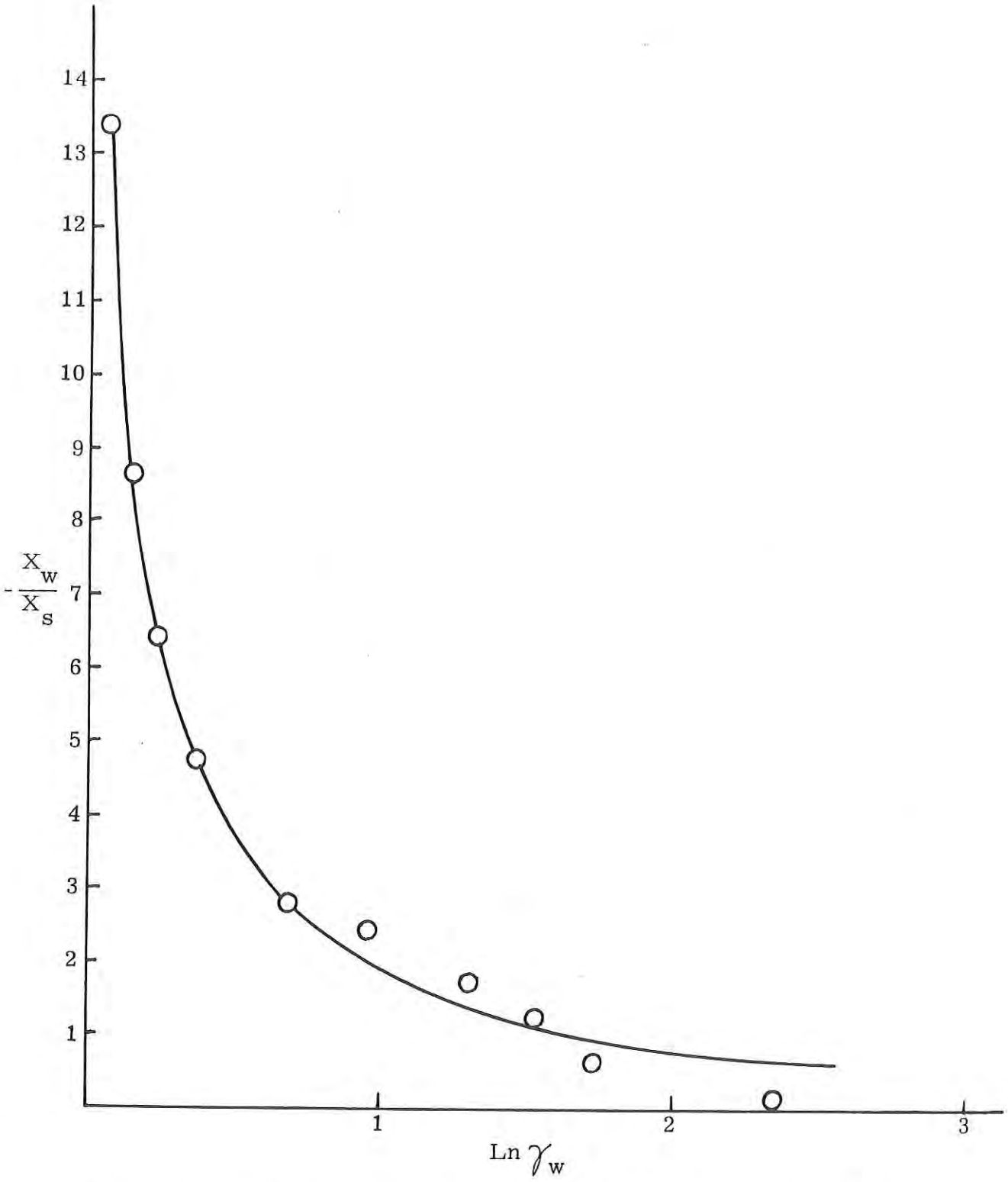

Figure 5-18 --Evaluation of activity coefficient for solids (γ_s) of precooked freeze-dried beef (plate temperature 105°F) by graphical integration.

Table 5-7 --Some thermodynamic parameters of precooked freeze-dried beef (plate temperature 145°F).

P/P_0	M	a_s	γ_s	$-\tilde{\Delta}G_m$	$\tilde{\Delta}S_m$	$-\tilde{\Delta}H_m$	$\overline{\Delta G_m}$	$\overline{\Delta S_m}$	$-\overline{\Delta H_m}$	$\overline{\Delta H_w}$
.05	2.1	1.000	2.106	923.701	1.375	517.595	2.008	.003	1.126	53.6
.1	3.2	0.381	1.026	1058.510	1.312	671.011	2.903	.004	1.841	57.5
.15	4.3	0.171	.560	1088.829	1.224	727.321	3.593	.004	2.401	55.8
.2	5.2	0.083	.312	1081.050	1.153	740.512	4.050	.004	2.775	53.4
.3	6.4	0.024	.106	1043.888	1.068	728.455	4.521	.005	3.156	49.3
.4	7.1	0.009	.041	1011.024	1.023	708.881	4.717	.005	3.308	46.6
.5	8.5	.003	.019	938.351	0.994	644.774	4.994	.005	3.512	41.3
.6	10.9	.001	.009	828.398	0.833	582.372	5.310	.005	3.733	34.2
.7	14.2	.0009	.004	710.537	0.720	497.855	5.563	.006	3.899	27.5
.8	18.4	.0006	.002	598.547	0.617	416.317	5.700	.006	3.967	21.6
.9	27.4	.0004	.001	443.902	0.476	303.316	5.671	.006	3.875	14.1
.95	35.7	.0002	.0008	355.958	0.397	238.705	5.470	.006	3.676	10.3

$$\ln \gamma_s = \int_{1.108}^{\frac{X_w}{X_s}} - \frac{X_w}{X_s} \quad \text{Ln}_{w} + \text{Ln } 2.106$$

The γ_s values at each moisture level are tabulated in Table 5-7. For example, at $a_w = 0.5$ the $\gamma_s = 0.019$ and

$$a_s = X_s \cdot \gamma_s \qquad \text{(equation 5-9)}$$

$$= (0.182)(.019) = .003$$

5. Computation of $\tilde{\Delta G}_m$, $\tilde{\Delta H}_m$ and $\tilde{\Delta S}_m$

From previous computations, all parameters in equations (5-6), (5-7) and (5-11) are known.

a. Molar free energy of mixing ($\tilde{\Delta G}_m$) is calculated by using equation (5-6):

$$\tilde{\Delta G}_m = (1.98726)(295.35)\ [0.818 \text{ Ln } (0.5) = 0.182 \text{ Ln } (.003)]$$

$$= -938.351 \text{ cal/g mole of mixture}$$

b. Using equation (5-7), the molar entropy of mixing was computed:

$$\tilde{\Delta S}_m = -(1.98726)\ [0.181 \text{ Ln } (.818) + .182 \text{ Ln } (.182)]$$

$$= 0.994 \text{ cal/g mole of mixture/°K}$$

c. Using equation (5-11), the molar enthalpy of mixing was computed:

$$\tilde{\Delta H}_m = -938.351 + 295.35\ (0.994)$$

$$= 644.744 \text{ cal/g mole of mixture}$$

6. Computation of $\overline{\Delta G}_m$, $\overline{\Delta H}_m$ and $\overline{\Delta S}_m$

The thermodynamic quantities expressed on molar basis are converted to mass basis by utilizing the quantity ($X_w \cdot MW_w + X_s \cdot EMW_s$) as a conversion factor.

$$\overline{\Delta G}_m = \frac{-938.351}{(0.818)(18) + (.182)(950)}$$

$$= 4.944 \text{ cal/g product}$$

Similarly $\overline{\Delta S}_m = .005$ cal/g product /°K and $H_m = 3.512$ cal/g product were obtained.

7. Computation of $\overline{\Delta H}_w$ and $\overline{\Delta H}_T$

a. The moisture content value was used to express the heat of adsorption values in terms of water as follows:

$$\overline{\Delta H}_w = \frac{\overline{\Delta H}_m}{0.085} = \frac{3.512}{.085} = 41.3 \text{ cal/g water}$$

b. The total enthalpy of adsorption is computed by adding the latent heat of condensation to the $\overline{\Delta H_w}$ value:

$$\overline{\Delta H_T} = 41.3 + 583.6 = 624.9 \text{ gal/g water}$$

The results obtained in this portion of the investigation will be presented as total enthalpy $(\overline{\Delta H_T})$ (cal/g water) versus moisture content in most cases. The total enthalpy value $(\overline{\Delta H_T})$ represents the sum of $\overline{\Delta H_w}$ and the latent heat of vaporization or condensation.

5.4.2. The Clausius-Clapeyron method and the Othmer procedure. Figure 5-19 shows the $(\overline{\Delta H_T})$ values for moisture adsorption for precooked freeze-dried beef (plate temperature 105°F) as determined by using the Clausius-Clapeyron method and the Othmer method (1940). As expected, the $\overline{\Delta H_T}$ decreased from about 1250 to 600 cal/g water as the moisture content increased from 2.5 to 30 percent (g water/100 g NFDM). At lower moisture levels, values were significantly higher and approached the latent heat of vaporization for pure water as the moisture content was increased. Figure 5-19 also reveals close agreement between total enthalpy of adsorption values $(\overline{\Delta H_T})$ determined by the Calusius-Clapeyron method and values determined by the Othmer method. This is as expected and can be attributed to the fact that Othmer (1940) developed the equation (5-3) from the Clausius-Clapeyron equation (4-3).

5.4.3. Comparison of the proposed method with the known method. Adsorption isotherm data for raw freeze-dried beef (Saravacos and Stinchfield, 1965) was used to compute $\overline{\Delta H_T}$ values by various methods. Figure 5-20 presents, in addition to $\overline{\Delta H_T}$ values by the Clausius-Clapeyron method and the Othmer method, the values of $\overline{\Delta H_T}$ by the proposed method for raw freeze-dried beef. The $\overline{\Delta H_T}$ values by the proposed method were significantly lower than the $\overline{\Delta H_T}$ values obtained by both the Clausius-Clapeyron method and the Othmer method. Above 25 percent moisture content all the three methods yielded similar values of $\overline{\Delta H_T}$. The total enthalpy values by the proposed method were computed utilizing an effective molecular weight of raw beef solids of 1075 which was obtained by Raoult's law at the water activity of 0.95. It must be pointed out that the $\overline{\Delta H_T}$ values obtained by the proposed method were computed using isotherm data at a single temperature (68°F), while the Clausius-Clapeyron method and the Othmer method required the use of isotherm data at several temperatures. Use of the Brunauer, Emmett, and Teller (BET) (1938) method allows evaluation of monomolecular moisture contents (M_1) and an energy constant (c). Figure 5-20 indicates the monomolecular moisture value was 6.94 g water/100 g NFDM and the corresponding $\overline{\Delta H_T}$ was 659.21 cal/g water. It is interesting to note that

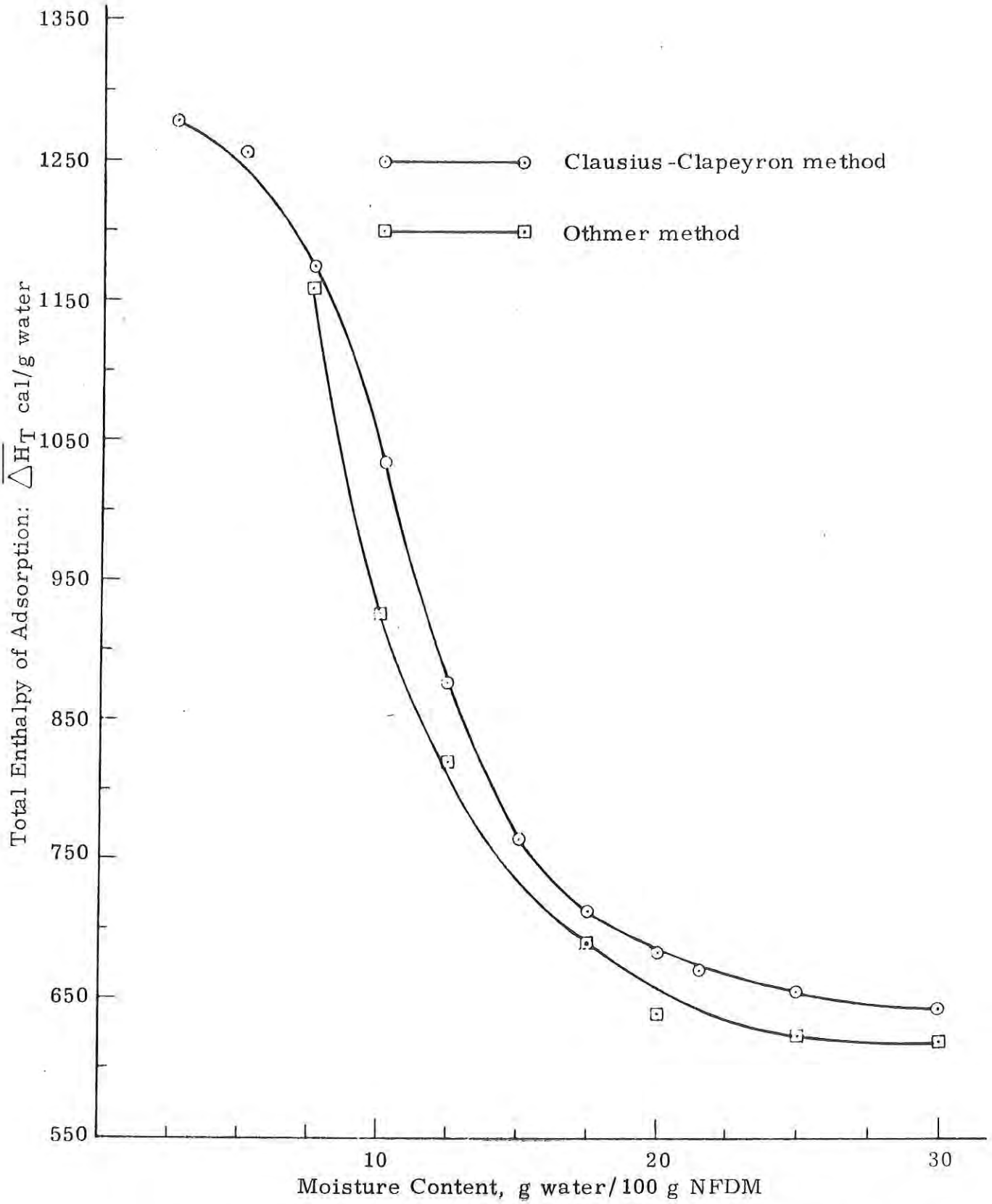

Figure 5-19 --Comparison of total enthalpy values ($\overline{\Delta H_T}$) by the Othmer method and the Clausius-Clapeyron method for precooked freeze-dried beef moisture equilibrium isotherms.

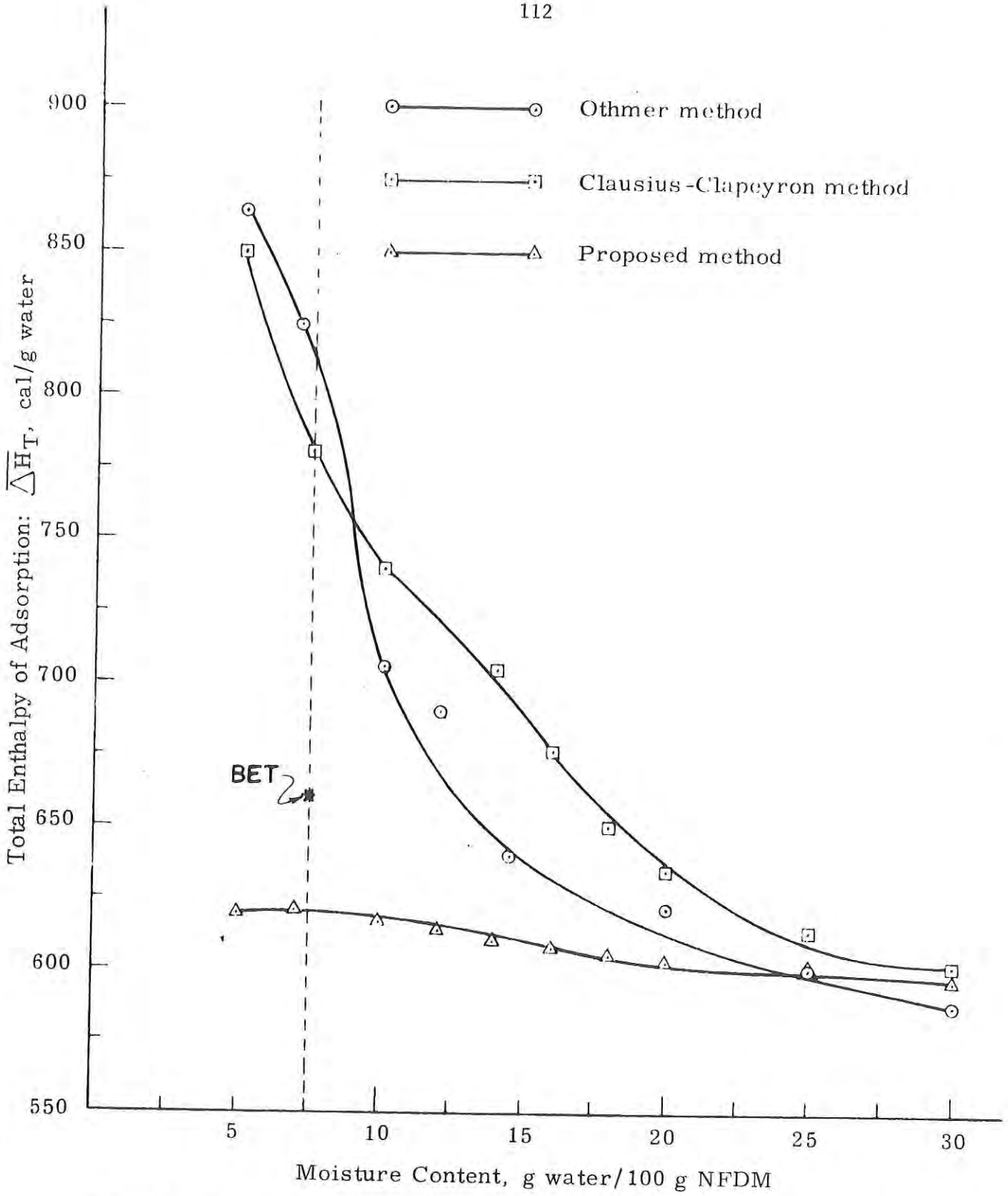

Figure 5-20 -- Comparison of total enthalpy values ($\overline{\Delta H}_T$) by the Othmer method, the Clausius-Clapeyron method and the proposed method at 68°F for raw freeze-dried beef moisture adsorption data (Saravacos and Stinchfield, 1965).

at the monomolecular moisture value, both the Clausius-Clapeyron and the Othmer method predicted significantly higher values of $\overline{\Delta H_T}$ than the proposed method the the BET method which were in close agreement.

The observed agreement between the $\overline{\Delta H_T}$ values obtained by the proposed tne BET methods is more evident in Table 5-8. Total heats of sorption values obtained by the four methods were tabulated in Table 5-8 for precooked freeze-fried beef, low heat non-fat dry milk and the raw freeze-dried beef. Once again, $\overline{\Delta H_T}$ values obtained by the Clausius-Clapeyron and the Othmer methods are significantly higher than the BET and the proposed method values.

5.4.4. Features of the proposed method. As indicated earlier in this section, the proposed method computes the $\overline{\Delta H_T}$ values using the equilibrium moisture isotherm data at one temperature. The values computed by the proposed method are expressed as cal/g mole of mixture which can be converted to cal/g of product while the $\overline{\Delta H_T}$ values obtained from the Clausius-Clapeyron method and the Othmer method are customarily expressed as cal/g mole water of cal/g water.

Figure 5-21 illustrates the significant change in shape of the curve when the $\overline{\Delta H_w}$ values were plotted on a mixture, solids and water basis. Figure 5-21 was plotted using moisture adsorption isotherm data for precooked freeze-dried beef at 72°F (plate temperature 109°F). First is should be pointed out that $\overline{\Delta H_w}$ can be converted to $\overline{\Delta H_T}$ by adding 583.6 cal/g water (latent heat of vaporization at 72°F). Close examination of results in Figure 5-21 leads to several interesting observations. $\overline{\Delta H_w}$ expressed as cal/g water decreased from 58 cal/g water to 10 cal/g water as the moisture content was increased from 3 percent to 44.5 percent. The heat of sorption expressed as cal/g product, however, results in an opposite relation; $\overline{\Delta H_w}$ (cal/g product) increased with the moisture content. Considerable similarity existed between $\overline{\Delta H_s'}$, expressed as cal/g solid and cal/g product.

Figure 5-22 presents the heats of sorption values expressed as cal/g product, for precooked freeze-dried beef (plate temperature 109°F) adsorption isotherms at 50°F, 72°F and 100°F. Figure 5-23 shows the similar results for precooked freeze-dried beef (plate temperature 145°F). In general, the heat of sorption increased with decrease in temperature. The plate temperature used in freeze-drying the product did not affect the magnitude of the heats of sorption values. However, as the freeze-drying temperature was increased, the heats of sorption values decreased somewhat. The relationship of those heats of sorption values with the heat evolved as sensed by a person when product is consumed will be discussed later. One significant observation from Figures 5-21, 5-22 and 5-23 would be the correlation between $\overline{\Delta H_w}$ values, expressed as

Table 5-8 --Comparison of total enthalpy values by various methods (total enthalpy values are expressed as cal/g water).

Temp.	M_1	BET	C-C[a]	Othmer Method	Proposed Method
a. Precooked Freeze-dried Beef					
50°F	10.63	671	983	922	648[b]
72°F	7.50	663	1173	1160	646
100°F	4.59	641	1257	1197	615
b. Raw Freeze-dried Beef (Saravacos and Stinchfield, 1965)					
50°F	6.87	659	791	830	636[c]
68°F	6.94	659	782	825	632
86°F	6.41	655	798	835	635
105°F	5.47	658	828	853	640
122°F	4.50	650	862	875	646
c. Low Heat Non-fat Milk (Heldman et al., 1965)					
35°F	10.06	676	889	833	627[d]
60°F	7.51	679	922	849	632
86°F	7.02	678	938	864	633
100°F	6.73	680	1021	922	634

[a] Clausius-Clapeyron method

[b] From adsorption data at 72°F (EMW_s = 775)

[c] From adsorption data at 68°F (EMW_s = 1075)

[d] From desorption data at 60°F. (EMW_s = 725)

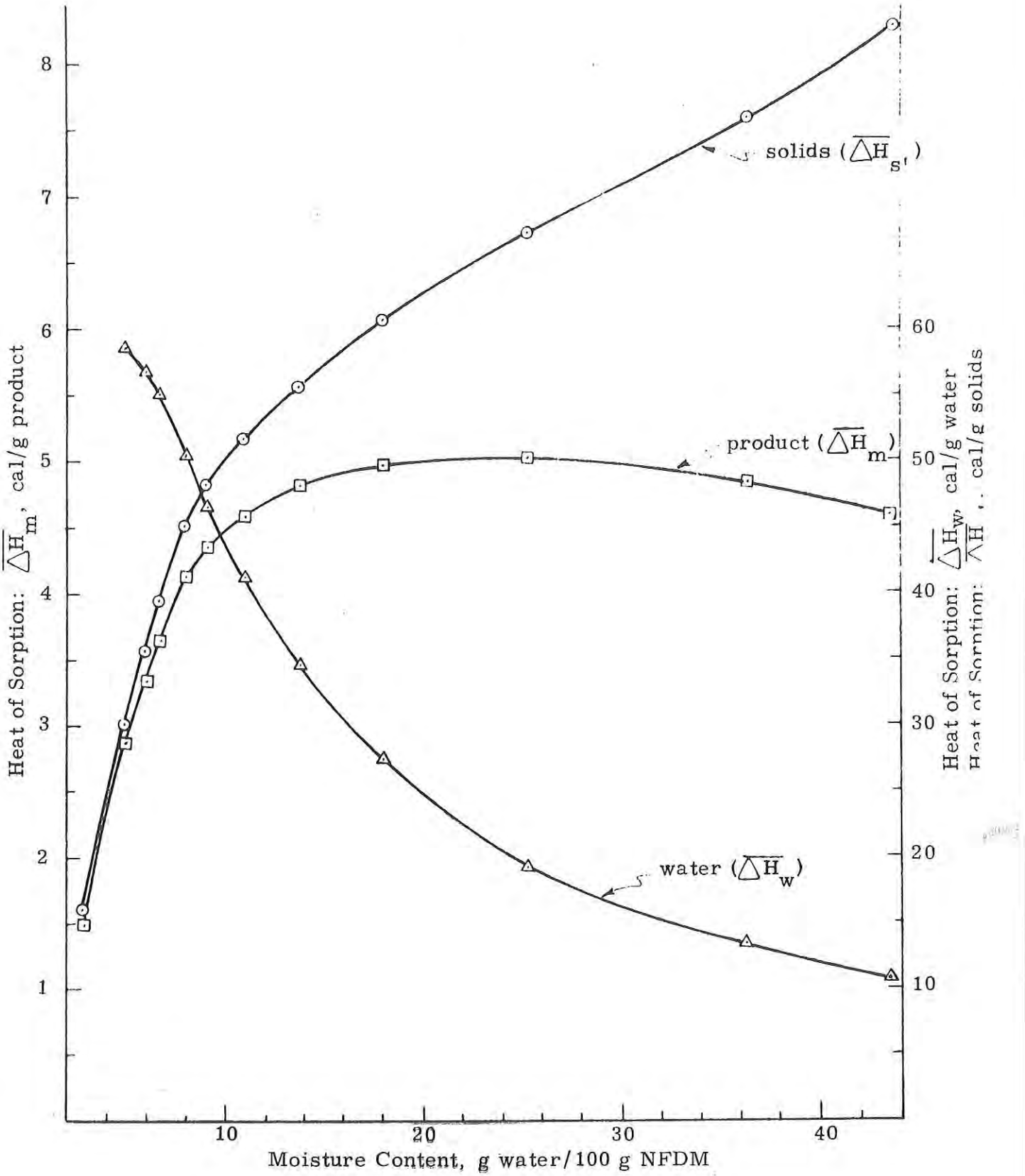

Figure 5-21 --Heat of adsorption values ($\overline{\triangle H_w}$) per g of product, per g of solids and per g of water for precooked freeze-dried beef adsorption isotherms (plate temperature 105°F).

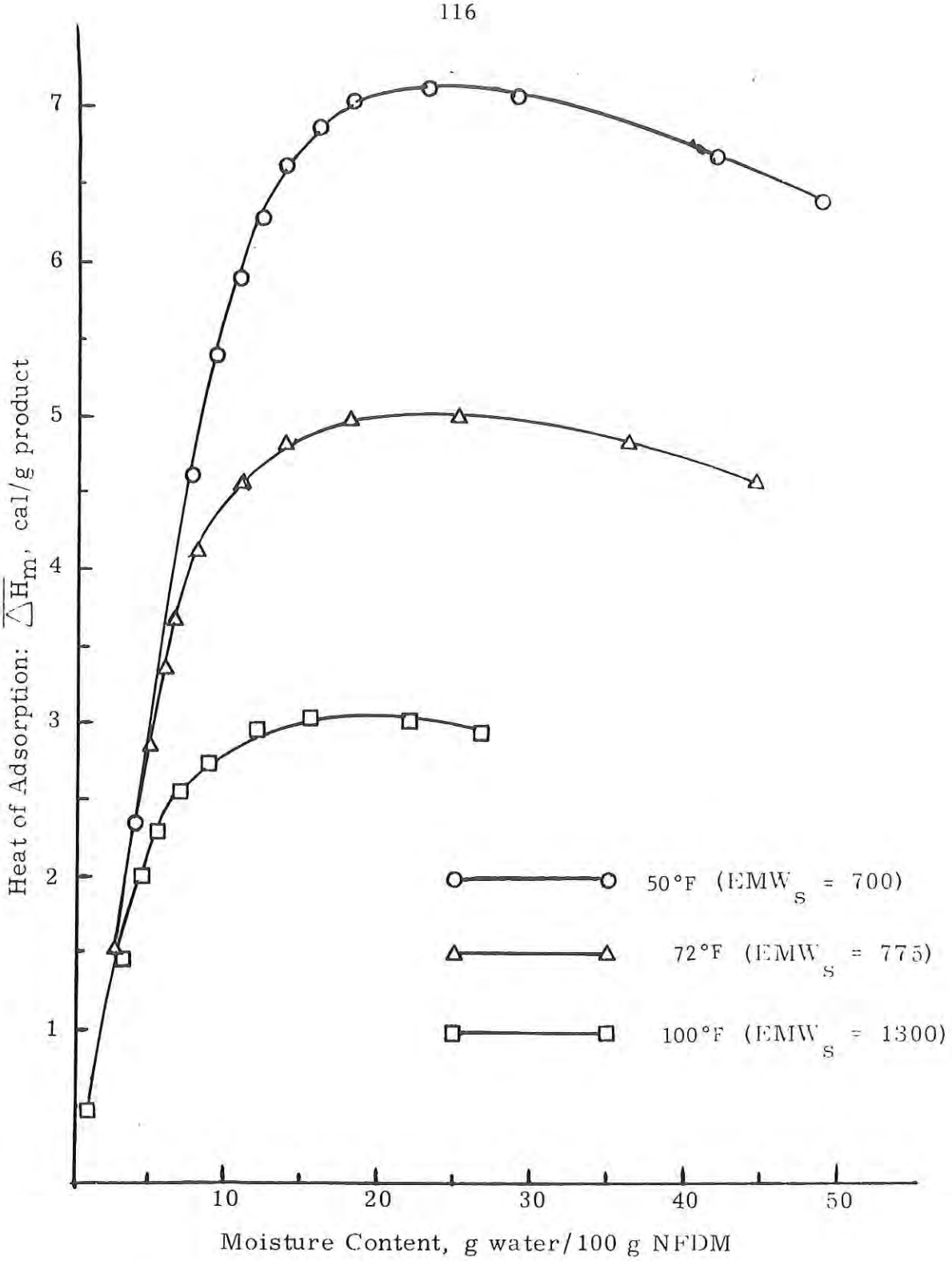

Figure 5-22 - Heat of adsorption values ($\overline{\triangle H_m}$) cal/g product by the proposed method for precooked freeze-dried beef adsorption isotherms (plate temperature 105°F).

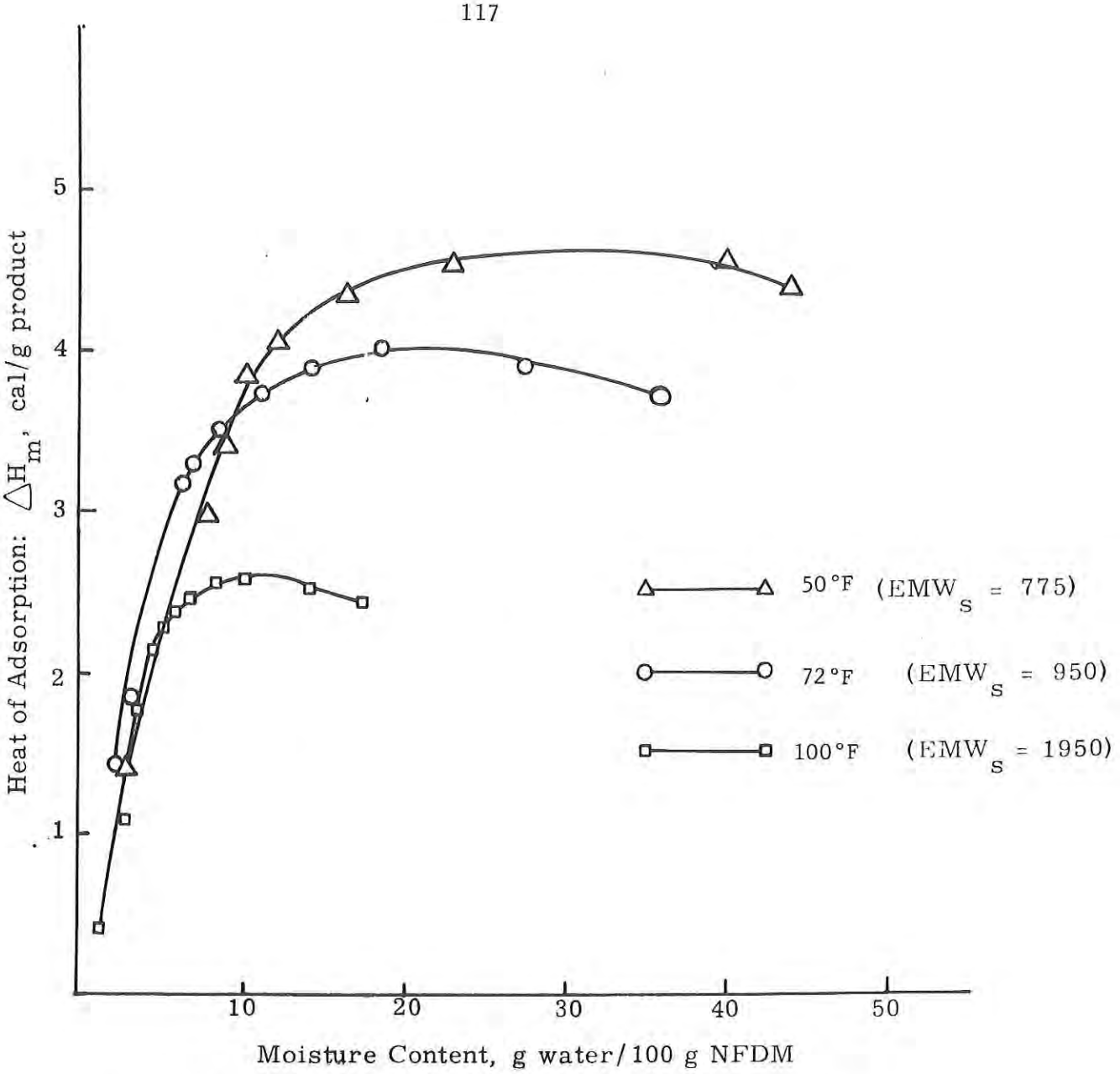

Figure 5-23 --Heat of adsorption values ($\overline{\triangle H_m}$) cal/g product by the proposed method for precooked freeze-dried beef adsorption isotherms (plate temperature 145°F

cal/g product, with the calorimetric heats of immersion. Thompson (1969) and Morrison and Hanlan (1957) indicated that the calorimetric values for heats of immersion for the precooked freeze-dried beef are approximately 1 cal/g product. This emphasizes the validity of the proposed method. It could be argued that the proposed method, due to its significant agreement with the BET values and the possible agreement with calorimetric heat of immersion values, is a better estimate of heats of sorption and hence the latent heats of vaporization. This also would mean that the more common methods of measuring the latents of vaporization and heats of sorption are predicting $\overline{\Delta H}_w$ values which are too high. Additional calorimetric investigations are needed to provide clarification of the situation.

At this point it may be worthwhile to closely examine the assumption of the proposed method and the Clausius-Clapeyron method. Probably the most objectionable assumption of the proposed method would be the use of Raoult's law for the evaluation of the effective molecular weight of the solids in a given food. An outstanding advantage of the proposed method, however, would be the use of non-ideality concept for food products. Reference to the development presented indicates that by setting activity of solids equal to one (dry solids as standard state) and the computation of activity coefficients for solids from the Gibbs-Duhem equation, non-ideality of food systems is accounted for. The use of Raoult's law for computation of effective molecular weight of solids can be justified since the partial heat of mixing or heat of immersion values were in the range of 1-5 calories for most food products. In addition, the close agreement of $\overline{\Delta H}_T$ values by the proposed method and the BET method provides additional evidence. The Clausius-Clapeyron method and the Othmer method assume that the liquid water in a given food system is in equilibrium with its vapor at the temperature of the isotherm. This assumption may be questionable due to the fact that food systems normally have water soluble components present which tend to lower the vapor pressure of the system. In addition, the vapor pressure exerted by the liquid water in the given food system could be lower than the one exerted by the pure water at the same temperature. The integrated form of the Calusius-Clapeyron equation assumes that the $\overline{\Delta H}_T$ is constant over the range of temperature studied. This assumption is somewhat questionable on the basis that the enthalpy change with respect to temperature for food systems may be significant. Finally, the Clausius-Clapeyron equation is applicable to only a reversible process, while the hysteresis commonly associated with biological products suggests that the sorption process for biological products is not strictly reversible.

In case calorimetric investigations indicate that the Clausius-Clapeyron method gives the more correct ($\overline{\Delta H}_T$) predictions, the difference from the proposed method must be attributed to low effective molecular weights used in the computation. Figure 5-24 illustrates the influence of the effective molecular weight (EMW_s) on the heats of sorption $\overline{\Delta H}_w$, expressed as cal/g water for precooked freeze-dried beef isotherm at 72°F. As the value of EMW_s was increased, the $\overline{\Delta H}_w$ values increased for a given moisture content. It appears from this discussion that the heats of sorption values obtained by using the proposed method are in good agreement with the calorimetric measurement values (about 1-6 cal/g product). This would also mean that the Raoult's law assumption

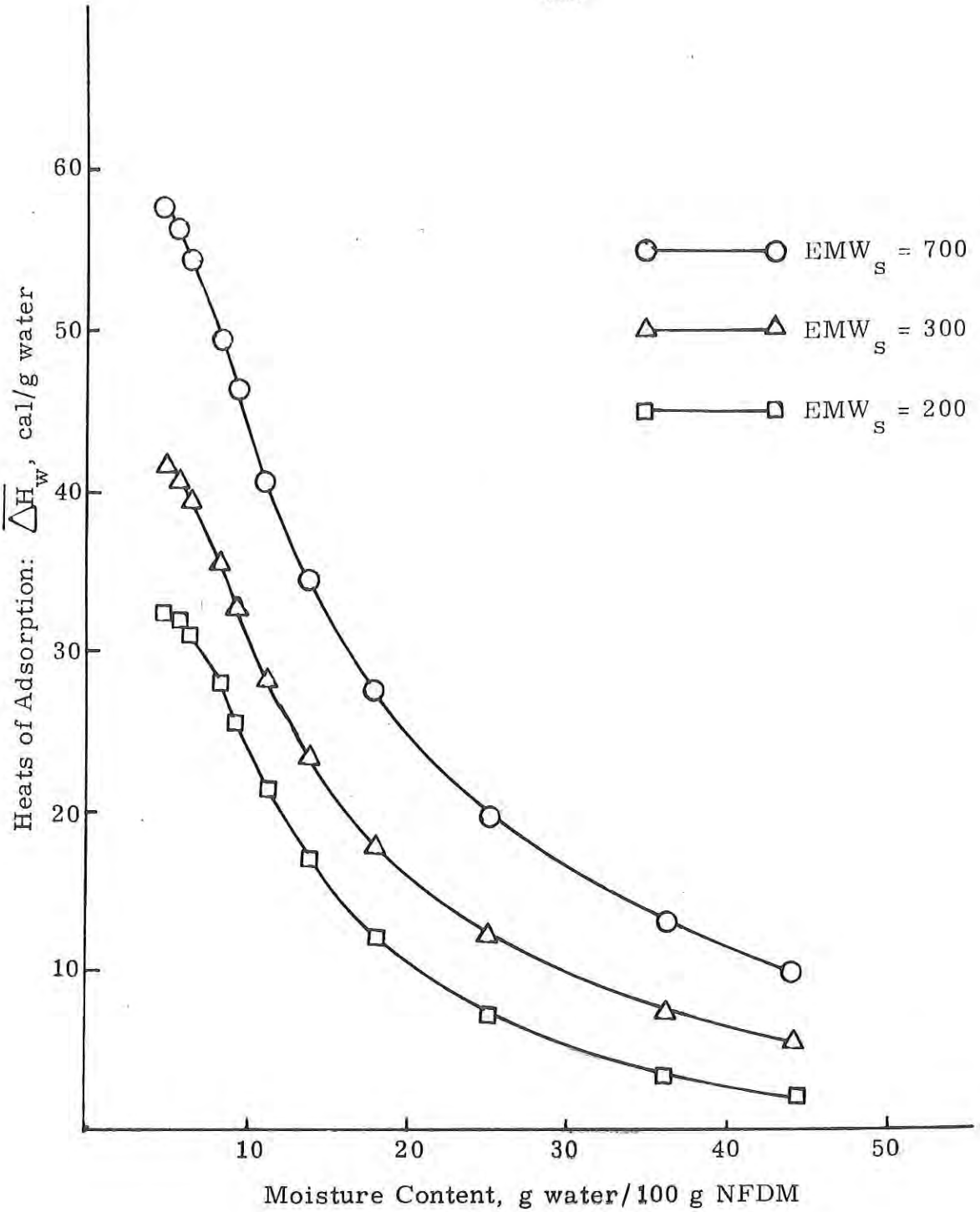

Figure 5-24 -- Effect of effective molecular weight of solids (EMW_s) on heats of sorption for adsorption data at 72°F of precooked freeze-dried beef (plate temperature 105°F).

to compute the effective molecular weight (EMW_s) is a reasonable assumption.

Additional investigations should reveal a more acceptable method of predicting these EMW_s values.

5.4.5. Applications of the proposed method. The total enthalpy values (ΔH_T) for precooked freeze-dried beef and raw beef were computed by the proposed method from the moisture equilibrium data and plotted versus moisture content (g water/100 g NFDM) as shown in Figure 5-25. The higher values of $\overline{\Delta H_T}$ were obtained for the precooked freeze-dried beef (72°F adsorption isotherm). Values from raw freeze-dried beef for adsorption data 68°F gave considerably lower values. Based on these observations, preheat treatments may tend to increase the heats of adsorption.

Table 5-8 illustrates the effect of temperature of sorption isotherm on $\overline{\Delta H_T}$ values by the proposed method. $\overline{\Delta H_T}$ values for the raw freeze-dried beef (Saravacos and Stinchfield, 1965) and low heat non-fat dry milk (Heldman et al., 1965) seem to have increased slightly with the increase in sorption temperature. While the $\overline{\Delta H_T}$ values for the precooked freeze-dried beef have decreased with the increased in temperature, this behavior is difficult to explain. It may be recalled that the total enthalpy values ($\overline{\Delta H_T}$) represent a sum of the heat of sorption ($\overline{\Delta H_w}$) and the latent heat of vaporization. The latent heat of vaporization values are 10 to 100 fold higher than the $\overline{\Delta H_w}$ values, depending on moisture content. In addition, the heats of sorption values ($\overline{H_w}$) do not change significantly from product to product when calculated by using the proposed method.

Figures 5-22 and 5-23 also illustrate the influence of temperature on values of the same product, precooked freeze-dried beef, at two different plate temperatures of freeze drying. As mentioned previously, when the temperature of the isotherm measurement was increased, the $\overline{\Delta H_w}$ values decreased slightly. With the increase in plate temperature of freeze-drying, the $\overline{\Delta H_w}$ value was decreased. There is a significant effect of temperature on the shape of the isotherm; at lower isotherm temperature normally the product adsorbs more moisture.

In Figure 5-26 heats of sorption values ($\overline{\Delta H_w}$) expressed as cal/g water are plotted versus the moisture content (g water/100g NFDM) utilizing the adsorption and desorption data at 72°F for precooked freeze-dried beef (plate temperature 105°F). Figure 5-26 revealed, first, as expected, the $\overline{\Delta H_w}$ value decreased as the moisture content was increased for both adsorption and desorption. Secondly, the values of the heats of desorption were slightly higher than the corresponding values of heats of adsorption. This is similar to the common observation that the desorption equilibrium moisture values are higher than the corresponding adsorption equilibrium moisture values. The higher values of heats of desorption than the corresponding values of heats of adsorption may be due to molecular shrinkage occurring during desorption (Chung and Pfost, 1967).

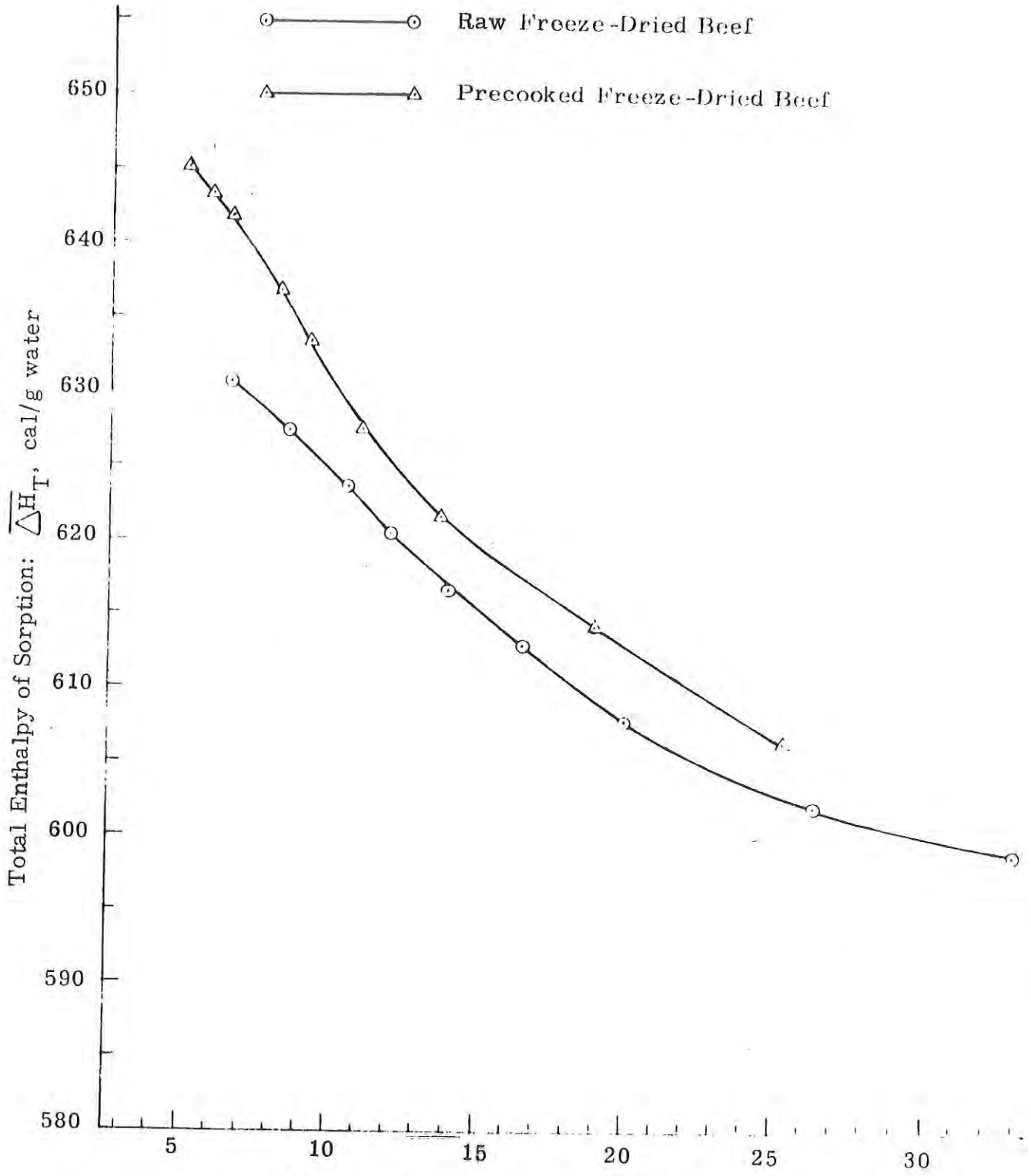

Figure 5-25 -- Total enthalpy values of sorption ($\overline{\Delta H}_T$) for a raw freeze-dried beef adsorption isotherm at 68°F (EMW_s = 1025) and precooked freeze-dried beef adsorption isotherm (plate temperature 105°F) at 72°F (EMW_s = 775).

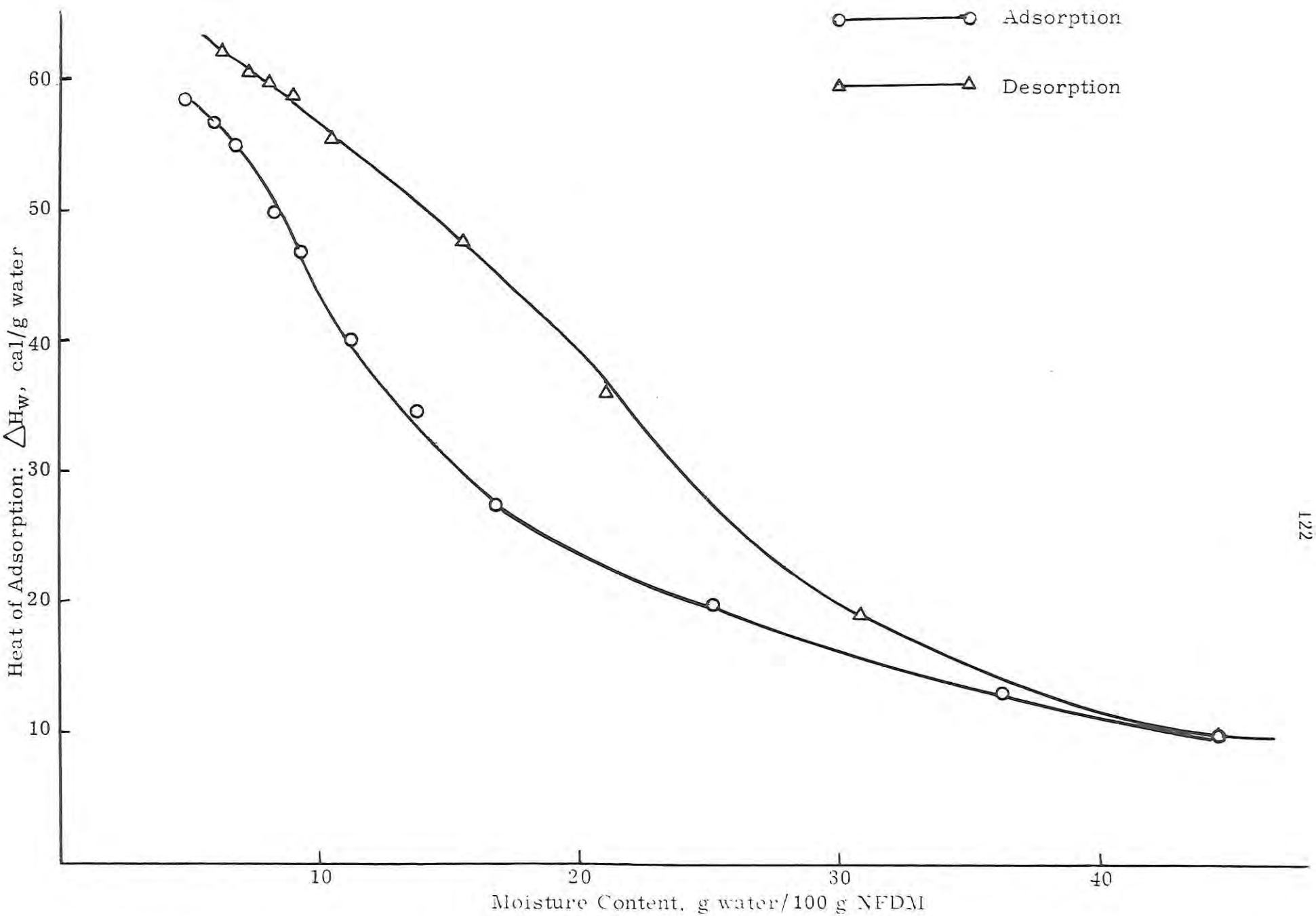

Figure 5-26 --Heat of adsorption and heat of desorption values (cal/g water) for precooked freeze-dried beef at 72°F isotherm (plate temperature 105°F).

Figure 5-27 presents the total enthalpy of adsorption ($\overline{\Delta H_T}$) for raw freeze-dried beef, the water insoluble component of beef, and the water soluble component of beef (Palnitkar and Heldman, 1970). The contribution to total enthalpy of adsorption $\overline{\Delta H_T}$ by the water insoluble component of beef was higher that that of the water soluble component (Sarcoplasmic fraction) of beef. The $\overline{\Delta H_T}$ values were computed using the proposed method for the adsorption isotherm data at 72°F for raw freeze-dried beef, water soluble component and water insoluble component. These results would indicate that a higher proportion of the total heat of adsorption $\overline{\Delta H_T}$ for freeze-dried beef is from the water insoluble component.

Figure 5-28 illustrates the total enthalpy of adsorption ($\overline{\Delta H_T}$) for raw freeze-dried beef, actomyosin, collagen and water soluble component of beef (Palnitkar and Heldman, 1970). The contribution to the total enthalpy of adsorption by collagen was higher than that of the water soluble components and the actomyosin. Collagen represents a portion of water insoluble portion of raw beef and may explain the larger contribution of both water insoluble component and collagen in the total enthalpy value of raw beef. Somewhat higher values of heats of sorption for water insoluble components than the water soluble components may be due to the fact that less energy is required to remove water from solution than solids.

5.5. Thermodynamic Parameters.

Straight line plots of the BET 2-parameter equation in the relative vapor pressure range, 0.05 to ≤ P/Po ≤ 0.3 were made. The monolayer capacity (Vm) together with the energy constants (c) are tabulated in Table 5-9. Figure 5-29 illustrates the effect of isotherm temperature on Vm, the effect of plate temperature on Vm during adsorption and desorption and the differences in Vm during adsorption and desorption.

The results obtained by utilizing the Harkins-Jura equation are summarized in Table 5-10. A considerable divergence is apparent between the Vm values obtained by the two methods. However, these differences appear within the limits (see for example Kapsalis, et al., 1964). In general, the desorption isotherm for the 145°F plate temperature product showed anomalous behavior which is expected from the strongly unique form of the raw data obtained.

Close observation of Tables 5-9 and 5-10 reveal that the monomolecular moisture value obtained by using the Harkins-Jura equation were slightly higher than the similar values computed by using BET equation for precooked freeze-dried beef (plate temperature 105°F), for both adsorption and desorption moisture equilibrium isotherms. The precooked beef freeze dried at 145°F plate temperature showed an opposite behavior, the BET monolayer values were higher than that of the Harkins-Jura monolayer value for adsorption isotherms while desorption isotherms exhibited an opposite effect. The moisture equilibrium isotherm temperature did not show a consistant influence of monomolecular layer moisture values.

5.6. Product Texture

The results obtained by sensory panel and by the objective method (Instron) were utilized in measuring the texture characteristics of precooked freeze-dried beef. The data was obtained for six different equilibrium relative

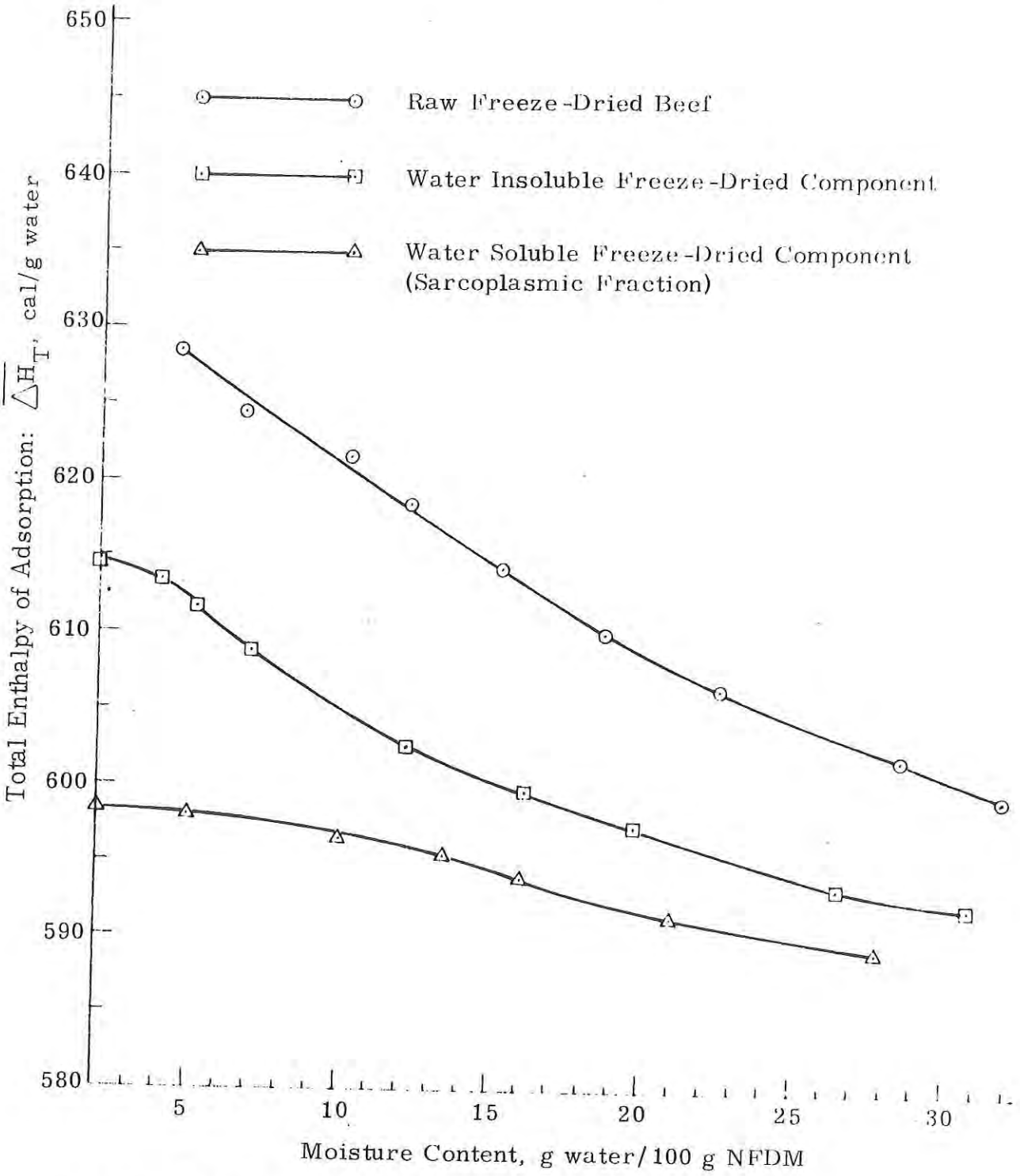

Figure 5-27 --Total enthalpy values of adsorption ($\overline{\triangle H_T}$) at 72°F for raw freeze-dried beef (EMW_S = 1100), water soluble freeze-dried component (EMW_S = 1175) and water insoluble freeze-dried component (EMW_S = 1300).

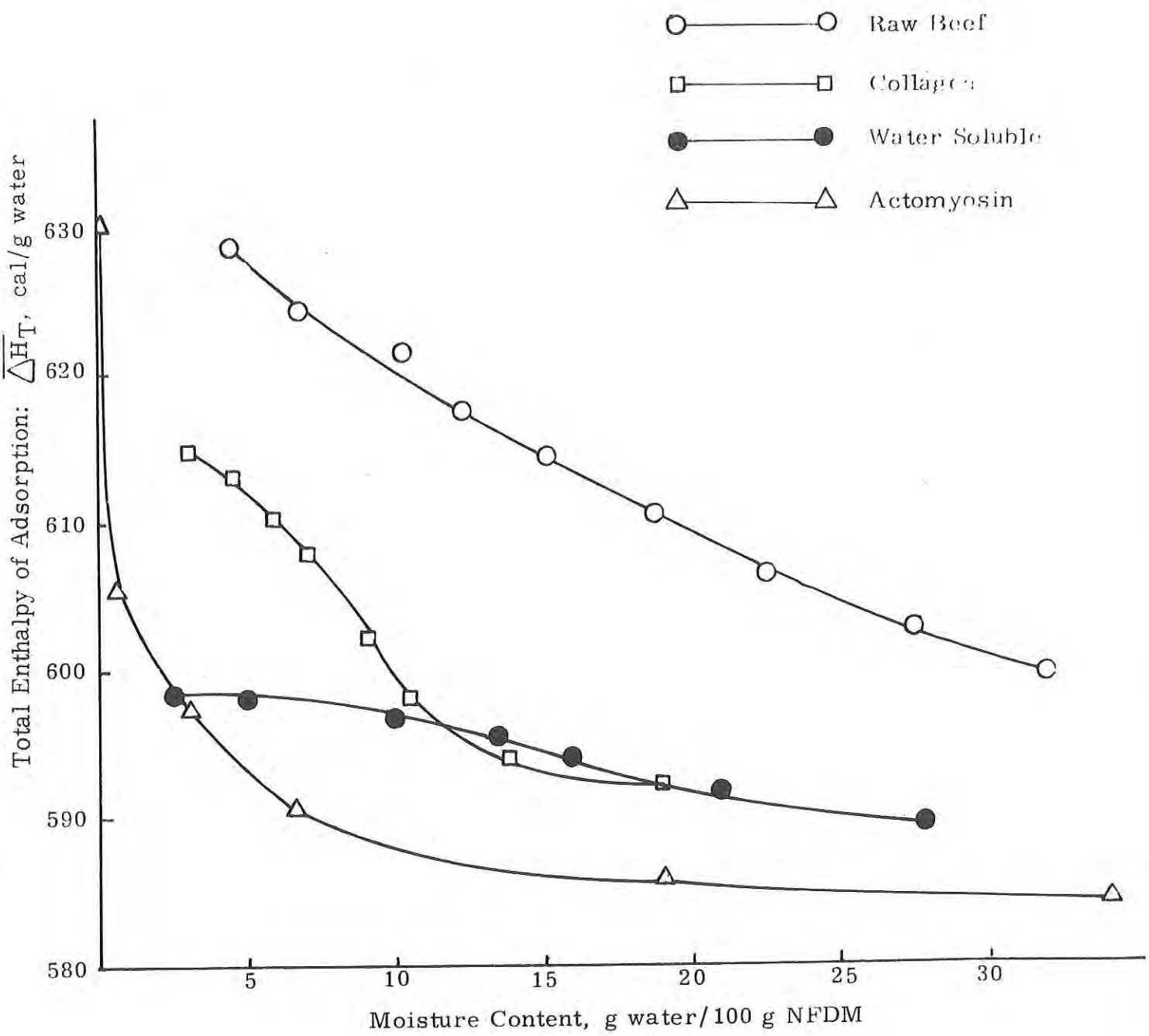

Figure 5-28 -- Total enthalpy values of adsorption ($\overline{\Delta H_T}$) at 72°F for raw freeze-dried beef (EMW_S = 1100), water soluble freeze-dried component (EMW_S = 1300), freeze-dried collagen (EMW_S = 2000) and freeze-dried actomyosin (EMW_S = 1050).

TABLE 5-9. BET parameters for precooked freeze-dried beef.

Plate temperature = 105°F

	Adsorption		Desorption	
Temp. °F	Vm	C	Vm	C
40	.148	9.88	.101	152.0
50	.1063	13.44	.1034	64.47
72	.0750	11.59	.0607	40.99
100	0.0459	6.6	0.0582	38.18

Plate temperature = 145°F

	Adsorption		Desorption	
Temp. °F	Vm	C	Vm	C
40	.0806	9.65	.0910	25.6
50	.0733	11.37	.0833	26.67
72	.0629	9.08	.0845	16.9
100	.0500	6.15	.0750	266.7

TABLE 5-10. Harkins Jura parameters for precooked freeze-dried beef.

Plate temperature = 105°F ($Vm = A^{\frac{1}{2}}$)

	Adsorption		Desorption	
Temp. °F	A	$A^{\frac{1}{2}}$	A	$A^{\frac{1}{2}}$
40	.0274	.166	.0266	.163
50	.01731	.1315	.02144	.1464
72	.01014	.1006	.00938	.09685
100	.004332	.06581	.00714	.08449

Plate temperature = 145°F

	Adsorption		Desorption	
Temp. °F	A	$A^{\frac{1}{2}}$	A	$A^{\frac{1}{2}}$
40	.00661	.0813	.0135	.116
50	.00732	.0856	.01244	.1115
72	.005851	.0765	.01301	.1095
100	.002399	.0489	.0363	.1621

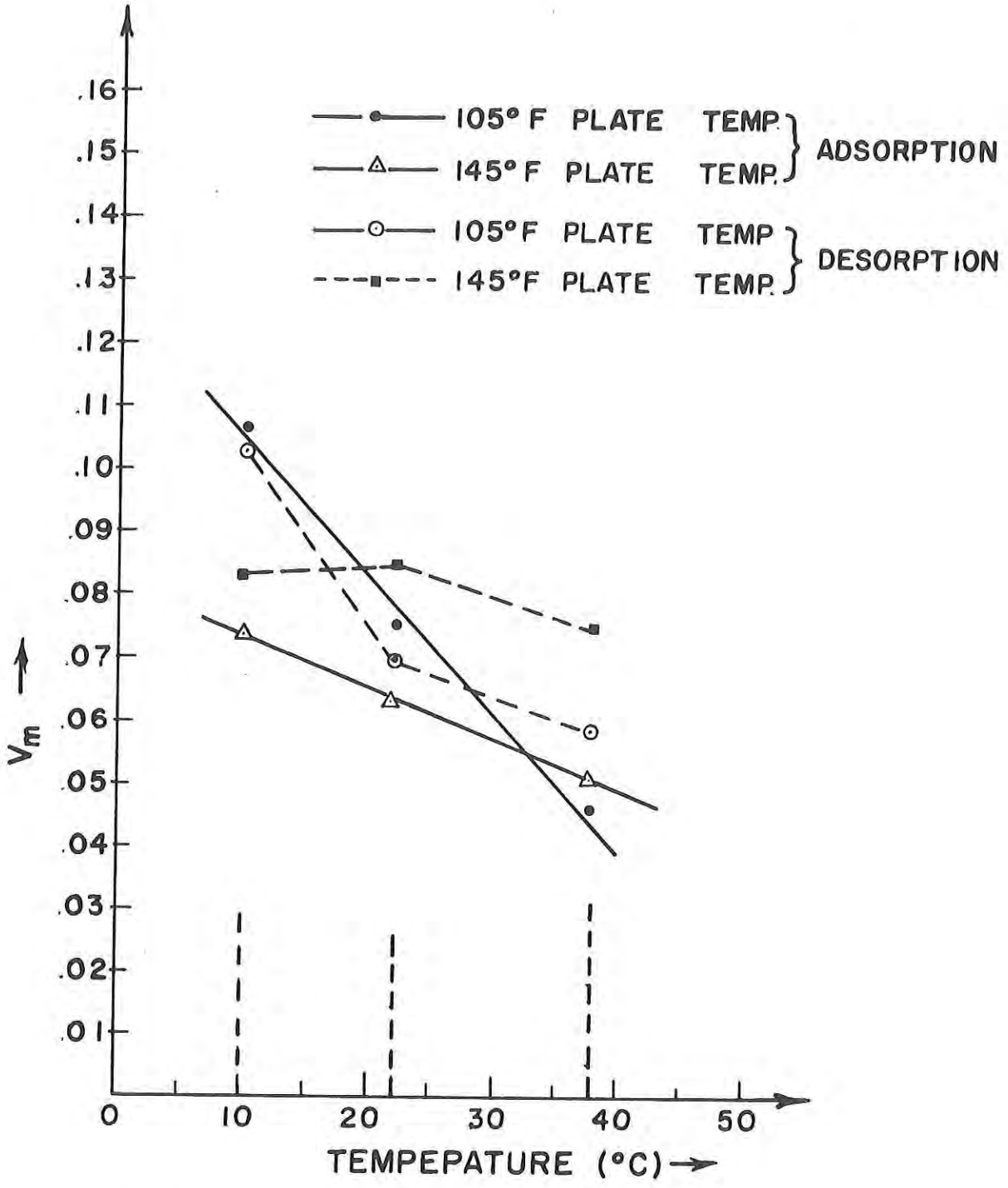

Figure 5-29 Plots showing (1) effect of isotherm temperature on v_m. (2) effect of plate temperature on v_m. (3) differences in v_m during adsorption and desorption.

* v_m = unimolecular moisture content (B-E-T)

humidities and four different conditioning temperatures for product freeze-dried at two different plate temperatures.

5.6.1. Sensory panel results. The results in Figure 5-30 illustrates the influence of equilibrium relative humidity and plate temperature on precooked freeze-dried beef hardness at 39°F as detected by the sensory panel. Data at additional temperatures (52°F, 70°F and 100°F) are presented in the appendix (Figures A-1, A-2 and A-3). There appears to be a predominate trend toward higher hardness values when the product was equilibrated in the 60 to 80% relative humidity range. There is one obvious exception at the 52°F and 39°F conditioning temperature where a lower value was obtained and there is no explanation. An analysis of variance on the means of data obtained at 70°F and 100°F supports the statement that equilibrium relative humidity does have a significant influence on hardness at the 5% level (see Table 5-11).

The chewiness data at 39°F (Figure 5-31) indicate that a maximum in this in this value may exist at around 80% equilibrium relative humidity, also. Additional data at 52, 70 and 100°F is presented in the appendix (Figures A-4, A-5 and A-6). Although this observation is not obvious at the 70°F conditioning temperature, a prevalent trend at all temperatures is the lower chewiness values at the 100% E.R.H. than at 60 or 80% E.R.H. In most cases, the chewiness values tend to increase as the equilibrium relative humidity is increased from 0 toward 60 or 80% E.R.H. A statistical analysis of mean chewiness values indicated that the influence of equilibrium relative humidity was significant at the 5% level, also.

Figure 5-30 illustrates the influence of plate temperature on sensory hardness values, also. There appears to be no consistent relationship at any equilibrium relative humidity except near 0% where product dried at the 105°F plate temperature had the highest hardness value. This consistent relationship is not evident at any other equilibrium relative humidity.

The influence of plate temperature on the chewiness parameter is illustrated in Figure 5-31. Product dried at the 105°F plate temperature gave somewhat higher chewiness values more consistently than revealed by hardness data. At the 52°F conditioning temperature, chewiness values for 105°F plate temperature product were considerably higher at all equilibrium relative humidities except at and near 100°F.

The influence of conditioning temperature on hardness is presented in Figure 5-32. The hardness values presented for a 145°F plate temperature does not reveal a consistent trend in data. There may be some tendency for the 52°F conditioning temperature to produce product with higher hardness when considering 105°F data (Table A-5). The product obtained from a 52°F conditioning temperature has consistently higher chewiness values for 105°F plate temperature (Table A-10). This trend is not consistent, however, since product from 100°F conditioning has considerably higher hardness values than product from 70°F conditioning temperature at the higher equilibrium relative humidities.

5.6.2. Objective (Instron) measurements. The hardness of precooked freeze-dried beef as indicated by force measurements by the Instron Testing Machine

Table5-11 Analysis of variance data for mean hardness values obtained by sensory panel for two conditioning temperatures* two plate temperatures and 6 relative humidity conditions.

Source	DF	SS	MS	F Calculated	F 5%	F 1%
Total	23	4.5711				
Equilibrium Relative humidity (ERH)	5	2.7254	.5451	6.0298**	5.05	10.97
Conditioning Temp (C.T.)	1	0.1601	.1601	1.7710		
Plate Temp (P.T.)	1	0.0988	.0988	1.0929		
ERH x C.T.	5	0.5138	.1027	1.1360		
ERH x P.T.	5	0.5977	.1194	1.3207		
C.T. x P.T.	1	0.0241	.0241	.2665		
Error (ERH x C.T. x P.T.)	5	0.4518	.0904			

* Conditioning temperatures: $70^{\circ}F$ $100^{\circ}F$
Plate Temperatures $105^{\circ}F$ $145^{\circ}F$
Equilibrium Relative humidity 0, 20, 40, 60, 80 and 100

** significant at 95% level of confidence.

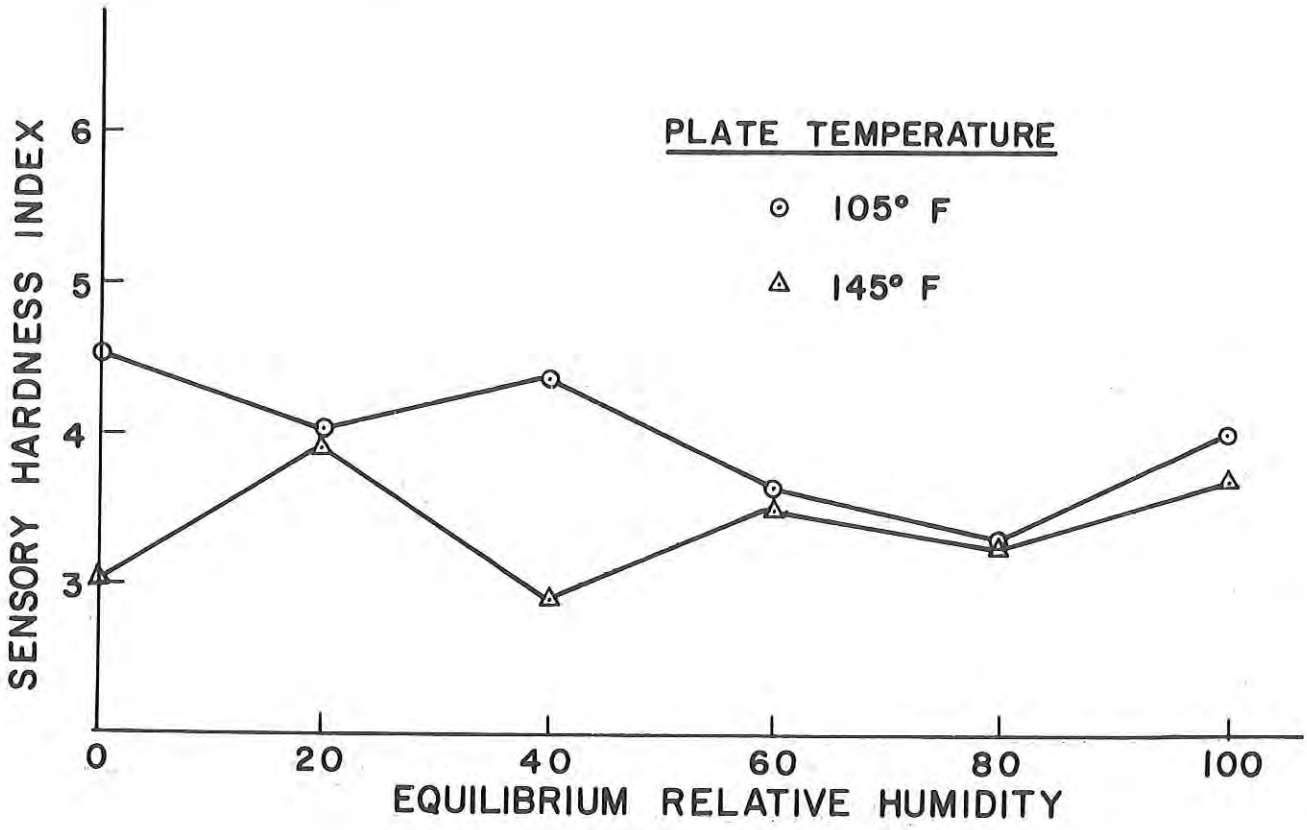

Figure 5-30. Sensory panel hardness of precooked freeze-dried beef at two different plate temperatures and conditioned at 39°F.

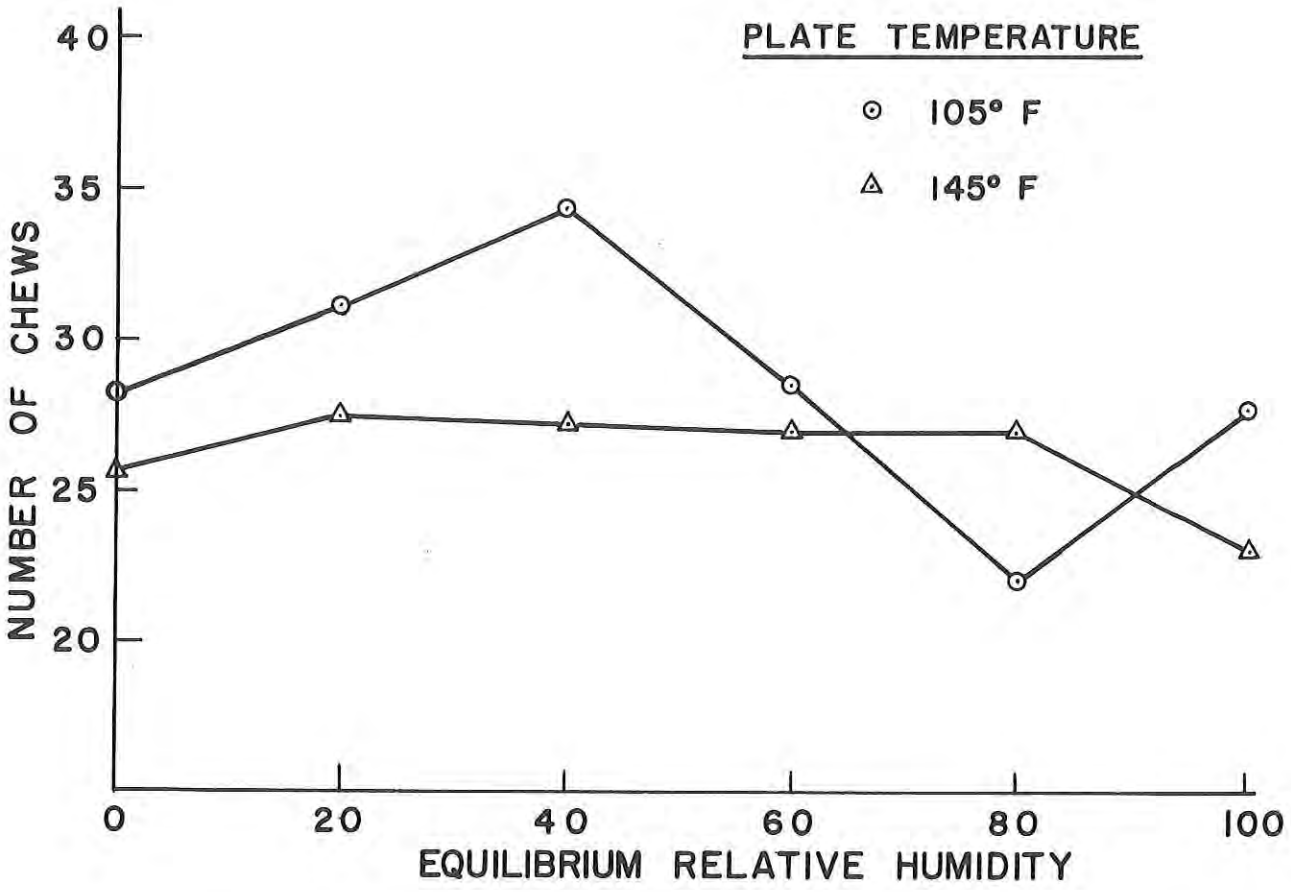

Figure 5-31. Sensory panel chewiness of precooked freeze-dried beef at two different plate temperatures and conditioned at 30°F.

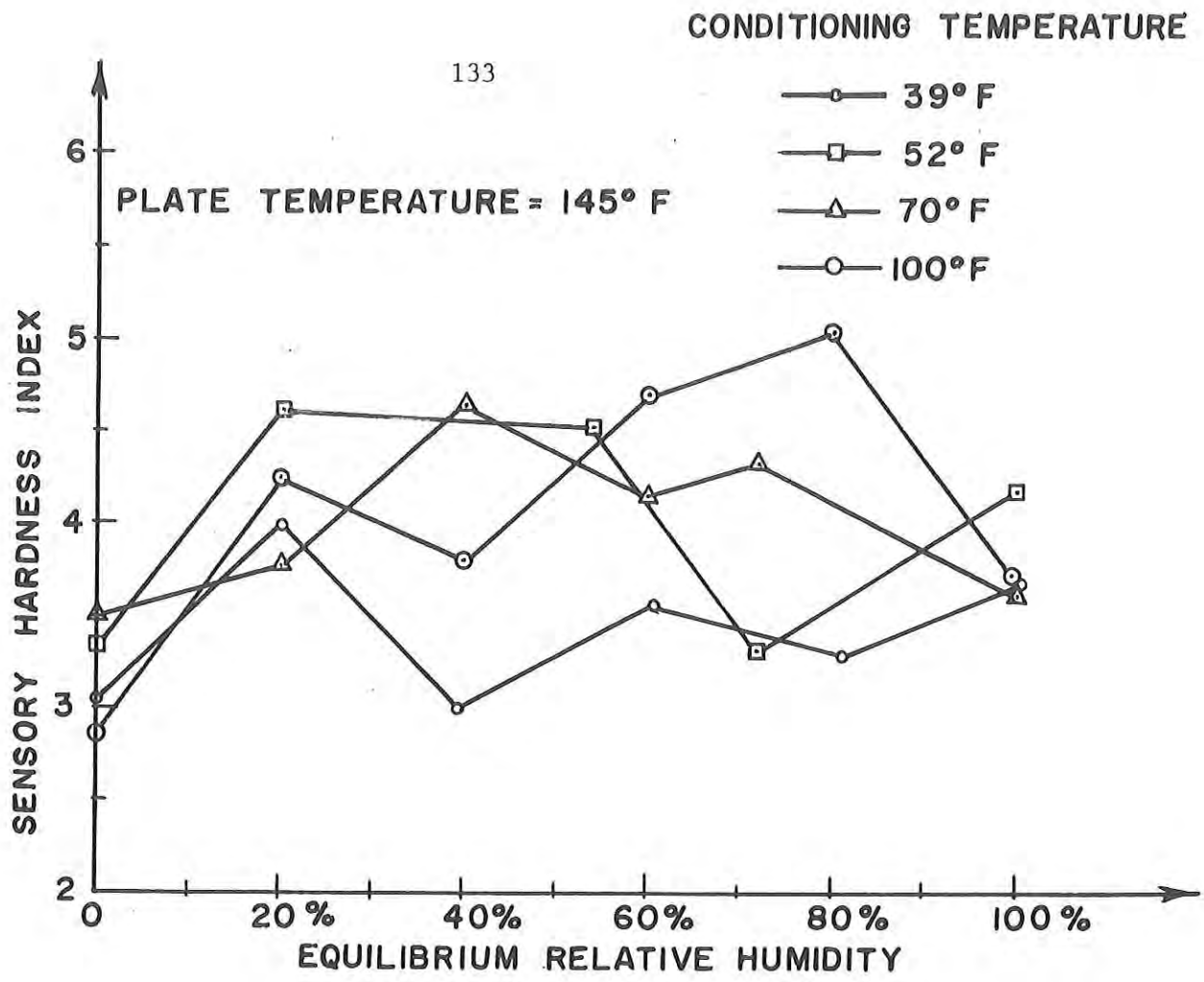

Figure 5-32. Sensory panel hardness of pre-cooked beef freeze-dried at two different plate temperatures and conditioned at 145°F.

are presented in Figure 5.33. Additional data for temperatures at 52, 70, and 100°F are presented in appendix (Figure A-7, A-8 and A-9). The results reveal that the hardness index decreased consistently as the equilibrium relative humidity increased. There was some indication at all four conditioning temperatures 39, 52, 70 and 100°F) that the hardness index may be relatively constant until an equilibrium relative humidity of 60 to 70% is reached. Above this level, the hardness value decreases significantly. This particular observation is most obvious at the 100°F conditioning temperature.

A trend toward lower chewiness values measured by the Instron Testing Machine at the higher equilibrium relative humidities is evident in Figure 5.34 and in appendix (Figure A-10, A-11, and A-12). The very obvious exception is product with 145°F plate temperature at the 70°F conditioning temperature. The results obtained at the 100°F conditioning temperature reveal a relationship very similar to hardness data at the same conditioning temperature. In all situations except one, the 60 to 70% equilibrium relative humidity tends to be the point above which chewiness values begin to decrease rapidly.

Any influence of plate temperature on the hardness index measured by the Instron is not obvious. The hardness of 105°F plate temperature product is higher somewhat more frequently when examining these results in Tables A-6, A-7, A-8 and A-9. The same statement cannot be made about the influence of plate temperature on chewiness values.

It is nearly impossible to visualize any influence of conditioning temperature on chewiness as measured by the Instron Testing Machine as illustrated in Figure 5.35. Although some consistent trends may exist at a given equilibrium relative humidity, these trends may be reversed at different conditions.

5.6.3. Heat evolved during sensory evaluation. As indicated on Table A-10 members of the sensory panel were requested to evaluate the heat evolved during mastication of the dry beef cubes. The evaluation was on a four-point basis from none (1) to evident (4) and will be called a heat evolution index.

The results obtained from the sensory evaluation of heat evolution are presented in Figure 5.36 and in appendix Figures A-13 and A-14). At all three temperatures (52°, 70° and 100°F), a decrease in the heat evolved with increasing equilibrium relative humidity is evident. The magnitude of the decrease is from slightly above the midpoint in the available range for the dry sample to no detected heat evolved for the rehdyrated sample.

There does not appear to be a consistent influence of plate temperature in the freeze-drier on heat evolved during mastication of the resulting product. The product dried with a plate temperature of 145°F was given the highest heat evolution index most frequently, but the results seem too inconsistent to draw a conclusion.

The influence of conditioning temperature on heat evolved is not obvious as illustrated in Figures 5.37 and 5.38. There does seem to be some tendency for the heat evolution index to be lower at 52°F. Examination of Table A-16 indicates that values obtained for a 39°F conditioning temperature are significantly lower at all equilibrium relative humidities above approximately 40%.

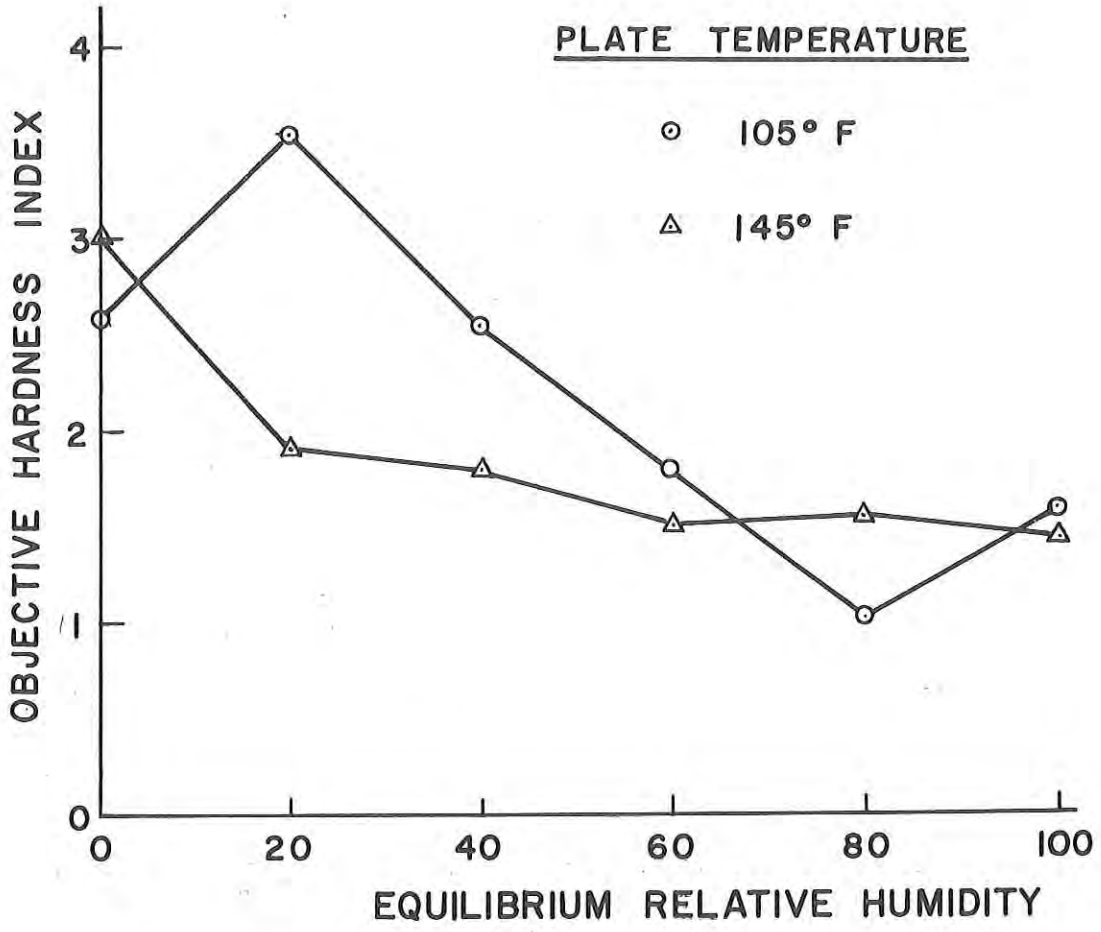

Figure 5.33. Instron hardness index of precooked freeze-dried beef at two plate temperatures and conditioned at 39°F.

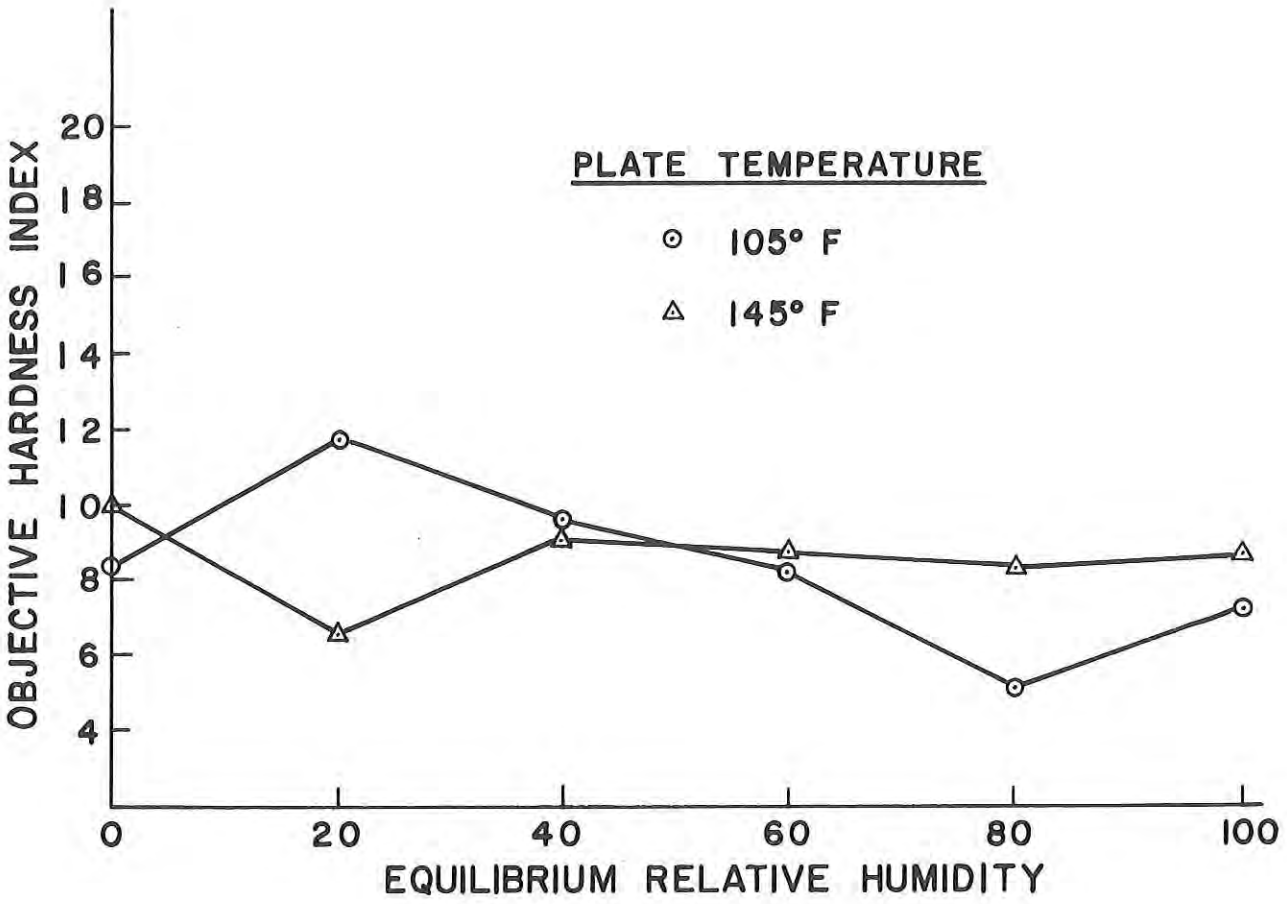

Figure 5-34. Instron chewiness index of precooked freeze-dried beef at two plate temperatures and conditioned at 39°F,

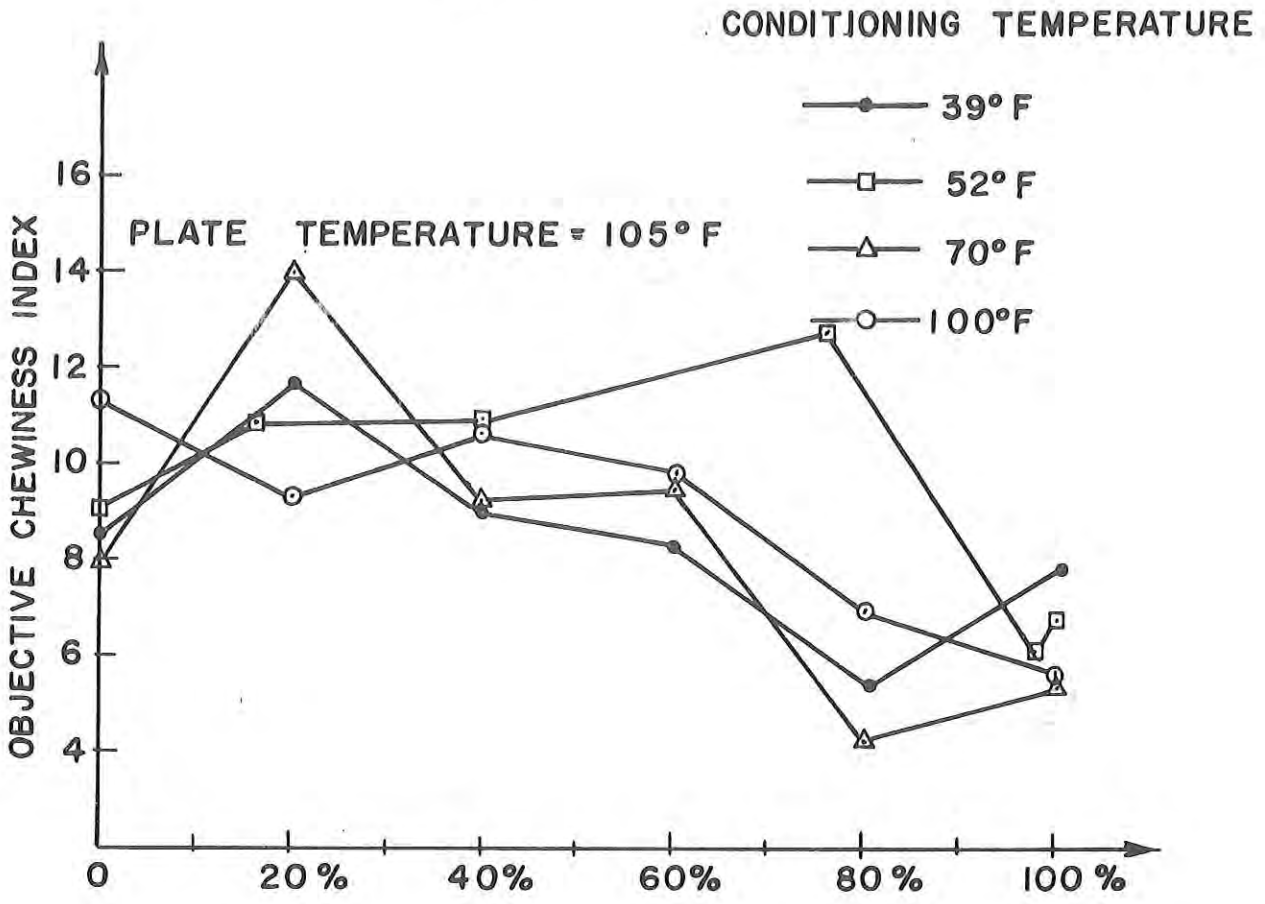

Figure 5-35. Influence of conditioning temperature on Instron chewiness index of pre-cooked beef freeze-dried at 105°F.

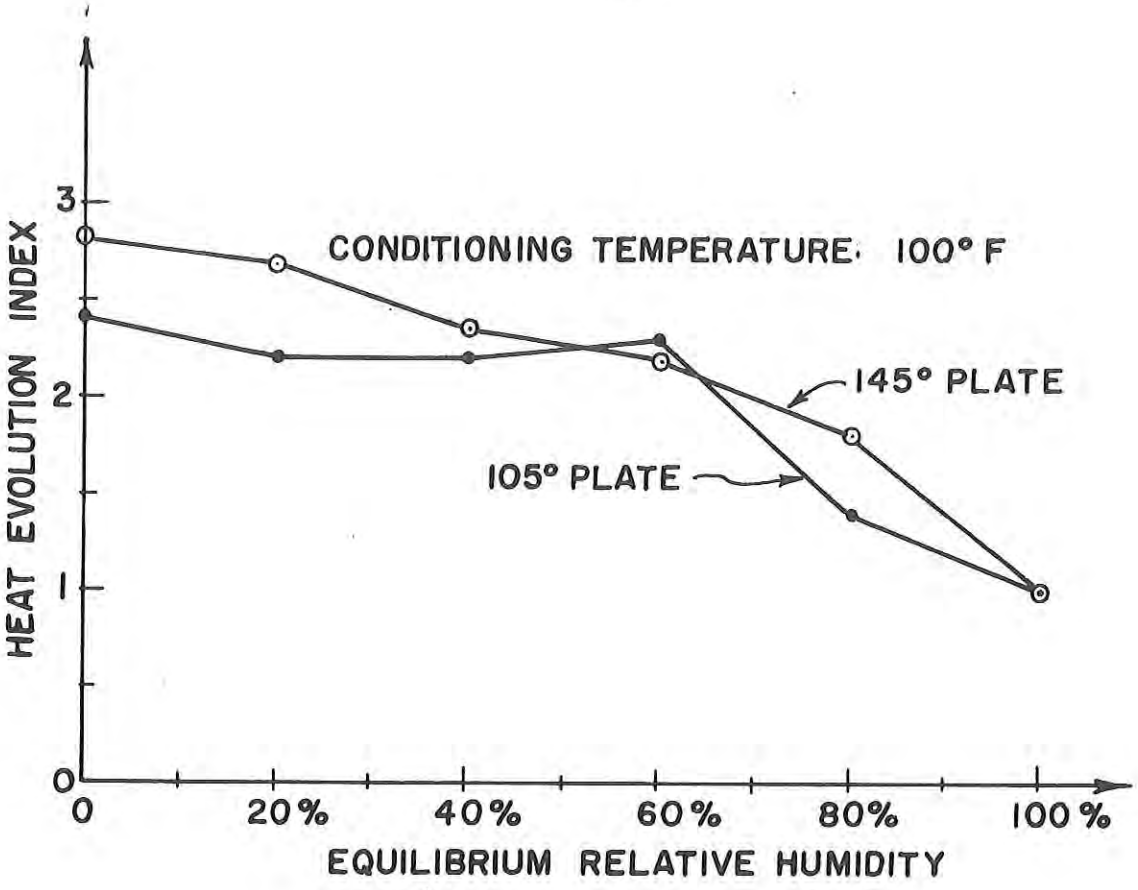

Figure 5-36. Influence of plate temperature on heat evolved from pre-cooked freeze-dried beef as detected by sensory panel for 100°F conditioning temperature.

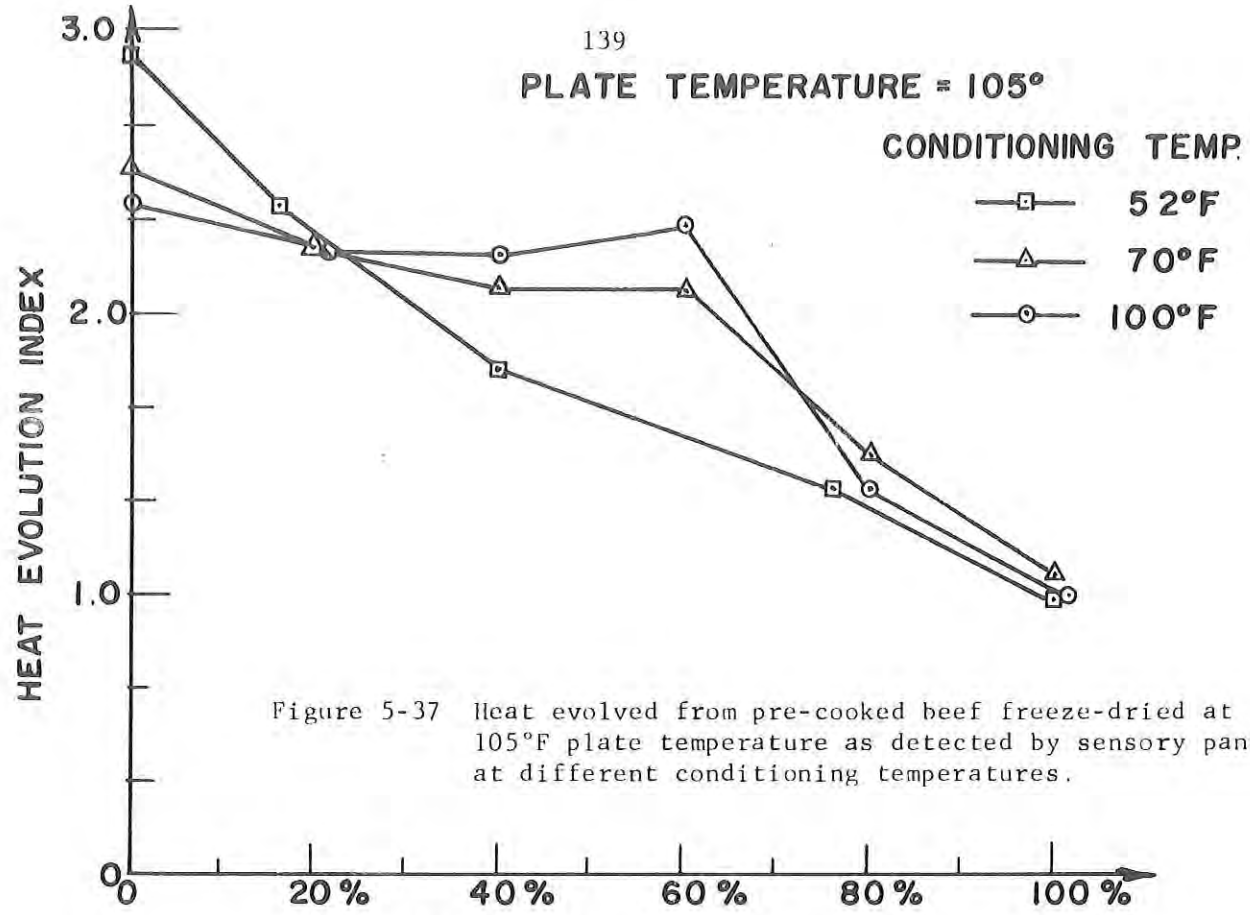

Figure 5-37 Heat evolved from pre-cooked beef freeze-dried at 105°F plate temperature as detected by sensory panel at different conditioning temperatures.

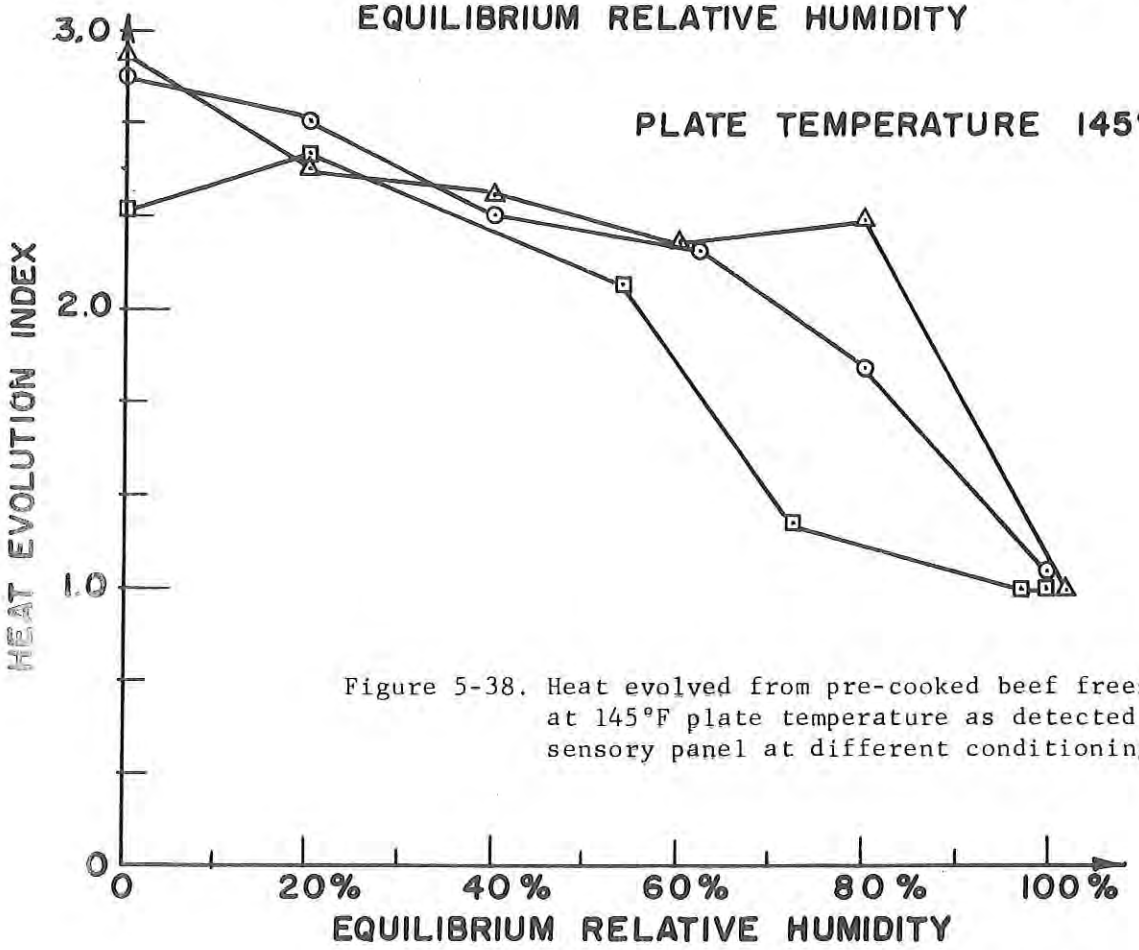

Figure 5-38. Heat evolved from pre-cooked beef freeze-dried at 145°F plate temperature as detected by sensory panel at different conditioning temperatures.

5.6.4. Correlation between sensory panel and objective measurement. The mean values of hardness and chewiness indices from the sensory panel were correlated with the same mean values for the objective measurement. The results revealed a correlation coefficient of 0.1533 for the hardness values and a coefficient of 0.0507. for chewiness values. Both of these coefficients must be considered poor and tend to emphasize the unexplained variations which exist in the data.

There are several factors which must contribute to the poor correlation obtained. The first and probably the most important factor was the product. Beef, as well as any food product, is nonhomogeneous and anisotropic. After preparation of the cube specimens used throughout this investigation, it was obvious from visual observation that significant differences existed within a given cube and from one cube to another. An attempt was made to overcome these variation through the measurement of relatively large number of specimens (15-20) by the objective method. The same approach was not possible with the sensory panel since each member received a different specimen, so that product variations would contribute to variations by both methods but more so to the sensory panel measurements.

The second factor would relate only to hardness measurement by the sensory panel. For this particular parameter, the range of values set up by the Texture Profile method is not adequate for freeze-dried beef. As is evident from results, all specimens were placed in the 3 to 5 range, which did not allow for adequate differentiation between the different factors being investigated.

5.7. Texture Characteristics of Precooked Freeze-dried Beef

One of the objectives of this investigation was to determine the optimum characteristics for a food product to be consumed at dry or intermediate moisture contents. The influence of several factors on the texture of pre-cooked freeze-dried beef have been evaluated. These factors include: a) equilibrium relative humidity, b) plate temperature during freeze-drying, and c) conditioning temperature before evaluation. The texture parameters (hardness and chewiness) have been evaluated by sensory and objective (Instron) techniques.

5.7.1. Influence of equilibrum relative humidity on texture. Both the sensory panel and Instron data indicate that hardness and chewiness decreased after reaching an equilibrium relative humidity of approximately 60 to 80%. Examination of the mean sensory panel values indicated that the hardness and chewiness tends to increase until the 60 to 80% range is reached. A statistical analysis of hardness and chewiness data obtained from Instron measurements produced the curves presented in Figures 5.39 and 5.40. By assuming a second order relationship between texture (hardness or chewiness) and equilibrium relative humidity, the appropriate coefficients for the model equations (See Tables 5-12 and 5-13) were determined utilizing all available data. These results reveal that the influence of equilibrium relative humidity was maximum at 40% and did not influence hardness or chewiness at 80%.

All data obtained and analyzed supports information presented by Kapsalis (1967) indicating that hardness of pre-cooked freeze-dried beef increases as moisture content increases to equilibrium levels above that of the dry product. The Kapsalis (1967) report indicated that the hardness was still increasing when the product was at a equilibrium relative humidity of 66%. However, the Kapsalis

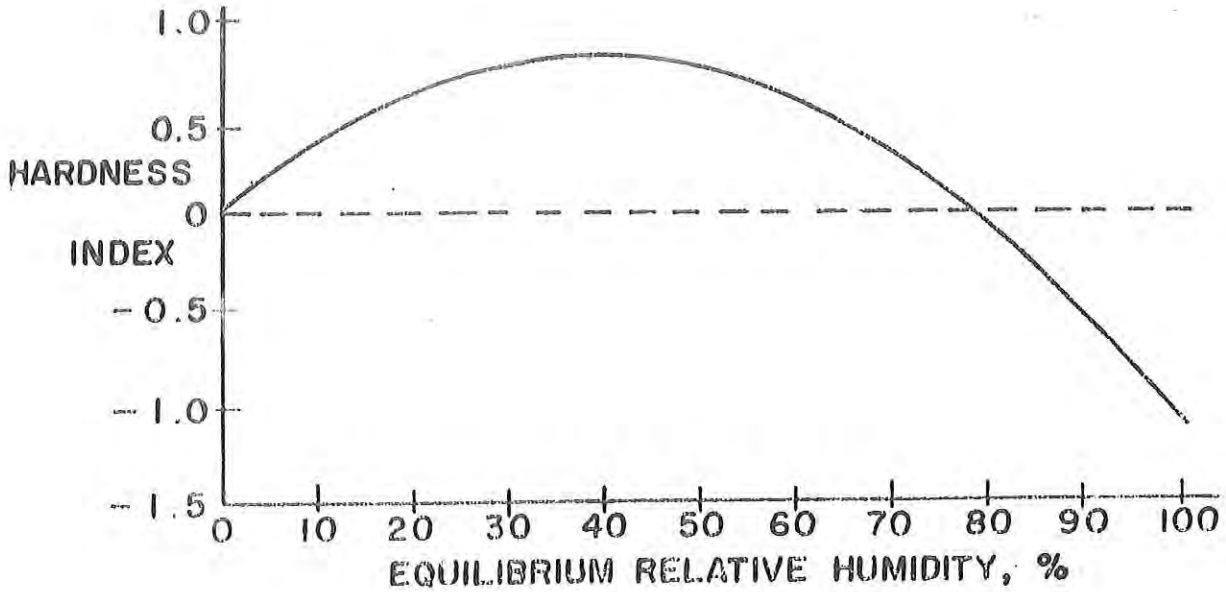

Figure 5-39. Statistical fit of all hardness data from Instron tests illustrating influence of equilibrium relative humidity.

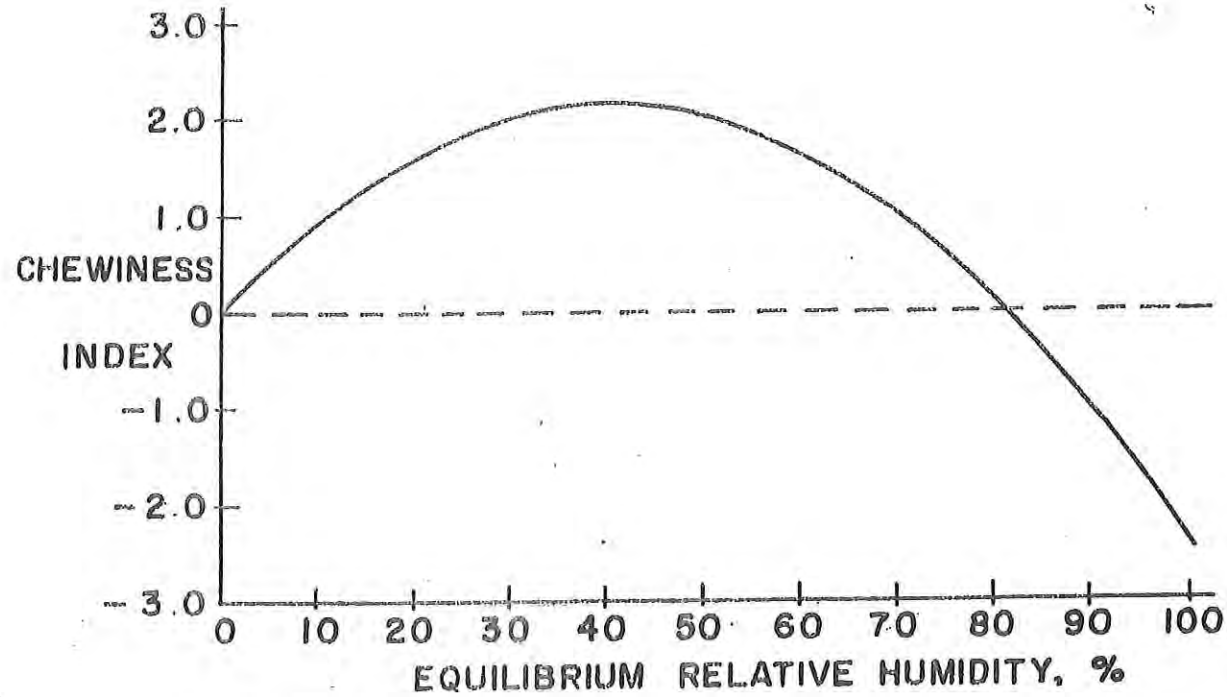

Figure 5-40. Statistical fit of all chewiness data from Instron tests illustrating influence of equilibrium relative humidity.

Table 5-12

Hardness model:

$$Y = \mu + P_i + C_j + (PC)_{ij} + b_1(R.H.) + b_2 (R.H.)^2$$

$\mu = 2.778 \pm 1.705$

$P_1 = 0.1826 \pm 0.0661$ — $P_1 \rightarrow$ plate effect at $105^{\circ}F$

$P_2 = -0.1826 \pm 0.0661$ — $P_2 \rightarrow$ plate effect at $145^{\circ}F$

$C_2 = 0.0701 \pm 0.0964$ — $C_2 \rightarrow$ condition temp ($52^{\circ}F$) effect

$C_3 = 0.1578 \pm 0.0894$ — $C_3 \rightarrow$ condition temp ($70^{\circ}F$) effect

$C_4 = -0.2279 \pm 0.0961$ — $C_4 \rightarrow$ condition temp ($100^{\circ}F$) effect

$(PC)_{12} = 0.0029 \pm 0.0960$

$(PC)_{13} = 0.4195 \pm 0.0894$

$(PC)_{14} = -0.4224 \pm 0.0931$

$(PC)_{22} = -0.0029 \pm 0.0960$

$(PC)_{23} = -0.4195 \pm 0.0894$

$(PC)_{24} = +0.4224 \pm 0.0931$

$b_1 = 0.0395 \pm 0.0068$

$b_2 = -0.0005 \pm 0.00006$

Table 5-13

Chewiness model:

$$Y = \mu + P_i + C_j + (PC)_{ij} + b_1(RH) + b_2(RH)^2$$

$\mu = 9.948 \pm 4.788$

$P_1 = 0.8301 \pm 0.1940$

$P_2 = -0.8301 \pm 0.1940$

$C_2 = 0.5074 \pm 0.2831$

$C_3 = 0.3688 \pm 0.2624$

$C_4 = -0.8762 \pm 0.275$

$(PC)_{12} = -0.5101 \pm 0.2819$

$(PC)_{13} = +1.2319 \pm 0.2624$

$(PC)_{14} = -0.7218 \pm 0.276$

$(PC)_{22} = +0.5101 \pm 0.2819$

$(PC)_{23} = -1.2319 \pm 0.2624$

$(PC)_{24} = +0.7218 \pm 0.276$

$b_1 = 0.1053 \pm 0.0200$

$b_2 = -0.0013 \pm 0.0002$

(1967) data was obtained for product which had been stored for 5½ months while the data in the present investigation were obtained immediately after conditioning. As Kapsalis (1967) points out, any changes in texture should be emphasized by length of storage.

5.7.2. Influence of plate temperature on texture. Examination of mean hardness and chewiness values obtained from sensory and Instron measurements does not permit the statement of a definite conclusion regarding the influence of plate temperature. The majority of the hardness and chewiness data obtained from the sensory panel indicated that the 105°F plate temperature produced precooked freeze-dried beef with a higher hardness index and higher chewiness value. This is supported by an analysis of variance of Instron data for hardness and chewiness presented in Tables 5-14 and 5-15, which indicated that plate temperature has a significant influence on both parameters at the 1% level. The influence is illustrated in Figures 5.41 and 5.42 where it is evident that the 105°F plate temperature product had a positive influence on the chewiness index and on the hardness index at all conditioning temperatures except 100°F.

The differences in texture due to plate temperature used during freeze-drying must be attributed to the influence of heat on product components. This same influence is apparent when examining equilibrium moisture content data. The reason for this type of influence is not obvious since the equilibrium moisture contents on 105°F plate temperature product were higher and the same product had higher hardness and chewiness values.

5.7.3. Influence of conditioning temperature on texture. The influence of conditioning temperature on hardness and chewiness of pre-cooked freeze-dried beef is probably the least obvious when examining mean values of each parameter. There was some indication from panel data that higher hardness and chewiness values were obtained on product conditioned at 52°F.

An analysis of variance of the Instron data (Tables 5-14 and 5-15) revealed that the influence of conditioning temperature on hardness was significant at the 5% level while the influence on chewiness was significant at the 1% level. In addition, it is obvious from Figures 5.41 and 5.42 that the influence of conditioning temperature is dependent on plate temperature. For the 105°F plate temperature, the hardness and chewiness values were highest at 70°F. For the 145°F plate temperature product, both parameters were lowest at 70°F. There appears to be no explanation for the type of interaction between condition temperature and plate temperature revealed.

It should be pointed out that the coefficients (b_1 and b_2) in Tables 5-14 and 5-15 are those which describe the influence of equilibrium relative humidity. As indicated, these coefficients are significant at the 1% level, also. In addition, a correlation coefficient of 0.7 was computed for the relationship between hardness and chewiness as measured by the Instron procedure.

5.8. Relationship Between Predicted Heats of Immersion and Sensory Results.

A trained taste panel consisting of eight members was asked to evaluate the heat evolved during mastication of beef cubes of a four-point scale from none (1) to evident (4). Table A-11 illustrates the sample score sheet used in the sensory evaluation. The precooked freeze-dried beef cubes were equilibrated to a given conditioning temperature and relative humidity. Four

Table5-14 Analysis of Variance on Hardness Index from Instron Data

Source	d.f.	SS	MS	F-ratio
Plate temperature (P)	1	16.699	16.699	7.632**
Conditioning temperature (C)	2	14.173	7.086	3.239*
Interaction, PXC	2	63.606	31.803	14.535**
b_1 [(R.H.)]	1	74.018	74.018	33.829**
b_2 [$(R.H.)^2$]	1	154.439	154.439	70.585**
Error	508	1111.492	2.188	

** significant at 0.01 level

* significant at 0.05 level

Table 5-15 Analysis of Variance on Chewiness Index from Instron Data

Source	d.f.	SS	MS	F-ratio
Plate temperature	1	345.202	345.202	18.3123**
Conditioning temperature	2	190.989	95.494	5.0658**
Interaction,	2	421.069	210.535	11.1684**
b_1 [(R.H.)]	1	525.035	525.035	27.8521**
b_2 [$(R.H.)^2$]	1	852.188	852.188	45.2069**
Error	508	9576.231	18.851	

**significant at 0.01 level

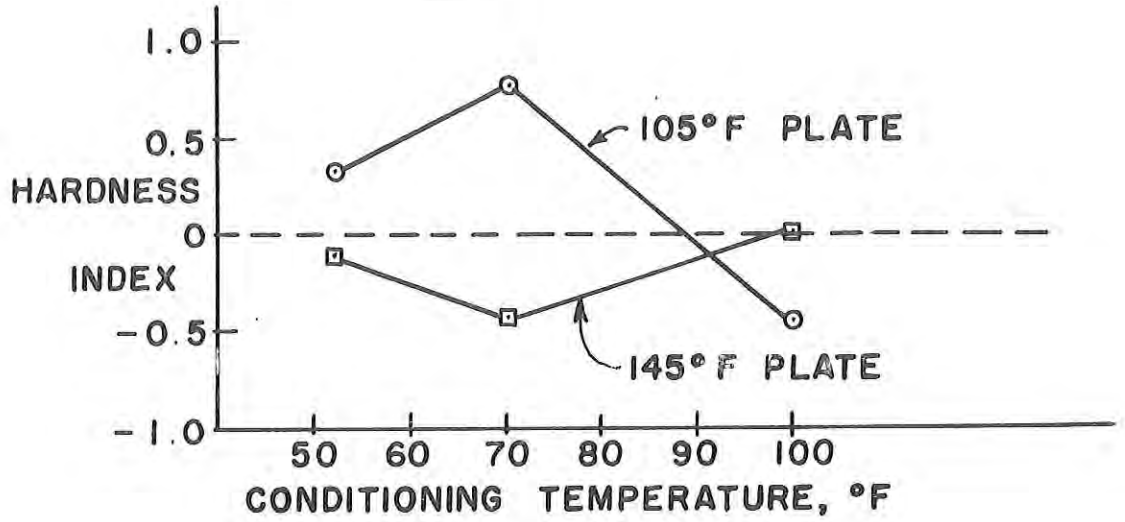

Figure 5.41. Statistical illustration of influence of plate temperature and conditioning temperature on hardness as measured by Instron.

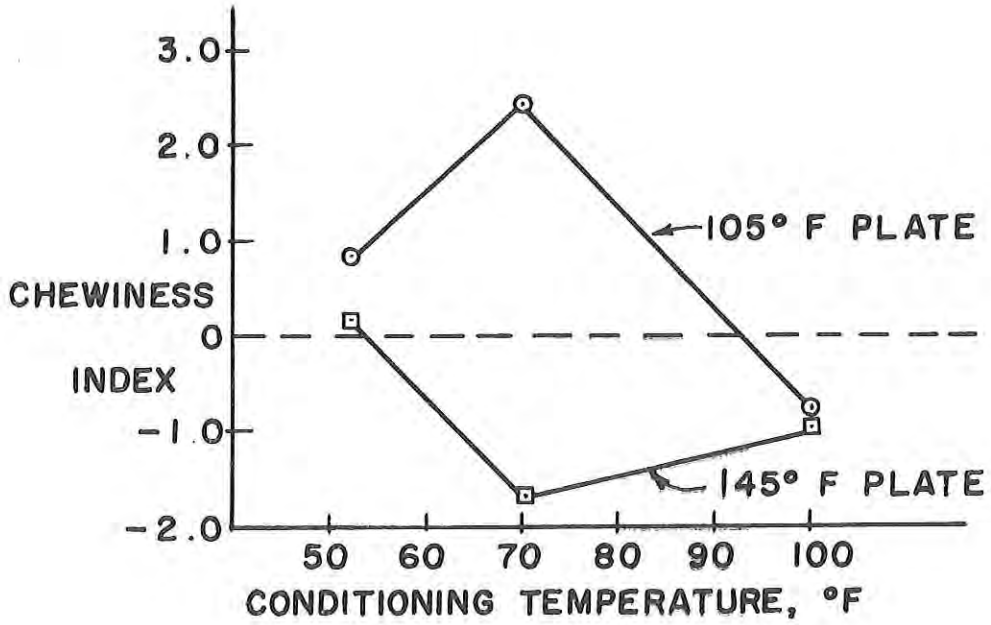

Figure 5.42. Statistical illustration of influence of plate temperature and conditioning temperature on chewiness as measured by Instron.

conditioning temperatures and five relative humidity conditions were employed in equilibrating the beef cubes. The panel members reported the heat evolved during mastication of a preconditioned beef cube as heat evolution index. Table (5-16) shows the heat evolution index values obtained from the sensory evaluation.

As mentioned previously, the heats of sorption values ($\overline{\Delta H}_w$) were obtained by using the proposed method and the moisture adsorption isotherm data at three different isotherm temperatures for precooked freeze-dried beef. Figures 5-22 and 5-23, illustrate the heats of sorption values for precooked freeze-dried beef powder freeze-dried at 105°F and 145°F respectively.

Figure (5-43) represents the general trend of the heat of sorption as determined by the proposed method and the heat evolved as sensed by taste panel members. It appears that the heat of sorption and the heat evolved as sensed by a person are indirectly related. The heat of sorption increased with the moisture content up to about 25 percent moisture level and then decreased slightly, while the heat evolved as sensed by the panel members decreased with an increase in moisture content.

Table (5-16) indicates that the heat evolved as sensed by the judges decreased with the increase in equilibrium relative humidity or water activity for all the three conditioning temperatures. The panel members assigned slightly higher value of heat evolved to a dry product (low moisture level) than a wet product. Table (5-16) did not show the consistent influence of plate temperature (105°F and 145°F) used in the freeze-drying of the beef cubes on the heat evolved during mastication of the product. However, the heats of sorption values (cal/g product) calculated by utilizing the proposed method indicated that the values are slightly influenced by the plate temperature used in freeze-drying.

Careful examination of Figure (5-43) revealed that the panel members sense the heat evolved while masticating the beef cubes in a peculiar manner. In order to illustrate this, the heats of immersion values (heats of sorption) obtained by the proposed method were plotted as difference in the maximum heat of immersion (which occurred at some intermediate moisture value) and the heats of immersion values at various moisture levels versus the equilibrium relative humidity. In addition to the differences in the heats of immersion, the heat evolved as sensed by the panel members was also plotted against the equilibrium relative humidity in the same Figure (5-44).

Figure (5-44) indicated that there seems to be a similar relation between the heats of immersion values expressed as differences and the manner in which the judges sensed the heat evolved during mastication of beef cubes. It seems that the panel members sensed the heat evolved as difference in taking preconditioned beef cube from its initial conditions (temperature and water activity) to some optimum condition existing in their mouth before swallowing the sample. This results in the panel members reporting higher amounts of heat evolved for a dry beef cube and somewhat lower values of heat evolved for the wet beef cubes. It should be pointed out that the judges experienced difficulties in judging the small differences in heat evolved during mastication of the beef cubes. Also, the heats of sorption values were based on the powder form of the product and were expressed as cal/g product while the heat evolved as sensed by the panel members was based on the beef sample in the form of

Table 5-16 Heat Evolution Index Values obtained from Sensory Panel.

Temp. (°F)	~0%	~20%	~40%	~60%	~80%	100%
	(Plate Temperature = 105°F)					
39	2.7	2.1	1.1	1.0	1.0	1.0
52	2.9	2.4	1.8	1.4	1.0	1.1
70	2.55	2.21	2.10	2.1	1.5	1.10
100	2.4	2.21	2.2	2.3	1.38	1.0
	(Plate Temperature = 145°F)					
39	2.65	2.0	1.1	1.0	1.0	1.3
52	2.36	2.58	2.1	1.2	1.0	1.0
70	2.9	2.5	2.417	2.2	2.3	1.0
100	2.8	2.68	2.35	2.2	1.8	1.0

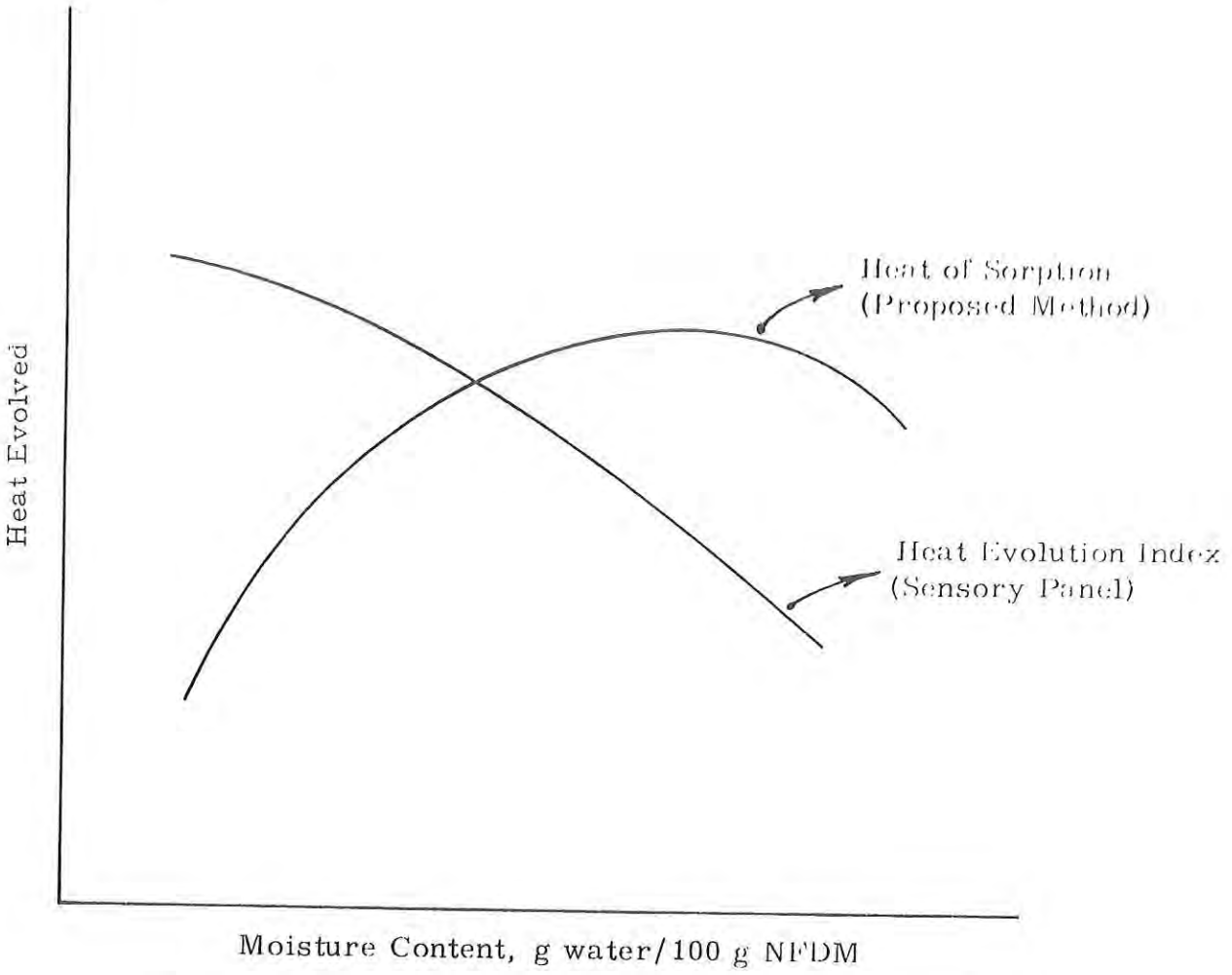

Figure 5-43 --General trends of heat evolved as measured by the sensory panel and the heat of sorption computed from moisture equilibrium isotherm data by the proposed method for precooked freeze-dried beef (plate temperature 105°F).

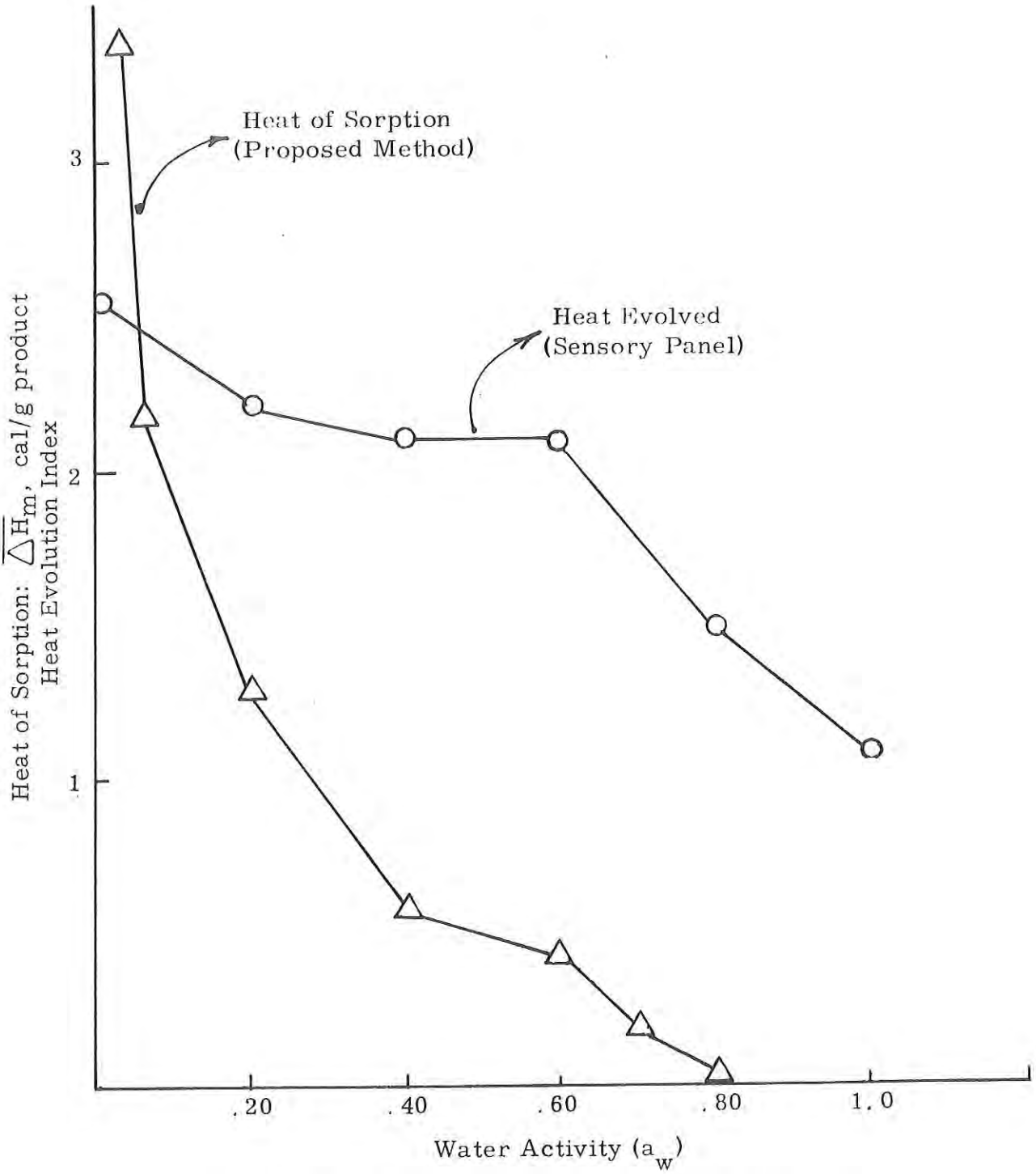

Figure 5-44 --Correlation between the difference in heat of sorption from moisture sorption data as calculated by the proposed method and the heat evolution index from the sensory panel for precooked freeze-dried beef (plate temperature 105°F).

cubes, the weight of which was dependent upon the conditioning temperature and relative humidity at which it was equilibrated.

5.9. Influence of Storage on Product Texture

The texture of the freeze-dried beef cubes was measured at 1-month intervals during storage at two temperatures (39°F and 100°F) and four water activities (0, 0.25, 0.5, 0.75). In addition, samples from two different plate temperatures (105°F and 145°F) during freeze-drying were utilized. The texture was expressed in terms of two parameters; hardness and chewiness. The mean of 15 replicate values is presented for each situation in Table A.12 for hardness and Table A.13 for chewiness.

5.9.1. Influence of plate temperature. The influence of storage time on texture seemed to be most evident at the 100°F and 0.75 water activity storage condition. The influence of plate temperature on hardness and chewiness is revealed in Figures 5.45 and 5.46, respectively. In both cases, the product freeze-dried with 105°F plate temperature seemed to have higher hardness and chewiness values after one and two months of storage. After 4 and 5 months, the hardness and chewiness values were higher for the 145°F plate temperature product. There is no obvious explanation for these relationships or for the rather significant decrease in both texture parameters occurring after six months of storage. This change was most evident for the 105°F plate temperature product.

5.9.2. Influence of storage temperature. The influence of storage temperature on texture of beef freeze-dried at 145°F plate temperature and stored at water activity of 0.75 is illustrated in Figures 5.47 and 5.48. High temperature storage (100°F) seems to have a detrimental influence on both hardness and chewiness since the parameter values are higher at the 100°F storage temperature throughout the storage period. The chewiness parameter seems to be much more sensitive to the differences caused by storage temperature. There appears to be a slight increase in hardness with storage at 100°F up to 5 months, while storage at 39°F seems to maintain the hardness parameter at a relatively constant value. The increase in the chewiness parameter at 100°F is much more obvious although the value is as high after 2 months of storage as at 5 months. Except for an increase in chewiness at 4 months, the values are relatively constant at 39°F storage. The decrease in all texture values at 6 months of storage has no apparent explanation.

5.9.3. Influence of water activity. The relationship between storage time and water activity seems relatively obvious in Figures 5.49 and 5.50. During the initial 2 to 3 months of storage at 100°F, the beef freeze-dried at 105°F seems to be relatively stable in that hardness and chewiness values do not change at any of the water activities investigated. Beginning with the third month, however, both hardness and chewiness values increase for product stored at water activities of 0.5 and 0.75. This increase results in maximum values for hardness and chewiness at 5 months of storage while product stored at water activities of 0 and 0.25 does not change in texture.

5.9.4. Statistical analysis. The results of an analysis of variance conducted on both hardness and chewiness data is presented in Table 5.17. The values in the table indicate the significance level at which variations existed in the variables considered. In general, those results indicate that the influence of most variables considered increased with storage time.

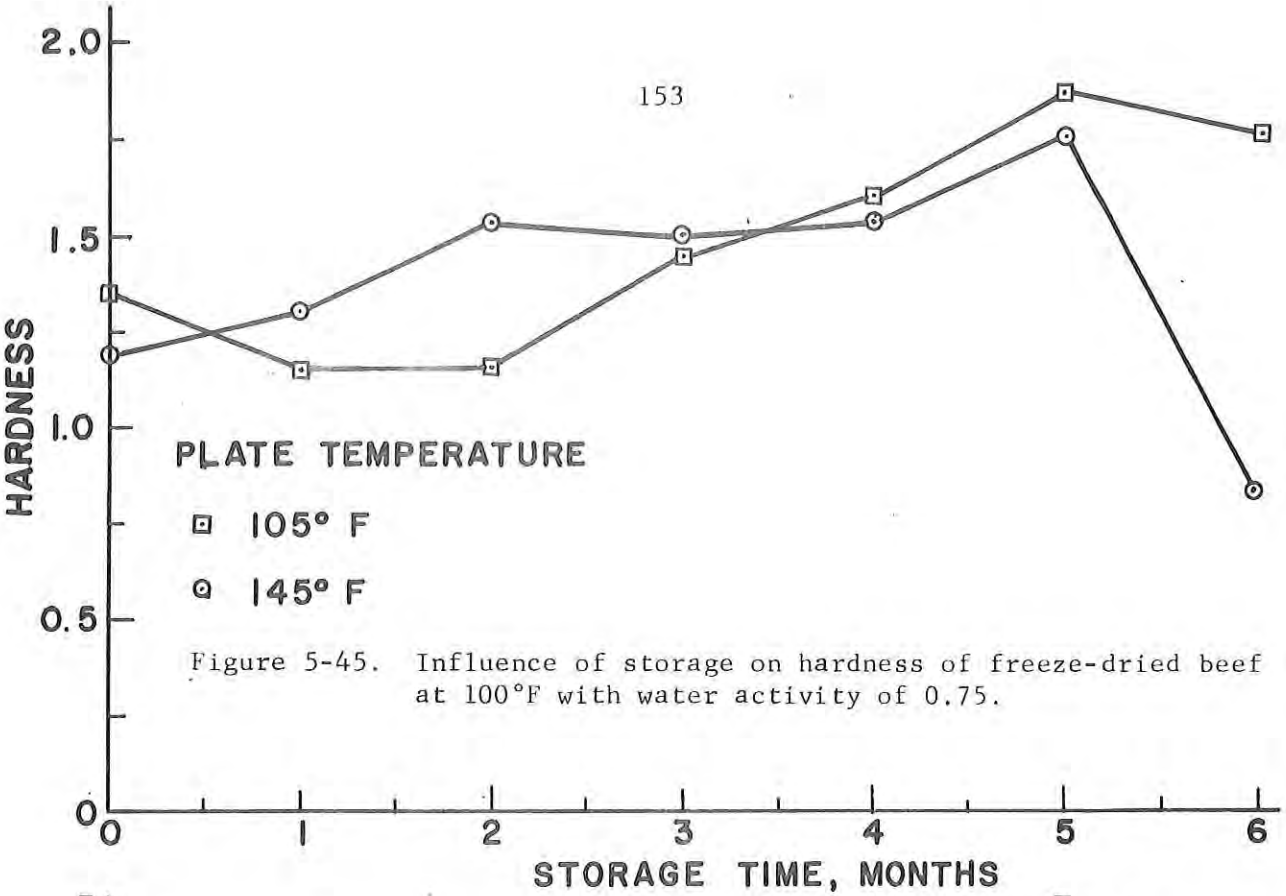

Figure 5-45. Influence of storage on hardness of freeze-dried beef at 100°F with water activity of 0.75.

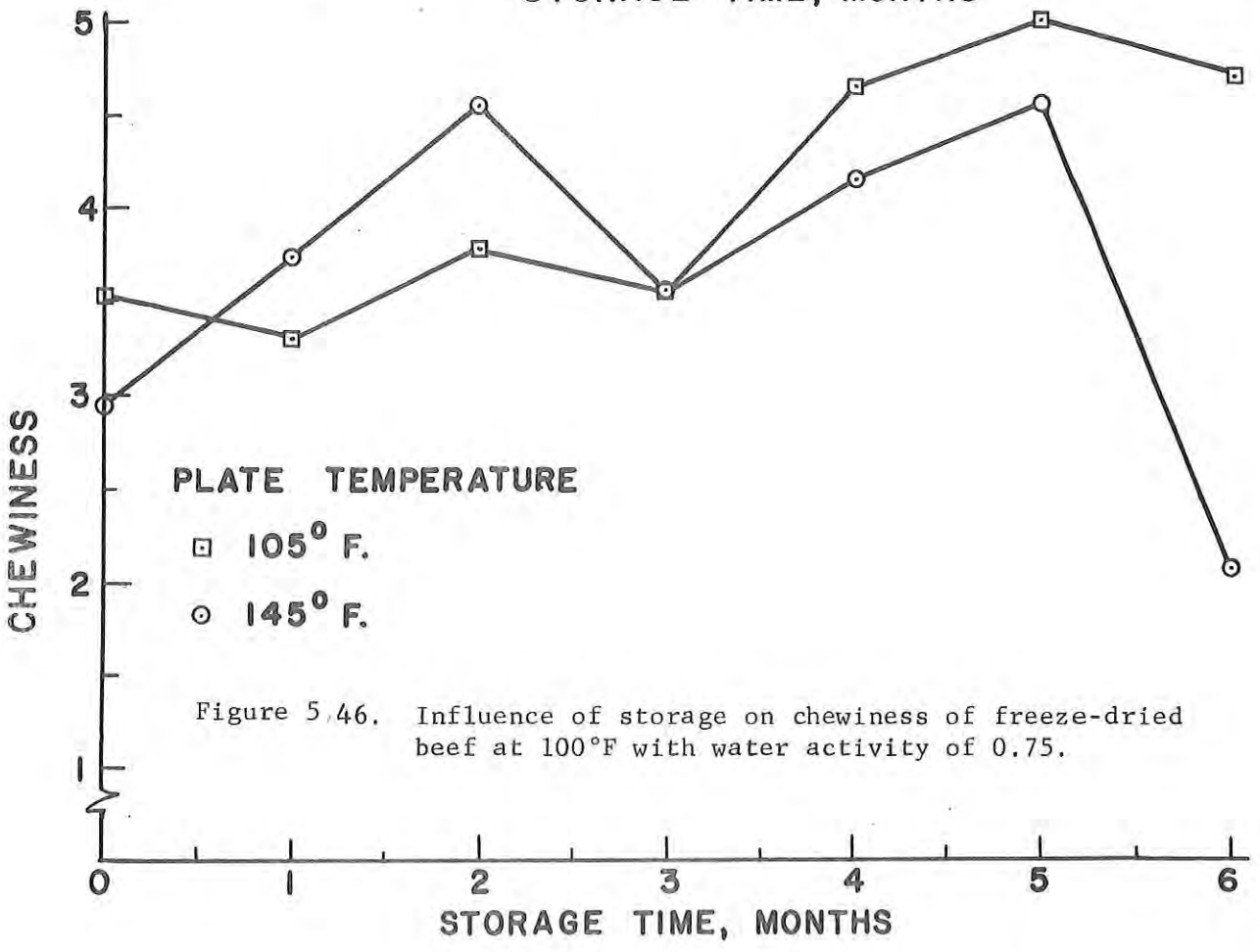

Figure 5.46. Influence of storage on chewiness of freeze-dried beef at 100°F with water activity of 0.75.

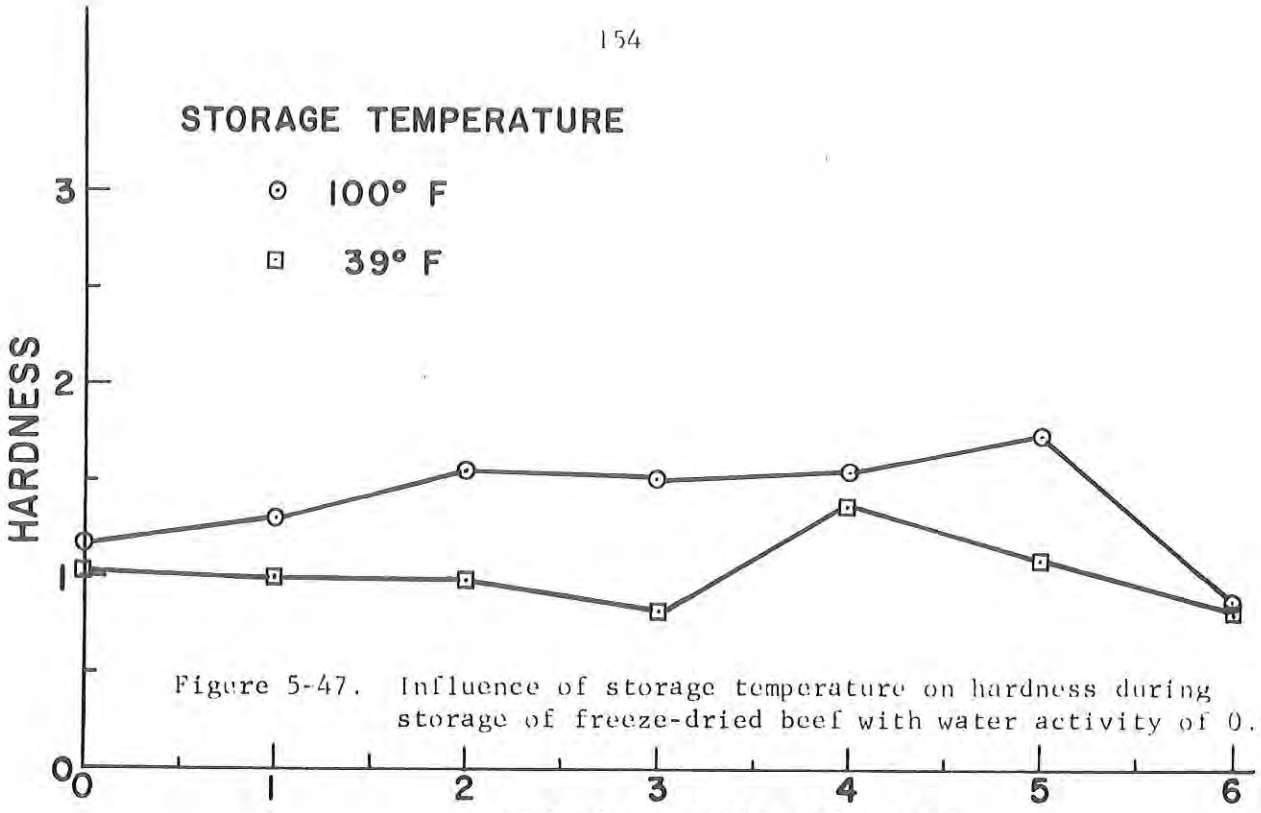

Figure 5-47. Influence of storage temperature on hardness during storage of freeze-dried beef with water activity of 0.75.

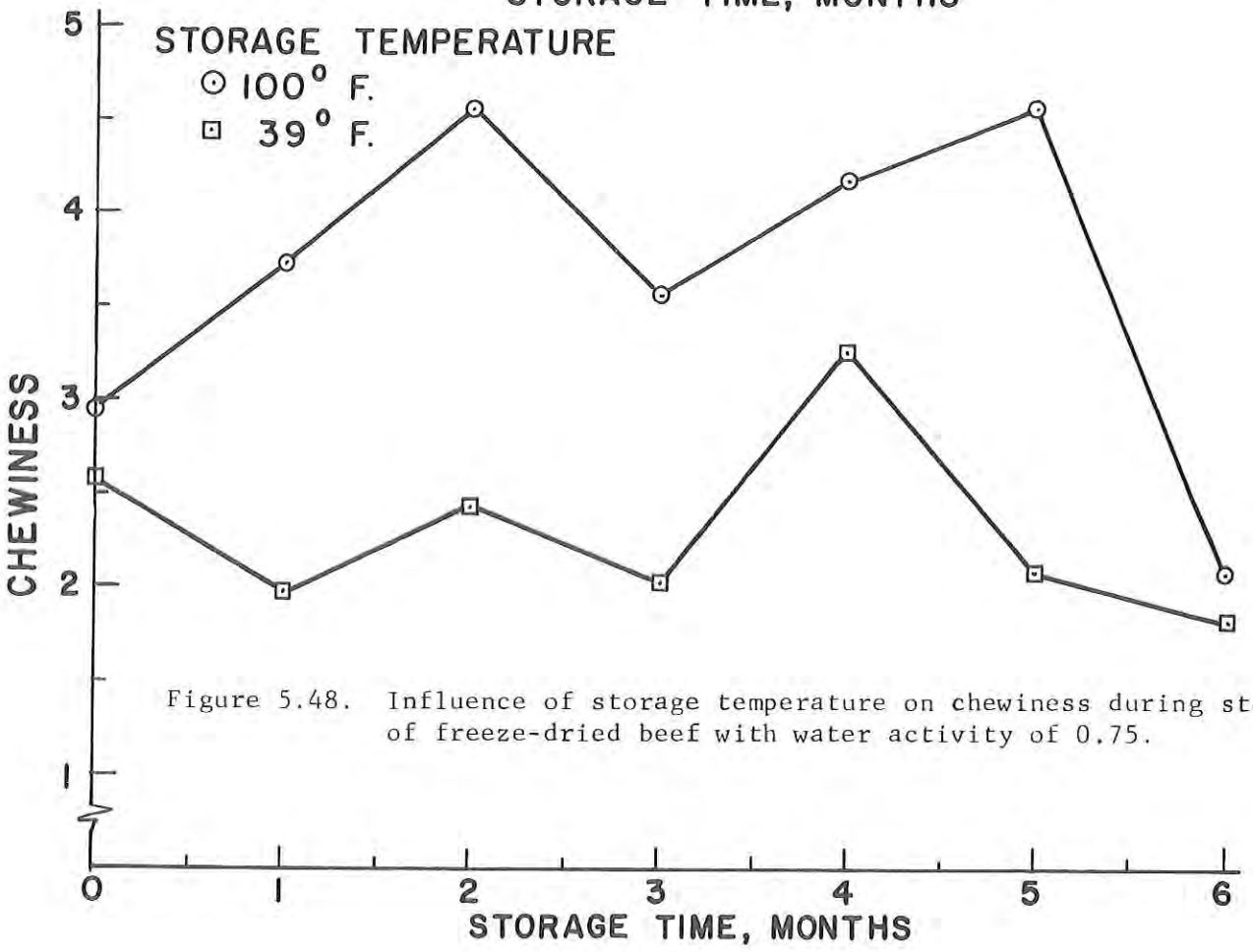

Figure 5.48. Influence of storage temperature on chewiness during storage of freeze-dried beef with water activity of 0.75.

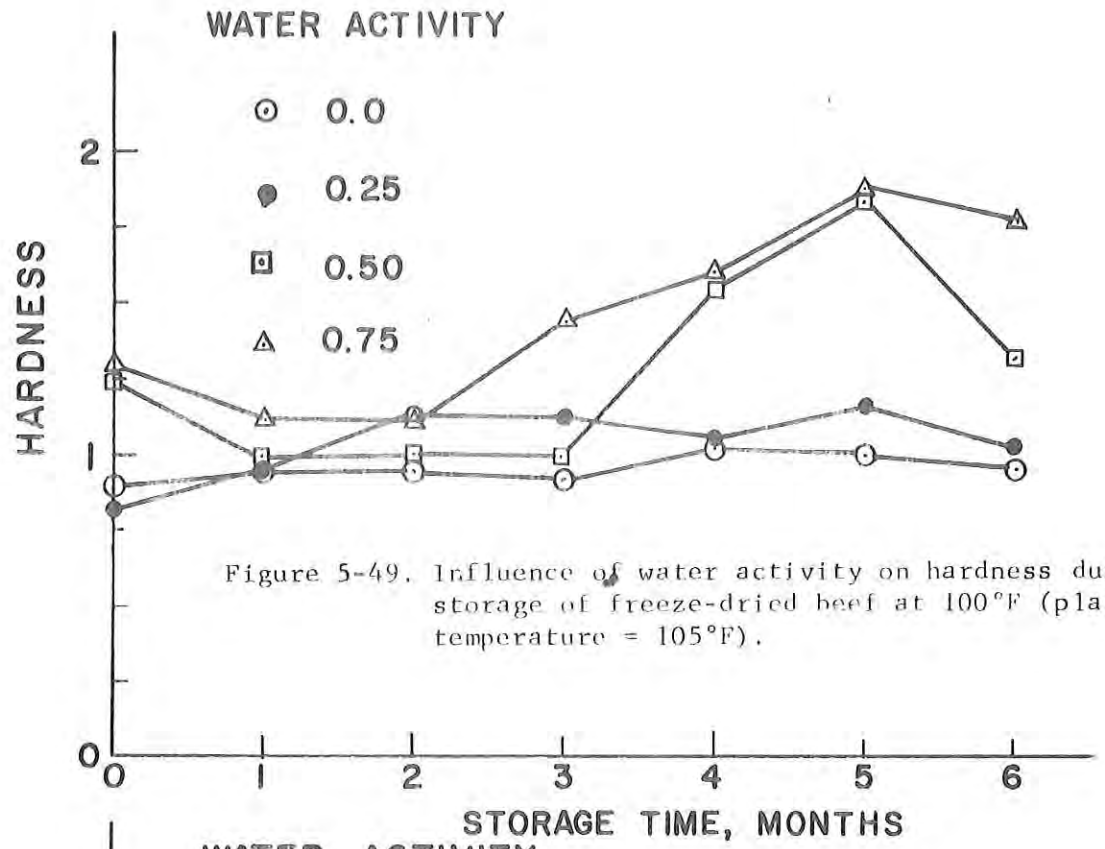

Figure 5-49. Influence of water activity on hardness during storage of freeze-dried beef at 100°F (plate temperature = 105°F).

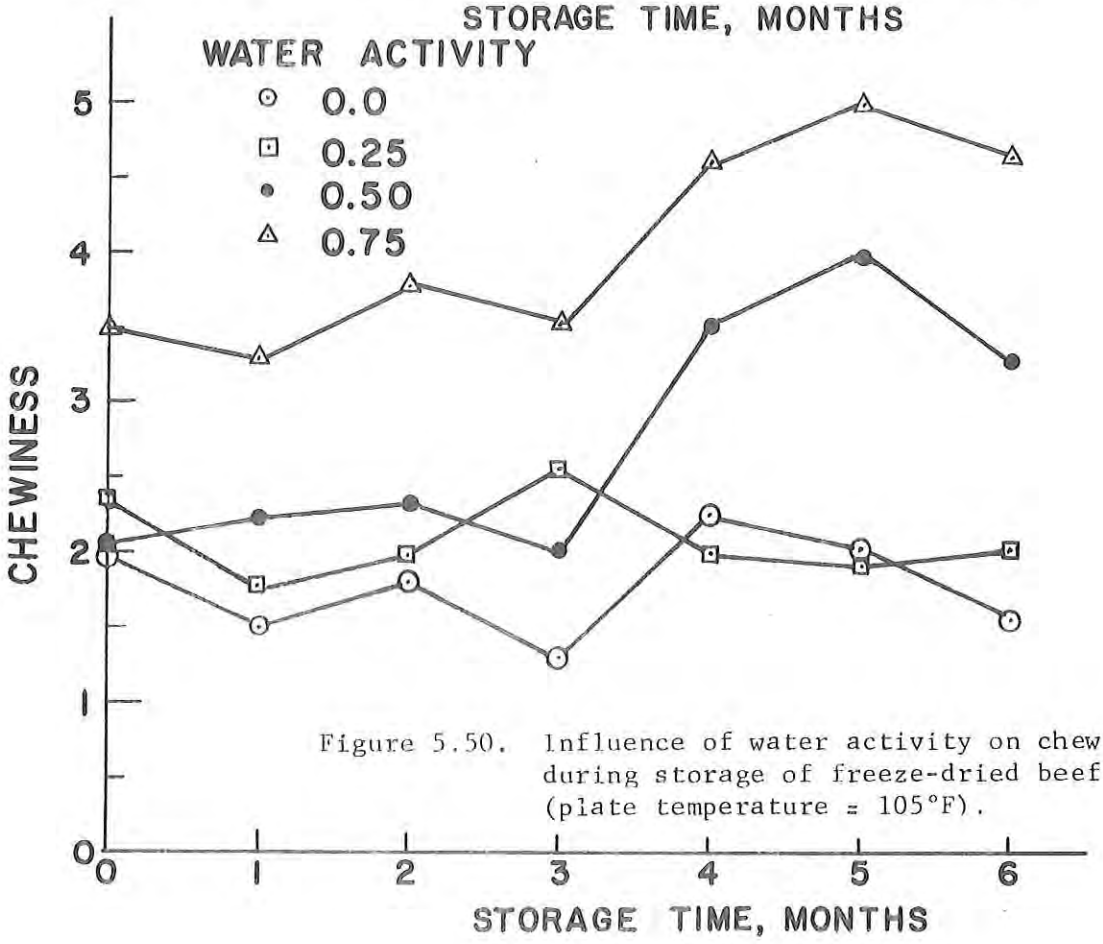

Figure 5.50. Influence of water activity on chewiness during storage of freeze-dried beef at 100°F (plate temperature = 105°F).

Table 5.17. Statistical significance of various processing and storage parameters on texture of freeze-dried beef.

Variable	Month of Storage 0	1	2	3	4	5	6	Overall
				(Hardness)				
Plate temp.	0.720	0.021	0.001	0.002	0.061	0.019	0.065	<0.0005
Storage temp.	0.224	0.018	0.011	0.636	0.857	< 0.0005	<0.0005	<0.0005
Water activity	0.294	0.293	0.022	0.468	0.728	0.102	0.049	0.169
Replicates	0.252	0.976	0.165	0.503	0.898	0.408	0.064	--
				(Chewiness)				
Plate temp.	0.072	0.003	0.297	0.295	0.767	0.365	0.162	0.003
Storage temp.	0.223	<0.0005	0.183	0.098	0.033	0.002	<0.0005	<0.0005
Water activity	0.017	<0.0005	0.001	0.013	0.003	<0.0005	0.001	<0.0005
Replicates	0.060	0.758	0.749	0.880	0.966	0.170	0.384	--

The influence of plate temperature on hardness appears to become significant beginning at 1 month of storage and continues through 5 months. After six months of storage, the significance level was the same as variability among replicates. In general, the same relationships existed between plate temperature and the chewiness parameter. The overall significance levels indicate a very definite influence of plate temperature on product hardness and a somewhat less significant influence on the chewiness parameter.

The statistical analysis indicates that the storage temperature may not have a significant influence on product hardness until reaching a storage time of 5 months. In the case of the chewiness parameter, the significance levels are sufficiently low at all times beginning with 1 month of storage supporting previous observations that the chewiness parameter may be more sensitive to variations in the product texture. An analysis of all data independent of storage time indicates that storage temperature has a definite influence on product hardness and chewiness.

The influence of water activity on product hardness seems somewhat questionable. The confidence levels are relatively close to corresponding levels for variations between replicate samples. This situation does not exist when analyzing the relationships between water activity and the chewiness parameter. Confidence levels obtained at storage times of one month or more are very low indicating a very definite influence of water activity on chewiness of the product. Analysis of all product samples confirms these observations, although the lack of observable influence on hardness may be related to the lack of sensitivity in the measurement of that particular parameter.

5.10. Relationships between Thermodynamic Parameters and Product Texture.

The thermodynamic parameters (differential free energy, enthalpy and entropy) were computed from the moisture equilibrium data. Tables 5.18 and 5.19 illustrate the thermodynamic properties of precooked freeze-dried beef for plate temperatures of 105°F and 145°F, respectively. The property values are presented for water activities of 0, 0.25, 0.50 and 0.75.

In general, the differential free energy ($\overline{\Delta G_w}$), differential enthalpy ($\overline{\Delta H_w}$) and differential entropy ($\overline{\Delta S_w}$) decreased as the water activity of the precooked freeze-dried beef increased. The only exception to this relationship was at the 100°F conditioning temperature with 145°F plate temperature product where the enthalpy and entropy values were maximum at 0.5 water activity.

In order to establish the relationship between product texture and thermodynamic parameters, the product chewiness parameter was plotted versus differential entropy ($\overline{\Delta S_w}$) as illustrated in Figures 5.51 and 5.52. The chewiness parameter was selected since previous analysis had indicated that it was a more sensitive parameter to changes than hardness. The differential entropy seems to be an appropriate thermodynamic parameter to utilize since variations with water activity are the same as for other thermodynamic parameters.

Table 5-18

Thermodynamic properties of precooked freeze-dried beef
(plate temperature 105°F)

Temperature 39°F

w.a.	$-\overline{\Delta G_w}$ *	$-\overline{\Delta H_w}$ *	$-\overline{\Delta S_w}$ **
0.0	∞	-	-
0.25	42.47	310.72	0.97
0.50	21.24	120.25	0.36
0.75	8.32	99.63	0.33

Temperature 100°F

w.a.	$\overline{\Delta G_w}$ *	$\overline{\Delta H_w}$ *	$\overline{\Delta S_w}$ **
0.0	∞		
0.25	47.57	496.30	1.44
0.50	23.79	640.5	1.98
0.75	9.87	430.4	1.35

* $\overline{\Delta G_w}$ - cal/g water

$\overline{\Delta H_w}$ - cal/g water

** $\overline{\Delta S_w}$ - cal/g water/ °C

Table 5-19. Thermodynamic properties of precooked freeze-dried beef (plate temperature 145°F)

Temperature 39°F

w.a.	$-\overline{\Delta G_w}$ *	$-\overline{\Delta H_w}$ *	$\overline{\Delta S_w}$ **
0.0	∞		
0.25	42.47	299.12	0.92
0.50	21.24	113.00	0.33
0.75	8.82	69.12	0.22

Temperature 100°F

w.a.	$-\overline{\Delta G_w}$ *	$-\overline{\Delta H_w}$ *	$-\overline{\Delta S_w}$ **
0.0	∞	316.82	0.87
0.25	47.57	130.71	0.34
0.50	23.79	86.82	0.25
0.75	9.87		

* $\overline{\Delta G_w}$ - cal/g water

$\overline{\Delta H_w}$ - cal/g water

** $\overline{\Delta S_w}$ - cal/g water / °C

Figure 5-51. Relationships between differential entropy and chewiness at 39°F.

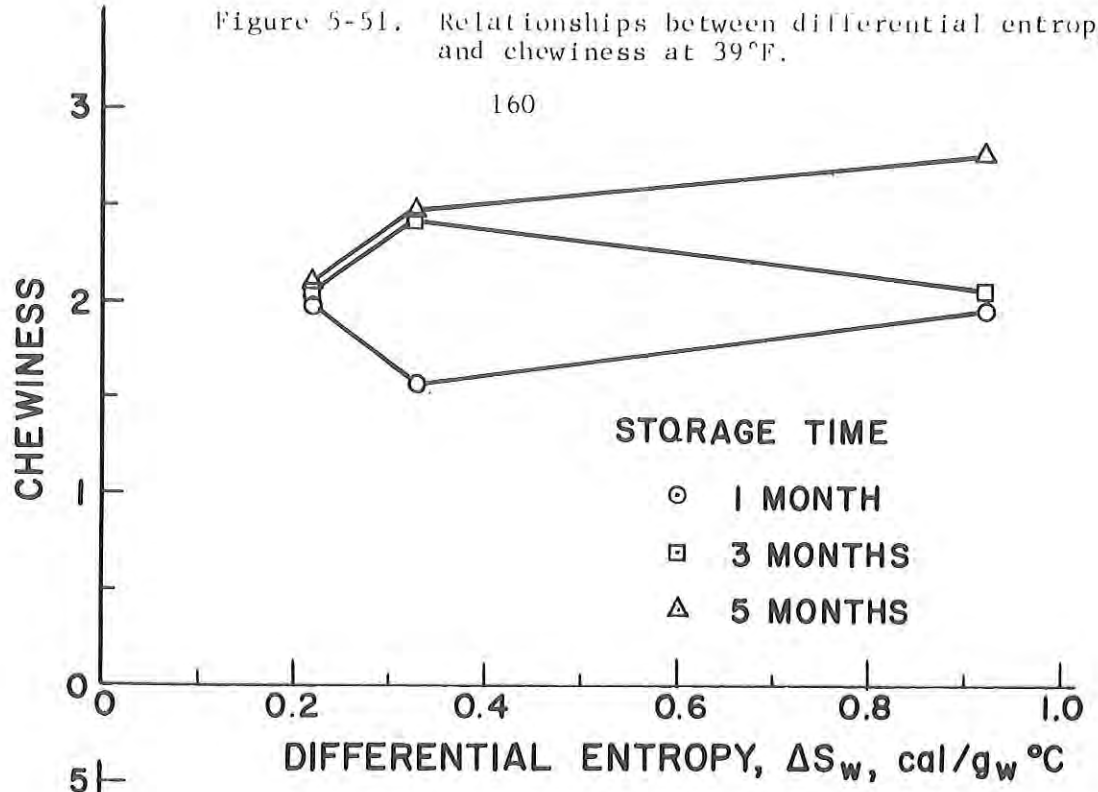

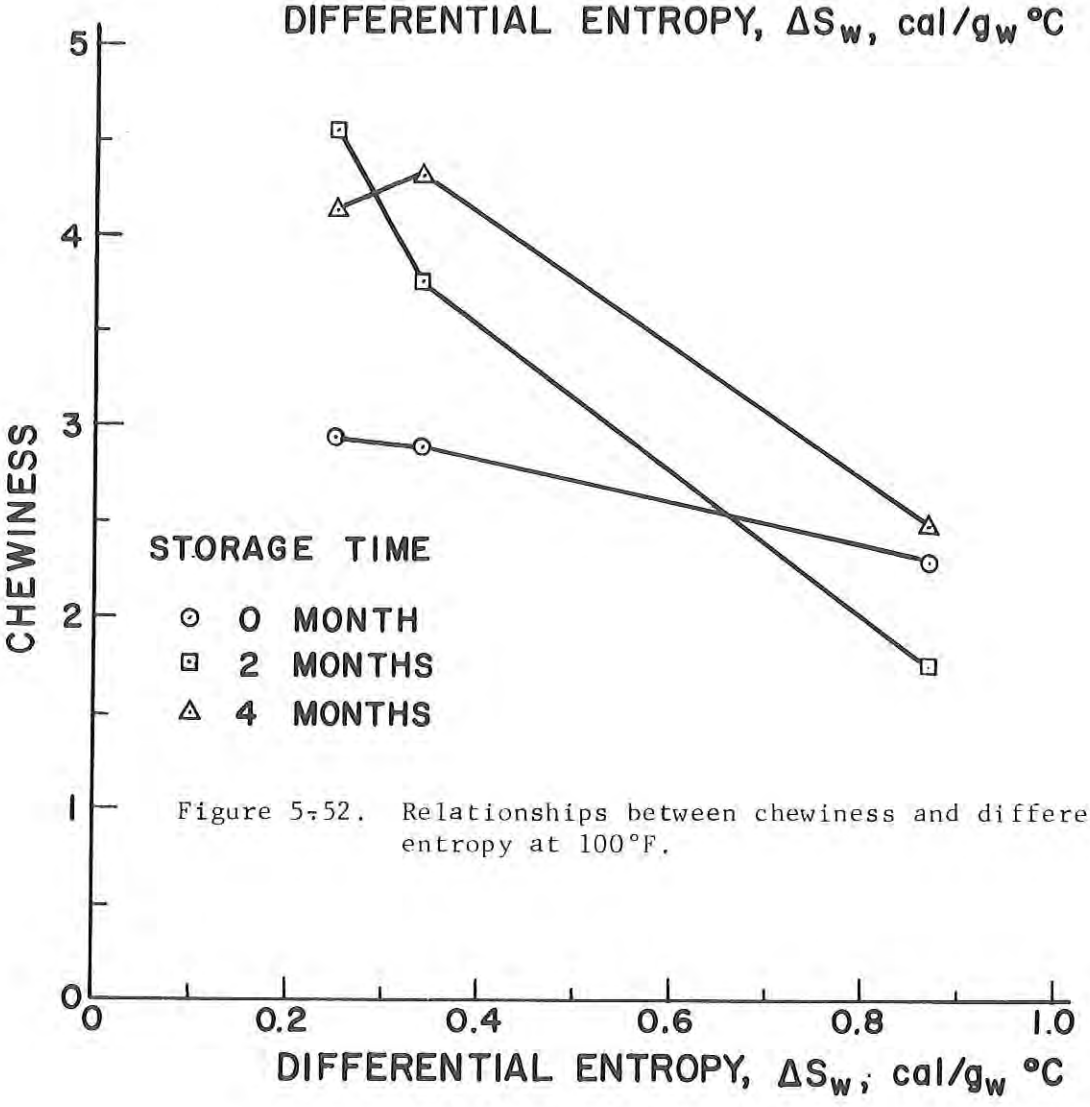

Figure 5-52. Relationships between chewiness and differential entropy at 100°F.

The results in Figure 5.51 illustrate the relationship obtained at 39°F. In general, it would appear that chewiness changes very little with increasing differential entropy. Although three different storage times are presented, it would be very difficult to draw a conclusion related to change of texture at 39°F with change in thermodynamic parameters.

At the 100°F storage temperature (Figure 5.53), a more obvious relationship exists. An initial observation reveals that all results indicate that chewiness is decreasing with increasing differential entropy. This is as expected since higher entropy values were obtained at higher water activities, which corresponded to lower chewiness values. It seems logical that higher entropy should have more desirable texture since lower entropy implies a tight structure expected for less desirable texture.

In addition to the general relationship between product chewiness and differential entropy, there appears to be a changing relationship with increased storage time. At the beginning of storage, the chewiness decreases only slightly with increasing entropy. As storage time increases to 2 and 4 months, the decrease in texture with increases in the thermodynamic parameter becomes more evident. Those results would indicate that extended storage at high temperature (100°F) results in more significant changes in product texture as related to the thermodynamic parameters.

5.11. Relationship Between Engineering Parameters and Product Texture.

5.11.1. Impact tests. The mean energy absorption values at various equilibrium relative humidities (E.R.H.) are presented in Table 5-20 and illustrated on Figure 5.53.

TABLE 5-20 Mean energy absorbed in impact test.

E.R.H. %	15	30	50	70	92
Energy Absorbed, ft.-lb.	0.152	0.216	0.236	0.215	0.187

The results reveal relatively little effect of water activity on the capability of the cube samples to absorb energy. An analysis of variance also failed to detect a significant effect of water activity.

The quantity of energy absorbed increased to a maximum at a water activity of 0.5, and decreased at water activities greater than that. Although the maximum value of energy absorbed was 50% greater than the minimum value it is difficult to justify drawing any conclusions regarding a definite relationship between equilibrium relative humidity and energy absorbed. For example, a quadratic type of function would seem adequate for describing the curve on Figure 5.53, but this could not be supported by statistical analysis. Further, it may be worthwhile to note that the one value of 0.54 ft.-lb. at 15% E.R.H. is an isolated instance and probably due to inhomogeneities in that particular sample. It has the effect of decreasing the value for energy absorbed at $a_w = 0.15$ to a level which is probably not typical. This one value could also be the cause for finding differences in energy absorbed due to the location in the muscle from which the sample was taken, a conclusion that can barely be drawn at the 95% confidence level.

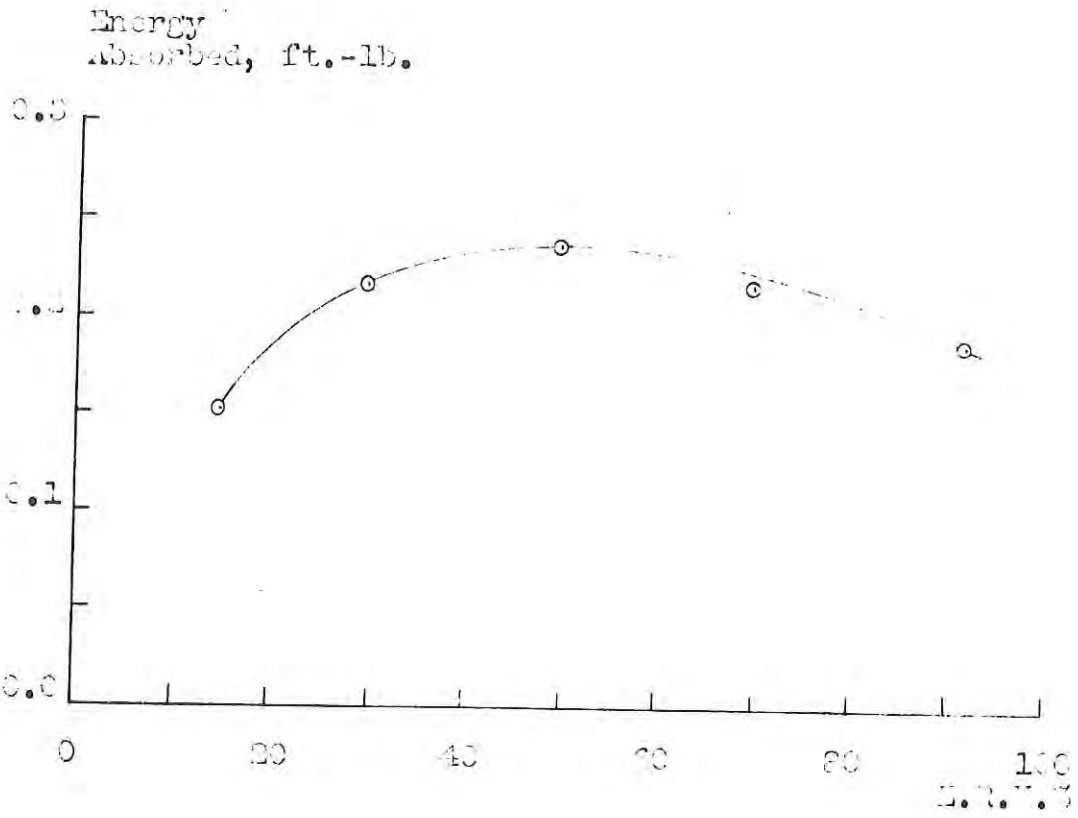

Figure 5-53 Energy absorbed (under impact loading) by 0.4 inch cubes of pre-cooked, freeze-dried beef, at different equilibrium relative humidities.

It is evident from Figure 5.54 that energy absorbed cannot be taken as a good guide for predicting water activity, and consequently texture parameters. These results tend to illustrate that energy absorbed is insensitive to changes in the hardness index. It may be concluded therefore that the impact test does not appear to offer information which could lead to predicting texture indices.

5.11.2. Accuracy of viscoelastic models. Three different approaches were adopted for estimating the parameters in both models. Accuracy of the models was checked not only by the experimental data of the test used for parameter estimation but also by independent tests. The concept underlying this approach is illustrated on Figure 5.55.

Figure 5.55 illustrates that the relaxation test data allowed all four parameters E_1, E_3, η_1, η_3 to be estimated for Model 1, which was then used to predict cyclic and creep functions. Similarly, the cyclic tests were used to estimate A, B, λ and C in Model 2(b), and the equation for that model subsequently predicted both creep and relaxation responses. The third approach used both the relaxation and cyclic tests to determine the coefficients in Model 2(a). The creep test results were employed for comparison purposes between Models 1, 2(a) and 2(b).

As will be discussed below, except for the failure of Model 1 to predict the cyclic response, the models appear to give satisfactory predictions. Since all of the parameters in Model 1, and three of the four in Model 2(a) were evaluated from relaxation tests, these models should give close agreement with the experimental relaxation data. Once the equation for a model gives a solution whose function is similar to the experimental pattern, then it only remains to calculate the optimum values of the constants in the model which give best agreement with experimental results. This optimization procedure was accomplished by using the GAUSHAUS non-linear estimation method.

Figures 5.56, 5.57, 5.58, 5.59 and 5.60 illustrate a comparison between the models and experimental data for the relaxation tests. The differences which may exist between Model 1 and Model 2 as time approaches infinity may not be obvious. Reference to equations (16) and (17) will show that stress (σ) for Model 1 reduces to zero after an infinite time, whereas, in Model 2, the stress will approach a constant value: $\sigma(t=\infty) = A\ \varepsilon_o$ Within the time periods considered in the present experiments however, large differences between both models were not apparent.

The relaxation function suggested by the model whose parameters were estimated without using relaxation data, i.e., Model 2(b), agrees exceptionally well with experimental results at equilibrium relative humidities of 70% and 92%. For the lower water activities the predicted stresses are higher than the experimental values for about the first five seconds, and approximately 25% too low for times greater than that. One possible explanation for this lack of agreement may be related to the fact that the parameters in Model 2(b) were determined from the cyclic tests, which gave results somewhat inconsistent from what the relaxation data indicate. For example, a strain of 0.15 is applied instantaneously to the sample in a relaxation test but in a cyclic test the application is gradual, e.g., over 7.2 seconds when the deformation rate is 0.5 inch/min. Some stress should have "relaxed" during this time period.

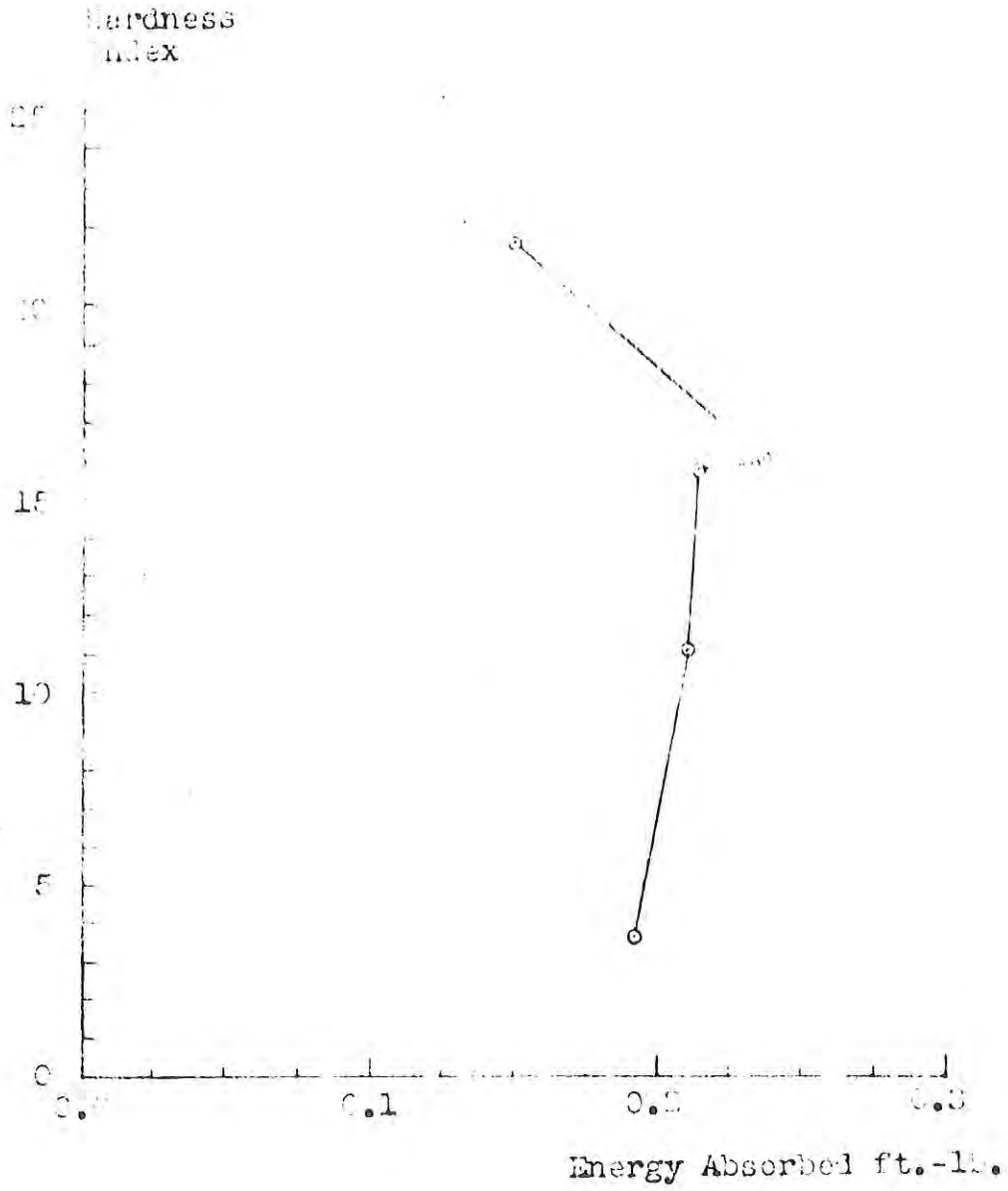

Figure 5-54 Relationship of energy absorbed under impact loading to Hardness Index for pre-cooked freeze-dried beef.

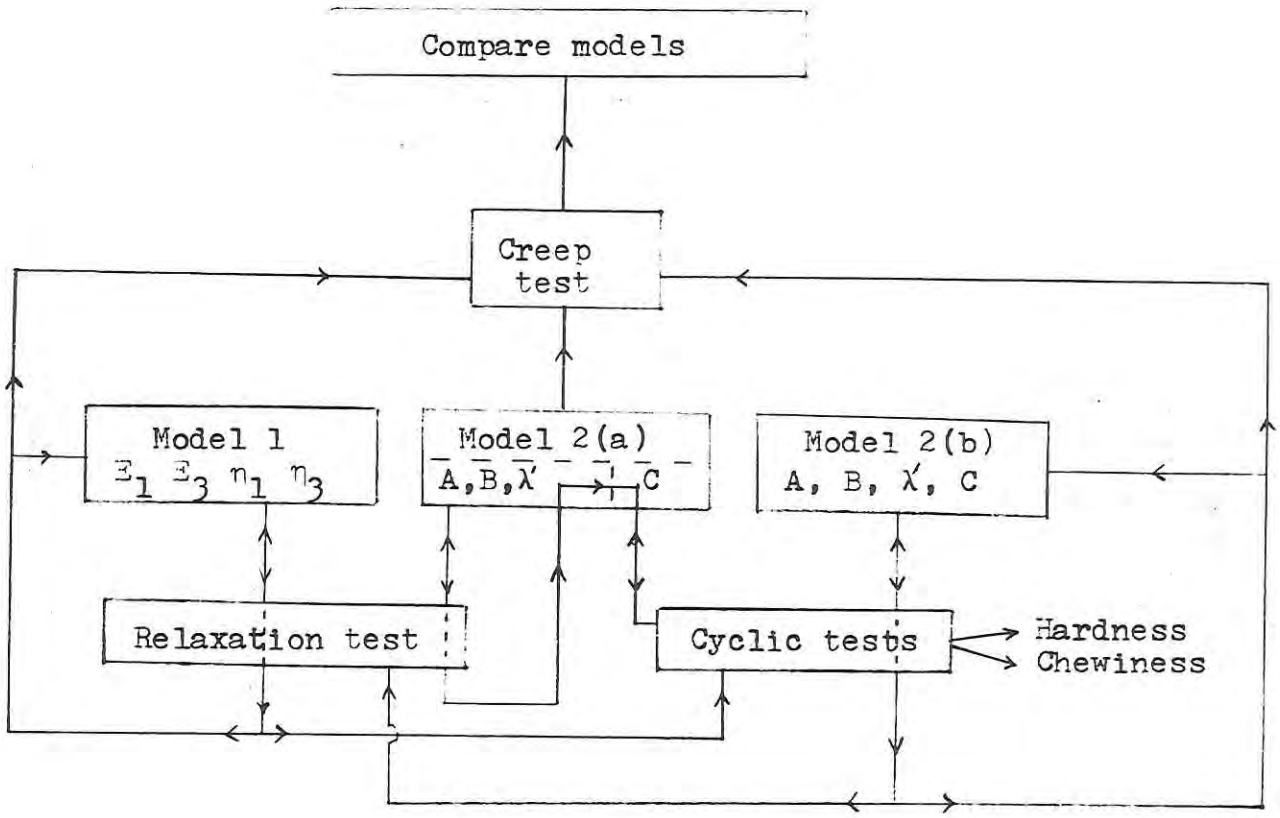

Figure 5-55 Parameter estimation, function predictions, and model comparison at each water activity.

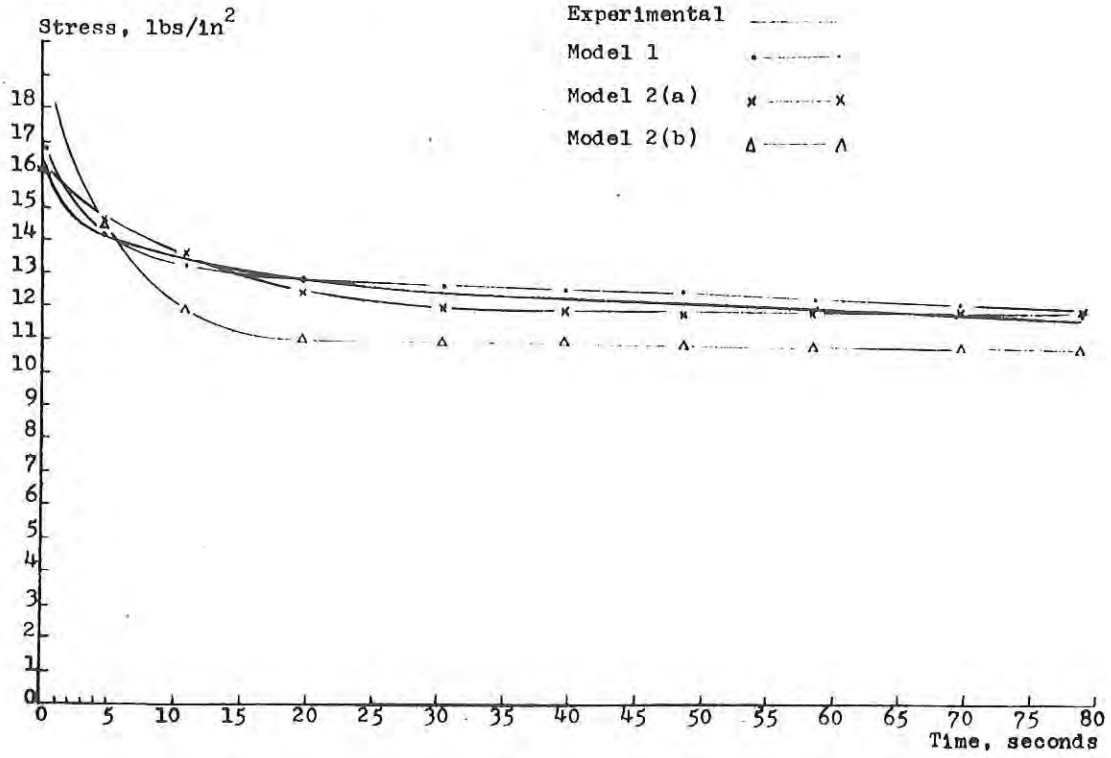

Figure 5-56 Experimental results and theoretical predictions for relaxation test - 80°F., 15% R.H.

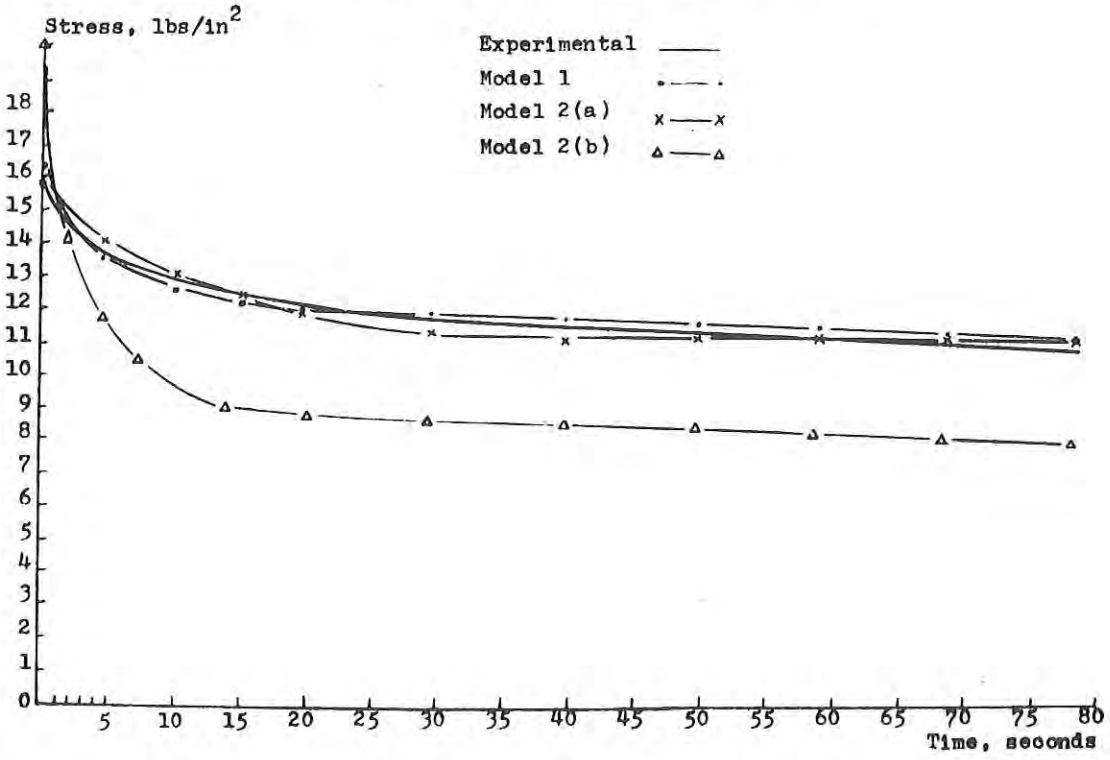

Figure 5-57 Experimental results and theoretical predictions for relaxation test - 80°F., 30% R.H.

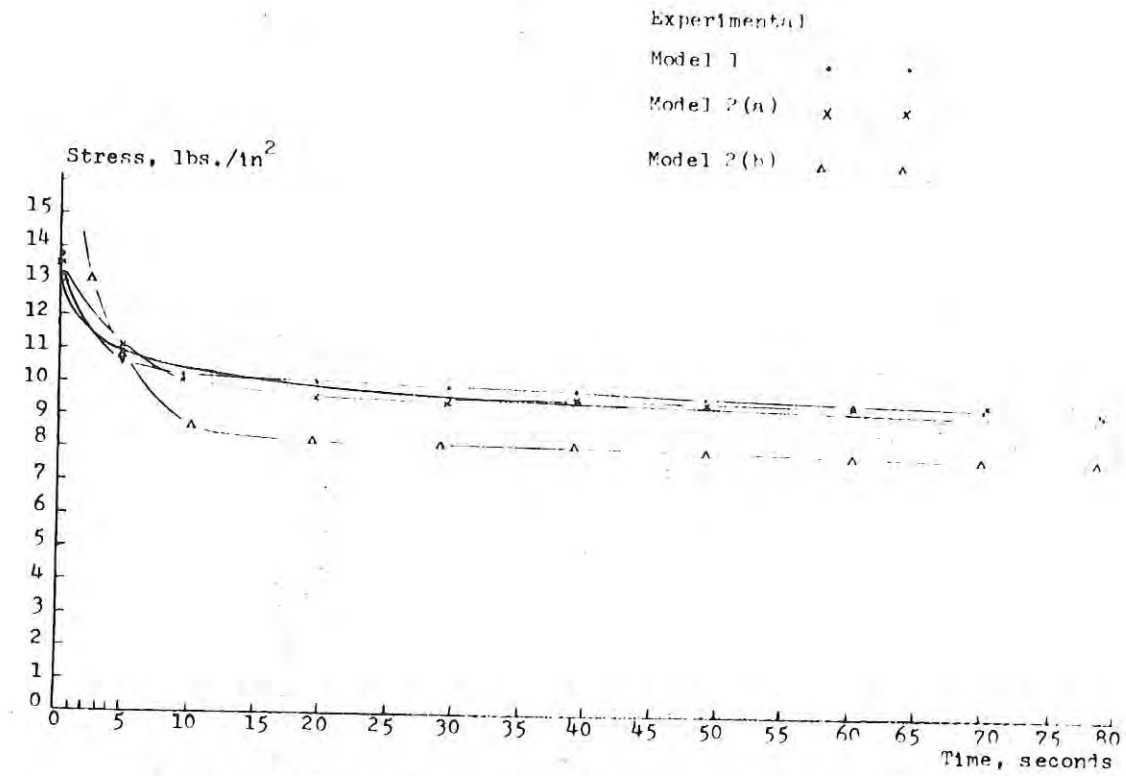

Figure 5-58 Experimental results and theoretical predictions for relaxation test - 80°F., 50% R.H.

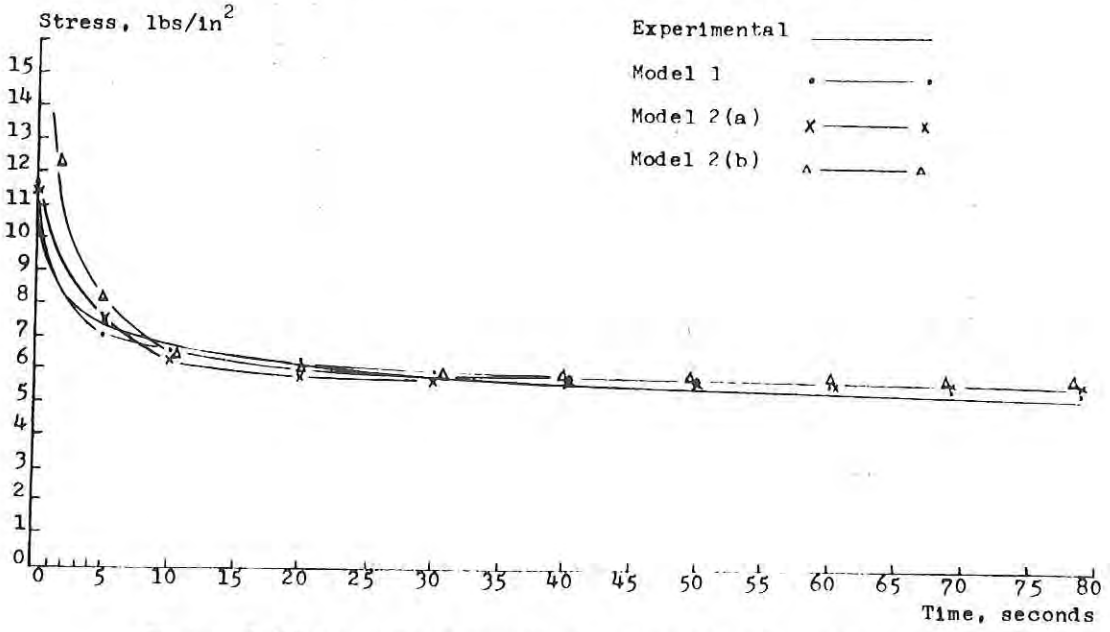

Figure 5-59 Experimental results and theoretical predictions for relaxation test - 80°F., 70% R.H.

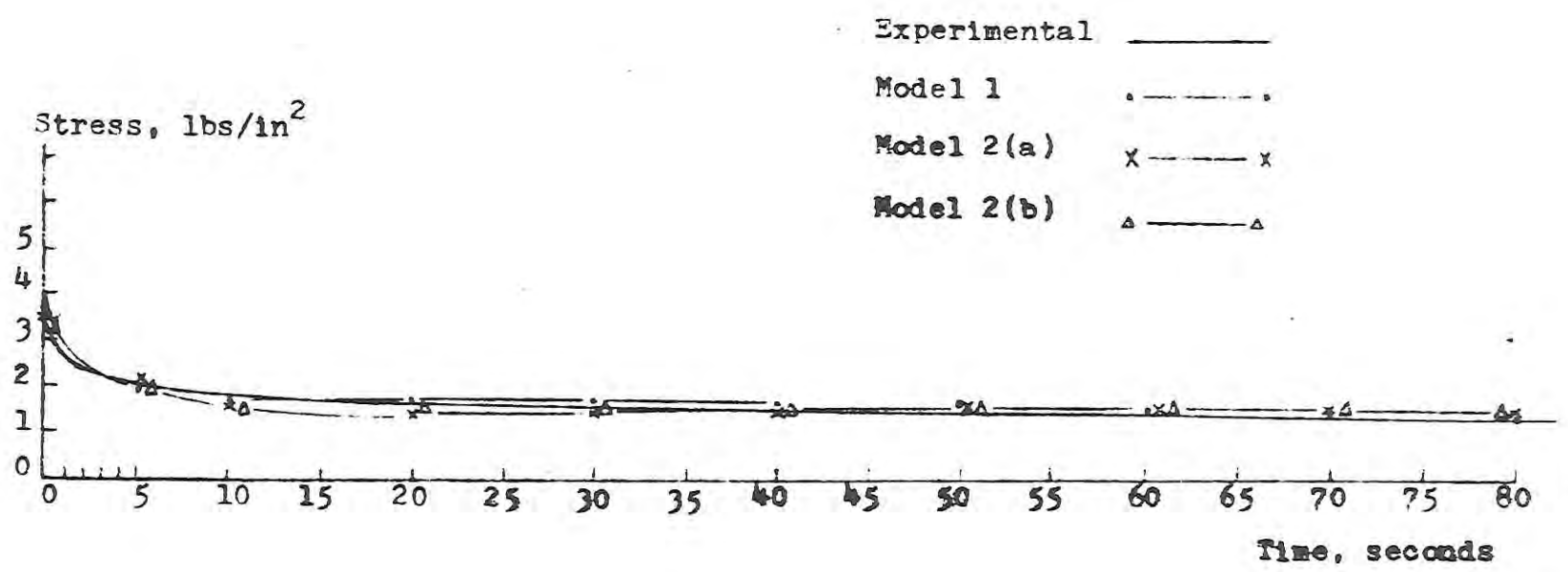

Figure 5-60. Experimental results and theoretical predictions for relaxation test - 80°F., 92% R.H.

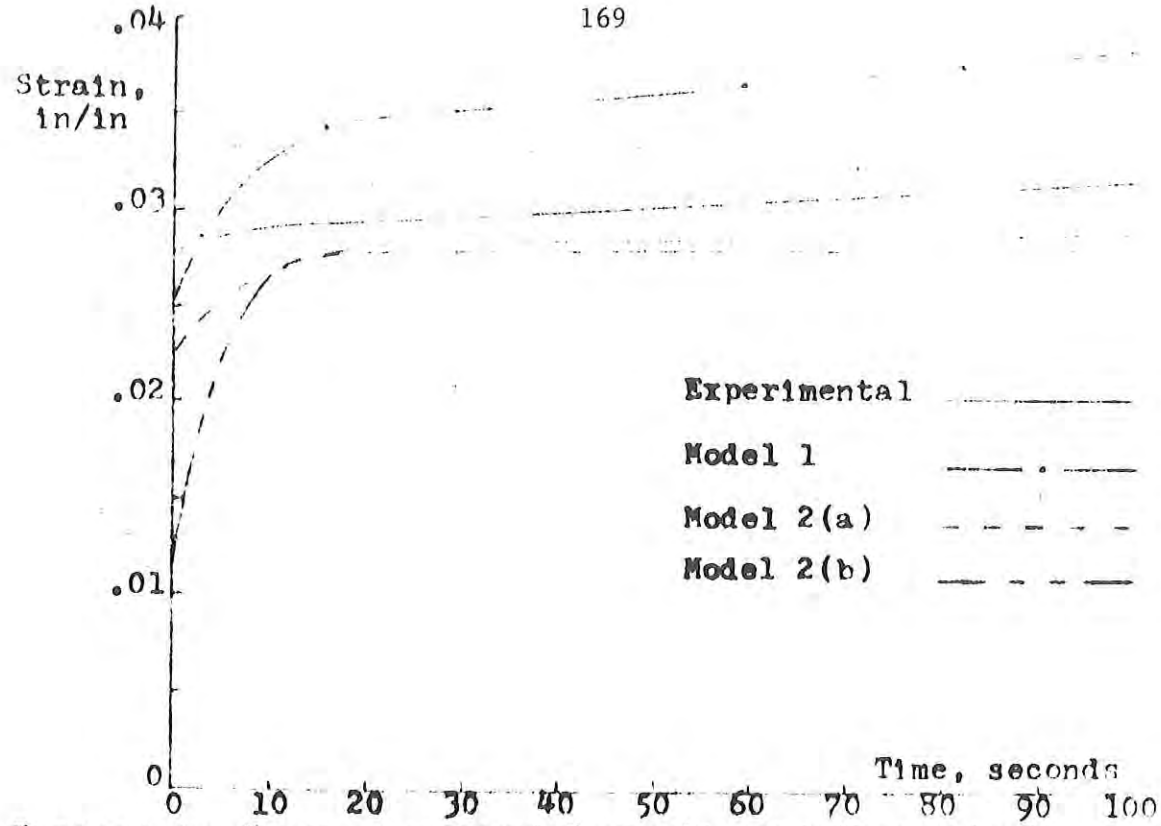

Figure 5-61. Creep experimental results and theoretical predictions - 80°F., 15% R.H.

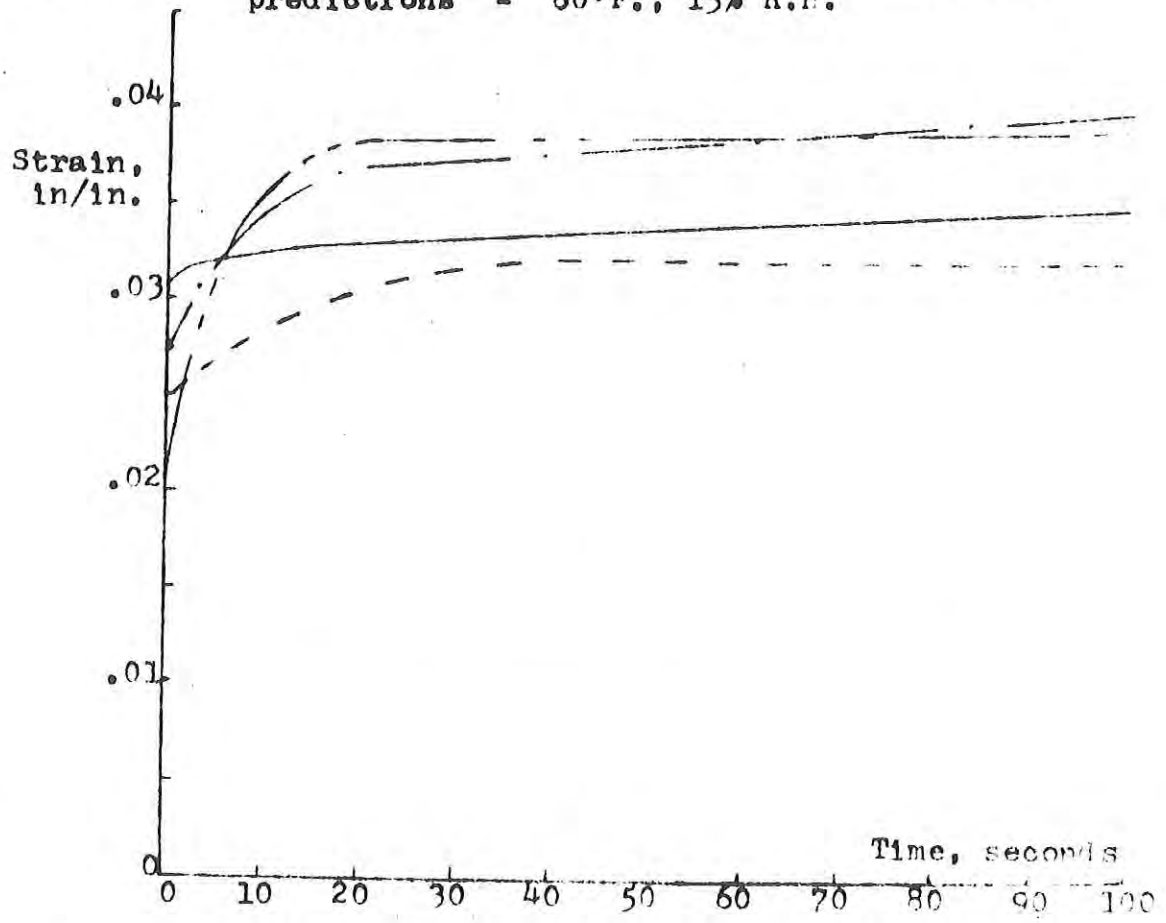

Figure 5-62. Creep experimental results and theoretical predictions - 80°F., 30% R.H.

Therefore the cyclic stress when strain reaches 0.15 should be lower than the relaxation stress for the same strain at time, t = 0. But the experimental results at the lower water activities showed that the maximum stress for a cyclic test was greater than the maximum stress for a relaxation test.

The very high relaxation stresses predicted by Model 2(b) for times less than five seconds substantiate the above explanation. Indeed, this same apparently inconsistent behavior eliminates the possibility that Model 1, with parameters estimated from the relaxation experiments, could accurately product cyclic stress behavior.

Such discrepancies between initial stress, σ_o, during relaxation loading and maximum stress, σ_{max}, under cyclic load application can perhaps be attributed to at least four possibilities: (a) differences in the samples tested; (b) the effect of sudden loading in a relaxation test, (c) a possible work-hardening effect during gradual compression in cyclic tests, or (d) changes in the product at different water activities.

Random errors due to sample differences is a strong possibility for the relaxation results, since only five replications were run at each equilibrium relative humidity. However, fifteen cyclic tests at each water activity should have been sufficient to account for product differences. Further, the trends for both types of experimental results are the same -- it is the relative magnitude of the stress values which is surprising.

It is conceivable that the sample structure would be more susceptible to fracture or yielding under sudden impacting than under more gradual force application. Also, at lower moisture contents the product structure seemed more brittle than at higher moisture levels. The fact that Model 2(b) predicts relaxation much better at higher moisture contents, when presumably the product is less brittle, would support the contention that manner of loading combined with changes in the product structure at increased moisture levels is the most acceptable explanation for the apparent inconsistancies.

The fourth possible reason mentioned was a work-hardening effect. This behavior is exhibited by many engineering materials and it could also be true of low moisture foods, i.e., the product becomes more resistant to compression as deformation is increased.

The use of the relaxation data to estimate parameters would lead to predictions of cyclic stresses which would be too low, as all ready discussed. However, the failure of Model 1 to predict cyclic response with any degree of accuracy must lead to the conclusion that a simple linear viscoelastic model is inadequate to describe the general stress-strain relationship for precooked freeze-dried beef. Nevertheless, such models may be very suitable for specific tests such as creep or relaxations.

For example, the four element model proposed gives the best fit of all the three models to relaxation curves, and also gives suitable predictions for creep at 0.15, 0.30 and 0.50 water activities (Figures 5.61, 5.62 and 5.63). At the higher water activities, creep predictions indicate that all four coefficients, E_1, E_3, η_1 and η_3, are too low (Figures 5-63, 5-64. Specifically,

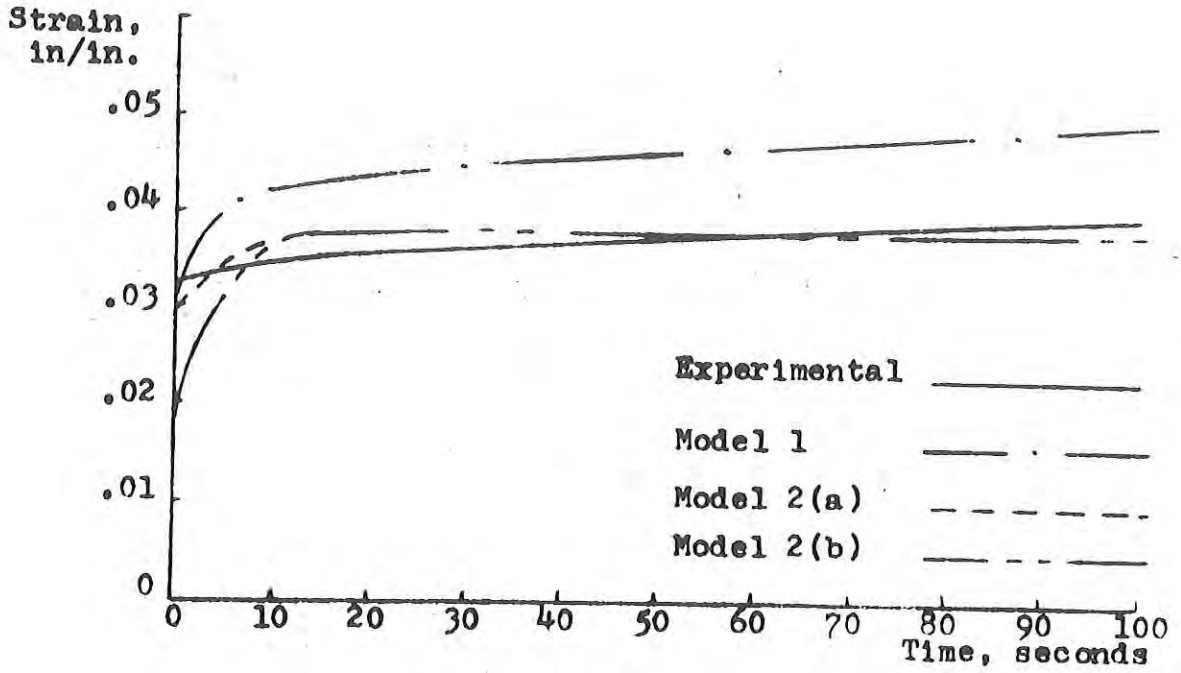

Figure 5-63. Creep experimental results and theoretical predictions - 80°F., 50% R.H.

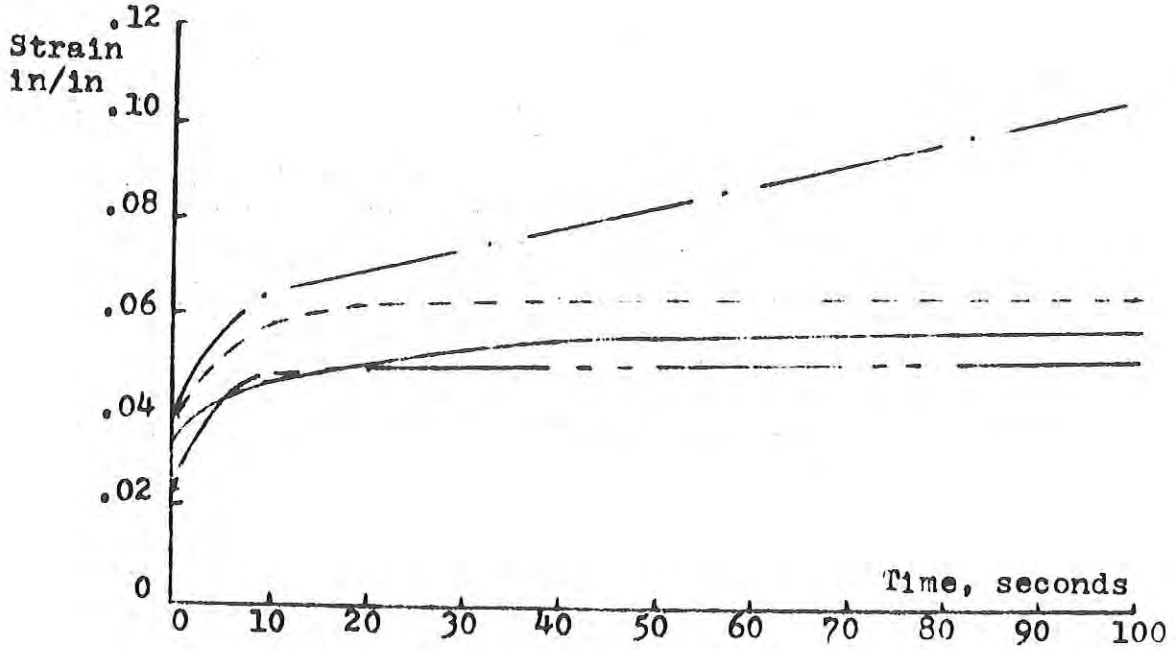

Figure 5-64. Creep experimental results and theoretical predictions - 80°F., 70% R.H.

increasing the values the η_1 and E_1 would decrease the rate of change of strain, and also the magnitude of strain. These changes would also have the effect of increasing the predicted cyclic stress to a value nearer the experimental value. Unfortunately, such changes would lead to inaccurate predictions of the relaxation function.

Model 2(b), whose coefficients were calculated from cyclic test data, describes cyclic behavior excellently. It can also satisfactorily predict creep strain at all water activities (Figures 5.61, 5.62, 5.63, 5.64 and 5.65). The fact that relaxation stresses predicted are too high for times below five seconds, and too low for times greater than that, is due to the exponential term $(B\, e^{-t/\lambda'})$, being determined to satisfy cyclic results. The inconsistencies between cyclic and relaxation data discussed above meant that this term, for times near $t = 0$, would make too high a contribution to predicted relaxation stress. Nevertheless, even allowing for this inaccuracy, the predicted relaxation stresses are reasonable estimates of the experimental results.

The combination of cyclic and relaxation data utilized to determine the constant parameters in Model 2(a) overcomes the irregularities in results between both tests. Only one part of Model 2 is applicable under relaxation conditions:

$$A\epsilon + B\epsilon e^{-t/\lambda'}$$

and this can be satisfactorily fitted to the experimental data for the relatively short time periods being considered. Using this part of the model to predict cyclic response (i.e., omitting the term $C\int_{t_n}^{t} d\epsilon$), it was found that for the loading parts of the cycle ($0 < t < t_1$ and $t_2 < t < t_3$) predicted stresses were too low, whereas the opposite was the case during unloading. Thus the term $C\int_{t_n}^{t} d\epsilon$ plays an important role, since it increases the predicted stress for loading conditions, but decreases it when strain -- and therefore stress -- is being decreased. The result is very good predictions, as illustrated on Figures 5.66, 5.67, 5.68, 5.69 and 5.70. In addition, when comparing the predictions by models with results of creep experiments, the predictions by Model 2(a) were in closer agreement than either Model 1 or Model 2(b). The approach used to evaluate the parameters of Model 2(a) would therefore seem to give the most acceptable general model.

To avoid confusion, the cyclic curves resulting from the solution of Model 1 have not been included in Figures 5.66, 5.67, 5.68, 5.69 and 5.70. The maximum theoretical stresses were only one-fourth to one-third the values of the experimental stresses, as illustrated by the results presented in Table 5.21.

5.11.3. Influence of water activity on model parameters. Two different methods were used for calculating mean parameters. One approach used for the parameters estimated from relaxation data involved the determination of a mean relaxation response at each water activity. From the mean curve thus obtained, optimum mean parameter values were estimated using the GAUSHAUS non-linear estimation procedure. Parameter estimates were also made from each individual curve. The coefficients estimated in this manner included E_1, E_3,

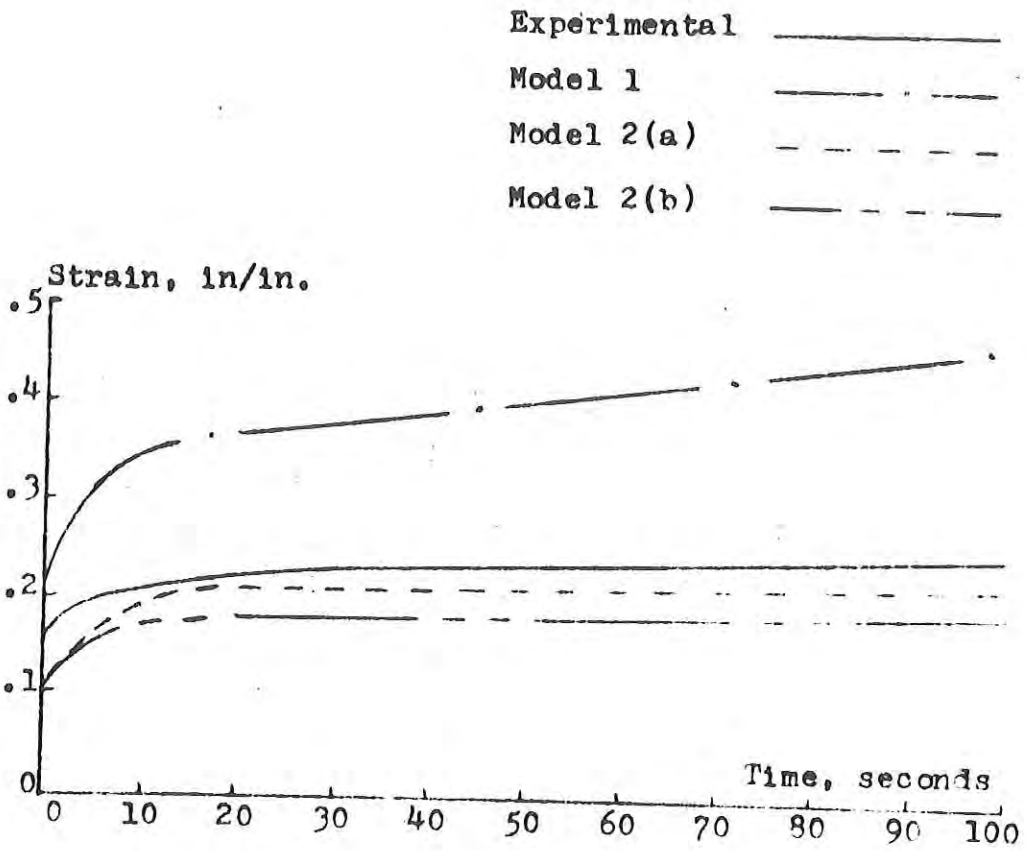

Figure 5-65. Creep experimental results and theoretical predictions - 80°F., 92% R.H.

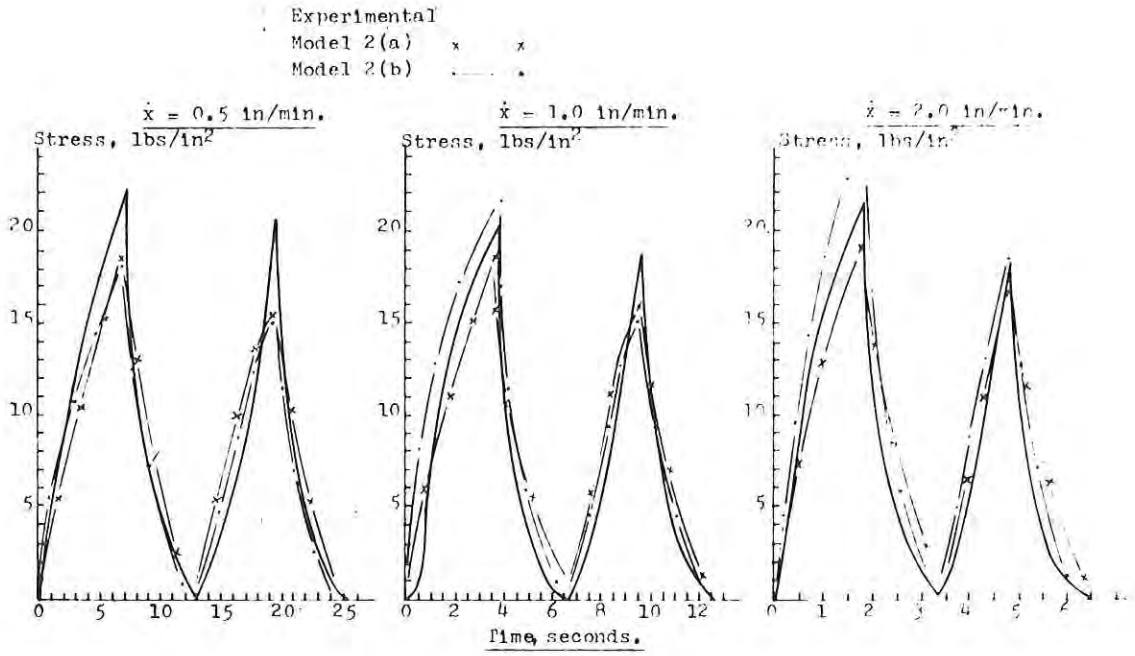

Figure 5-66 Experimental results and theoretical predictions for cyclic tests - 80°F., 15% R.H.

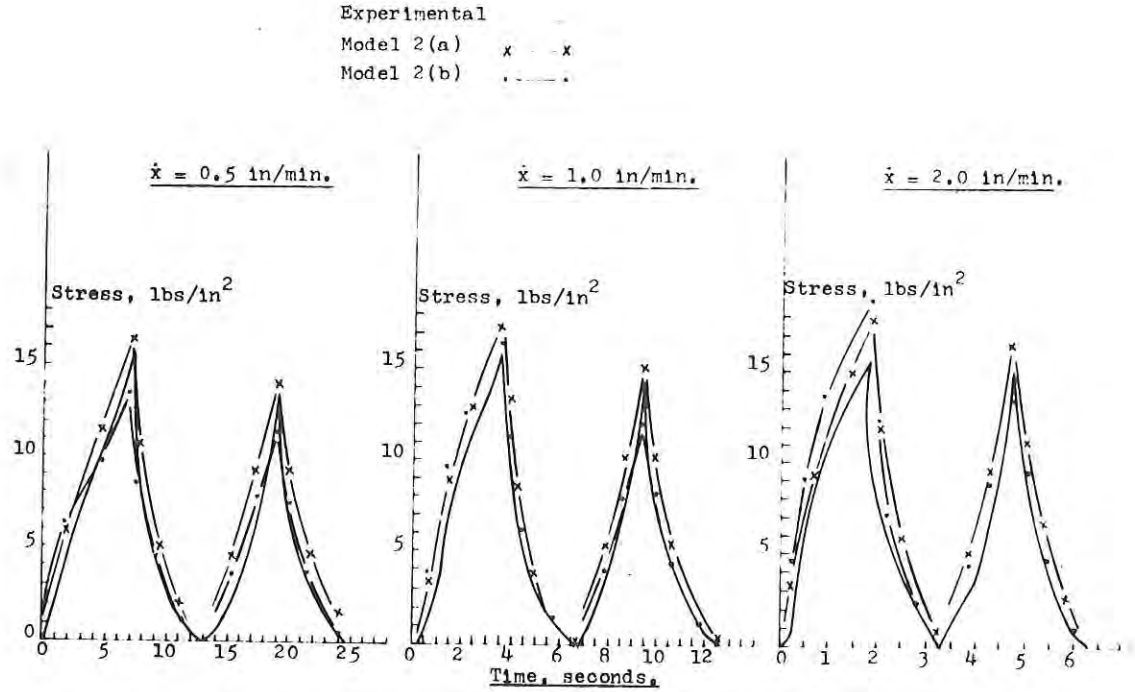

Figure 5-67 Experimental results and theoretical predictions for cyclic tests - 80°F., 30% R.H.

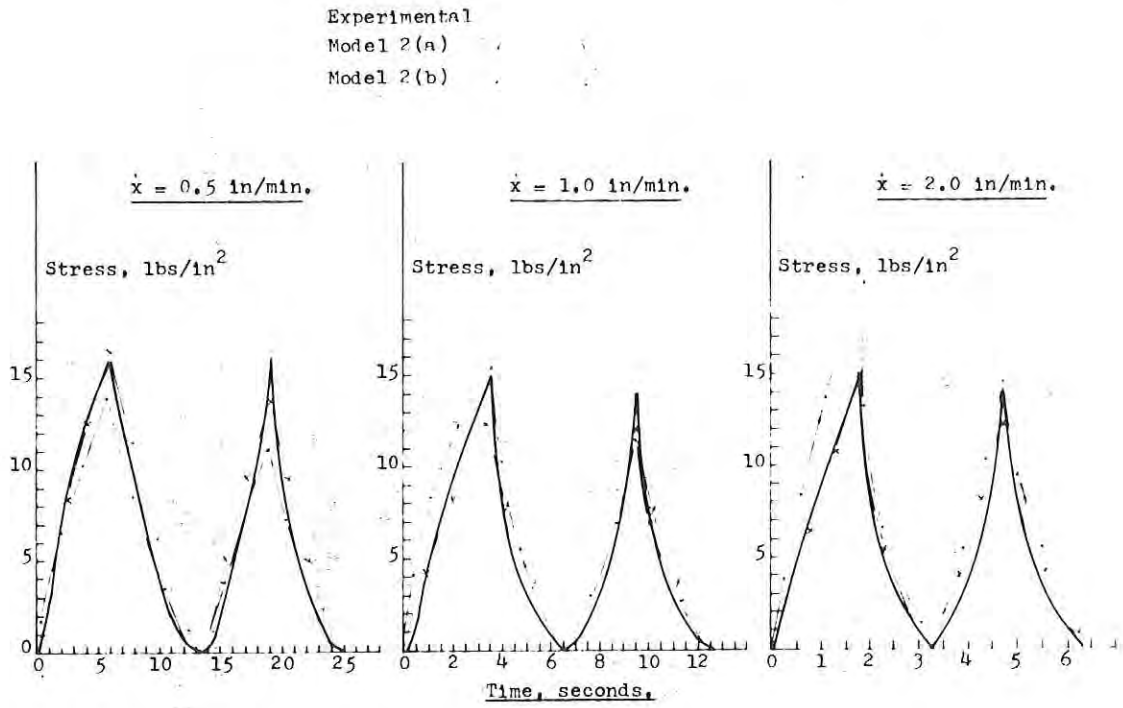

Figure 5-68 Experimental results and theoretical predictions for cyclic tests - 80°F., 50% R.H.

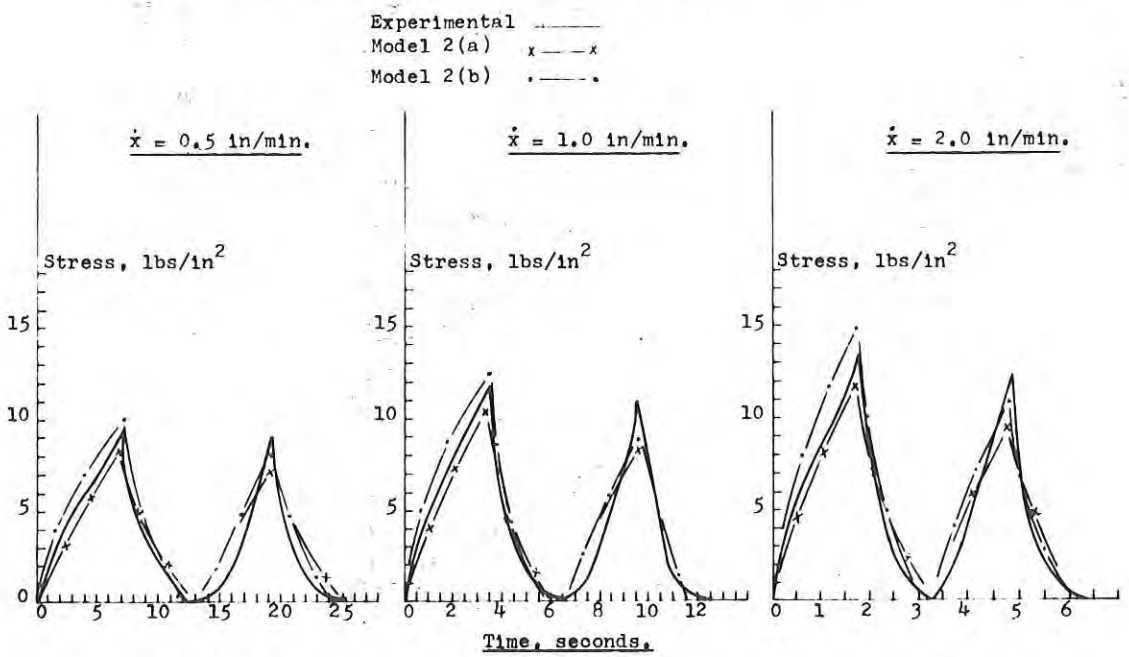

Figure 5-69 Experimental results and theoretical predictions for cyclic tests - 80°F., 70% R.H.

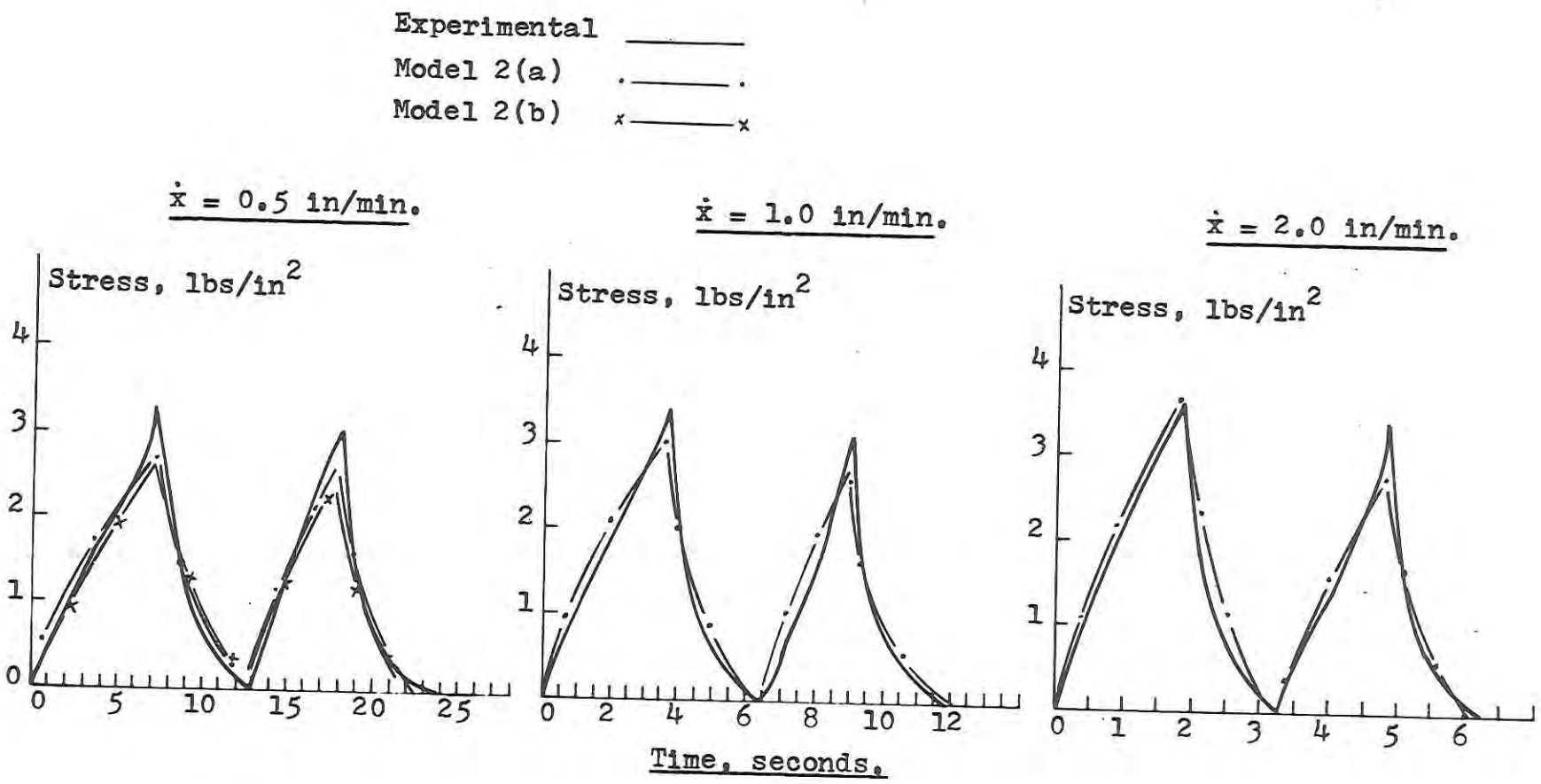

Figure 5-70. Experimental results and theoretical predictions for cyclic tests - 80°F., 92% R.H.

Table 5-21. Mean experimental and predicted values for texture parameters, hardness and chewiness.

a_w		Hardness	Chewiness
0.15	Model 1	5.1	4.7
	Model 2 (a)	18.5	19.4
	Model 2 (b)	22.5	19.6
	Experimental	21.3	18.7
0.30	Model 1	4.2	3.8
	Model 2 (a)	17.3	15.6
	Model 2 (b)	16.3	13.6
	Experimental	15.6	13.1
0.50	Model 1	5.5	5.3
	Model 2(a)	13.7	12.0
	Model 2(b)	16.5	13.4
	Experimental	15.8	13.8
0.70	Model 1	4.0	3.9
	Model 2(a)	9.8	8.3
	Model 2(b)	12.8	11.7
	Experimental	10.9	9.1
0.92	Model 1	1.2	1.0
	Model 2(a)	3.1	2.6
	Model 2(b)	3.1	2.8
	Experimental	3.4	2.9

η_1 and η_3 in Model 1, and A, B and λ' in Model 2(a).

The second approach merely estimated the arithmetic mean of fifteen values for each parameter at every water activity, using experimental cyclic results. In addition to C in Model 2(a), all four parameter means in Model 2(b) were calculated by this method.

Analysis of variance tests revealed that water activity levels had a significant effect, at the 99% confidence level, on every parameter except λ' in Model 2(b). This conclusion could be anticipated from the large decrease in parameter values at the higher equilibrium relative humidities, particularly at 92%.

Mean parameter values for the various models are presented in Tables 5.22, 5.23 and 5.24. The general trend is one of decreasing parameter values with increasing moisture content. At the lower water activities relatively little change is evident, but any statistically significant differences between means indicate that the parameter value at the lower equilibrium relative humidity is higher than the corresponding parameter value at the next highest a_w.

The main inconsistent difference of statistical significance was C at 0.30 in Model 2(a). The explanation for the low value in this instance is that A, B and λ' had been previously computed from the relaxation tests. An examination of and comparison between the relaxation and cyclic test results at 0.30 and 0.50 water activities will show that the relaxation response for 0.50 is 10% to 15% lower than that at 0.30. Statistical analysis confirmed significant differences between both of these responses. Yet the cyclic results at these water activities were quite similar.

Use of A, B and λ' calculated from the relaxation experiment to determine C in Model 2(a) from cyclic data meant that the relaxation differences must be compensated for when fitting the model to the cyclic results. Accordingly, since B at 0.30 estimated from relaxation was much higher than B at 0.50, the corresponding values for C estimated from cyclic results should differ in the opposite direction. Again, this was the case and was supported by statistical analysis. Dunnett's supplementary test confirmed the similarity between cyclic results at 0.30 and 0.50 water activity, there being no significant difference between Model 2(b) constants at these two levels.

It should be emphasized that relationships between model parameters and water activity cannot be compared directly with results in Kapsalis (1967) or Reidy and Heldman (1970) as discussed earlier. Both reports indicated that hardness of precooked freeze-dried beef increased slightly with water activity level up to 0.5-0.6. At higher water activities, the values decreased significantly. The latter trend is definitely confirmed by all results which also suggest that further research concentrated at water activities of 0.5-1.0 is warranted, to more precisely define the magnitude of change occurring in hardness of the product at different intervals in this water activity range. Similarly, further research should be conducted to confirm texture changes which occur in the a_w range of 0.0-0.5. Kapsalis (1967) and Reidy and Heldman (1970) did not illustrate that statistically significant differences existed between individual means at the lower equilibrium relative humidities, but based their conclusions on the trend of the means. The increase in toughness found by Kapsalis (1967) was very small

TABLE 5-22. Model 1: Parameter values estimated from mean relaxation data.

a_w	0.15	0.30	0.50	0.70	0.92
E_1	112.6	109.1	94.2	81.3	25.0
E_3	402.6	351.0	249.3	132.3	13.2
η_1	64760	55474	55052	6375	2494
η_3	1819.6	2023.2	672.9	412.1	37.8

TABLE 5- 23 Model 2 (a): Mean parameter values; A, B, λ', estimated from relaxation data; C from cyclic test data.

a_w	0.15	0.30	0.50	0.70	0.92
A	79.2	73.9	63.5	38.3	9.7
B	28.5	31.0	27.0	38.9	13.3
λ	10.63	11.36	4.85	4.09	4.53
C	37.5	16.9	30.0	23.2	6.9

TABLE 5-24 Model 2(b): Mean parameter values estimated from cyclic test data.

a_w	0.15	0.30	0.50	0.70	0.92
A	72.8	55.0	53.9	41.0	13.2
B	164.0	91.0	107.9	87.0	10.8
λ	2.52	3.53	2.69	2.65	3.72
C	34.0	22.9	25.6	20.0	4.9

from one level to another, whereas the results of Reidy and Heldman (1970) show considerable variation among samples at any one water activity. It would appear therefore that the results included in this report neither confirm or contradict previous work at lower water activities. They might more appropriately lead to the conclusion that texture of precooked freeze-dried beef is affected very little by increasing equilibrium relative humidity up to 50% but decreases significantly for higher water activities.

The smaller stresses required to deform the samples at higher moisture contents could be due to the adsorbed moisture being less tightly bound. Being relatively loose, this moisture might bring about a lubricating effect on the product components when subjected to externally applied stresses. Kapsalis' (1967) suggestion that cross-linking, which occurs to a greater extent above 20% R.H., has a toughening effect on meat could possibly explain the relatively stable values of hardness and chewiness found at 30% and 50% R.H.

It is interesting to note from Figure 5.71 that the changes which occur in hardness of the product as equilibrium relative humidity increases, are almost inversely related to the isotherm especially at a_w greater than 0.50. This would suggest that textural changes in the product may be closely related to water binding properties. As previously suggested however, further research is required to establish precisely the textural changes occurring at moisture contents below the monomolecular layer level, i.e., corresponding to 20%-25% equilibrium relative humidity.

5.11.4. Use of the models to predict texture parameter. As previously discussed, Model 1 failed to predict stress-strain behavior for cyclic loading conditions and consequently was inadequate for predicting texture. The poor comparison between actual and predicted texture indices is evident from Figures 5-72 and 5.73.

However, an accurate linear relationship appears to exist between chewiness and hardness:

$$C = (0.59)H + 3.61$$

where C represents chewiness and H hardness. Therefore is a correlation exists between any model parameter value and hardness, it would be possible to arrive at reasonable estimates for both texture parameters.

For example, use of the free spring element (E_1) in Model 1, to predict hardness gives values of 16.9, 16.4, 14.1, 12.2 and 3.8 compared to 21.3, 15.6, 15.8, 10.9 and 3.4, respectively (Figure 5.74). None of the other parameters (E_3, η_1, η_3) in Model 1 show a consistent relationship with either chewiness or hardness. The values of η_1 change in a relatively similar manner to hardness values between 15% and 50% E.R.H. but at higher relative humidities the large decrease in magnitude is not consistent with changes in texture.

Model 2 satisfactorily predicts cyclic response and therefore the texture profile from which hardness and chewiness are estimated. Any of the other texture parameters suggested by Szezesniak, et al. (1963) can also be found from the profile predicted by Model 2. The better predictions of Model 2(b) compared to 2(a) (Figures 5.72 and 5.73) can be attributed to the fact that all of the model constants in 2(b) were evaluated from cyclic data. The fact that this model -- 2(b) -- can also give satisfactory predictions for three different

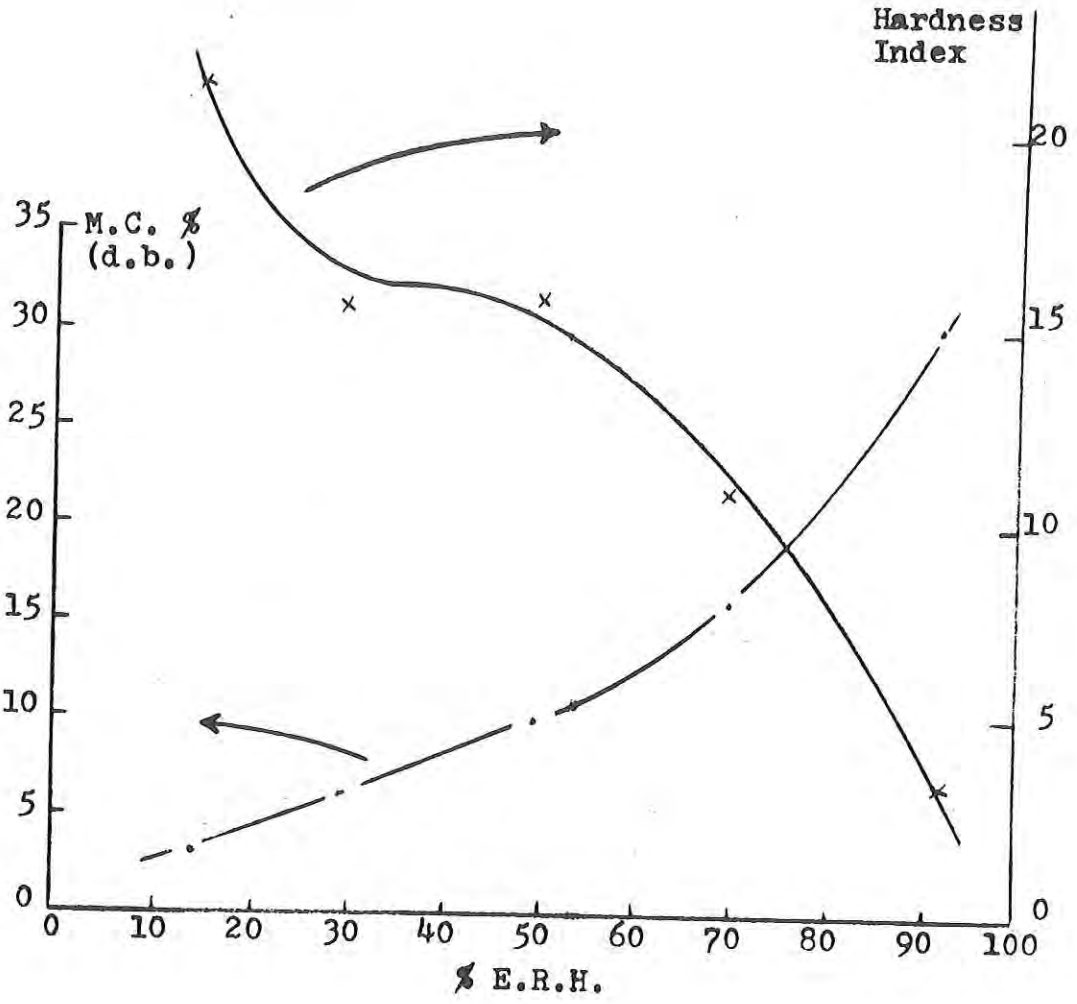

Figure 5-71 Moisture content and Hardness Index vs. Equilibrium Relative Humidity for pre-cooked freeze-dried beef at 80°F.

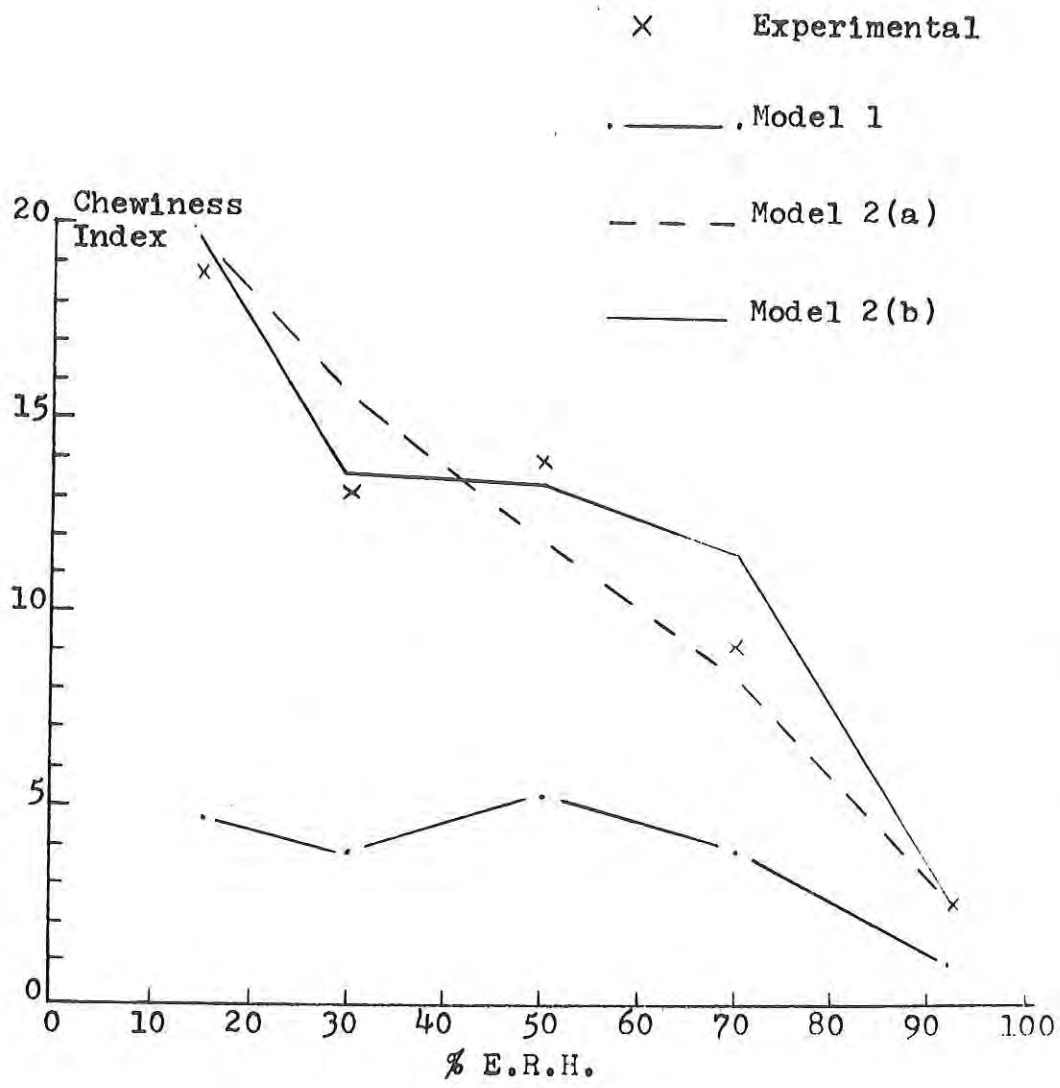

Figure 5-72 Mean experimental and predicted values for texture - Chewiness Index.

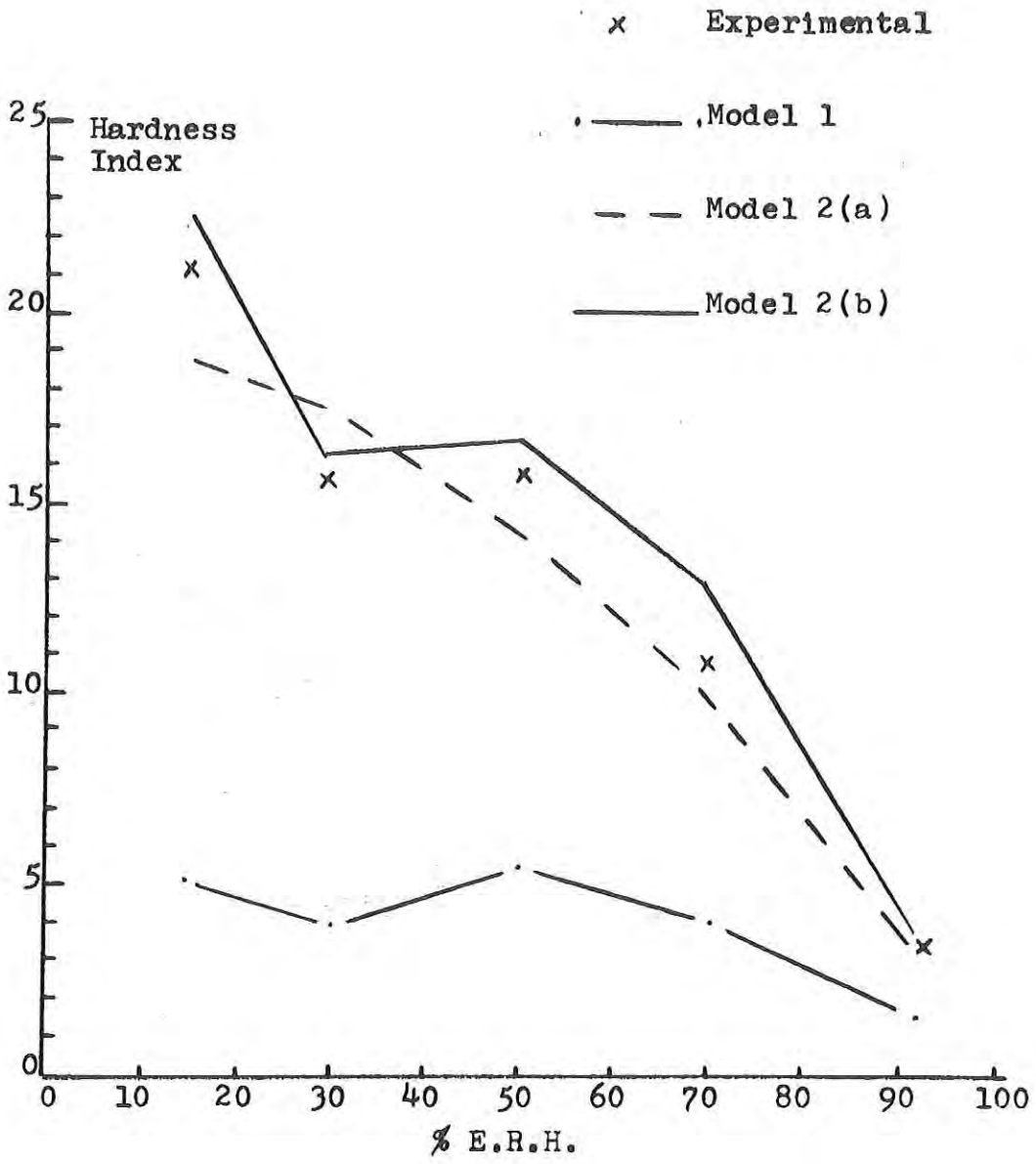

Figure 5-73 Mean experimental and predicted values of texture - Hardness Index.

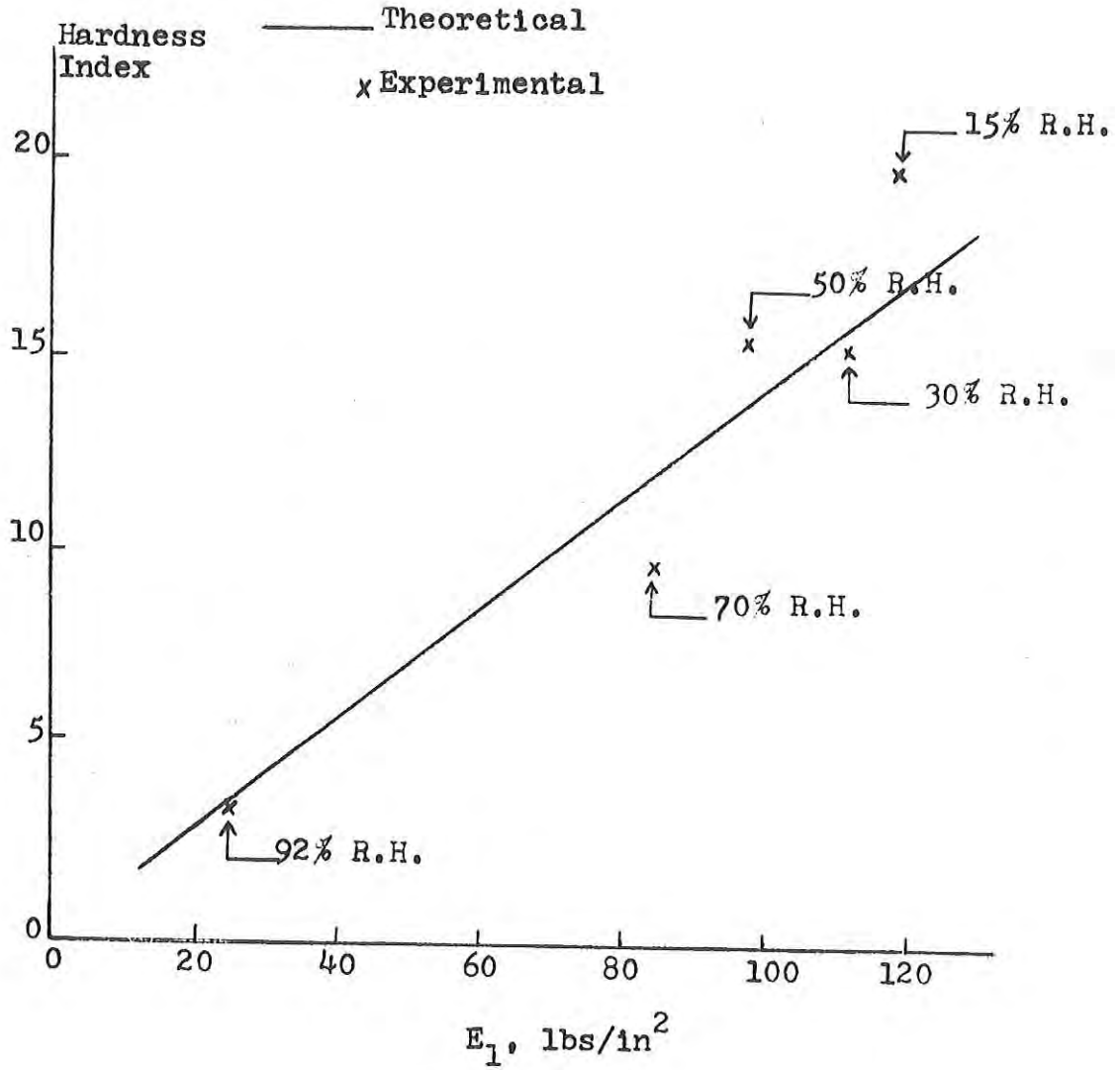

Figure 5-74 Comparison of experimental values of the Hardness Index with theoretical values predicted by the free spring (E_1) in Model 1.

tests, yet utilizes only one of them for parameter estimation, makes it particularly attractive.

The parameter A in Model 2(a) could possibly be used to give an approximation of hardness since the relative ratios at various water activities are similar to hardness ratios. The value predicted for hardness at 30% E.R.H. would be too high, again on account of the poor agreement between the relaxation and cyclic behavior frequently referred to. None of the other parameters in Model 2(a), used individually, could be used to indicate texture.

To predict textural parameters using Model 1 and Model 2 it is necessary to consider the total equations (3-67) and (3-78) and not merely any one or two terms. The magnitude of some terms, however, have more influence on hardness and chewiness than others. In Model 1, a relatively weak free spring, i.e., a low value for E_1, will result in very low hardness values because most of the strain will occur in this element. Little energy will be absorbed and therefore the stress response for the second compression cycle will be very similar to that for the first cycle.

Should the free spring be strong, however, the strain will occur in either the dashpot or the Kelvin part of the model, depending on the relative strength of these elements. For example, if the viscosity value, η_1 of the dashpot is low, then more deformation will occur through this element. Since the dashpot absorbs energy, the stress in the second and subsequent compression cycles will be much lower than for the first cycle, and consequently the chewiness index will be lower than if the model had a stronger free dashpot.

In Model 2, both A and C are the parameters most influencing hardness. The term $(B_\epsilon\ e^{-t/\lambda'})$ will largely determine the quantity of energy absorbed. The magnitude of (λ') will determine how fast the energy in this whole term is absorbed, and therefore will seriously affect chewiness values.

It should be emphasized however, that no single parameter is either model can independently predict either the hardness or chewiness indices.

6. Conclusions

Based on the analysis and discussion of results obtained in this investigation of the thermodynamic and rheological properties of freeze-dried beef, the following statements can be presented:

1. Equilibrium moisture content isotherms for freeze-dried beef are typical of isotherms for biological materials in terms of shape, influence of temperature and hysteresis.
2. The use of a 105°F plate temperature during freeze-drying produces a higher equilibrium moisture content and lower water activity during moisture adsorption than a 145°F plate temperature.
3. The connective tissue and sarcoplasmic fraction components of beef protein contribute significantly to isotherm shape at lower water activities.
4. The precooking process produces a significant influence on the shape of desorption isotherms for freeze-dried beef.
5. A generalized theory of moisture adsorption in biological materials allows accurate prediction of moisture equilibrium isotherms for freeze-dried beef.
6. The use of a numerical model of a calorimeter allows the evaluation of relative errors in measurement of heats of immersion and other thermodynamic parameters for dry foods.
7. The use of basic thermodynamic parameters for prediction of thermodynamic heats results in predictions which are low when compared to experimental results. The concept of effective molecular weight can be introduced to facilitate the prediction.
8. Texture parameters of freeze-dried beef (hardness and chewiness) were maximum at water activities of 0.4 to 0.6 before storage while the influence of platen temperature and conditioning temperature is not obvious.
9. Predictions based on thermodynamic analysis and experimental results from sensory panel indicated that heat evolved during moisture adsorption by the product decreases with increasing water activity.
10. Higher storage temperature (100°F) produces larger texture parameters (hardness and chewiness) in freeze-dried beef with an increase in storage time while low temperature storage (39°F) maintains the texture parameters near initial values.
11. The influence of storage on the freeze-dried beef texture parameters is most obvious at higher water activities (0.5 and 0.75) and high temperature storage (100°F). At low water activities (0 and 0.25), the texture parameter remained low, even at 100°F storage temperature.
12. Relationships between freeze-dried beef texture and thermodynamic parameters are evident only at 100°F storage temperature where increasing differential entropy results in lower texture parameter values.

13. A four element viscoelastic model provides a good description of freeze-dried beef properties over the entire range of water activities.

14. A four element semi-empirical viscoelastic model can be used to describe the cyclic response necessary to predict texture parameters of freeze-dried beef.

15. In general, all results on freeze-dried beef texture indicate that parameters are relatively constant between water activities of 0 and 0.7, while all parameters decrease significantly above water activity of 0.7.

16. Based on the equilibrium moisture isotherms, the 105°F platen produces the more desirable freeze-dried beef since the product has higher moisture content at a given water activity than product dried with 145°F plate temperature. This influence is not significant enough to detect in texture investigations.

17. Storage temperature for freeze-dried beef should be as low as possible since product texture is not influenced by six months of storage at 39°F even at water activities as high as 0.75.

18. Storage time for freeze-dried beef should be limited to 3 months at 100°F at water activities of 0.5 and 0.75. Beyond 3 months at these conditions, the product texture is not stable.

19. The most appropriate processing and storage conditions for freeze-dried would include 105°F platen temperature with 39°F storage at water activities of 0.75 or higher. These conditions should provide the most stable product texture for storage periods up to 6 months.

REFERENCES

Abbott, J. A., G. B. Backman, R. F. Childers, J.V. Fitzgerald and F. J. Matusik. 1968. Sonic techniques for measuring texture of fruits and vegetables. Food Technol. 22 : 101.

Adamson, A. W. 1967. The Physical Chemistry of Surfaces. (Second edition), Interscience Publishers. New York.

Allada, S.R. and Quon, D. 1966. Chem. Engr. Progress Symposium Series. Heat Transfer - Los Angeles. 151.

Babbitt, J. D. 1942. On the adsorption of water vapor by cellulose. Canadian J. of Research. 20(A). No. 9. pp. 143-172.

Ball, C.O., W. E. Clauss and E. E. Stier. 1957. Factors affecting quality of prepackaged meats. 1. Physical and organotepic tests. Food Technol. 11: 277.

Bangham, D.H. and W. Sever (1925). An experimental investigation of the dynamical equation of the process of gas-sorption. Phil. Magazine. 6(49): 935.

Barakat, H.Z. and Clark, J.A. 1966. Trans. ASME, J. Heat Transfer. Series C. 88:421.

Berger, R.L., Chick, Yu-Bing-Fok, and Davids, N. 1968. Rev. Scient. Instrum. 39:362.

Bockian, A.H., S.G. Anglemier and L.A. Sather. 1958. A comparison of an objective and subjective measurement of beef tenderness. Food Technol. 12: 483.

Boelter, L.M.K., Cherry, V.H. and Johnson, H.A. 1942. Heat Transfer Notes. University of California (Berkeley).

Bone, D. 1970. Structuring intermediate moisture foods. Paper presented at Innovation in Food Engineering Conference. San Francisco, California (March 23-26).

Bourne, M.C and N. Mondy. 1967. Measurement of whole potato firmness with a universal testing machine. Food Technol. 21: 97.

Bourne, M.C. 1966. A classification of objective methods for measuring texture and consistency of foods. J. Food Sci. 31: 1011.

Bourne, M.C. 1967. Deformation testing of foods 1. A precise technique for performing the deformation test. J. Food Sci. 32: 601.

Bourne, M.C. 1968. Texture profile of ripening fears. J.Food Sci. 33:223.

Bourne, M.C. 1967. Deformation testing of foods 2. A simple spring model deformation. J. Food Sci. 32: 605.

Bowen, R.M. 1967. Lectures on Continuum Mechanics. Sandia Laboratory. Albuquerque, New Mexico.

Brandt, M.A., E.Z. Skinner and J.A. Coleman. 1963. Texture profile method. J. Food Sci. 28: 404.

Bratzler, L.J. 1932. Measuring the tenderness of meat by means of a mechanical shear. M.S. Thesis. Kansas State College, Kansas.

Brockman, M.C.1969. Development of intermediate moisture foods for military use. Paper presented at the 29th Annual Meeting of Institute of Food Technologists. Chicago, Illinois.

Brunauer, S.; Emmett, P.H.; and E. Teller. 1939. Adsorption of gases in multimolecular layers. J.Am. Chem. Soc. 60: 309.

Brunauer, S. 1945. The Adsorption of Gases and Vapors. Vol. 1. Princeton University Press, Princeton.

Burrill, L.M., I. Deethardt and R. L. Staffle. 1962. Two mechanical devices compared with taste panel evaluation for measuring tenderness. Food Technol 16:145.

Calvet, E. and Pratt, H. 1963. Recent Progress in Microcalorimetry. Translated by Skinner, H.A. MacMillan, New York.

Charm, S.E. 1963. Fundamentals of Food Engineering. A.V. I. Publishing Co., Westport, Conn.

Charm,S.E. 1963. The direct determination of shear stress - shear rate behavior of foods in the presence of a yield stress. J. Food Sci. 28: 107.

Chung, D.S. and H. B. Pfost. 1967. Adsorption and desorption of water vapor by cereal grains and their products. Parts I, II, and III. Transactions of A.S.A.E. 10:552.

Clark, R.L. 1968. A Constitutive Equation to Determine Mechanical Properties of Cottonseed Subjected to Normal Stress. Ph.D. Thesis, Department of Agricultural and Biological Engineering, Mississippi State University, Mississippi.

Clark, R.L., W.R. Fox and G.B. Welch. 1968. Representation of Mechanical Properties of Non-linear Viscoelastic Materials by Constitutive Equations. Journal No. 1698. Ag. Exp. Sta., Mississippi State University, Mississippi.

Coelingh, M.B. 1939. Kolloid Z. 87:251.

Cohan, L.H. 1938. Sorption hysteresis and the vapor pressure of concave surfaces. J.Am. Chem. Soc. 60:433.

Copeland, L.E., and T.F. Young. 1961. A thermodynamic theory of adsorption. Advances in Chemistry 33:348.

Cranston, R.W. and F.A. Inkley. 1957. The determination of pore structure from Nitrogen adsorption isotherms. Advances in Catalysis. 9:143.

Cuendet, L.S, Larson,E.E. Norris, C.G, and W.F. Geddes. 1954. The influence of moisture content and other factors on the stability of wheat flours at 37.8° C. Cereal Chem. 31:362.

Davis, S., and A.D. McLaren. 1948. Free energy, heat and entropy changes accompanying the sorption of water vapor by proteins. J. Polymer Sci. 3:16.

Deatherage, F.E. and G. Garnatz. 1952. A comparative study of tenderness determination by sensory panel and by shear strength measurement. Food Technol. 6:260.

de Boer, J.H. 1958. The shapes of capillaries. In Structure and Properties of Porous Materials. Edited by Everett and Stone. Butterworths Scientific Publications, London, p. 68.

Diener, R.C. and D.R. Heldman. 1968. Methods of determining rheological properties of butter. ASAE Trans. 11(3): 444.

Dole M. and A.D. McLaren. 1947. The free energy, heat and entropy of sorption of water by proteins and high polymers. J.A. Chem. Soc. 69: 651.

Dollimore, D. and G.R. Heal. 1964. An improved method for the calculation of pore size distribution from adsorption data. J. of Appl. Chem. pp 109-114.

Eirich, F.Q. ed. 1958. Rheology, Theory and Applications. Academic Press, New York.

Elder, A.L. and R.J. Smith. 1969. Food rheology today. Food Technol. 23: 629.

Fennema, O.R. 1970. Nature and characteristics of water in food and biological systems. Paper presented at Highlights of Food Science Conference, Michigan State University, East Lansing, Michigan (March 23-25).

Finney, E.E., C.W. Hall and G.E. Mase. 1964. Theory of linear viscoelasticity applied to potato. J. Ag. Eng. Res. 9(4): 307.

Finney, E.E. 1963. The Viscoelastic Behavior of Potato Solarum Tuberosum, Under Quasi-Static Loading. Ph.D. Thesis, Agricultural Engineering Department, Michigan State University.

Flood,E.A. 1967. The Solid-Gas Interface Vols. I and II. Marcel Dekker, Inc., New York.

Flügge, Wilhelm. Viscoelasticity. Blaisdell Publishing Company, Waltham, Mass. 1967.

Foster, A.G. 1932. The sorption of condensable vapors by porous solids. Part I. The applicability of the capillary theory. Trans. Faraday Soc. 28:645.

Foster, A.G. 1948. Pore size and pore distribution. Discussions Faraday Soc. 3:41.

Friedman, H.H., J.E. Whitney and A.S. Szczesniak. 1963. The texturometer - a new instrument for objective texture measurement. J.Food Sci. 28: 390.

Frish, H.L. and R. Simha. 1956. The viscosity of colloidal suspensions and macromolecular solutions. In Rheology, Theory and Applications. F.R. Eirich Ed. p.525. Academic Press, New York.

Fung, Y.B. 1968. Biomechanics. Applied Mechanics Reviews. 21(1):1.

Gibbs, J.W. 1875. Cited from S. Glasstone. 1946. Textbook of Physical Chemistry. D. Van Nostrand Co., New York.

Gregg S.J. and K.W. Sing 1967. Adsorption Surface Area and Porosity. Academic Press, London, and New York.

Halsey, Jr., G.D. 1948. Physical adsorption on non-uniform surfaces. J. Chemical Physics. 16:931.

Hammerle, J.R. 1968. Failure in a thin viscoelastic slab subjected to temperature and moisture gradients. Unpublished Ph.D. Thesis Penn. State University.

Hansen, R.W. 1952. The development and testing of equipment to measure the resistance of potatoes to brusing and injury. Unpublished M.S. Thesis. North Dakota Agricultural College.

Harrington, G. and A.M. Pearson. 1962. Chew count as a measure of tenderness of pork loins with various degrees of marbling. J. Food Sci. 27:106.

Haut, R.C. and R.W. Little. 1969. Rheological properties of canine anterior cruciate ligaments. ASME Publication 69-BHF-9 ASME, United Engineering Center 345 East 47th Street, New York, New York.

Heldman, D.R., Hall C.W. and T. I. Hedrick. 1965. Vapor equilibrium relationship of dry milk. J. of Dairy Sci. 48:845.

Heldman D.R., Hall, C.W. and T. I. Hedrick. 1965. Equilibrium moisture contents and moisture adsorption rates of dry milks. Humidity and moisture Vol.11 page 22. Reinhold Pub. Corp. Proceedings of 1963 International Symposium on Humidity and Moisture, Washington,D.C.

Henderson, S.M. 1952. A basic concept of equilibrium moisture. Agr. Eng. 33: 29.

Hildebrand, J.H., and R.L. Scott. 1950. The Solubility of Non-electrolytes. 3rd Edition. Reinhold Publishing Corp., New York.

Hofer, A.A., and H. Mohler. 1962. Zur Aufnahmetechnik von sorption-sisothermen und ihre Anwendung in der Lebensmittelindustrie. Trav. Chim. Aliment et'd Hygiene 53:274.

Hohner, G.A. and D.R. Heldman, 1970. Computer simulation of freezing rates in foods. Paper presented at the 30th Annual Meeting of Institute of Food Technologists, San Francisco, California.

Hohner, G.A. 1970. An Analysis of Heat and Mass Transfer in Atmospheric Freeze-Drying. Ph.D. Thesis. Agricultural Engineering Department. Michigan State University, East Lansing.

Huelsen, W.A. and W.P. Bemis. 1955. Artificial drying and rehydration of popcorn. University of Illinois. Agr. Experiment Station. Bull. 593. Urbana, Illinois.

Huff, E.R. 1967. Measuring tine-dependent mechanical properties of potato tubers, equipment, procedure, results. ASAE Trans. 10(3): 414.

Kapsalis, J.G. 1967. Hygroscopic equilibrium and texture of freeze-dried foods. Technical Report 67-87 - FL, U.S. Army, Natick, Mass.

Karel, M. and J.T. R. Nickerson. 1964. Effect of relative humidity, air and vacuum on browning on dehydrated orange juice. Food Technol. 18:104.

Katz, J.R. 1933. The Laws of Swelling. Trans. Faraday Soc. 29:279.

Kramer, A. and B.A.Twigg. 1959. Principles and instrumentation for the physical measurement of food quality with special reference to fruit and vegetable products. Adv. in Food. Res. 9:153.

Kramer, A. 1959. Glossary of some terms used in the sensory (panel) evaluation of foods and beverages.Food Technol. 13:733.

Kramer, A., G.J. Burkhardt and H.P. Rogers. 1951. The shear-press, a device for measuring food quality. Canner. 112: 34.

Kramer, A. 1961. The shear press-a basic tool for the food technologist. The Food Scientist 7: 16.

Kühn, I. 1964. A new theoretical analysis of adsorption phenomena. Introductory part: The characteristic expression of the main regular types of adsorption isotherms by a single simple equation. J. Colloid Science. 19:685.

Kuprianoff, J. 1958. Bound water in foods. In Fundamental Aspects of Dehydration of Foodstuffs. Society of Chemical Industries, London, England.

Labuza, T.P. 1968. Sorption phenomena in foods. Food Technol. 22:263.

Labuza, T.P., Tannenbaum, S.R., and M. Karel. 1970. Water content and stability of low moisture and intermediate moisture foods. Food Technol. 24:543.

Lazan, B.J. 1965. Internal friction, damping and cyclic pasticity. A.S.T.M. Special Technical Pub. No. 378.

Lowe, B. 1949. Organoleptic tests developed for measuring the palatability of meat. Proc. Recip. Meat Conference. 2: 111.

Magness, J.R. and G.F. Taylor. 1925. An improved type of pressure tester for the determination of fruit maturity. U.S.D.A. Circular No. 350.

Malvern, L.E. 1967. Introduction to the Mechanics of a Continuous Medium. Prentice-Hall, Englewood Cliffs, N.J.

Martin, W.M. 1937. The tenderometer. Canner, 80:108.

Martin,H.F. 1958. Factors in the development of oxidative rancidity in ready-to-eat crisp oatflakes. J.Sci. Food Agr. 12:817.

Matz, S.A.1962. Food Texture. A.V.I. Publishing Co., Inc.Westport, Conn.

McClelland, T.H. and R.E. Spielrein. 1957. An investigation of ultimate bending strength of some common pasture plants. J. Ag. Eng. Res. 2:288.

Meeter, D.A. 1964. Program GAUSHAUS, Numberical Analysis Laboratory, University of Wisconsin, Madison.

Metzner, A.B. 1956. Non-Newtonian technology; Fluid mechanics, mixing and heat transfer. Adv. in Chem. Eng. 1.

Miyada, D.A. and A.L. Tappel. 1956. Meat tenderization 1; Two mechanical devices for measuring texture. Food Technol. 10:142.

Mitchell, J.H. and J. J. Enright. 1957. Effect of low moisture level on thermostability of active dry yeast. Food Technol. 11:359.

Mohsenin, N. and H. Gochlich. 1962. Techniques for determination of mechanical properties of fruits and vegetables as related to design and development of harvesting and processing machinery. J. Agr. Engr. Res. 7:300.

Mohsenin, N.N. 1966. Physical Properties of Plant and Animal Materials. Department of Agricultural Engineering, The Pennsylvania State University, University Park, Pa.

Mohsenin, N.N. and H.E. Cooper and L.D. Tukey. 1963. Engineering approach to evaluation of textural factors in fruits and vegetables. A.S.A.E. Trans. 6(2):85.

Morrison, J.A., and J.F. Hanlan. 1957. Second International Congress of Surface Activity II. Editor Schlman, Butterworths, London.

Morrow,C.T.1965. Viscoelasticity in a Selected Agricultural Product. M.S. Thesis. in Agricultural Engineering. The Pennsylvania State University, Pa.

Morrow, C.T. and N.N. Mohsenin. 1966. Consideration of selected agricultural products as viscoelastic materials. J.Food Sci. 31:686.

Morrow, C.T. 1969. Engineering analysis of mechanical behavior of caramel and solid chocolate. A.S.A.E. Paper No. 69-875.

Ngoddy, P.O. 1969. A generalised theory of sorption phenomena in biological materials. Ph.D. Thesis. Agr. Eng. Dept., Michigan State University, East Lansing, Michigan.

Othmer, D.F. 1940. Correlating vapor pressure and latent heat data. Ind. and Eng. Chem. 32:841.

Palnitkar, M.P. and D.R. Heldman. 1970. Equilibrium moisture characteristics of freeze-dried beef component . Paper presented at the 30th Annual Meeting of Institute of Food Technologists, San Francisco, California.

Palnitkar, M.P. 1970. Thermodynamic characteristics of low and intermediate moisture food. Unpublished Ph.D. thesis. Michigan State University.

Pearson, A.M. 1963. Objective and subjective measurements for meat tenderness. Proceedings Meat Tenderness Symposium, Campbell Soup Company, Camden, N.J.

Polany, M. 1914. Verhandl. Deutsch. Physik. Ges. 18:55.

Prager, W. 1956. In Rheology, Vol. 1 . F.R. Eirich, (ed.) Academic Press. Inc., New York.

Proctor, B.E., S. Davison, C.J. Malecki and M. Welch. 1955a. A recording strain-gauge denture tenderometer for foods, 1. Instrument evaluation and initial tests. Food Technol. 9 :471.

Reidy, G. A. 1970. Relationships between engineering and texture parameters for low and intermediate moisture foods. Unpublished Ph.D. Thesis, Michigan State University.

Reidy, G.A. and D.R.Heldman. 1970. Measurement of texture parameters of freeze-dried beef. Paper presented at 30th Annual Meeting of Institute of Food Technologists, San Francisco, California. May, 1970.

Richtmyer, R.D. 1957. Difference Metods for Initial Value Problems. Interscience, N.Y.

Roby, M.T., and M. Simon. 1959. Improvement of potato granule quality by fluidized bed finish drying. Food Technol.13:327.

Rockland, L.G. 1957. A new treatment of hygroscopic equilibria: Application to walnuts and other foods. Food Research. 22:604.

Rockland L.B., Swerthout, D.M. and R.A. Johnson. 1961. Studies on english (persian) walnuts: Stablization of kernels. Food Technol. 15:112.

Rockland L.B. 1969. Water activity and storage stability. Food Technol. 23:1241.

Ross, S. and J.P. Oliver. 1964. On Physical Adsorption. Interscience Publishers, New York, London, Sidney.

Rodriguez-Arias,J.H. 1956. Desorption isotherms and drying rates of shelled corn in the temperature range of 40 to 140°F. Ph.D. Thesis, Agr. Eng. Dept. Michigan State University, East Lansing, Michigan.

Salwin, H. 1959. Defining minimum moisture contents for dehydrated foods. Food Technol. 13:594.

Salwin,H.1963. Moisture levels required for stability in dehydrated foods. Food Technol. 17:34.

Saravacos, G.D. and R. M. Stinchfield (1965). Effect of temperature and pressure on the sorption of water vapor by freeze-dried food materials. J. of Food Science. 30(5):779.

Schultz, H.W. 1957. Mechanical methods of measuring tenderness of meat. Proc. Recip. Meat Conference 10:17.

Scott, W.J. 1957. Water relations of food spoilage organisms. Advan. Food Res.7:83.

Sherman, P. 1969. A texture profile of food stuffs based upon well defined rheological properties. J. Food Sci. 34:458.

Shama, F. and P. Sherman. 1966. The texture of ice cream, 2. Rheological properties of frozen ice cream. J. Food Sci. 31:699.

Shama, F. and P.Sherman. 1966. The texture of ice cream, 3. Rheological properties of milk and melted ice cream. J. Food Sci. 31:707.

Shull, C.G. 1948. The determination of pore-size distribution from gas adsorption data. J. Am. Chem. Soc. 70:1405.

Smith, S. E. 1947. The sorption of water vapor by high polymers. J. Am. Chem. Soc. 69:646.

Somers, G.F. 1965. Viscoelastic properties of storage tissues from potato, apple and pear. J. Food Sci. 30(6):922.

Stamm, A.J. and R.M. Seborg 1935. Adsorption compression on cellulose and Wood I. . Phys. Chem. 39:133.

Stamm, A.J. 1938. Calculations of void volume in wood. Industrial and Engr. Chem. 30 (11):1280.

Strohman,D.R. and R.R. Yoerger. 1967. A new equilibrium moisture content equation. Transactions of A.S.A.E. 10:675.

Stitt, F. 1958. Moisture equilibrium and the determination of dehydrated foods. In Fundamental Aspects of the Dehydration of Foodstuffs. Society of Chemical Industries, London, England.

Strasser, J. 1969. Detection of quality changes in freeze-dried beef by measurement of sorption isobar hysteresis. J. Food Sci. 34:18.

Sunner, S. and Wadso, I. 1966. Sci.Tools. 13:1.

Swietoslawski, W. 1946. Microcalorimetry. Reinhold Publishing, New York.

Szczesniak, A.S., K. Sloman, M. Brandt and E. Skinner. 1963. Objective measurement of texture of fresh and freeze-dehydrated meats. Proc. 15th Res. Conf. Am. Meat Inst. Found., University of Chicago.

Szczesniak,A.S., M. Brandt and H. Friedman. 1963. Development of standard rating scales for mechanical parameters of texture and corelation between the objective and sensory methods of texture evaluation. J. Food Sci. 28:397.

Szczesniak, A.S. 1963. Objective measurements of food texture. J. Food Sci. 28:410.

Szczesniak, A.S. 1963. Classification of textural characteristics. J. Food Sci. 28:385.

Taylor,A. A. 1961. Determination of moisture equilibria in dehydrated foods. Food Technol. 15:536.

Thompson, D.R. 1970. An analysis of selected techniques in microcalorimetry. Ph.D. Thesis, Agr. Eng. Dept. Michigan State University, East Lansing, Michigan.

Triebold,H.O. and W. A. Aurand. 1963. Food Composition and Analysis. D. VanNostrand Co.,Inc. Princeton,New Jersey.

U.S. Army Natick Laboratories. 1965. Report No. 11 (Final) on Fundamental Aspects of Meat Texture, submitted by General Foods Corporation under contract no. DA19-129-QM-1844 (01-5147). 1965.

Viswanathan, B. and M.V.C. Sastri 1967. computation of pore size distribution in terms of surface area. J. of Catalysis: 8:312.

Webb, B.D, Bayliss, M.E., and L.R. Richardson. 1960. Relation of interspace relative humidity to growth of molds and heating in feed ingredients and feed mixes. J. Agr. Food Chem. 8:371.

Wheeler, A. 1945. Report #S-9829. Circulated to the PAW "Recommendation 41 Group" of the Petroleum Industry, June 1945; presented at A.A.A.S. Gordon Conference on Catalysis 1945 and 1946.

Wilhoit, R. C. 1967. XXXIII. Recent developments in calorimetry. Part 1. Introductory Survey of Calorimetry. J. Chem. Ed. 44:A571.

Wu, Y.C. and L.E. Copeland. 1961. Thermodynamics of adsorption. The Barium Sulfate-Water system. Advan. in Chem. 33:357.

Young, J.H. and G.L. Nelson. 1967. Research of hysteresis between sorption and desorption isotherms of wheat. Trans. of A.S.A.E. 10(6): 756.

Young, J.H. and G. L. Nelson. 1967. Theory of hysteresis between sorption and desorption isotherms in biological materials. Trans. A.S.A.E. 10(2):260.

Zoerb, G.C. 1958. Mechanical and rheological properties of grain. Unpublished Ph.D. Thesis. Michigan State University.

Zsigmondy, R. 1911. Z. Anorg. Chem. 71:356.

APPENDIX

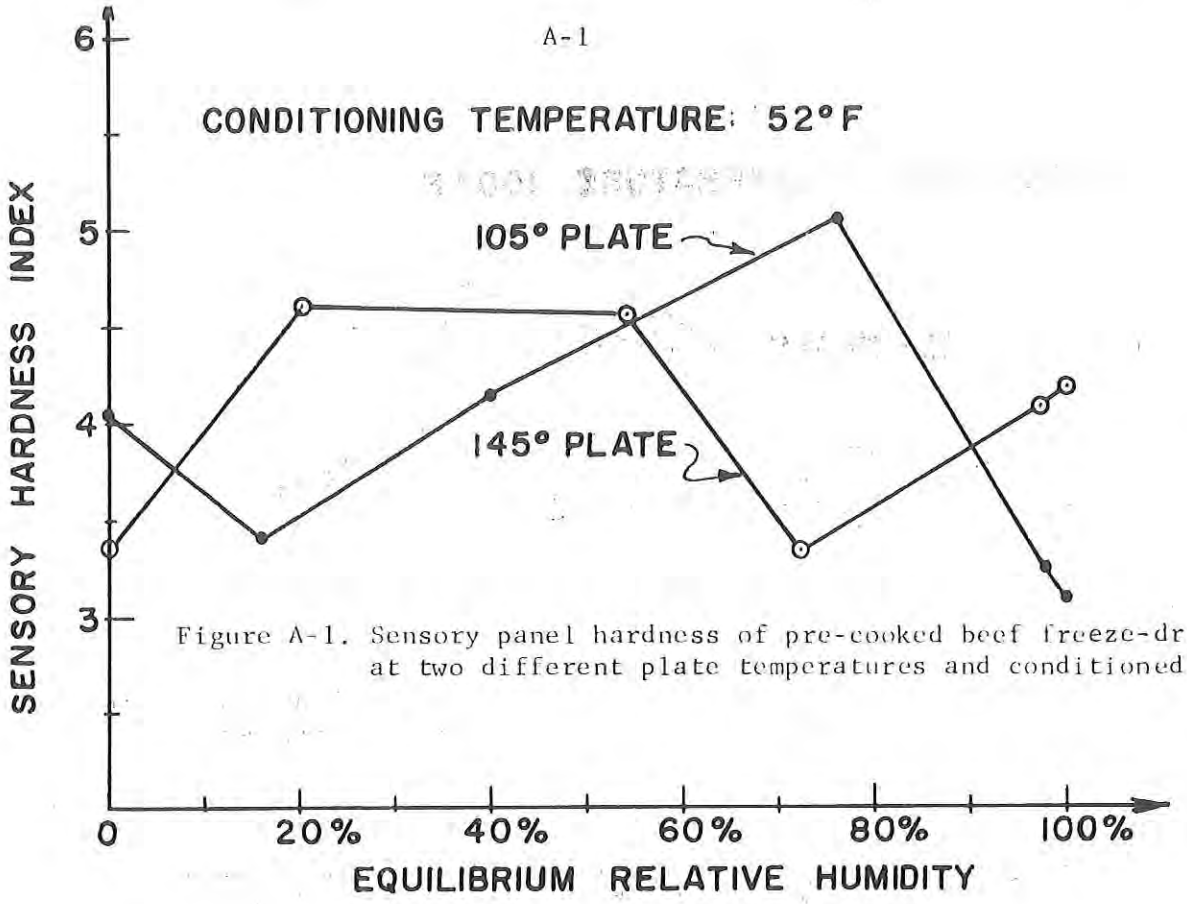

Figure A-1. Sensory panel hardness of pre-cooked beef freeze-dried at two different plate temperatures and conditioned at 52°F.

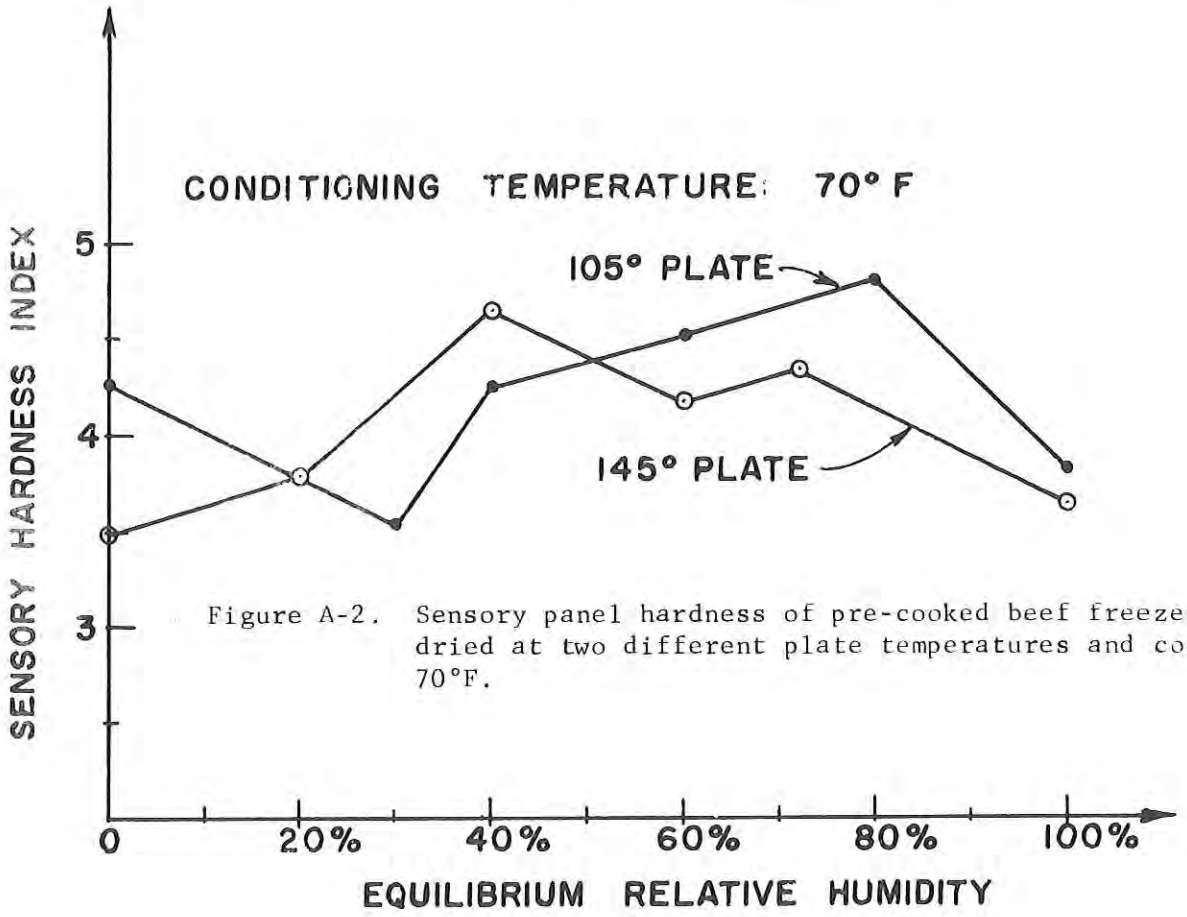

Figure A-2. Sensory panel hardness of pre-cooked beef freeze-dried at two different plate temperatures and conditioned at 70°F.

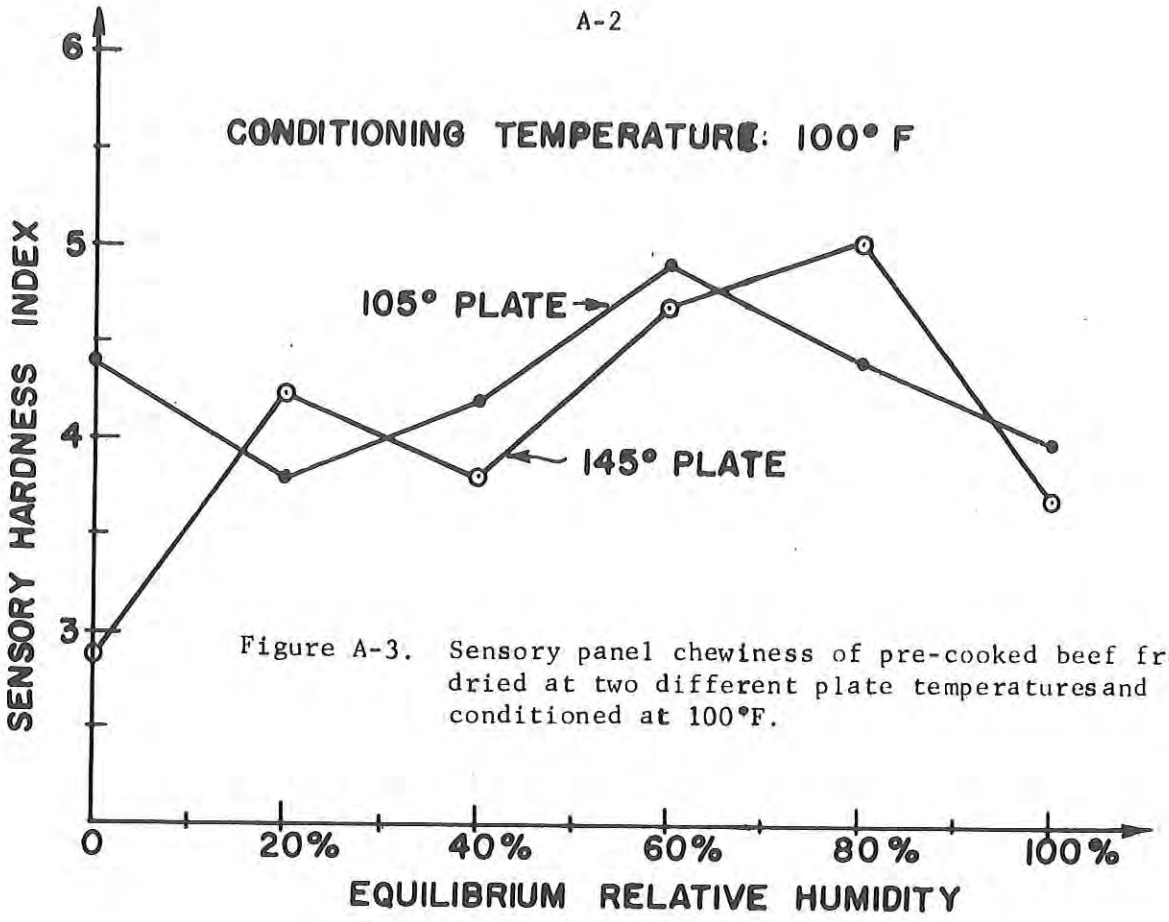

Figure A-3. Sensory panel chewiness of pre-cooked beef freeze-dried at two different plate temperatures and conditioned at 100°F.

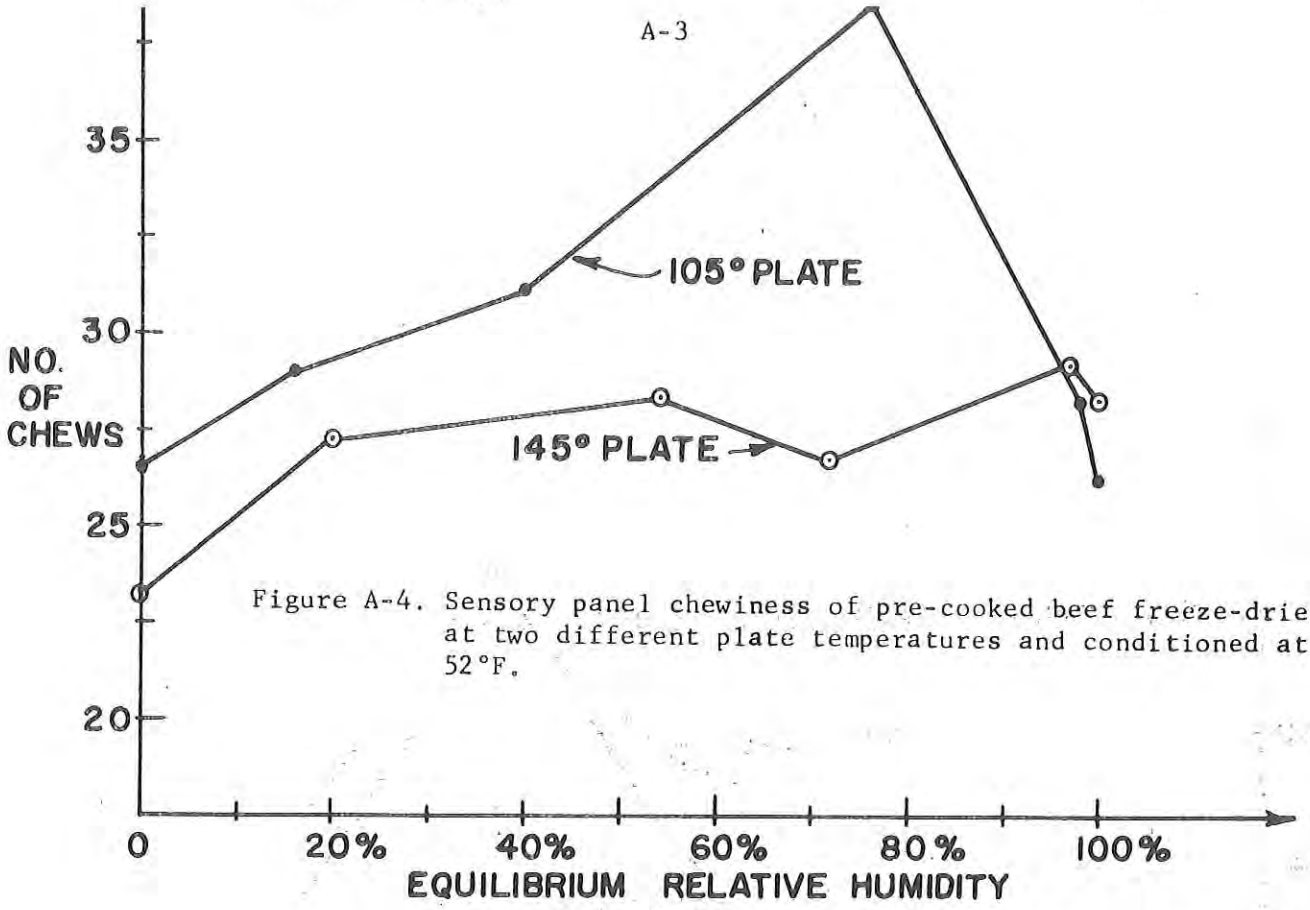

Figure A-4. Sensory panel chewiness of pre-cooked beef freeze-dried at two different plate temperatures and conditioned at 52°F.

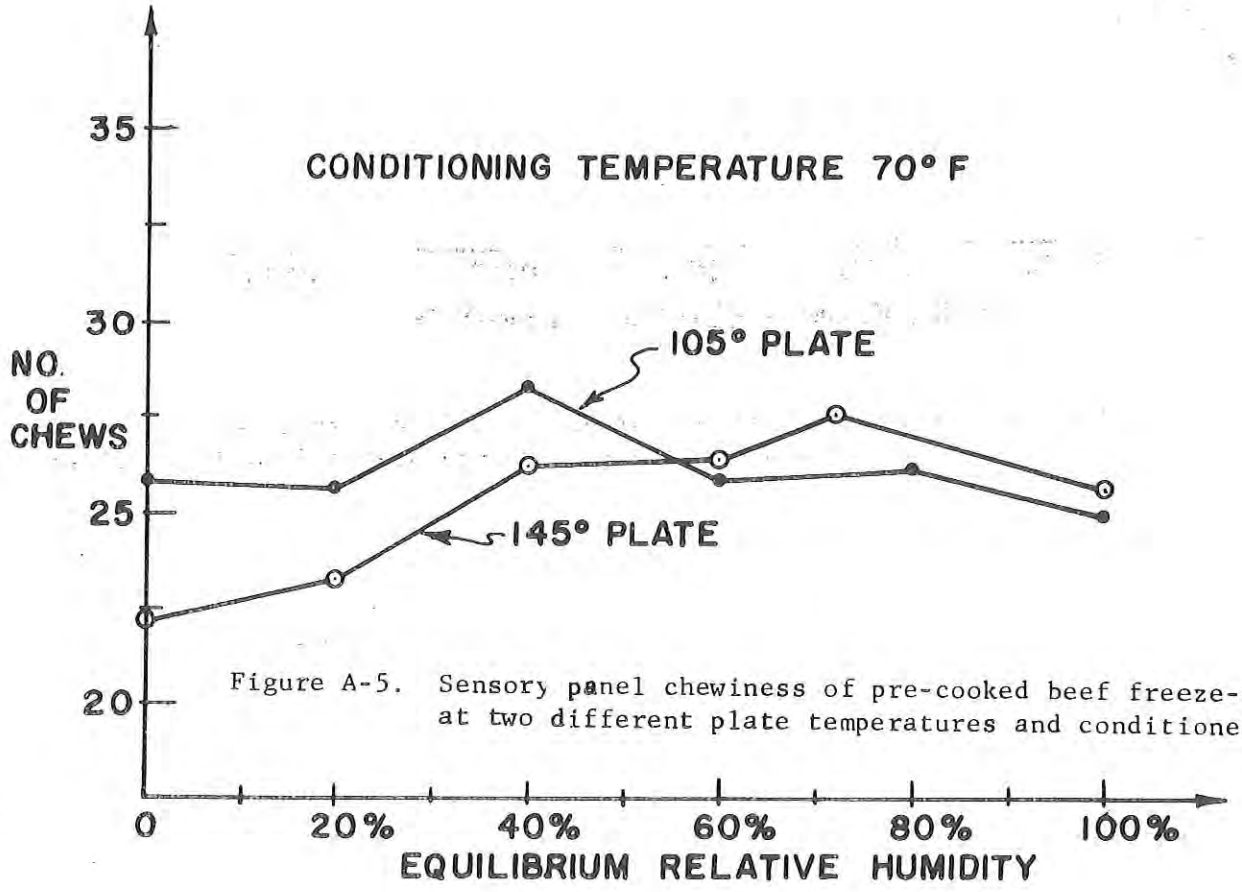

Figure A-5. Sensory panel chewiness of pre-cooked beef freeze-dried at two different plate temperatures and conditioned at 70°F.

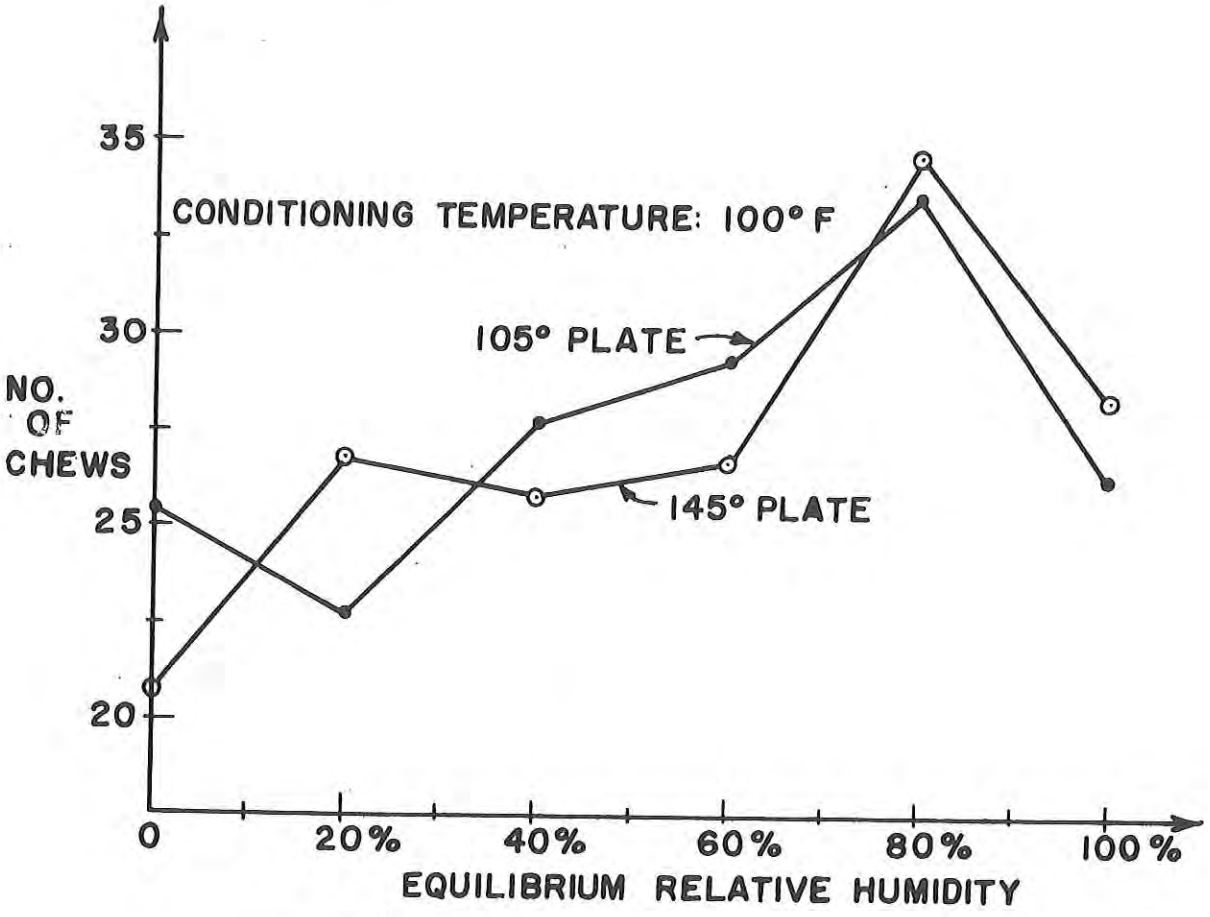

Figure A-6. Sensory panel hardness of pre-cooked beef freeze-dried at two different plate temperatures and conditioned at 100°F.

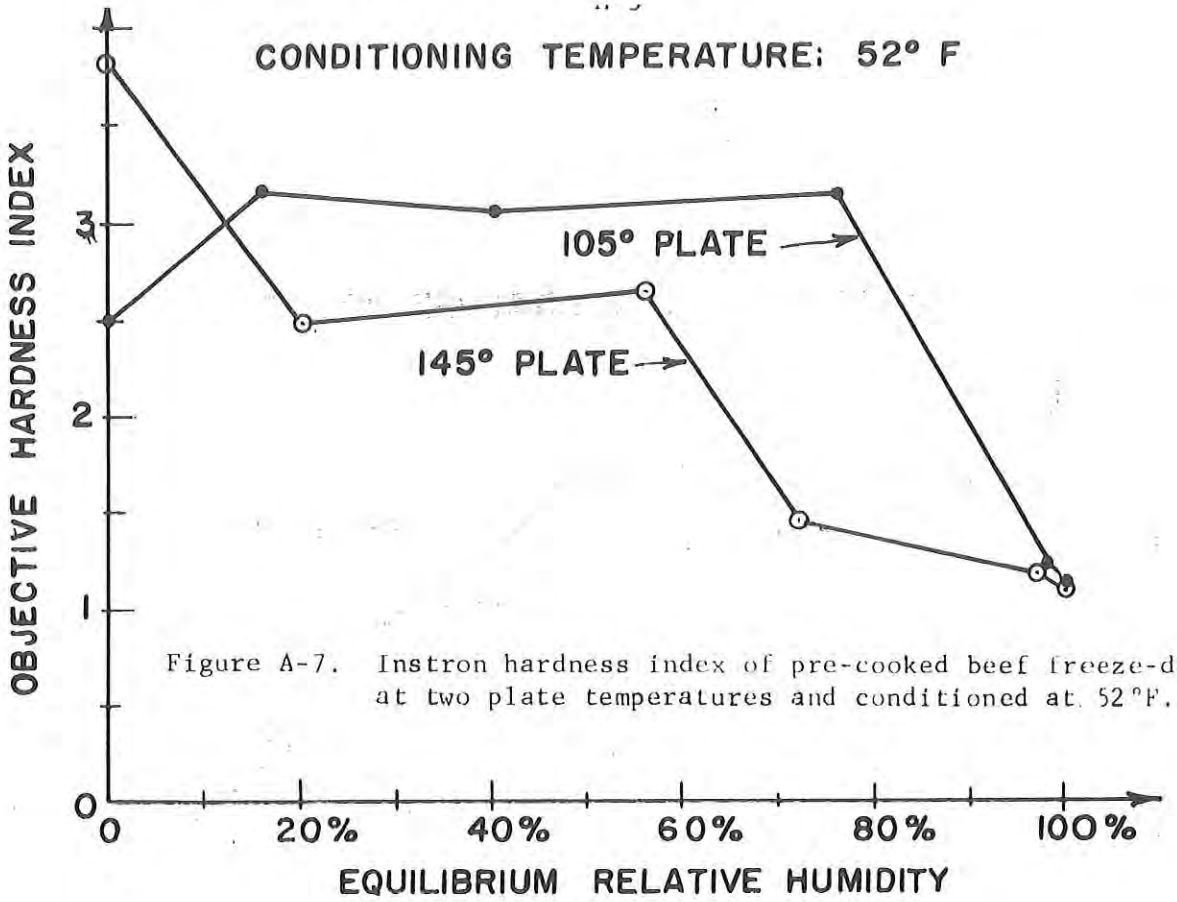

Figure A-7. Instron hardness index of pre-cooked beef freeze-dried at two plate temperatures and conditioned at 52°F.

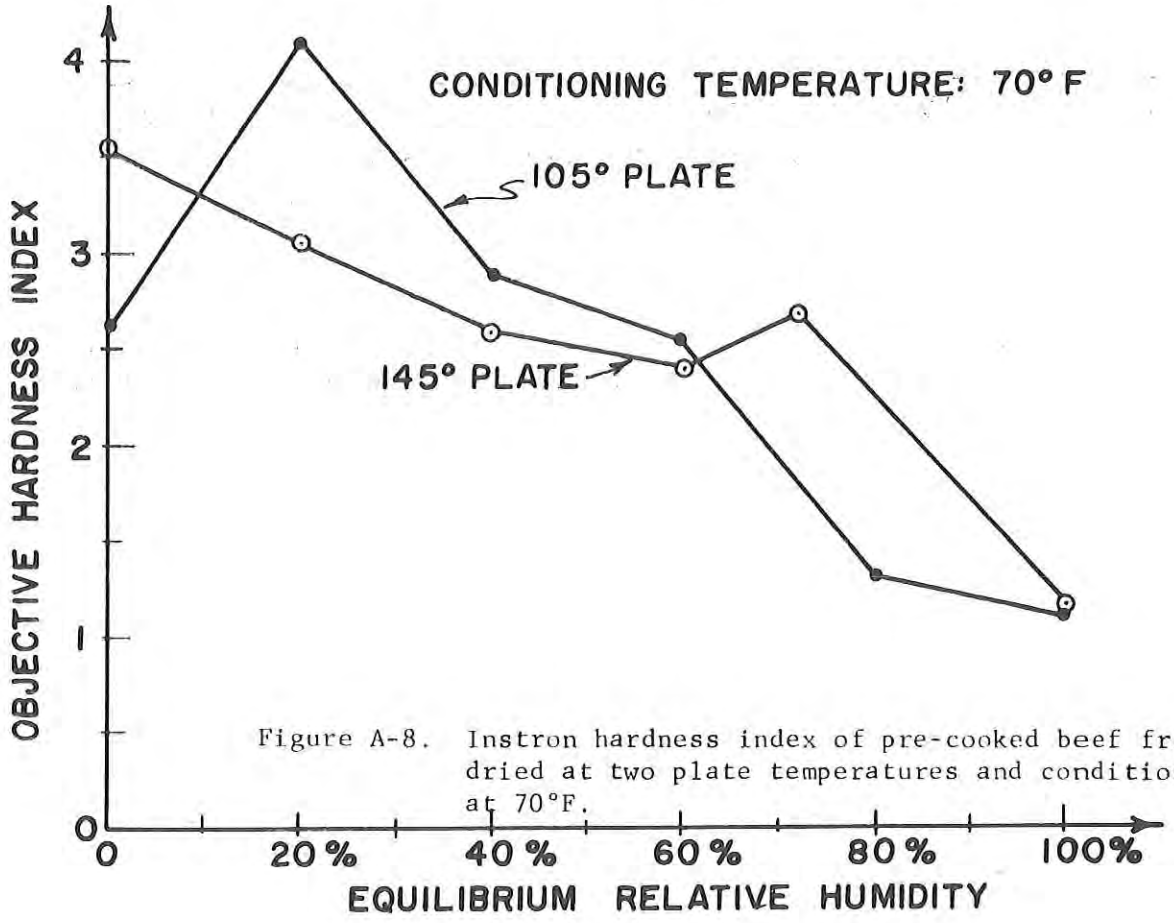

Figure A-8. Instron hardness index of pre-cooked beef freeze-dried at two plate temperatures and conditioned at 70°F.

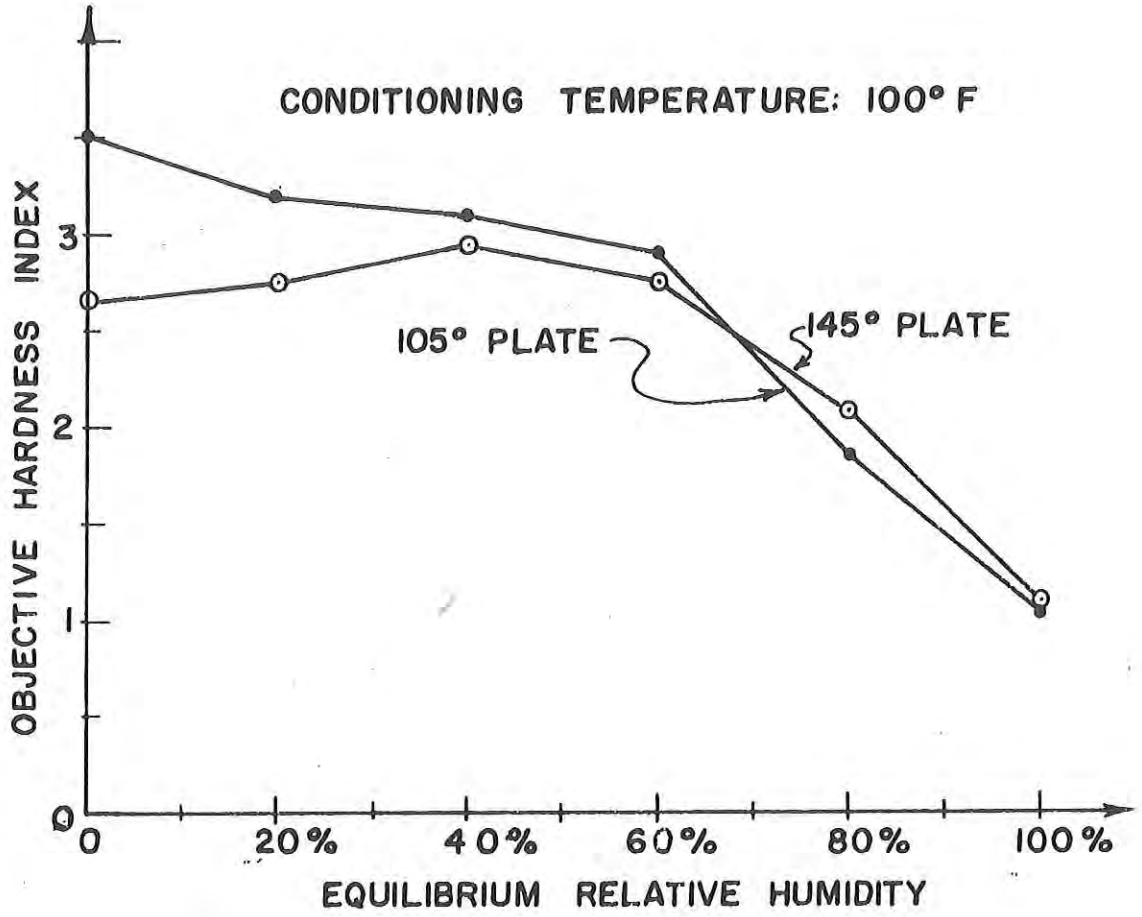

Figure A-9. Instron hardness index of pre-cooked beef freeze-dried at two plate temperatures and conditioned at 100°F.

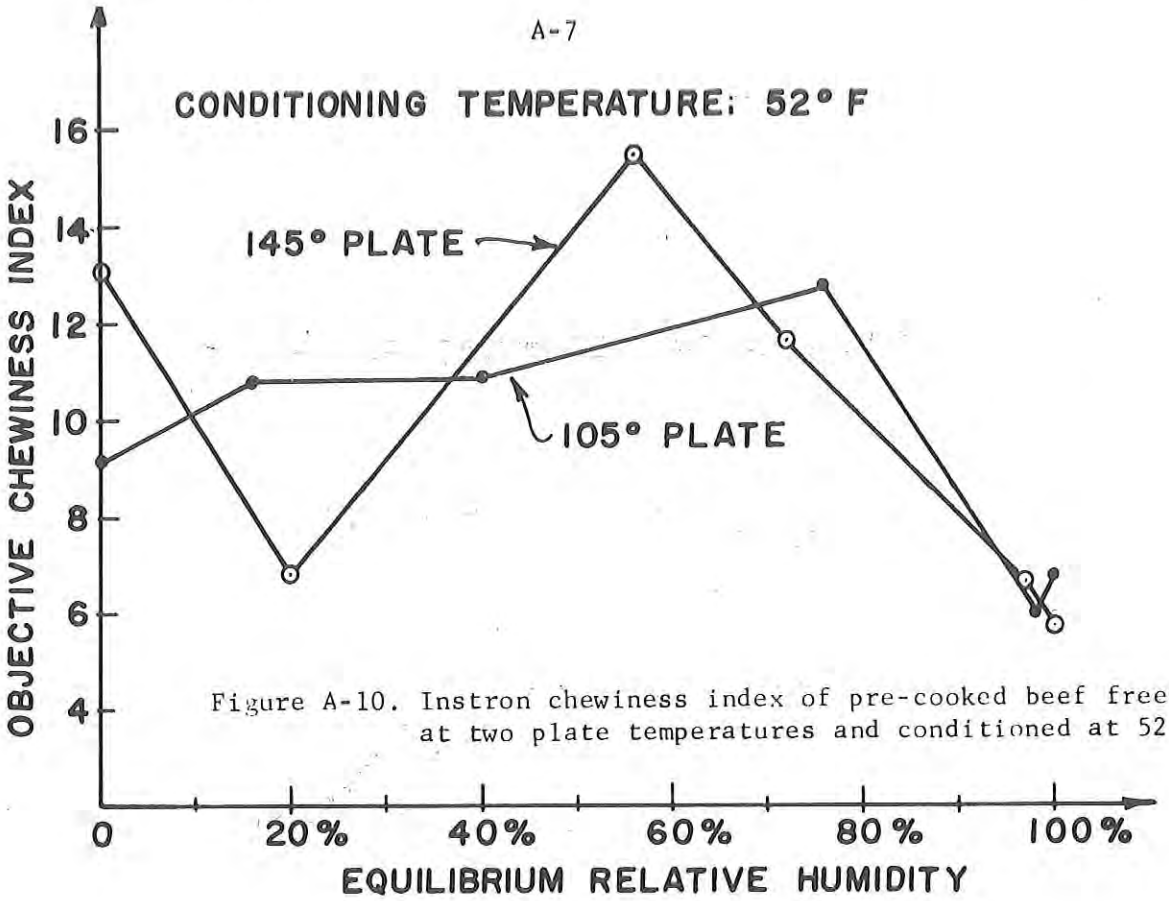

Figure A-10. Instron chewiness index of pre-cooked beef freeze-dried at two plate temperatures and conditioned at 52°F.

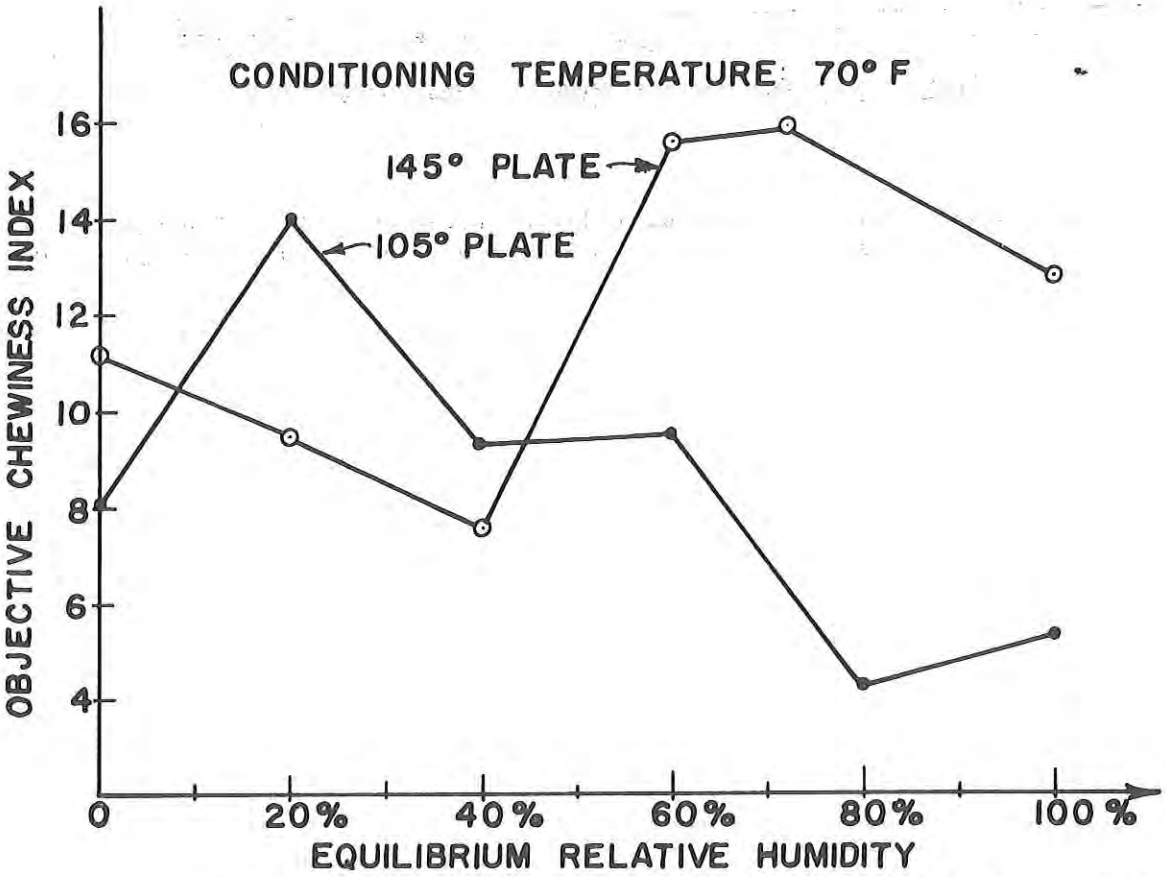

Figure A-11. Instron chewiness index of pre-cooked beef freeze-dried at two plate temperatures and conditioned at 70°F.

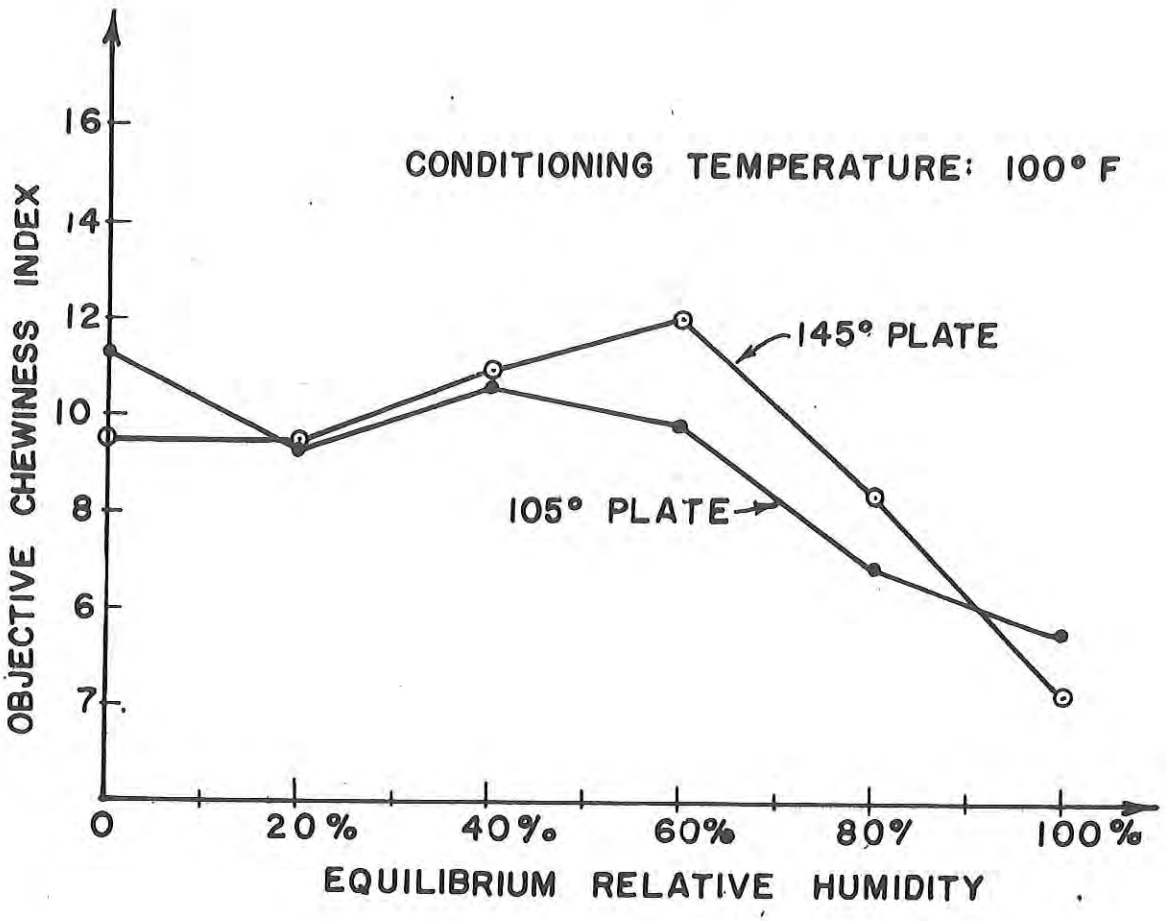

Figure A-12. Instron chewiness index of pre-cooked beef freeze-dried at two plate temperatures and conditioned at 52 °F.

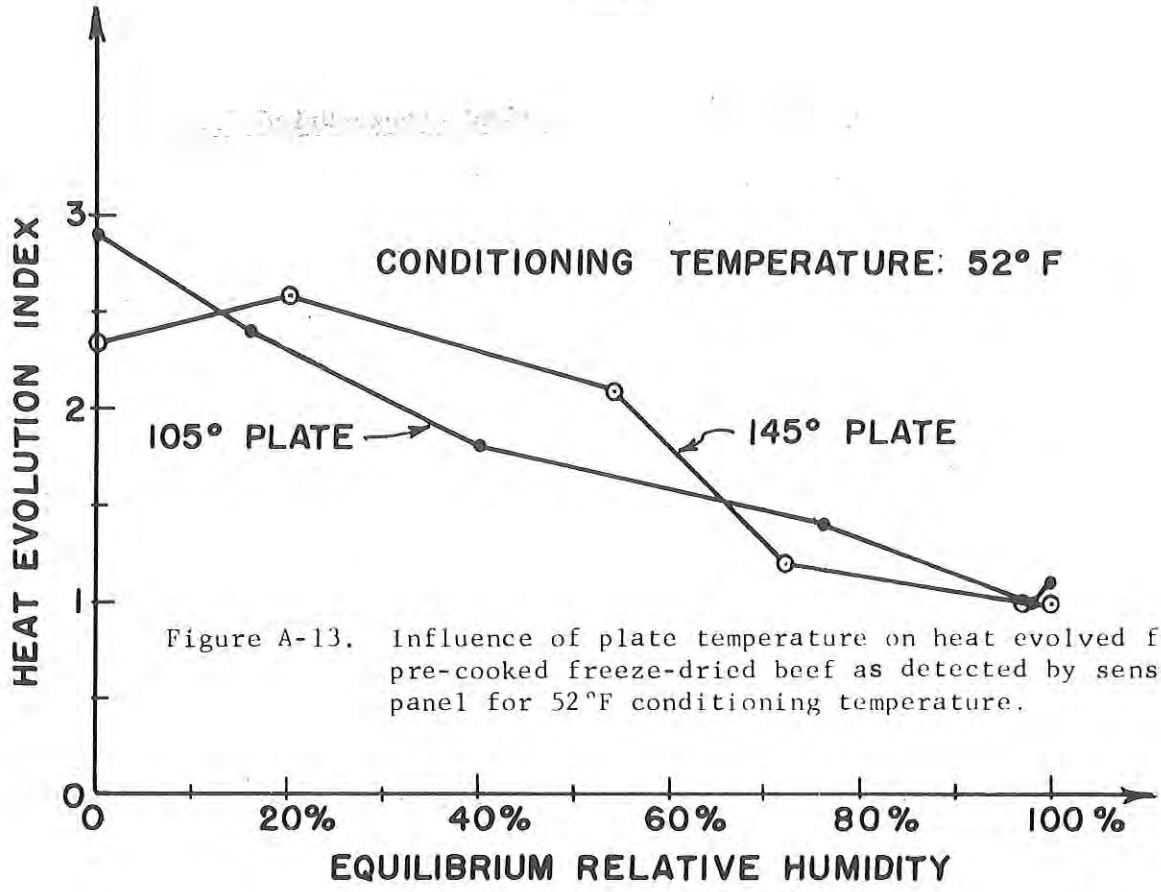

Figure A-13. Influence of plate temperature on heat evolved from pre-cooked freeze-dried beef as detected by sensory panel for 52°F conditioning temperature.

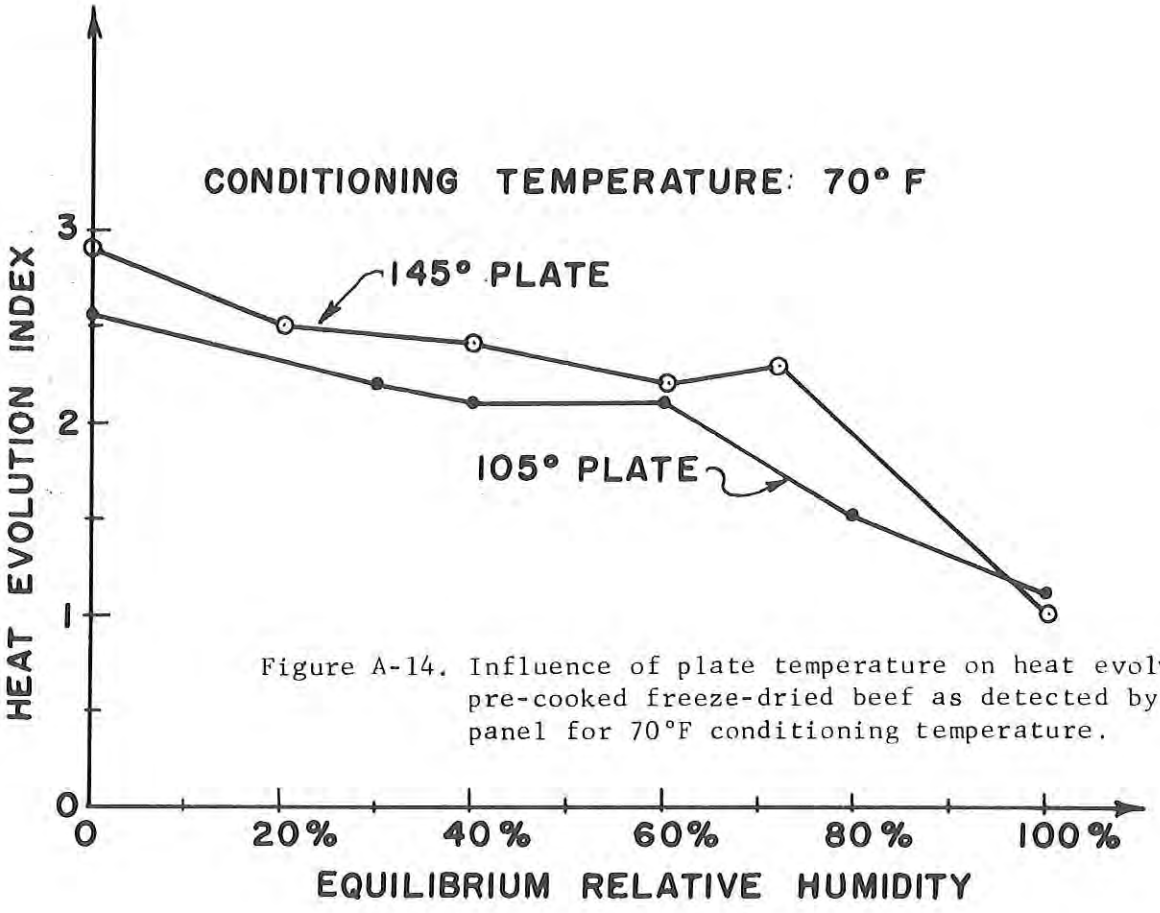

Figure A-14. Influence of plate temperature on heat evolved from pre-cooked freeze-dried beef as detected by sensory panel for 70°F conditioning temperature.

Table A-1 Equilibrium Moisture Content of Pre-cooked Freeze-Dried Ground Beef.

plate temperature = 105°F

sample size = 100-150 milligrams

	A D S O R P T I O N in (N.F.D.)			
P/Po	40°F	50°F	72°F	100°F
0.0000	0.000	0.000	0.000	0.000
0.005	0.007	0.003	0.002	0.001
0.010	0.013	0.011	0.0033	0.0011
0.020	0.025	0.019	0.0110	0.0022
0.030	0.035	0.027	0.0160	0.0055
0.050	0.055	0.041	0.0280	0.011
0.100	0.100	0.077	0.049	0.022
0.150	0.120	0.093	0.059	0.027
0.200	0.130	0.106	0.066	0.033
0.300	0.139	0.121	0.082	0.044
0.400	0.154	0.137	0.093	0.055
0.580		0.160	.112	0.07
0.600	0.230	0.181	0.138	0.088
0.700		0.23	0.18	0.12
0.800	0.391	0.286	0.253	0.154
0.900	0.506	0.418	0.363	0.220
0.950	0.567	0.484	0.445	0.264

Table A-2 Equilibrium Moisture Content of Pre-cooked Freeze-Dried Ground Beef.

plate temperature = 105°F

sample size = 100-150 milligrams

DESORPTION

in (N.F.D.)

P/Po	40°F	50°F	72°F	100°F
0.000	0.066	0.044	0.011	.033
0.005	0.069	0.046	0.018	.034
0.010	0.071	0.050	0.0219	.0351
0.020	0.077	0.055	0.0270	.0384
0.030	0.082	0.066	0.033	.0417
0.050	0.091	0.077	0.044	.043
0.100	0.108	0.099	0.063	.055
0.150	0.120	0.110	0.072	.058
0.200	0.128	0.121	0.080	.066
0.300	0.141	0.138	0.090	.077
0.400	0.155	0.150	0.104	.093
0.480		0.16	0.112	.050
0.600	0.226	0.209	0.154	.148
0.700		0.285	0.210	
0.800	0.458	0.467	0.308	.236
0.900	0.526	0.533	0.505	.280
0.950	0.541	0.549	0.522	.302

Table A-3 Equilibrium Moisture Content of Pre-cooked Freeze-Dried Ground Beef.

plate temperature = 145°F

sample size = 100-150 milligrams

	A D S O R P T I O N in (N.F.D.)			
P/Po	40°F	50°F	72°F	100°F
0.000	0.000	0.000	0.000	0.0000
0.005	0.004	0.0032	0.0021	0.0010
0.010	0.007	0.0087	0.0032	0.0021
0.020	0.014	0.0140	0.0087	0.0054
0.030	0.019	0.0190	0.0110	0.0087
0.050	0.030	0.0270	0.0210	0.0100
0.100	0.051	0.0430	0.0320	0.0210
0.150	0.062	0.0540	0.0430	0.0290
0.200	0.070	0.0650	0.0520	0.0350
0.300	0.084	0.0800	0.0640	0.0460
0.400	0.100	0.0900	0.0710	0.0520
0.600	0.145	0.1230	0.1090	0.0680
0.800	0.233	0.2300	0.1840	0.0980
0.900	0.335	0.3510	0.274	0.1420
0.950	0.408	0.4390	0.357	0.1750

Table A-4 Equilibrium Moisture Content of Pre-cooked Freeze-Dried Ground Beef.

plate temperature = 145°F

sample size = 100-150 milligrams

D E S O R P T I O N

in (N.F.D.)

P/Po	40°F	50°F	72°F	100°F
0.000				
0.005				
0.010	0.020	0.022	0.018	.0100
0.020	0.033	0.026	0.022	0.076
0.030	0.042	0.040	0.024	0.080
0.050	0.056	0.048	0.040	0.082
0.100	0.077	0.062	0.060	0.092
0.150	0.088	0.080	0.070	0.100
0.200	0.097	0.090	0.084	0.102
0.300	0.110	0.104	0.104	0.116
0.400	0.128	0.122	0.120	0.122
0.600	0.186	0.180	0.163	0.140
0.800	0.504	0.524	0.285	0.160
0.900	0.532	0.560	0.385	0.170
0.950	0.539	0.576	0.445	0.175

Table A-5 Hardness Index Values Measured by Sensory Panel

Temp. (°F)	Equilibrium Relative Humidity ~0%	~20%	~40%	~60%	~80%	~100%
	(Plate Temperature = 105°F)					
39	4.55	4.03	4.37	3.63	3.37	3.925
52	4.05	3.4	4.15	5.05	3.23	3.1
70	4.27	3.52	4.25	4.51	4.8	3.8
100	4.4	3.8	4.2	4.?2	4.43	4.0
	(Plate Temperature = 145°F)					
39	3.01	3.98	2.91	3.53	3.33	3.69
52	3.35	4.62	4.56	3.32	4.09	4.19
70	3.49	3.77	4.64	4.16	4.33	3.62
100	2.87	4.25	3.80	4.69	5.04	3.71

Table A-6 Hardness and Chewiness Data obtained by Instron Testing Machine for Precooked Freeze-dried Beef conditioned at 100°F.

	Equilibrium Relative Humidity											
	~0%		~20%		~40%		~60%		~80%		100%	
	H	C	H	C	H	C	H	C	H	C	H	C
					(Plate Temperature = 105°F)							
	3.84	11.68	5.50	13.80	2.41	8.36	1.61	5.85	1.25	4.46	.53	2.06
	2.77	9.45	2.24	7.84	3.72	11.46	2.72	10.22	1.96	7.21	1.10	4.76
	4.72	15.67	2.97	8.26	3.67	13.18	2.94	11.48	1.68	5.53	.75	2.86
	4.89	14.31	2.02	6.86	3.19	11.05	2.60	8.63	1.04	3.38	1.25	5.98
	2.21	7.54	3.18	9.58	2.17	8.15	3.35	10.12	1.66	6.31	1.02	6.61
	2.78	9.05			2.36	9.03	2.99	10.18	1.43	5.37	.95	7.03
	3.42	10.91			2.06	8.51	3.86	11.34	2.56	10.92	1.05	6.64
	2.34	9.17			1.59	6.93	2.74	12.12	1.44	5.02	1.33	7.46
	5.25	17.62			4.74	13.88	3.37	8.28	4.77	18.15	.74	4.29
	3.75	12.81			2.03	7.24			1.51	5.88	.86	4.77
	2.77	12.34			3.21	10.61			1.81	6.93	1.13	5.66
	2.80	8.32			3.06	7.40			1.02	4.02	1.02	6.01
	3.51	11.41			3.11	10.28			1.34	5.47	1.11	6.92
	5.35	12.62			4.31	15.20			2.52	7.53	1.08	5.47
	2.78	7.98			4.82	18.51			1.52	5.17	1.32	6.04
	3.77	11.46							1.92	7.57	1.22	6.24
	2.22	8.93							2.09	9.96		
	3.47	11.73							1.32	5.06		
	3.51	11.31							1.36	5.17		
	3.84	11.34							2.78	8.89		
(Mean)	3.50	11.28	3.18	9.27	3.10	10.65	2.91	9.80	1.85	6.90	1.03	5.55
					(Plate Temperature = 145°F)							
	2.35	7.61	1.77	7.06	2.34	8.33	3.56	21.15	4.25	20.22	1.08	2.81
	5.12	22.22	2.43	7.49	3.12	11.65	1.37	7.22	5.25	22.64	1.14	5.35
	1.36	3.88	3.95	11.35	3.16	11.12	2.50	9.65	2.00	9.70	1.06	2.72
	2.97	13.79	2.07	7.36	2.74	10.43	3.28	12.96	1.35	4.72	1.23	5.88
	2.94	9.38	1.80	6.47	3.75	12.00	3.16	13.74	2.40	8.99	.96	4.06
	2.83	9.09	3.65	10.47	2.52	9.61	1.33	5.92	2.66	9.33	1.13	3.77
	1.44	5.26	2.50	7.27	2.66	12.99	2.17	7.60	1.44	5.54	.50	1.48
	2.55	7.48	3.95	13.15	3.57	15.07	2.85	8.43	1.08	3.48	1.04	3.56
	3.68	9.19	1.50	7.21	2.58	11.81	2.02	7.35	1.23	4.28	1.57	8.05
	2.58	7.73	3.78	16.06	2.77	12.94	4.27	21.43	0.75	3.39		
	2.32	8.43			2.60	9.54	5.10	23.98	1.02	3.91		
					3.10	10.67	2.70	12.50	1.38	4.97		
					2.83	9.34	1.72	6.96				
					2.40	9.58	2.75	11.27				
					5.04	11.32	3.17	20.58				
					2.58	8.95	2.31	8.29				
					3.49	14.83	4.00	11.15				
					2.28	8.13	1.34	6.51				
					2.36	10.45						
(Mean)	2.65	9.46	2.74	9.39	2.94	10.99	2.76	12.04	2.07	8.43	1.08	4.19

H = Hardness values
C = Chewiness values
Value at bottom of each column represent mean value for that column.

Table A-7 Hardness and Chewiness Data obtained by Instron Testing Machine for Precooked Freeze-dried Beef conditioned at 70°F.

Equilibrium Relative Humidity											
~0%		~30%		~40%		~60%		~80%		100%	
H	C	H	C	H	C	H	C	H	C	H	C
				(Plate Temperature = 105°F)							
3.66	9.79	5.25	16.80	3.11	9.54	2.62	9.50	.71	2.27	.96	3.90
2.84	10.51	1.45	6.73	3.47	18.11	3.06	11.45	1.13	4.89	.84	3.98
1.83	7.61	2.66	9.49	2.22	7.83	4.50	15.62	.67	2.17	1.05	6.06
2.82	7.30	4.62	16.87	3.92	9.68	2.08	8.64	1.28	3.78	1.15	5.94
2.63	8.64	2.67	8.14	4.06	9.23	2.08	9.39	2.46	7.36	1.68	8.75
2.27	6.85	2.30	7.62	2.67	8.13	3.20	12.14	1.73	5.15	.98	4.30
2.32	6.39	5.50	22.35	2.84	9.04	2.28	6.17	1.18	3.83	1.76	9.72
2.57	9.32	2.52	7.54	3.00	7.17	1.83	6.61			1.10	6.34
2.44	7.62	3.78	10.00	2.34	8.01	2.28	8.72			.87	4.00
2.50	6.34	2.97	10.14	2.64	10.33	2.25	7.40			.82	3.79
1.48	4.56	5.75	19.91	3.22	10.39	2.61	10.44			1.06	4.24
2.02	5.67	1.79	8.80	1.95	7.58	1.61	7.05			.72	3.76
2.24	7.90	2.31	6.76	2.24	8.30	2.67	10.06			1.36	5.94
3.69	10.92	4.04	12.85	2.24	8.08	3.22	12.07			.92	4.18
2.67	9.95	2.65	10.16	2.44	8.00	2.63	10.32			.65	3.01
3.93	12.82	2.22	7.05	2.35	7.59	2.65	10.60			1.74	9.54
1.48	3.26	4.04	12.97	3.88	12.74	2.62	11.02			.71	3.78
2.94	10.28	4.71	15.64	1.78	4.62	2.88	9.82			1.38	6.11
2.76	7.92			3.30	10.07	1.46	5.44			.83	3.09
3.10	6.43			3.11	8.78	2.03	6.98			1.40	6.68
				3.70	11.34						
(Mean) 2.61	8.00	4.08	13.99	2.88	9.26	2.53	9.47	1.31	4.21	1.10	5.36
				(Plate Temperature = 145°F)							
3.50	10.99	1.76	4.11	1.86	5.63	6.91	24.51	5.20	20.32	1.08	11.87
2.61	8.24	3.90	13.88	2.27	7.05	7.22	23.76	5.15	21.19	0.98	18.05
3.93	17.01	2.59	10.59	2.53	7.48	3.82	12.05	7.92	19.85	1.62	17.33
3.55	13.78	3.16	9.43	3.71	9.56	4.60	14.09	7.73	21.19	1.21	13.28
4.34	13.81	2.65	6.75	3.94	8.65	5.38	16.76	3.25	12.07	0.79	8.95
3.67	10.09	2.10	6.81	1.67	5.67	5.80	16.66	7.82	22.94	1.68	19.16
3.60	8.54	2.67	10.15	1.23	4.06	5.09	18.60	2.64	8.36	0.82	7.41
3.62	10.05	3.02	12.38	2.94	9.04	4.09	14.58	6.15	20.47	1.14	10.61
3.00	8.98	2.32	8.15	3.30	10.38	4.61	15.14	9.00	20.11	0.73	7.29
3.49	10.24	3.25	7.37	2.33	7.18	7.52	20.59	4.82	10.00	1.02	11.92
		3.18	9.21			3.62	11.76	2.93	10.19	1.76	16.99
		2.50	9.00			6.17	20.45	4.11	13.35	0.84	8.30
		2.66	6.42			3.42	14.37	3.51	10.85	1.42	16.16
		2.47	8.60			3.37	9.48	6.98	21.67	0.71	6.67
		2.60	8.08			3.53	15.81	7.75	20.63	1.38	17.11
		4.69	18.44			3.92	9.71	3.74	9.42		
		5.50	1.73			2.20	10.03	3.02	11.22		
		2.47	10.29			3.46	11.75	5.96	15.67		
		3.11	9.95			7.08	19.13	3.91	14.35		
		4.55	16.07			3.60	12.01	5.39	13.83		
(Mean) 3.53	11.17	3.06	9.38	2.58	9.47	2.39	15.56	2.68	15.88	1.15	12.74

H = Hardness values

C = Chewiness values

Value at bottom of each column represent mean value for that column.

Table A-8 Hardness and Chewiness Data obtained by Instron Testing Machine for Precooked Freeze-dried Beef conditioned at 52°F.

Equilibrium Relative Humidity

~0%		~20%		~40%		~60%		~80%		100%	
H	C	H	C	H	C	H	C	H	C	H	C
				(Plate Temperature = 105°F)							
1.65	4.15	3.69	13.01	3.25	10.16	2.09	7.00	1.45	7.21	1.10	6.23
3.37	12.10	2.14	8.99	4.16	12.44	1.16	3.04	0.82	3.56	1.04	7.04
4.1	15.37	2.49	9.77	3.42	10.67	3.12	9.36	0.82	4.10	1.21	6.80
2.65	9.24	3.91	12.90	3.35	12.10	1.62	6.66	1.24	6.67	1.00	6.09
1.81	6.48	2.41	9.97	2.13	9.17	4.80	18.96	1.58	7.61	0.77	4.93
2.43	7.38	2.36	6.92	1.83	7.77	5.30	25.88	1.70	7.57	1.37	8.27
3.38	12.90	3.76	12.78	4.18	14.83	3.33	13.24	1.17	6.12	1.20	7.14
2.96	9.55	3.76	12.51	1.81	5.87	3.94	17.92	1.30	7.10	1.96	12.07
1.86	5.18	3.80	13.27	1.61	6.02	5.30	20.54	1.50	7.03	0.87	5.73
3.71	11.54	3.17	8.10	2.36	9.30	5.25	21.84	0.93	3.67	0.76	3.41
2.44	9.58			1.43	6.44	1.86	7.65			1.02	5.88
3.17	10.94			5.40	16.96	3.28	10.97			1.57	8.16
				5.20	18.14	1.60	5.84				
				2.87	10.08	4.43	17.55				
				3.02	11.07	2.66	11.36				
				3.66	13.59	0.96	3.07				
				2.07	8.88	2.96	15.88				
				4.39	17.38						
				1.62	6.38						
(Mean) 2.49	9.09	3.15	10.82	3.04	10.91	3.16	12.75	1.25	6.06	1.16	6.81
				(Plate Temperature = 145°F)							
3.30	8.09	4.34	8.64	3.02	7.53	1.66	24.58	0.83	4.42	1.03	6.75
3.41	11.74	2.76	8.78	3.70	10.05	1.24	15.88	0.64	3.27	1.24	5.21
2.38	10.68	1.34	4.82	3.40	10.42	1.51	18.73	0.84	4.06	1.16	7.08
2.44	10.31	2.05	7.47	1.67	5.24	2.01	12.95	1.30	7.00	1.27	5.86
5.02	16.02	3.39	7.88	3.86	9.73	1.76	9.92	1.63	9.03	1.39	9.15
4.82	10.38	2.62	7.99	1.70	4.81	1.07	5.62	1.54	8.84	0.92	4.53
4.63	8.03	3.15	7.80	2.12	6.79	1.10	6.68	1.16	8.15	0.70	3.24
4.66	15.68	2.20	7.18	1.72	5.39	1.22	6.31	1.58	8.73	1.20	6.45
3.67	27.90	1.70	4.37	3.31	10.18	2.01	10.98	0.66	3.15	0.96	3.93
3.65	11.71	1.20	3.48	2.90	7.49	0.92	4.34	1.72	9.95	1.15	4.88
				2.80	9.13						
				2.70	6.03						
				2.76	8.40						
				1.13	3.68						
				1.90	7.96						
				2.76	8.04						
				1.74	6.69						
				2.47	7.49						
				4.51	11.89						
				2.87	7.66						
(Mean) 3.80	13.05	2.48	6.84	2.65	15.45	1.45	11.60	1.19	6.66	1.10	5.71

H = Hardness values
C = Chewiness values
Value at bottom of each column represent mean value for that column.

Table A-9 Hardness and Chewiness Data obtained by Instron Testing Machine for Precooked Freeze-dried Beef conditioned at 39°F.

	Equilibrium Relative Humidity											
	~0%		~20%		~40%		~60%		~80%		100%	
	H	C	H	C	H	C	H	C	H	C	H	C
	(Plate Temperature = 105°F)											
	2.18	7.29	3.46	10.58	1.11	5.05	1.85	9.23	1.81	8.60	1.42	8.13
	1.93	6.46	3.82	12.50	1.43	5.48	1.81	8.09	1.92	10.52	1.10	5.11
	2.38	7.60	3.12	13.10	2.28	7.02	2.44	11.38	1.77	8.13	1.77	4.72
	4.79	16.23	5.15	21.76	3.17	11.81	1.80	6.67	.51	2.86	1.06	6.33
	2.07	5.13	3.79	10.03	3.45	11.46	2.40	12.17	.78	4.23	1.45	10.81
	3.07	11.36	2.97	5.56	1.41	4.63	1.16	4.79	.62	2.78	2.03	4.42
	2.63	7.53	3.60	11.75	4.94	20.15	1.69	9.23	.96	5.39	1.04	4.80
	2.95	9.65	5.15	14.45	1.04	3.86	1.44	8.13	1.34	7.76	1.38	10.91
	2.27	7.20	2.40	8.33	0.95	3.57	1.48	3.29	1.12	6.27	2.06	2.39
	1.71	6.06	2.95	9.93	1.11	3.54	1.92	9.69	.54	2.07	.80	11.09
	2.33	4.88			3.05	10.98			1.06	5.72	2.08	8.98
	3.08	10.44			2.98	12.38			.69	4.75	1.98	10.40
					1.62	5.84			.60	2.87		
					5.20	22.22			.95	4.27		
					4.35	14.97			1.26	6.84		
									1.06	4.24		
									.53	2.63		
									.77	3.33		
(Mean)	2.62	8.32	3.64	11.80	2.54	9.53	1.80	8.27	1.02	5.18	1.54	7.34
	(Plate Temperature = 145°F)											
	2.18	7.38	2.50	9.06	2.03	7.57	1.76	7.91	1.13	5.65	.68	3.76
	1.58	7.51	2.07	6.29	2.02	11.62	2.06	11.44	1.26	5.57	1.14	6.96
	3.13	11.04	1.93	5.61	1.62	7.99	0.92	5.93	.44	2.39	1.30	8.82
	2.57	6.69	2.45	7.49	1.94	9.86	2.08	11.57	2.30	12.40	2.10	11.33
	3.15	10.13	1.56	8.57	2.18	9.96	2.16	11.37	2.40	9.43	2.08	12.25
	2.11	12.65	1.95	5.89	1.76	9.13	1.02	6.32	1.07	5.47	1.46	8.62
	2.55	10.23	1.00	3.21	1.85	9.69	1.29	7.64	2.38	12.42	1.27	7.37
	3.65	8.92	1.52	4.69	2.01	10.76	2.06	11.70	1.04	6.26	1.32	8.23
	5.5	17.93	1.83	6.03	1.61	9.76	1.18	6.96	1.49	16.82	2.08	12.48
	2.58	7.65	2.44	8.91	1.15	6.52	0.73	4.34	1.91	7.76	1.18	6.61
	2.53	6.12									1.85	11.51
	1.88	7.48									1.09	6.46
	3.67	11.02										
	4.87	14.57										
	3.36	9.57										
(Mean)	3.02	9.93	1.93	6.58	1.82	9.29	1.53	8.52	1.54	8.42	1.46	8.70

H = Hardness values
C = Chewiness values
value at bottom of each column represent mean value for that column.

Table A-10

SENSORY PANEL

Score Sheet Guide

I. Hardness Evaluation for Freeze-dried Beef

A. Orient specimen so that product fibers are perpendicular to direction of bite.

B. Place specimen between molar teeth and bite down evenly to evaluate force required to compress.

C. Compare force required to standards in order to assign scale value.

D. Remember that hardness scale value is based on the very first response obtained from the specimen.

E. Assign a scale value to the nearest 0.25 point (7, 7.25, 7.5, 7.75, 8) and record.

II. Chewiness Evaluation for Freeze-dried Beef

A. Orient specimen in mouth the same as for hardness test.

B. Apply a force equal to that required to penetrate a gum drop in one-half second.

C. Chew the specimen at a rate of one chew per second with same force in each chew until the specimen is ready to swallow.

D. Be sure the specimen is as close to the condition at the time of swallowing as standards were at this point.

E. Record the number of chews.

III. Heat Evolved During Chewiness Evaluation

A. During the chewiness evaluation, try to sense an increase in temperature in the mouth (on tongue or palate).

B. Use the four-point scale on the score sheet to indicate your evaluation.

Table A-11

TEXTURE SCORE SHEET

NAME _____ DATE _____

Hardness — Unknown

	I	II	III	IV	V
1. Cream Cheese					
2. Egg White					
3. Frankfurter					
4. Cheese					
5. Olives					
6. Peanuts					
7. Carrots					
8. Almonds					
9. Rock Candy					

Chewiness (Record number of chews and scale number)

1.					
2.					
3.					
4.					
5.					
6.					
7.					

Heat evolved

1. None					
2.					
3.					
4. Evident					

TABLE A-12 Influence of storage time and conditioning on the hardness of the precooked freeze-dried beef.

Storage Temp = 39°F Plate Temp = 105°F

RH/Time	0	1	2	3	4	5	6
0	.9404	0.88245	1.07227	1.02960	1.21387	1.19333	1.22173
25	1.1359	0.96820	1.23446	1.05760	1.31287	0.89587	1.15087
50	.9946	1.09313	1.02566	1.33473	1.65007	1.00373	0.72147
75	0.8390	.85240	0.73206	0.87000	0.88147	0.88040	.72700

Storage temp = 39°F Plate Temp = 145°F

RH/Time	0	1	2	3	4	5	6
0	1.0735	1.19500	1.24533	1.43467	1.96027	1.18773	.40320
25	1.0660	0.99733	1.72300	1.10307	1.35647	1.14393	.88953
50	.9606	0.97660	0.93566	1.16020	0.84580	0.96027	.71093
75	1.0394	0.99833	0.98678	0.81527	1.38860	1.09613	.81787

Storage Temp = 100°F Plate Temp = 105°F

RH/Time	0	1	2	3	4	5	6
0	.9162	0.94420	0.91466	.88293	1.11367	1.08147	.94520
25	1.2789	0.94787	1.15973	1.13687	1.08327	1.17300	1.04420
50	.8715	0.98767	0.99995	.98173	1.55200	1.77520	1.34827
75	1.3616	1.16060	1.16200	1.46546	1.61373	1.87880	1.76253

Storage Tem = 100°F Plate Temp = 145°F

RH/Time	0	1	2	3	4	5	6
0	1.0073	1.00020	1.09193	1.00147	1.15600	1.06247	1.16220
25	1.0092	1.48266	1.04080	0.93900	1.17920	1.12680	1.15120
50	1.1058	1.31953	1.46526	1.37073	1.50647	1.43440	1.32640
75	1.1968	1.30580	1.54484	1.50173	1.53933	1.76406	0.84653

TABLE A-13 Influence of storage time and conditioning on the chewiness of the precooked freeze-dried beef.

STORAGE TEMP = 39°F PLATE TEMP = 105°F

RH/Time	0	1	2	3	4	5	6
0	1.7750	1.39907	3.29531	2.22508	2.67477	2.84503	2.29373
25	2.5390	1.94857	2.78120	2.55889	3.16825	2.05711	2.61899
50	2.3427	2.02621	2.71710	2.43155	3.09799	2.48313	1.86283
75	2.6092	1.77843	1.44640	2.08015	2.19598	1.96437	1.77107

STORAGE TEMP = 39°F PLATE TEMP = 145°F

RH/Time	0	1	2	3	4	5	6
0	2.3380	1.38932	1.97336	1.76135	1.54649	1.67824	2.38143
25	2.7692	1.94556	3.35750	2.04215	3.07461	2.78125	2.17761
50	1.9670	1.59963	1.79426	2.44105	1.96283	2.46627	1.74780
75	2.5931	1.98393	2.43317	2.04970	3.27981	2.08768	1.81402

STORAGE TEMP = 100°F PLATE TEMP = 105°F

RH/Time	0	1	2	3	4	5	6
0	2.0236	1.51752	1.83278	1.32817	2.25159	2.01707	1.57079
25	2.3614	1.77065	1.96840	2.58456	1.97855	1.97498	2.16527
50	2.0165	2.28684	2.32462	2.04093	3.53917	4.19078	3.24371
75	3.5329	3.31389	3.79751	3.54577	4.65334	5.00360	4.71823

STORAGE TEMP = 100°F PLATE TEMP = 145°F

RH/Time	0	1	2	3	4	5	6
0	2.2480	2.19890	1.17446	2.16939	2.62075	1.79843	2.26413
25	2.3033	4.59206	1.76513	2.09805	2.49619	2.54366	2.17953
50	2.9220	4.09782	3.78523	3.09611	4.34364	3.27314	3.08436
75	2.9618	3.73023	4.56058	3.57214	4.17675	4.55846	2.08407

Table A-14 Chewiness Values Measured by Sensory Panel

Temp. (°F)	Equilibrium Relative Humidity ~0%	~20%	~40%	~60%	~80%	~100%
	(Plate Temperature = 105°F)					
39	28.25	31	34.3	28.7	22.1	27.68
52	26.4	29	31.1	38.4	28.3	26.3
70	25.74	25.68	28.2	25.89	26.1	24.89
100	25.5	22.8	27.7	29.3	33.56	26.2
	(Plate Temperature = 145°F)					
39	25.55	27.5	27.1	27.0	27.0	23.2
52	23.1	27.2	28.36	26.72	29.3	28.2
70	22.2	23.2	26.2	26.35	27.57	25.55
100	20.7	26.8	25.8	26.7	34.66	28.3

FOOD LABORATORY DISTRIBUTION LIST

Food Chemistry

Copies

1 - Commanding General
U. S. Army Combat Development Command
ATTN: CDCMS-O
Fort Belvoir, Virginia 22060

1 - Commanding General
US Army Materiel Command
ATTN: AMCRD-JI
Department of the Army
Washington, D. C. 2031

2 - Commanding Officer
U.S. Army Combat Development Command
Supply Agency
ATTN: CDCSA-R
Fort Lee, Virginia 23801

2 - Commanding Officer
U.S. Army Medical Nutrition Laboratory
Fitzsimons General Hospital
Denver, Colorado 80240

1 - Commanding Officer
U.S. Navy Subsistance Office
ATTN: Mrs. Marjorie Kehoe
Washington, D. C. 20390

1 - Commanding Officer
U.S. Air Force Service Office (AFLC)
ATTN: Mrs. Germaine Gotshall
2800 South 20th Street
Philadelphia, Pennsylvania 19101

1 - Commanding Officer
U.S. Army Foreign Science & Technical Center
ATTN: AMXST-GE (Victoria Dibbern)
220 7th Street, N.E.
Charlottesville, Virginia 22901

1 - Commanding General
U.S. Army Medical Research & Development Command
ATTN: SGRD-MDI-N
Washington, D. C. 20314

2 - Commandant of the Marine Corps
Headquarters U.S. Marine Corps
ATTN: Code AX-44
Washington, D. C. 20380

2 - Commandant of the Marine Corps
Headquarters U.S. Marine Corps
ATTN: Code COB-2
Washington, D. C. 20380

1 - Commandant of the Marine Corps
Headquarters U.S. Marine Corps
ATTN: Code A04G
Washington, D. C. 20380

1 - Commandant of the Marine Corps
Headquarters U.S. Marine Corps
ATTN: CSY-4
Washington, D. C. 20380

1 - Commanding General
Marine Corps Supply Activity
ATTN: Code 826
1100 South Broad Street
Philadelphia, Pennsylvania 19146

1 - Director AF Hospital Food Service
ATTN: Lt. Col. Chaska
Headquarters USAF/SGB-1
6B153 James Forrestall Building
Washington, D. C. 20314

1 - Director
Division of Biology & Medicine
U.S. Atomic Energy Commission
Washington, D. C. 20545

FOOD LABORATORY DISTRIBUTION LIST

Food Chemistry

Copies

1 - Library
USDA, Southern Marketing & Nutrition Research Division
P.O. Box 19687
New Orleans, Louisiana 70119

5 - U.S. Department of Agriculture
Animal & Plant Health & Inspection Service
ATTN: Director, Standards & Services Division
Washington, D. C. 20250

1 - USDA, National Agricultural Library
Current Serial Record
Beltsville, Maryland 20705

1 - Administrator
Agricultural Research Service
U.S. Department of Agriculture
ATTN: Dr. Sam R. Hoover
Washington, D. C. 20250

1 - Dr. I. A. Wolff, Director
Eastern Marketing & Nutrition Research Division
Agricultural Research Service
U.S. Department of Agriculture
Wyndmoor, Pennsylvania 19118

1 - Dr. C. H. Fisher, Director
Southern Marketing & Nutrition Research Division
Agricultural Research Service
U.S. Department of Agriculture
1100 Robert E. Lee Blvd.
New Orleans, Louisiana 70119

1 - Dr. C. H. Harry Neufeld, Director
Southeastern Marketing & Nutrition Research Division
Agricultural Research Service
U.S. Department of Agriculture
P.O. Box 5677
Athens, Georgia 30604

1 - Mr. Dean F. Davis, Acting Director
Market Quality Research Division
Agricultural Research Service
U.S. Department of Agriculture
Federal Center Building
Hyattsville, Maryland 20782

2 - Headquarters 12th Support Brigade
ACofS Services
ATTN: Food Advisor
Fort Bragg, North Carolina 28307

1 - Chief, U.S. Army Food Service Center
ATTN: Dir/Commissary Operations
Fort Lee, Virginia 23801

1 - Dr. K. C. Emerson
Assistant for Research
Office of Assistant Secretary of the Army (R&D)
Department of the Army
Washington, D. C. 20310

2 - Dr. Frank R. Fisher
Executive Director, ABMPS
National Academy of Sciences
National Research Council
2101 Constitution Avenue
Washington, D. C. 20418

1 - CDR Harold J. Janson, MSC, USN
Head, Food Service Branch
Bureau of Medicine & Surgery
Navy Department
Washington, D. C. 20390

1 - Dr. Louis J. Ronsivalli
Fishery Products Technology Laboratory
U.S. Department of Commerce
National Oceanic & Atmospheric Administration
National Marine Fisheries Service
Northern Region
Emerson Avenue
Gloucester, Massachusetts 01930

FOOD LABORATORY DISTRIBUTION LIST

Food Chemistry

Copies

1 - R. J. Reynolds Tobacco Company
ATTN: J. E. Roberts
Winston-Salem, North Carolina 27102

1 - HQDA (DARD-ARL)
WASH DC 20310

1 - Subsistence Management Policy Director
ATTN: OASD (I&L)
Pentagon 2B323
Washington, D. C. 20301

3 - Office of the Coordinator of Research
University of Rhode Island
Kingston, Rhode Island 02881

3 - Exchange & Gift Division
Library of Congress
Washington, D. C. 20540

1 - Headquarters, USAF (AF/RDPS)
DCS/Research & Development
Washington, D. C. 20330

1 - Subsistence & Culinary Arts Department
U.S. Army QM School
Fort Lee, Virginia 23801

1 - Logistics Library
Bunker Hall2
Fort Lee, Virginia 23801

2 - HQDA (DALO-TSS)
WASH DC 20310

2 - Chief, US Army Food Service Center
ATTN: Dir/Food Service Operations
Fort Lee, Virginia 23801

1 - Commanding Officer
Edgewood Arsenal
ATTN: SMUEA-TS-L
Edgewood Arsenal, Md. 21010

1 - Stimson Library
ATTN: Documents Librarian
U.S. Army Medical Field Service School
Brooke Army Medical Center
Fort Sam Houston, Texas 78234

1 - U.S. Department of Agriculture
Consumer & Marketing Service
ATTN: Chief, Product Standards Branch
Standards and Services Division
Washington, D. C. 20250

1 - Assistant Director for Isotopes Development
Division of Applied Technology
U.S. Atomic Energy Commission
Washington, D.C. 20545

1 - Dr. Nicholas Raica, Jr.
Chief, Nutrition Branch and Gnotobiotic Laboratory
Chemistry Division
U.S. Army Medical Research and Nutrition Laboratory
Fitzsimons General Hospital
Denver, Colorado 80240

1 - Commanding General
U.S. Army Medical Research and Development Command
ATTN: SGRD-IDS
Washington, D. C. 20314

5 - Chief, Food Service Division
Walter Reed General Hospital
Washington, D. C. 20012

18 - NRC Committee Members

FOOD LABORATORY INTERNAL DISTRIBUTION LIST

Copies

22 - Program Coordination Office, Food Laboratory, NLABS
(12 for transmittal to Defense Documentation Center)

2 - Technical Library, NLABS

7 - Division Chiefs, Food Laboratory, NLABS

2 - Marine Liaison Officer, NLABS

3 - Air Force Liaison Officer, NLABS

1 - Special Assistant for DOD Food Program, ATTN: Dr. E. E. Anderson, NLABS

1 - US Army Representative for DOD Food Program, NLABS

1 - US Air Force Representative for DOD Food Program, NLABS

1 - US Navy Representative for DOD Food Program, NLABS

2 - Chief, Quality Assurance and Engineering Office, ATTN: Standardization Management and Quality Assurance Branch (Mr. Richman), NLABS

3 - Director, General Equipment and Packaging Laboratory, NLABS

3 - Director, Pioneering Research Laboratory, NLABS

25 - Project Officer, Food Laboratory, NLABS

10 - Alternate Project Officer, Food Laboratory, NLABS

Unclassified
Security Classification

DOCUMENT CONTROL DATA - R & D

(Security classification of title, body of abstract and indexing annotation must be entered when the overall report is classified)

1. ORIGINATING ACTIVITY *(Corporate author)*
Agricultural Engineering Department
Department of Food Science and Human Nutrition
Michigan State University
East Lansing, Michigan 48823

2a. REPORT SECURITY CLASSIFICATION
Unclassified

2b. GROUP

3. REPORT TITLE
INVESTIGATION OF THE ENERGETICS OF WATER BINDING IN DEHYDRATED FOODS AT VERY LOW MOISTURE LEVELS IN RELATION TO QUALITY PARAMETERS

4. DESCRIPTIVE NOTES *(Type of report and inclusive dates)*
Final (1967 - 1970)

5. AUTHOR(S) *(First name, middle initial, last name)*
Dennis R. Heldman, Fred W. Bakker-Arkema, P. O. Ngoddy, G. A. Reidy, M. P. Palnitkar and D. R. Thompson

6. REPORT DATE	7a. TOTAL NO. OF PAGES	7b. NO. OF REFS
June 1972	220	140

8a. CONTRACT OR GRANT NO.	9a. ORIGINATOR'S REPORT NUMBER(S)
DAAG 17-67-C-0165	72-10-FL
b. PROJECT NO. 1J062110A034	9b. OTHER REPORT NO(S) *(Any other numbers that may be assigned this report)* FL-139
c.	
d.	

10. DISTRIBUTION STATEMENT
Approved for public release; distribution unlimited

11. SUPPLEMENTARY NOTES	12. SPONSORING MILITARY ACTIVITY
	U. S. Army Natick Laboratories Natick, Massachusetts 01760

13. ABSTRACT

The thermodynamic and texture properties of low and intermediate moisture foods are discussed on the basis of the moisture sorption isotherm. Information is presented on the effects of final plate temperature in the freeze-drier and of in-package relative humidity on the textural properties under different storage conditions.

DD FORM 1 NOV 68 1473 REPLACES DD FORM 1473, 1 JAN 64, WHICH IS OBSOLETE FOR ARMY USE.

Unclassified
Security Classification

14. KEY WORDS	LINK A		LINK B		LINK C	
	ROLE	WT	ROLE	WT	ROLE	WT
Quality	8		7			
Parameters	8					
Water	9		6		9	
Bound water	9		6		9	
Dehydrated foods	5		7		5	
Thermodynamics			6		8	
Activation			6		8	
Moisture content	9					